Regulation of Fibrin Clot Structure by the Fibrinogen α- and γ-chains and its Relationship to Thrombosis

Helen Ruth McPherson

Submitted in accordance with the requirements for the degree of
Doctor of Philosophy

The University of Leeds
Faculty of Medicine and Health
School of Medicine
Discovery and Translational Science Department

Year 2022

Intellectual Property and Publication Statements

The candidate confirms that the work submitted is his own, except where work which has formed part of jointly authored publications has been included. The contribution of the candidate and the other authors to this work has been explicitly indicated below. The candidate confirms that appropriate credit has been given within the thesis where reference has been made to the work of others.

Publications which have arisen from the work presented in this thesis:

Fibrinogen αC-subregions critically contribute blood clot fibre growth, mechanical stability, and resistance to fibrinolysis. McPherson HR, Duval C, Baker SR, Hindle MS, Cheah LT, Asquith N L, Domingues MM, Ridger VC, Connell SDA, Naseem KM, Philippou H, Ajjan, RA, Ariëns RAS. eLife. 2021; 10: e68761. doi: 10.7554/eLife.68761. Methods from this paper appear in the method section (Chapter 2). Results and adapted figures and discussions from this paper appear in Chapter's 3, 4 and 5.

I performed all the experiments in this section unless stated otherwise. Cédric Duval performed *in vivo* murine experiments. Stephen Baker assisted with micro-rheology experiments. Matthew Hindle performed the platelet incorporation assay and assisted with analysis. Lih Cheah performed platelet fibrinogen interaction assay and assisted with analysis. I performed data analysis, wrote, and submitted the manuscript for publication. All authors on the paper critically reviewed the manuscript prior to publication. Robert Ariëns and Ramzi Ajjan helped plan the work, design experiments, interpret results and edit the manuscript

Acknowledgements

Firstly, I would like to thank my supervisor Professor Robert Ariëns, for his support, guidance, and exchange of ideas during my time as a PhD student and the opportunity to participate in many collaborations and projects. Additionally, for offering me the opportunity to do a PhD, which is something I never thought I would achieve.

I would also like to thank Professor Ramzi Ajjan for his valuable advice, encouragement, and support during my PhD.

I would like to take the time to thank those who have collaborated with me on this thesis Dr Cédric Duval, Dr Stephen Baker, Dr Lih Cheah, Dr Matthew Hindle and Dr Kingsley Simpson. I have appreciated everyone's contribution and greatly treasured the discussions regarding this project and others. Furthermore, I would like to thank Cédric for welcoming me and showing me the ropes all those years ago.

I greatly appreciate the support I have received from Dr Karen Porter and for being a welcoming ear when I was in doubt.

I am grateful to the members (past and present) of the Ariëns and Philippou groups for all the times you have made me laugh and smile in particular Nathan, Adomas, Sam, Lewis, Natalie, and Julia. I will always cherish the times we had together and appreciate how you all supported me through the years. I would like to thank the lovely "level 5 ladies", who welcomed me to the LICAMM all those years ago and who I have had the pleasure of sitting with ever since.

I would like to thank Jess my first lab partner at university, for all the lovely care packages she has sent me while writing up. I greatly treasure our friendship and we certainly had some experimental disasters during university.

I would like to thank my family, for all their support over the years and for the adventures we have had together. Kingsley who has always supported me and encouraged me to believe in myself. I look forward to what the next chapter brings for us together.

I am grateful to the British Society of Thrombosis and Haemostasis for the travel grants I received to attend the ISTH Congress in Berlin and Melbourne to present my projects.

Publications and Presentations

Publications

Fibrin Protofibril Packing and Clot Stability are Enhanced by Extended Knob-hole Interactions and Catch-slip Bonds. Asquith NL, Duval C, Zhmurov A, Baker S, McPherson HR, Domingues MM, Connell SDA, Barsegov V, Ariëns RAS. Submitted to Blood Advances 2022 Jul 12;6(13):4015-4027

Fibrinogen αC-subregions Critically Contribute Blood Clot Fibre Growth, Mechanical Stability, and Resistance to Fibrinolysis**.** McPherson HR, Duval C, Baker SR, Hindle MS, Cheah LT, Asquith N L, Domingues MM, Ridger, VC, Connell SDA, Naseem KM, Philippou H, Ajjan, RA, Ariëns RAS**.** eLife. 2021; 10: e68761

Elimination of Fibrin γ-chain Cross-linking by FXIIIa Increases Pulmonary Embolism Arising from Murine Inferior Vena Cava Thrombi. Duval C, Baranauskas A, Feller T, Ali M, Cheah LT, Yuldasheva N, Baker SR, McPherson HR, Raslan Z, Bailey MA, Cubbon RM, Connell SD, Ajjan RA, Philippou H, Naseem KM, Ridger VC RA, Ariëns RAS. PNAS 2021 Vol. 118 No. 27 e2103226118

GPVI (Glycoprotein VI) Interaction With Fibrinogen Is Mediated by Avidity and the Fibrinogen αC-Region. Xu R, Gauer JS, Baker SR, Slater A, Martin EM, McPherson HR, Duval C, Manfield IW, Bonna AM, Watson SP, Ariëns RAS. ATVB 2021 2021;41:1092–1104

Impact of γ'γ' Fibrinogen Interaction with Red Blood Cells on Fibrin Clots*.* Guedes AF, Carvalho FA, Domingues MM, Macrae FL, McPherson HR, Sabban A, Martins IC, Duval C, Santos NC, Ariëns RA. Nanomedicine 2018 Oct;13(19):2491-2505

A Fibrin Biofilm Covers the Blood Clot and Protects from Microbial Invasion. Macrae FL, Duval C, Papareddy P, Baker S, Yuldasheva N, Kearney K, McPherson HR, Asquith N, Konings J, Casini A, Degen J, Connell SD, Philippou H, Wolberg AS, Herwald H, Ariëns RAS. JCI 2018;128(8):3356-3368

Sensing adhesion forces between erythrocytes and γ’ fibrinogen, modulating fibrin clot architecture and function*.* Guedes AF, Carvalho FA, Domingues MM, Macrae FL, McPherson HR, Santos NC, Ariëns RAS. Nanomedicine 2018 Apr;14(3):909-918

Thrombin and fibrinogen γ' impact clot structure by marked effects on intrafibrillar structure and protofibril packing. Domingues MM, Macrae FL, Duval C, McPherson HR, Bridge KI, Ajjan RA, Ridger VC, Connell SD, Philippou H, Ariëns RAS. Blood 2016 Jan 28;127(4):487-95

Clot structure and fibrinolytic potential in patients with post thrombotic syndrome. Bouman AC, McPherson H, Cheung YW, Ten Wolde M, Ten Cate H, Ariëns RAS, Ten Cate-Hoek AJ. Thromb Res. 2016 Jan;137:85-91

PIK3CA dependence and sensitivity to therapeutic targeting in urothelial carcinoma. Ross RL, McPherson HR, Kettlewell L, Shnyder SD, Hurst CD, Alder O, Knowles MA. BMC Cancer. 2016 Jul 28;16:553

Oral Presentations

Lack of Fibrinogen αC-subdomains Leads to Stunted Fibre Growth, Clot Instability and Increased Fibrinolysis. McPherson HR, Duval C, Baker SR, Hindle MS, Cheah LT, Asquith NL, Domingues MM, Ridger VC, Connell SD, Naseem KM, Philippou H, Ajjan RA, Ariëns RAS. BSHT 2021

Role of the fibrin αC region in mechanical strength, resistance to fibrinolysis and formation of a stable whole blood clot. McPherson HR, Duval C, Baker SR, Hindle MS, Cheah LT, Asquith NL, Domingues MM, Ridger VC, Connell SD, Naseem KM, Philippou H, Ajjan RA, Ariëns RAS. ECTH 2019

The fibrin αC region is critical for mechanical strength, resistance to fibrinolysis and the formation of a stable whole blood clot. McPherson HR, Duval C, Asquith N, Baker SR, Hindle MS, Domingues MM, Ridger VC, Connell SD, Naseem K, Philippou H, Ajjan RA, Ariëns RAS. ISTH 2019

The Fibrin αC Domain not only plays a role in lateral aggregation but also in longitudinal fibre growth. McPherson HR, Duval C, Asquith NL, Domingues MM, Baker SR, Ridger VC, Connell SD, Philippou H, Ajjan RA, Ariëns RAS. BSHT 2017

Role of fibrinogen αC domain in fibrin fibre lateral aggregation and αC connector region in longitudinal fibre growth; complex interactions of the αC region that regulate clot structure and function. McPherson HR, Duval C, Asquith N, Domingues MM, Baker S, Ridger VC, Connell SD, Philippou H, Ajjan RA, Ariëns RAS. ISTH 2017 – Awarded young investigator grant

Functional characterisation of fibrinogen γ' truncations. McPherson HR, Duval C, Domingues MM, Baker S, Ridger VC, Connell SD, Philippou H, Ajjan RA, Ariëns RAS. ISTH 2017

Poster Presentations

Loss of AGDV sequence and interaction with plasma factor(s) contribute to the effect of fibrinogen γ' on clot structure and function. McPherson HR, Duval C, Domingues MM, Baker S, Ridger VC, Connell SD, Philippou H, Ajjan RA, Ariëns RAS. BSHT 2017

Abstract

Cardiovascular disease (CVD) is a group of conditions that primarily affect the circulatory system. CVD is the leading cause of death worldwide, with thrombosis being a key contributor. Fibrin is a central component of the thrombus, and its structural and functional properties can influence thrombi function and impact the success of treatment. Fibrinogen is a protein composed of 3 pairs of polypeptide chains $(A\alpha,B\beta,\gamma)_2$, and the conversion to fibrin by thrombin, releasing the fibrinopeptides, forms a fibrous network supporting the clot.

Both the α- and γ-chains of fibrinogen are critical to protein function, but the exact functional regions are only partially understood. This requires further research, particularly as α- and γ chain variants, including γ', are associated with bleeding and thrombotic conditions. To delineate the roles of these chains on fibrin network characteristics, recombinant fibrinogen variants were produced in Chinese hamster ovary cells. Five γ'-chain truncations were produced, each displaying sequentially four less residues, together with full-length homodimer. Two αC-region truncations were produced; α390 (lacking the αC-domain) and α220 (missing the entire αC-region). Fibrinogens were studied in purified protein, plasma, and whole blood systems.

αC-region truncations altered clot structure, with α390 producing a denser clot composed of thinner fibres, while α220 resulted in a porous structure with stunted fibres and limited longitudinal fibre growth. Complete loss of the αC-region prevented whole blood clot contraction. Fibrinogen with γ'-chain residues showed fibre curvature and was mechanically weaker compared to wild-type.

The addition of γ'-fibrinogen to fibrinogen-deficient plasma produced clots with reduced maximum optical density without hindering whole blood clot contraction or incorporation of RBC or platelets.

This thesis highlights the distinct roles of the αC-domain and αC-connector in fibrin formation, fibre growth, clot structure and stability and shows that γ'-chain residues influence clot structure and decrease mechanical stability.

Table of Contents

List of Figures

List of Tables

List of Equations

List of Abbreviations

aPTT	**Activated Partial Thromboplastin Time**
AT	**Antithrombin**
BCA	**Bicinchoninic Acid Assay**
BHK	**Baby Hamster Kidney**
BSA	**Bovine Serum Albumin**
C-terminal	**C-terminal**
$CaCl_2$	**Calcium Chloride**
cDNA	**Complementary DNA**
CHO	**Chinese Hamster Ovary**
CO_2	**Carbon Dioxide**
COVID-19	**Coronavirus Disease 2019**
COS	**CV-1 in origin and carrying the SV40 genetic material,**
CV	**Column Volume**
CVD	**Cardiovascular Disease**
ddH_2O	**Double-distilled Water**
DMEM	**Dulbecco's Modified Eagle Medium**
DMSO	**Dimethyl Sulfoxide**
DNA	**Deoxyribonucleic Acid**
dNTP	**Deoxyribonucleoside Triphosphate**
DVT	**Deep-vein Thrombosis**
E.coli	**Escherichia coli**
EDTA	**Ethylenediaminetetraacetic acid**
ELISA	**Enzyme-linked Immunosorbent Assay**
FCS	**Foetal Calf Serum**
FpA	**Fibrinopeptide A**
FpB	**Fibrinopeptide B**
F	**Factor**
GP	**Glycoprotein**
HEBS	**Hepes, Sodium Chloride, and Sodium Phosphate Dibasic**
HMWK	**High-molecular-weight Kininogen**
ICU	**Intensive Care Unit**
IL-6	**Interleukin 6**
ITS	**Insulin, Transferrin and Sodium Selenite**
kDa	**Kilo Dalton**
LB	**Lysogeny Broth**
LDL	**Low-density Lipoprotein**
LMW	**Low Molecular Weight**
M	**Molar**

LSCM	**Laser-scanning Confocal Microscopy**
MERS-CoV	**Middle East Respiratory Syndrome Coronavirus**
MFI	**Medium Fluorescent Intensity**
MI	**Myocardial Infarction**
N-terminal	**Amino-terminal**
NO	**Nitric Oxide**
NaCl	**Sodium Chloride**
OD	**Optical Density**
PAI-1	**Plasminogen Activator Inhibitor 1**
PAR4	**Protease-activating Receptor 4**
PBS	**Phosphate Buffer Saline**
PE	**Pulmonary Embolism**
PK	**Pre-kallikrein**
PolyP	**Polyphosphate**
PCR	**Polymerase Chain Reaction**
PMSF	**Phenylmethylsulfonyl Fluoride**
PTM	**Post-Translational Modification**
PTS	**Post-Thrombotic Syndrome**
RBC	**Red Blood Cell**
SARS-CoV-1	**Severe Acute Respiratory Syndrome Coronavirus 1**
SARS-CoV-2	**Severe Acute Respiratory Syndrome Coronavirus 2**
SOC	**Super Optimal Broth**
SDS-PAGE	**Sodium Dodecyl Sulphate–polyacrylamide gel electrophoresis**
SFM	**Serum Free Medium**
siRNA	**Small Interfering RNAs**
SNP	**Single Nucleotide Polymorphisms**
TAE	**Tris, acetic acid and Ethylenediaminetetraacetic acid**
TAFI	**Thrombin Activatable Fibrinolysis Inhibitor**
TF	**Tissue Factor**
TFPI	**Tissue Factor Pathway Inhibitor**
t-PA	**Tissue Plasminogen Activator**
VSMC	**Vascular Smooth Muscle Cells**
VTE	**Venous Thromboembolism**
vWF	**von Willebrand Factor**
WBC	**White Blood Cells**
WT	**Wild Type**

Chapter 1 General Introduction

The ability of fibrinogen to be converted to fibrin to form insoluble clots for the prevention of blood loss is one of fibrinogen's most notable roles. In addition to its role within coagulation mediated haemostasis, fibrinogen has been shown to have role in microbial invasion, prognosis of solid tumours as well as secretion by tumours, angiogenesis, and thrombosis (Simpson-Haidaris and Rybarczyk, 2001; Laurens et al., 2006; Perisanidis et al., 2015; Macrae et al., 2018). The focus of this thesis is on the role of fibrinogen in thrombosis, and to gain further insights into how its structure impacts protein function.

1.1 Cardiovascular Disease

The umbrella term cardiovascular disease (CVD) covers a wide range of conditions that affect the heart and circulation. CVD ranges from inherited conditions to conditions that are associated with ageing such myocardial infarction (MI), stroke and vascular dementia. Taken together, CVD's are the leading cause of death worldwide, and in 2017 there were 17.7 million deaths directly attributed to CVD (Ritchie and Roser, 2019) (WHO https://www.who.int/data/gho/data/themes/mortality-and-global-health-estimates).

Furthermore, in addition to the deaths from CVD there are around 85 million people living with CVD in the Europe (Wilkins et al., 2017). Each year there is an increase in people living with CVD through a combination of factors such as ageing population and improved survival rates from MI and strokes. Currently, the long-term impact on patients who survived acute infections with SARS-CoV-2 (severe acute respiratory syndrome coronavirus 2) or coronavirus disease 2019 (COVID-19) and that had acute cardiovascular complications secondary to the infection are unknown. The complications range from stroke, deep-vein thrombosis (DVT), pulmonary embolism (PE), pulmonary micro thrombosis and the development of cardiac arrhythmias in patients. (Satterfield et al., 2021). CVD is a major health burden globally with both acute and long-term conditions.

Thrombosis is a key component in the pathophysiology of many CVD's, and the formation of thrombus or blood clot can occur in either the arterial or venous system (Cilia La Corte et al., 2011). Arterial thrombosis is responsible for MI or ischaemic stroke, which are generally caused by the formation of a platelet and coagulation activation driven thrombus secondary to the formation, enlargement, and rupture of an atherosclerotic plaque (Previtali et al., 2011; Tomaiuolo et al., 2017).

The formation of an atherosclerotic plaque occurs slowly over time and is driven by vascular inflammation associated with a combination of risk factors such as smoking, hypertension and diabetes mellitus as well as increased blood concentration of low-density lipoprotein

(LDL) (Figure 1) (Bentzon et al., 2014). Atherosclerosis involves a build-up of fatty and fibrous material in the intima, the innermost layer of arteries. Over time, the plaque can become more fibrous and can encroach on the arterial lumen impacting the blood flow (Libby et al., 2019). The deposition of LDL within the intima is a result of diminished barrier function of the vascular endothelium. Once present within the intima, LDL forms aggregates (Libby et al., 2019). These aggregates can enter vascular smooth muscle cells (VSMC) within the vessel wall. Circulating monocytes can migrate out from the vasculature and differentiate into macrophages which are able to engulf the LDL and in turn become pro-inflammatory transforming into foam cells once inside plaque (Hafiane, 2019; Beck-Joseph and Lehoux, 2021). With further accumulation of lipid and lipid-enlarged cells, the atherosclerotic plaque continues to develop. The extracellular matrix of the plaque contains collagen, elastin, proteoglycans and glycosaminoglycans which can aid with the entrapment of the lipids within the intima. The necrotic core is formed by the cell death of macrophages and VSMCs leading to an increased tissue factor (TF) content (Libby et al., 2019). Plaque rupture is the most frequent cause of thrombus, and is initiated by the exposure of the thrombogenic core to the blood through a gap in the fibrous cap of the plaque (Bentzon et al., 2014; Libby et al., 2019)

A thrombus can also form due to a breach of the vessel wall, where circulating platelets become engaged at the site of injury by interaction of von Willebrand factor (vWF) attached to exposed collagen fibres. vWF interactions with platelets occurs through the glycoprotein (GP) Ib-IX-V receptor complex (Tomaiuolo et al., 2017). The breach of the vessel wall also results in the exposure of TF allowing the activation of thrombin which converts fibrinogen into fibrin and is a potent activator of platelets (Bouchard et al., 2013). After initial platelet activation, further platelets are recruited to the site and aggregate together, which is mediated by fibrinogen and the $\alpha_{IIB}\beta_3$integrin also known as GP IIb/IIIa on the platelet surface (Hayward and Moffat, 2013). The platelet plug is stabilised by the conversion of fibrinogen to fibrin by thrombin (Tomaiuolo et al., 2017).

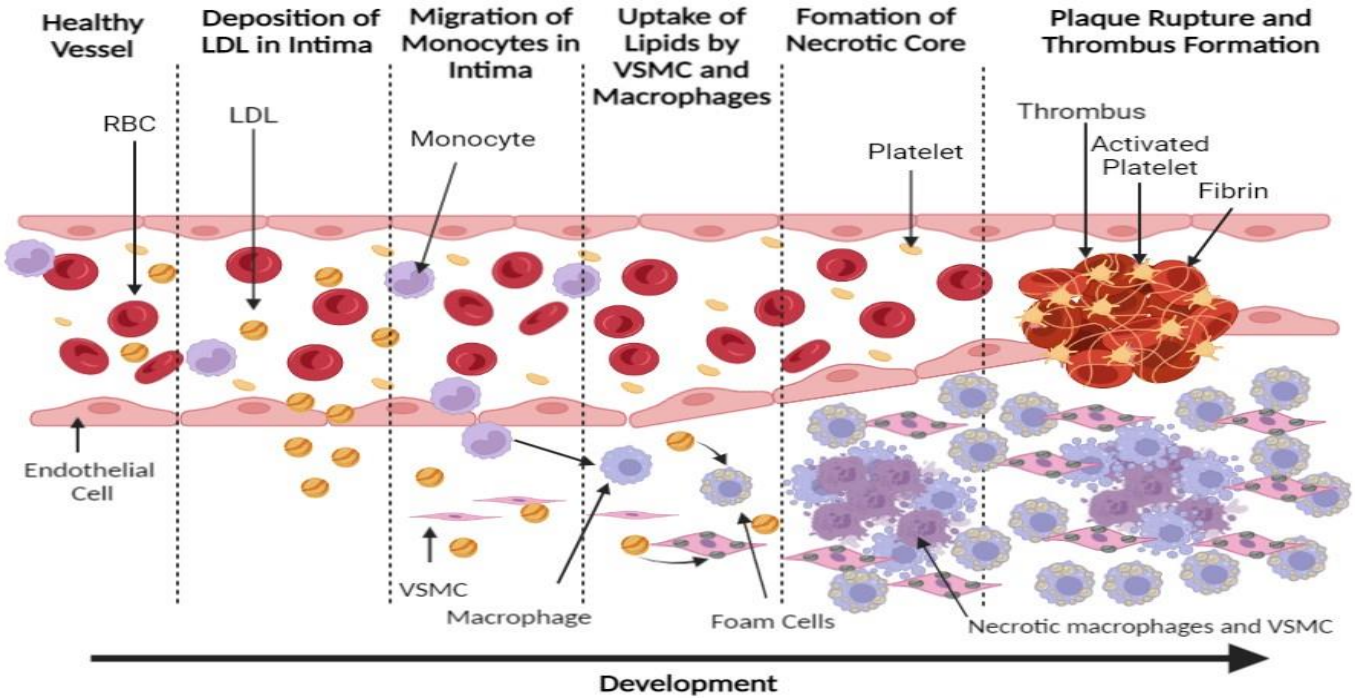

Figure 1 Development of Atherosclerosis

Representative schematic of development, rupture, and thrombus formation of an atherosclerotic plaque. Low-density lipoprotein (LDL) can escape the vasculature due to diminished barrier function of endothelial cells. Monocytes migrate out of the vasculature and differentiate into macrophages and engulf LDL along with vascular smooth muscle cells (VSMC). Macrophages become proinflammatory foam cells due to uptake of lipids. Necrotic core is formed by the death of VSMC and macrophages. The plaque causes vascular remodelling and vessel narrowing. Plaque rupture exposes flowing blood to thrombogenic core therefore triggering thrombus formation. Image created using Biorender.

In contrast to arterial thrombosis, venous thrombosis or venous thromboembolism (VTE) is associated with a triad of different factors, which include stasis or altered blood flow, hypercoagulability and changes in the vessel wall (endothelial dysfunction), and are known collectively as Virchow's triad (Esmon, 2009). Venous thrombosis is primarily observed as DVT and predominately within the deep veins of the lower limbs (Wolberg et al., 2015). Hospital-acquired VTE is estimated to be the most preventable of deaths amongst hospitalised patients (Hunt, 2009). Immobility results in stasis, and stasis-related risk factors are surgery, bed rest and pregnancy. A hypercoagulable state can result from an imbalance of anticoagulant mechanisms or an increase in procoagulant state. These can be caused by factors such as oral contraception medication, presence of the factor V Leiden gene variant and increased fibrinogen levels (Wolberg et al., 2015). In the venous system, the valve pockets of large veins are most sensitive to alterations in flow and stasis, and post-mortem studies have observed thrombi in femoral valve pockets (Sevitt, 1974). Alterations in the vascular environment can activate local endothelial cells and impair their normal, 'healthy' antithrombotic mechanisms by reducing tissue factor pathway inhibitor (TFPI) and nitric oxide (NO) release and Kruppel-like factor 2-mediated production of thrombomodulin to generate a prothrombotic imbalance (Atkins and Jain, 2007; Wolberg et al., 2015). Patients with spontaneous VTE, had higher levels of endothelial activation markers (vWF and P-selectin) in their plasma indicating endothelial dysfunction (Migliacci et al., 2007). Plasma studies into hypercoagulability have shown increased thrombin generation, increase in activation of coagulation factors which can result in the production of fibrin and formation of thrombi (Van Hylckama Vlieg et al., 2007; Brandts et al., 2007; Besser et al., 2008).

1.2 Haemostasis

1.2.1 Classical Coagulation Cascade

The clotting cascade is composed of serine protease zymogens, a transglutaminase, and modulating proteins or cofactors (Figure 2). This model was first proposed in 1964, by two different groups in the UK and the USA (MacFarlane, 1964; Davie and Ratnoff, 1964)**.** The cascade is separated into the intrinsic or contact pathway and extrinsic or tissue factor pathway. Both pathways converge into the common pathway at factor (F)X, ultimately resulting in thrombin generation and the conversion of fibrinogen to fibrin.

The extrinsic pathway is initiated by the exposure of TF on the surface of perivascular cells such as fibroblasts and smooth muscle cells following trauma to the vascular wall allowing contact with the blood. FVII binds to the exposed TF and in the presences of calcium ions and phospholipids activates FX. Once FX has been activated it forms the prothrombinase complex, which is composed of FXa, FVa, calcium ions and phospholipids, and converts

prothrombin to thrombin. Thrombin then converts fibrinogen to fibrin forming a fibrin fibre network which is stabilised by FXIIIa, a transglutaminase that is also activated by thrombin (Cilia La Corte et al., 2011).

The intrinsic pathway begins with FXII which is converted to its active form (FXIIa) by plasmin or Kallikrein with the co-factor high-molecular-weight kininogen (HMWK), in addition to autoactivation by interaction with negatively charged surfaces (Schmaier, 2008). FXII has been suggested to be activated by certain physiological negatively charged macromolecules such as extracellular RNA, collagen, and polyphosphate (PolyP). PolyP is secreted from the dense granules of activated platelets (Morrissey, 2012). Once activated, FXII can activate FXI producing FXIa which then activates FIX. Following the activation of FIX, the intrinsic tenase complex, which is composed of FIXa with the co-factor FVIIIa in the presence of calcium ions and phospholipids, activates FX leading to the common pathway and the generation of fibrin (McMichael, 2012).

The cascade models suggest that the pathways can operate independently of one another, but the clinical symptoms of patients deficient in certain factors point to an alternative situation *in vivo*. A prolonged activated partial thromboplastin time (aPTT) is observed in the clinical work-up of patients with deficiencies in either FXII, HMWK and pre-kallikrein (PK) however these deficiencies are not associated with a bleeding tendency (Gailani and Renne, 2007). Other intrinsic factors have variable bleeding tendencies. FXI (haemophilia C) has a variable bleeding tendency in some people, while serious bleeding is consistently observed in patients with haemophilia A (FVIII), highlighting that the extrinsic pathway alone it is not able to overcome deficiencies in the intrinsic arm of the coagulation pathway. In addition to these clinical observations, *in vitro* studies have shown activation of intrinsic factors (FIX) by extrinsic factors (FVIIa/TF), demonstrating crosstalk between the two pathways. (Lu et al., 2004).

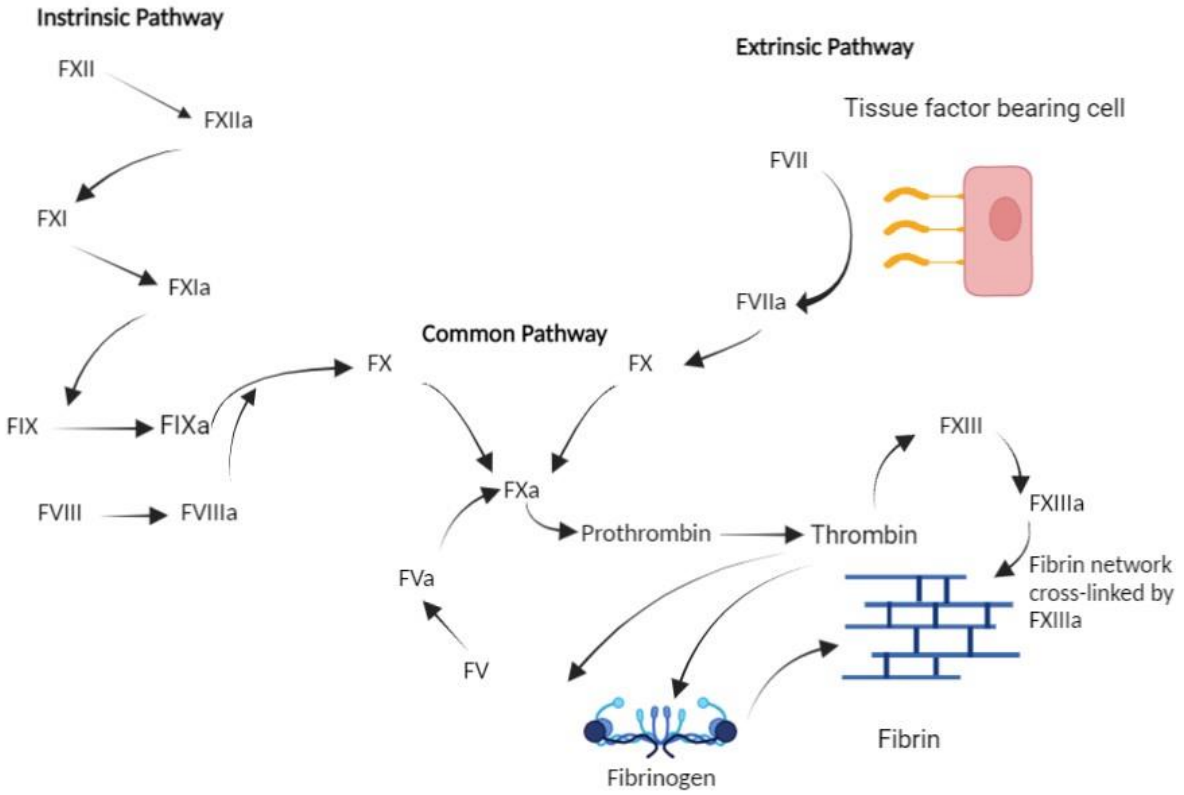

Figure 2 Classical Coagulation Cascade

Representative schematic of the classical coagulation cascade, clotting initiated by either intrinsic or extrinsic pathway, both pathways lead to the common pathway resulting in Factor (F) X activation (FXa) and eventual conversion of fibrinogen to fibrin. Image created using Biorender.

1.2.2 Cell Based Haemostasis Model

The cascade model does not fully reflect the *in vivo* situation, with the model implying that coagulation occurs via either the intrinsic or extrinsic pathway without major crosstalk between the two sides. Therefore, an alternative model has been proposed for coagulation which includes the influence of cells and their surfaces. In this model, the coagulation pathway is represented by 3 overlapping stages, the first stage being initiation, followed by amplification and finally propagation (Hoffman and Monroe, 2001).

1.2.2.1 Initiation

The initiation stage is triggered when blood is exposed to a TF-bearing cell and FVIIa binds to TF. The TF-FVIIa complex can activate FIX and FX in a limited capacity as well as auto-activate FVII. At a slow reaction rate FV can be activated directly by FXa. The generated FXa binds to FVa to form the prothrombinase complex, which generates a small amount of thrombin by the cleavage of prothrombin (Smith, 2009). If the FXa dissociates from the membrane surface of the TF bearing cells it is rapidly inactivated by antithrombin (AT) or tissue factor pathway inhibitor (TFPI), localising the generated FXa. Coagulation activation in this stage only continues if there is enough TF exposed at high enough levels to overcome the influence of the inhibitors (McMichael, 2012). In contrast to FXa, the generated FIXa can leave the TF-bearing cell surface and move to the surface of platelets of other nearby cells as it is not inhibited by TFPI, and the inhibition of FIXa by AT occurs more slowly compared to FXa. (Hoffman, 2003; Roberts et al., 2006)

1.2.2.2 Amplification Stage

After the initiation stage, the amplification stage is activated. The limited amount of thrombin generated through the initiation stage can disperse away from the initial site of TF exposure. Amplification results from the activation of platelets by the dispersed thrombin and through the binding of platelets to the exposed collagen (Hoffman and Monroe, 2001; Smith, 2009). Platelet activation gives rises to shape change, membrane rearrangements resulting in the exposure of phospholipids and results in the release of granules (Smith, 2009). Thrombin on the activated platelet surface cleaves both FXI and FV to their activated form. Thrombin removes vWF, which circulates in plasma in complex with FVIII, to release FVIII and activates the latter. The released vWF can mediate further platelet adhesion and aggregation leading to an increase in the number of activated platelets at the site of injury, therefore increasing the surface area for coagulation to take place on (Smith, 2009).

1.2.2.3 Propagation

In the propagation phase, the surface of activated platelets supports the generation of substantial amounts of tenase and prothrombinase complexes, leading to significant thrombin production (Hoffman and Monroe, 2001). The platelets activated during the amplification stage release granules which contain factors that cause further recruitment of platelets and mediate platelet-platelet interactions (Smith, 2009; Flaumenhaft, 2013). FIXa generated during the initiation phase binds to co-factor FVIIIa on the platelet surface. Further FIXa is generated on the platelet surface by FXIa-mediated cleavage of FIX. Once the tenase complex (FIXa–FVIIIa) is formed on the platelet surface, it generates further FXa, which binds to its co-factor FVa, to generate prothrombinase complexes (FXa,FVa and calcium ions) (Smith, 2009; McMichael, 2012). The now substantial numbers of prothrombinase complexes lead to a burst of thrombin generation and the conversion of fibrinogen to fibrin.

1.3 Fibrinogen

1.3.1 Production and Secretion

In healthy individuals, fibrinogen circulates in the plasma between 1.5-4 mg/mL with a half-life of 3-5 days (Bridge et al., 2014; Vilar et al., 2020). The fibrinogen protein is composed of two copies of three chains termed Aα, Bβ and γ. The genes encoding the fibrinogen chains are all located on chromosome 4, (4q23-32), clustered in a 50 kb region (Kant et al., 1985). Each chain is encoded by a separate gene: *FGA* for Aα, *FGB* for Bβ, and *FGG* for γ. The FGA mRNA undergoes splice variation to produce a major splicing isoform composed of five exons (Aα) and a minor isoform (1-3 % in circulation) of 6 exons termed AαE (Fish and Neerman-Arbez, 2012). The *FGB* gene has eight exons and encodes a single mRNA. The *FGG* gene produces two isoforms: a major form referred to as the γA, which is produced from the entire 10 coding exons, and a minor form known as γ' (10 % in circulation) where intron 9 is not spliced and 4 of the exon 10 encoded residues are replaced with 20 different residues at the carboxyl (C-) terminal (Fish and Neerman-Arbez, 2012). The Aα and γ genes exist on the same DNA (deoxyribonucleic acid) strand and are transcribed in the same direction, while the Bβ gene in contrast is found on the opposite DNA strand (Fuller and Zhang, 2001). The nascent polypeptides of the three fibrinogen chains each have a signalling peptide which is cleaved off in the endoplasmic reticulum, producing mature polypeptide chains of 610, 461 and 411 residues for the Aα, Bβ and γ-chains respectively (Weisel and Litvinov, 2017). Together the fibrinogen molecule has a molecular weight of 340 kDa, with the Aα chain at 66.5 kDa, the Bβ at 52 kDa, and the γ at 46.5 kDa. Some of the molecular weight is due to

co- and post-translational modifications to the Bβ and γ-chains, which are glycosylated (Weisel and Litvinov, 2017).

The primary source for plasma fibrinogen production is the hepatocyte (Vilar et al., 2020). In addition to basal expression of fibrinogen, fibrinogen is an acute phase response protein where increased hepatocyte fibrinogen expression is observed in response to interleukin 6 (IL-6) stimulation (Fuller et al., 1985). The three chains are encoded separately on independent polysomes and then translocated into the lumen of the endoplasmic reticulum for assembly (Redman and Xia, 2000). Within the endoplasmic reticulum the stepwise construction of fibrinogen involves formation of Aα-γ and Bβ-γ complexes, followed by the addition of third chain to create Aα-Bβ-γ, which then dimerises to form the complete fibrinogen molecule (Hartwig and Danishefsky, 1991; Huang et al., 1993; Redman and Xia, 2000). The stepwise assembly of fibrinogen is aided by the lectin-chaperone system (Tamura et al., 2013).

The post-translation modifications that are found on the secreted fibrinogen commence within the endoplasmic reticulum and are completed in the Golgi apparatus, as fibrinogen is a glycoprotein, the glycosylation most commonly occurs at residues Asn364 and Asn52 on the Bβ and γ-chain respectively (Cilia La Corte et al., 2011).

1.3.2 Fibrinogen Structure

The fibrinogen protein is 45 nm in length, with a central E-region, and two D-regions either side of the E-region, which are connected to the E-region by α-helical coiled coils composed of all three chains and the protein is held together by 29 disulphide bonds (Figure 3) (Mosesson, 2005; Weisel and Litvinov, 2017). Part of the α-helical coiled coils are within D and E regions. Most of the human structure has been crystallised and solved by X-ray crystallography (Spraggon et al., 1997; Kollman et al., 2009). Fibrinogen has several unstructured regions which are not amenable to crystallisation, and these have yet to be resolved by crystallography, although recent advances in NMR spectroscopy may change this. The unresolved areas are the amino (N-) terminal residues of Aα (residues 1-26), Bβ (residues 1-57) and γ-chain (residues 1-13) and C-terminal residues Aα (residues 201-610), Bβ (residues 459-461) and γ-chain (residues 395-411) (Weisel and Litvinov, 2017). There have been a number of alternative methods used to gain structural insight on to some of these areas, including electron microscopy, atomic force microscopy, cross-linking mass spectrometry and computational reconstruction (Veklich et al., 1993; Zhmurov et al., 2011; Protopopova et al., 2015; Klykov et al., 2020).

The central E-region is composed of the N-termini of all the 6 chains (Aα, Bβ and $\gamma)_2$, which chains are held together by 5 disulphide bonds forming a disulphide ring (Blombäck et al.,

1976; Mosesson, 2005). The residues involved in the disulphide ring are a pair at Aα 28, two pairs between Aα36 and Bβ65 and between two γ-chains at γ8 and γ9, with one of the γ-chains in an antiparallel orientation (Mosesson et al., 2001). The fibrinopeptides (Fp) are in the N-termini of the Aα and Bβ-chains and are termed FpA and FpB respectively and these are cleaved during the conversion to fibrin (Mosesson et al., 2001).

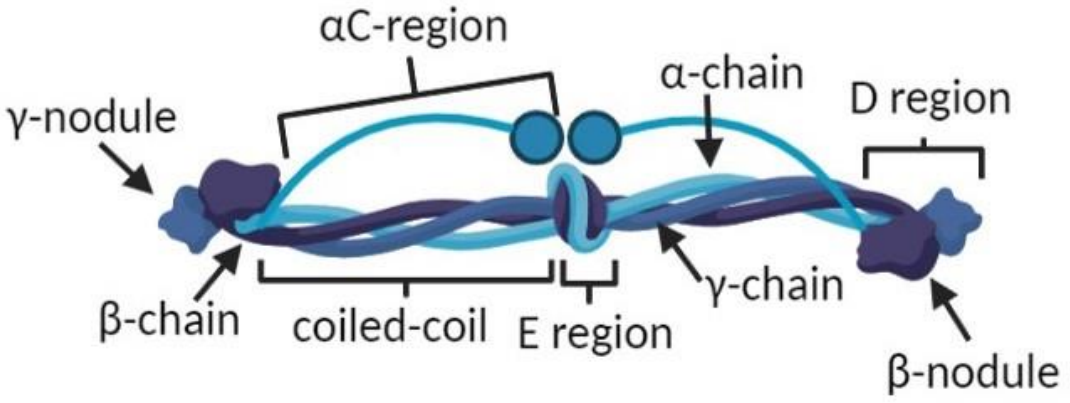

Figure 3 Structure of Fibrinogen

Fibrinogen is composed of a central E-region and two D-regions which connect to E-region by coiled coil regions. These regions are composed of two sets of three chains known as Aα, Bβ and γ. The αC-region which extends away from the main module, is composed of the Aα-chain. Image created in Biorender.

The D-region is where the Bβ and γ-chain terminate and have been observed by atomic force microscopy (AFM) to be larger than the E-region (Protopopova et al., 2017). The C-termini of the β- and γ-chains form the β- and γ-nodule respectively. These nodules consist of three domains: an N-terminal A-domain, a central B-domain and a C-terminal P-domain (Medved et al., 2009). The β- and γ-nodules are arranged relative to each other at 130°, with the β-nodule folded close to the coiled coil and the γ-nodule extending towards the distal position, associated by non-covalent interactions (Spraggon et al., 1997; Zhmurov et al., 2011). The disulphide bonds within the D-region form an asymmetric ring involving disulphide bonds between Bβ193 and Aα165, Aα161 and γ135 and Bβ197 and γ139 (Spraggon et al., 1997). Within the D-region there are both high and low affinity calcium ion binding sites. The high affinity site is termed γ1 in the γ-nodule and is associated with residues γ318, γ320, γ324 and γ322 and β-nodule residues β381-385, each with a coordinating water molecule (Yee et al., 1997; Everse et al., 1998). The low affinity binding sites are termed γ2 (located in the γ-chain loop residues 294-301) and β2 (residues Bβ261, Bβ398 and γ132) (Everse et al., 1999). The coiled-coil which connects the D- and E-regions, is composed of three right-handed α-helices which wrap around one another and create a left-handed supercoil (Doolittle et al.,

1978). There is a fourth helix bundle composed of residues Aα166-195, which starts at the lateral disulphide ring in the D-region, with the α-chain reversing out from the D-region to run back alongside the coiled-coil (Spraggon et al., 1997). Following the reverse loop along the coiled-coil, the α-chain extends to form the αC-region comprising residues Aα221-610 (Medved et al., 2009). The αC-region is composed of two subregions, the C-terminus known as the αC-domain residues Aα392-610 and an αC-connector region involving residues Aα221-391. This αC-connector connects the αC-domain to the rest of the protein (Medved and Weisel, 2021).

1.3.3 Fibrin Polymerisation

Fibrin polymerisation is initiated following the conversion of prothrombin to thrombin. Once thrombin is in its active form, it first cleaves FpA from the Aα-chain (Figure 4). The FpA is the first 16 residues of the Aα-chain, and the removal of FpA from the Aα-chain results in a new N-terminal sequence of Gly-Pro-Arg which are referred to as knobs 'A' (Cilia La Corte et al., 2011; Weisel and Litvinov, 2017). At a slower rate, FpB is cleaved next, which involves the first 14 residues of the β-chain. In analogy with the removal of FpA, a new N-terminal sequence of Gly-His-Arg termed knob 'B' is exposed after FpB cleavage (Blomback et al., 1978; Cilia La Corte et al., 2011).

Knobs 'A' interact with holes that are always available within the γ-nodules (in the D-region) of the interacting fibrin molecules, forming a half-staggered dimer (Erickson and Fowler, 1983). Knobs 'B' associate with the holes within the β-nodules in the D-region. Generating a D:D interface, a third fibrin module is then added to the half-staggered dimer. The D:D interface is composed of residues γ275-309, with residues γ275, γ308 and γ309 critical for elongation of fibrin stands (Everse et al., 1998; Doolittle et al., 1998; R.C. Marchi et al., 2006; Bowley et al., 2009). Fibrin monomers can continue to be added to the initial half-staggered dimer, resulting in the formation of extended two-stranded fibrin oligomers and then two-stranded protofibrils with the further inclusion of monomers (Weisel and Litvinov, 2017; Zhmurov et al., 2018). When protofibrils reach 0.5-0.8 μm in length they are able to aggregate laterally and produce fibres, which branch to form the 3D fibrin network (Hantgan et al., 1980; Chernysh et al., 2011). The αC-regions are released following FpB cleavage and interact with adjacent αC-regions, encouraging lateral aggregation (Weisel and Medved, 2001).

The fibrin network is stabilised by formation of ε-(γ-glutamyl)-lysyl bonds catalysed by FXIIIa between a number of glutamine and lysine residues in the α- and γ-chains (Pisano et al., 1968). The γ-γ-chain cross-links, which are the first to form, occur between residues γ-Lys406 and either γGln398 or γGln399 (Duval et al., 2014). Compared to the γ-chain, there are far

more sites involved in cross-linking of the α-chains, including five known reactive glutamines in the αC-region (Glut221, Glut223, Glut237, Glut328 and Glut366) and numerous lysine acceptor sites (Mouapi et al., 2016; Schmitt et al., 2019).

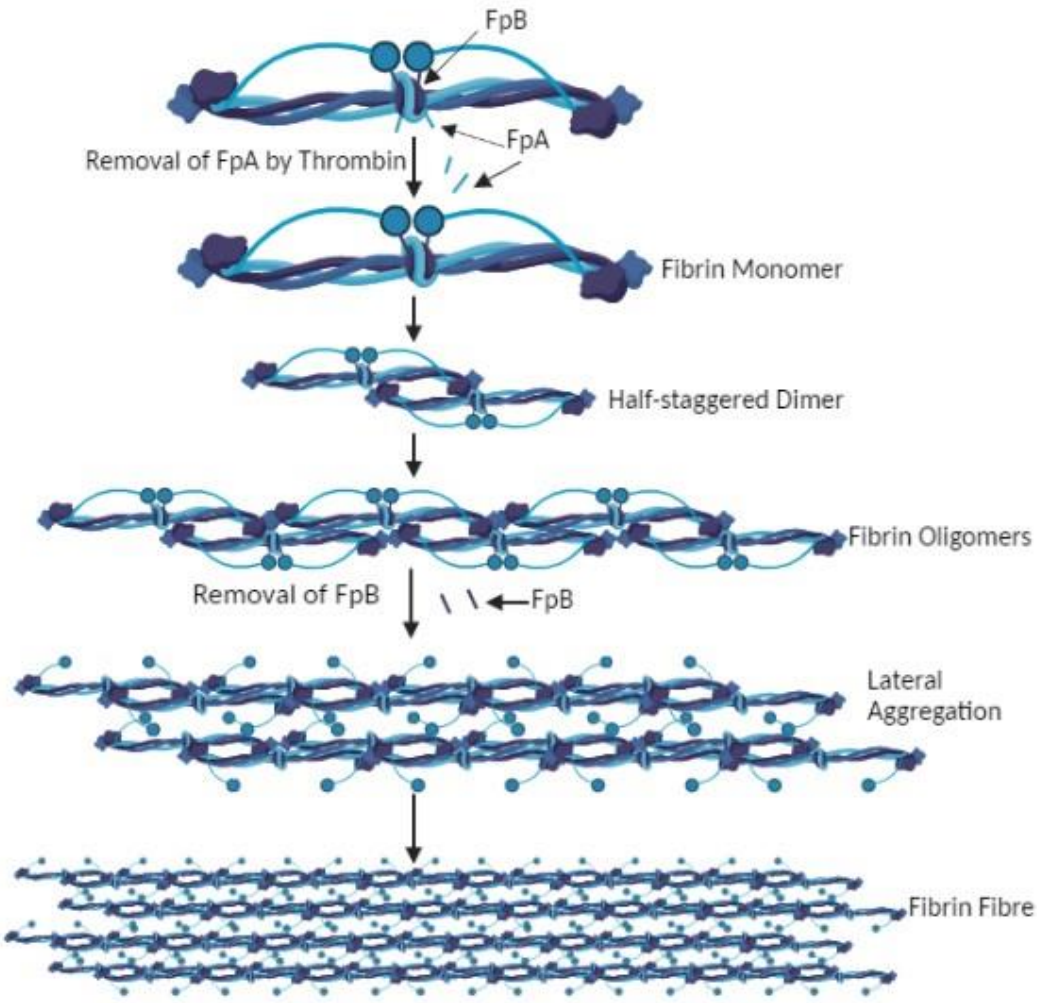

Figure 4 Fibrin Polymerisation

Fibrin polymerisation is initiated by thrombin through the release of fibrinopeptide A (FpA) making fibrin monomer. Fibrin monomer can form a half-staggered dimer, with the addition of more monomers, there is the formation of fibrin oligomers. The release of FpB allows lateral aggregation and development of fibrin fibre. Image created in Biorender.

1.3.4 Fibrinolysis

The process of fibrinolysis is tightly regulated, with fibrinolytic proteases and inhibitors, and any overactivity or deficiency in either side would tip the scales towards excessive bleeding or thrombosis respectively. The fibrinolytic system is composed of plasminogen, an inactive proenzyme, and its activators tissue-type plasminogen activator (t-PA) and urokinase (u-PA). t-PA mediated plasminogen activation in circulation is the main pathway for fibrin

breakdown (Lijnen, 2001). t-PA and plasmin activities are regulated by α_2-antiplasmin (plasmin), plasminogen activator inhibitor (PAI) 1 and 2 (t-PA and u-PA) and thrombin activatable fibrinolytic inhibitor (TAFI) (plasminogen) (Medved and Nieuwenhuizen, 2003; Medcalf and Keragala, 2021). The activation of plasminogen by t-PA to plasmin is enhanced in fibrin compared to fibrinogen (Hoylaerts et al., 1982). The binding sites for plasminogen and t-PA in fibrinogen are cryptic and are exposed on conversion to fibrin. t-PA and plasminogen binding sites are located within the fibrinogen αC-domain, Aα148-160 (for t-PA and plasminogen), D-region (for plasminogen), and D-region γ312-324 (for t-PA) (Schielen et al., 1989; Schielen et al., 1991; Yakovlev et al., 2000; Tsurupa and Medved, 2001; Hudson, 2017).

The initial breakdown of fibrin occurs in the αC-domains and the N-terminal β-chain (cleaved at βArg42), followed by multiple cleavages between the D- and E-regions (Longstaff and Kolev, 2015). The breakdown products include high and low molecular weight complexes: D-D-E_1 complex with the terminal products being D-Dimer, E_3 fragment and the remaining portions of the αC-region (Marder and Francis, 1983; Medved and Nieuwenhuizen, 2003). The cleavage products generate terminal lys-residues which provide additional binding sites for plasmin that further enhance fibrinolysis (Fleury and Anglés-Cano, 1991).

The rate of fibrinolysis is influenced by clot structure (fibre diameter and porosity) and composition (platelet and red blood cell (RBC) content) (Collet et al., 2000; Wohner et al., 2011; Whyte et al., 2017). Plasma clots that are composed of a tight fibre network of thin fibres are lysed more slowly than a loose fibre network of thick fibres. However, on an individual level, thin fibres are lysed faster than thick fibres (Collet et al., 2000). It was observed that plasmin cuts fibrin fibre perpendicularly to the fibre direction (Veklich et al., 1998). A further study into lysis of individual fibrin fibres used a combination of mathematical modelling and dynamic fluorescence microscopy (Lynch et al., 2022). Plasmin digestion occurred along the entire fibre with variable rates of digestion. The variation in the digestion rate is due to fibrin longitudinal sliding and loss of protofibril sections by plasmin digestion. The combination of both these activities result in local fibre thinning and eventual breakdown (Lynch et al., 2022).

Investigations by turbidimetric assay and Chandler loop of purified FXIII showed that FXIIIa reduced fibrinolytic resistance (Hethershaw et al., 2014). Other investigations under flow aimed at understanding the role of FXIIIa cross-linking in clot fibrinolysis using inhibition of FXIIIa, whole blood from healthy individuals and whole blood and plasma from a patient with FXIII deficiency (Mutch et al., 2010a). This study showed that thrombi lacking FXIIIa crosslinking lysed more quickly compared to clots containing FXIIIa.

The cellular component of a whole blood clot does not act as mere bystander in the process of fibrinolysis. Platelet-mediated contraction of whole blood clots results in clots that are more resistant to fibrinolytic degradation. The contracted clot permits less access to plasminogen and its activators to the fibrin network, and the presence of cross-linked α_2-antiplasmin further protects clots from degradation (Blinc et al., 1992; Aoki, 1993; Whyte et al., 2017). Upon platelet activation, the α-granules are released, which contain fibrinogen, vWF, pro-fibrinolytic proteins (plasminogen) and proteins that provide fibrinolytic resistance (α_2-antiplasmin , TAFI and PAI-1) (Flaumenhaft, 2013; Whyte et al., 2017). The contents of the α-granules demonstrate that platelets have a role in maintaining the balance between fibrinolysis and fibrinolytic resistance. Platelet subpopulations have been observed, including procoagulant phosphatidylserine (PS) expressing platelets and pro-aggregatory platelets (PS negative). The PS on the procoagulant platelets binds coagulation factors to drive the generation of thrombin whereas the pro-aggregatory platelets are characterised by the activation of $\alpha_{IIB}\beta_3$, which supports aggregation and clot contraction (Hindle et al., 2021). It has been observed that during clot contraction procoagulant platelets accumulate at the surface of the thrombus (Nechipurenko et al., 2019). Procoagulant platelets have been observed to have a protruding “cap”, which localises FXIIIa, plasminogen, PAI-1 and fibrinogen (Mitchell et al., 2014; Whyte et al., 2015; Podoplelova et al., 2016). Plasminogen in the cap contribute to thrombus lysis which was accelerated by flow (Whyte et al., 2015) . RBCs are another major component of a thrombus, and can influence clot structure and clot viscoelasticity (Gersh et al., 2009a). RBCs have been shown to increase lytic resistance by supressing t-PA activation of plasminogen (Wohner et al., 2011).

Experimentally, a fibrinolytic mixture can either be included in the clotting mixture (mirroring internal fibrinolysis) or added to a formed clot (external fibrinolysis). *In vivo* fibrinolysis occurs through internal fibrinolysis whereas thrombolysis used for stroke treatment largely involves external lysis. Furthermore, clot contraction can influence internal and external fibrinolysis, with contracted clots having enhanced internal fibrinolysis but reduced external fibrinolysis (Tutwiler et al., 2019). The influences of clot porosity, fibre diameter, accessibility of plasmin and presence of anti-fibrinolytic proteins within the fibrin clot, highlight the complex nature of fibrinolysis.

1.3.5 Clot Mechanics

Fibrin is often described as a viscoelastic polymer; meaning it has both elastic and viscous properties. These properties determine how clots or thrombi behave within the circulation and under the differing shear forces of the arterial or venous vasculature. Viscoelastic properties are covered by two laws; Hooke’s Law and Newton’s law. Hooke’s law describes

an elastic solid as the strain or deformation that is proportional to the stress or force applied per area, however the stress is independent of the rate of strain. Newton's law describes viscous materials as the stress is proportional to the rate of strain but independent of the strain itself (Weisel, 2004). The stiffness of the clot can be characterised by the elastic (reversible mechanical deformation) or storage modulus and the inelastic or irreversible component studied by the loss modulus or creep (slow irreversible mechanical deformation) (Weisel, 2004; Weisel and Litvinov, 2017).

Fibrin mechanics range from whole clot, fibre network and individual fibre levels. Fibrin clots have high extensibility and a loose volume with stretching, and when strain is applied to fibrin, the network of fibres becomes thinner, closer and bundled with α-helix to β-sheet conversion of the coiled-coils (Brown et al., 2009; Purohit et al., 2011; Litvinov et al., 2012). These bundled fibres align in the direction of strain. Rearrangement of the network has been observed in response to compressive deformation (Brown et al., 2009; Kim et al., 2014a). At the fibrin fibre level, fibres bend and buckle in the direction of deformation (Kim et al., 2014a).

Fibrin is highly extensible, resisting shear strain up to 250 % deformation, while investigations have shown that there were no permanent alterations in fibre or network structure with strains up to 25 % (Vos et al., 2020). However, above 25 % the fibres progressively aligned to the direction of strain and caused network stiffening (Vos et al., 2020). A fibrin fibre network is made from numerous fibres, and these fibres can have a range of extensibilities. Individual fibres have been shown to rupture when extended to 226 % for uncrosslinked fibres and 332 % for partially crosslinked fibres (Liu et al., 2006). Interestingly, authors observed some fibres that could extend to over 500 %, highlighting the heterogeneous nature of fibrin fibres. A further investigation into single fibrin fibres found that fully crosslinked fibres were less extensible, stiffer and less elastic than non-crosslinked fibres (Liu et al., 2010). Furthermore, fully crosslink and non-crosslinked fibres both showed time dependent softening (Liu et al., 2010).

Clinically the understanding of clot mechanics is important to understand why some patients experience emboli following DVT or how thrombi respond to treatment by mechanical thrombectomy.

1.4 Fibrinogen αC-region

The αC-region is the C-terminal portion of the α-chain and comprises two thirds of the α-chain residues 220-610 (Soria et al., 2019). The region is composed of two subregions, the αC-domain residues Aα392-610 and the αC-connector residues Aα221-391 which connects

the domain to the bulk of the fibrinogen protein (Medved et al., 2009). The αC-region contains numerous sites for interaction with other plasma proteins and receptors (Figure 5). Within the αC-domain there is an RGD motif (Aα572-574) involved in endothelial cell binding through integrin αvβ5, as well as numerous lysine residues utilised in FXIIIa cross-linking, with a high percentage of cross-linking occurring at Lys556 and Lys580 (Cheresh et al., 1989; Sobel and Gawinowicz, 1996; Cilia La Corte et al., 2011). The αC-region is the first part of fibrin that is targeted for proteolysis by plasmin. Within the αC-domain there is a binding site for plasmin with the first point of cleavage after Lys583 (Tsurupa and Medved, 2001). Also contained within the αC-connector is an α_2-antiplasmin incorporation site at residue Aα303 and various glutamines involved in FXIIIa-mediated cross-linking (Kimura and Aoki, 1986; Mouapi et al., 2016).

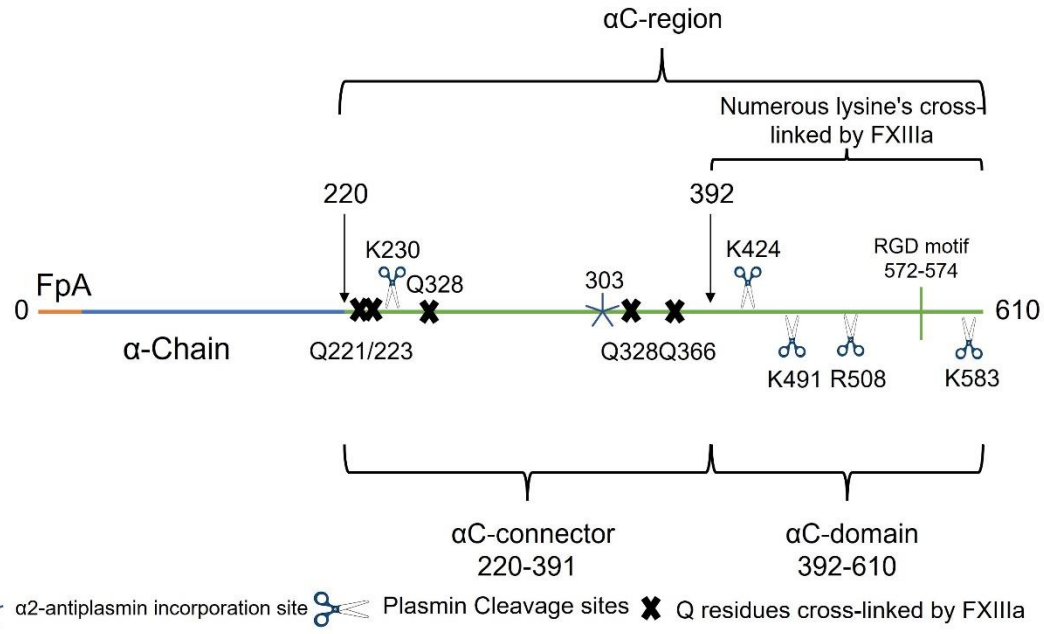

Figure 5 Schematic of αC-region Interaction Sites

Sites cleaved by plasmin, FXIIIa cross-linking sites and α2-antiplasmin incorporation site are highlighted in the αC-connector and αC-domain.

1.4.1 Structure of the αC-region

Although the αC-region has not been crystalised due to the region being sensitive to proteolysis within circulation and a large proportion of the region being relatively unstructured, there are areas within the region that are structured. AFM has been used to visualise the αC-region, showing the αC-connector as thin strands coming from the D-region terminating with a small compact globular structure indicating the αC-domain (Protopopova et al., 2017).

The αC-region length is highly variable and there are few conserved residues between species. Furthermore, the number of tandem repeats in the αC-connector and number of residues within the repeats differ between species (Doolittle and Kollman, 2006). The human αC-connector contains 10 repeats of 13 residues; however, both the bovine and rat repeats have 13 residues they have less repeats, 7 and 5 respectively. Furthermore, these repeats are absent in birds. The tandem repeats in the human αC-connector are located between Aα261-391. The tandem repeats are composed of tryptophan, and are rich in glycine, serine threonine and proline residues. Furthermore, there are few non-polar residues found within the αC-connector however it does contains an excess of glycine, serine, threonine, and proline, suggesting that it is unlikely to form a compact structure (Doolittle et al., 1979; Medved et al., 1983; Weisel and Medved, 2001).

In contrast to the αC-connector, the αC-domain has a large number of non-polar residues and the domain is rich in glycine, serine, threonine and proline residues alike the αC-connector (Doolittle et al., 1979; Weisel and Medved, 2001). Contrary to the αC-connector, which does not form a compact structure, the αC-domain consists of two subdomains, an N-terminal composed of β-sheet consisting of two β-hairpins and C-terminal is less structured (Burton et al., 2006; Burton et al., 2007; Tsurupa et al., 2009). The αC-domain has been reported to associate with the central E-region and to be released upon FpB cleavage by thrombin (Veklich et al., 1993; Litvinov et al., 2007; Protopopova et al., 2017; Medved and Weisel, 2021).

1.4.2 Fibrinolysis

The αC-domain contains the first point of cleavage during fibrinolysis at AαK583 and thus is partly degraded in circulation (Hudson, 2017). Three forms of fibrinogen, a high molecular weight (340 kDa), a low molecular weight (LMW) (305 kDa) and LMW' (270 kDa) are found in circulation at 70 %, 25 % and 5 % respectively (Holm et al., 1985). The LMW form has a truncated αC-region highlighting the susceptibility of the αC-region to proteolysis resulting in degradation (Holm et al., 1986). Fragments of the human αC-region were expressed in *E.coli* and showed plasminogen and t-Pa binding sites within the αC-domain, but no binding was observed in the connector (Tsurupa and Medved, 2001). Additional points of proteolysis are located at Aα508, Aα491, AαK230 and AαK206, leading to removal of most or the entire αC-region (Tsurupa et al., 2009).

1.4.3 Mechanical Investigations into the αC-region

A study of human, mouse, and chicken fibrinogens with variable lengths of αC-connectors showed 10, 5 and 0 repeats respectively (Falvo et al., 2008). The authors also observed

greater extensibility with the increased tandem repeat number, highlighting that the αC-connector provides elasticity in fibrin. Further investigations into the role of the extensibility of the αC-region compared recombinant WT fibrinogen and γQ398N/Q399N/K406R where the γ-chain cross-linking sites are mutated. AFM experiments using lateral force with these fibrinogens indicated that α-α cross-links provided substantial fibre elasticity and stiffness (Helms et al., 2012). As the αC-connector is roughly 60 nm in length, it may form numerous intermolecular and interprotofibrillar interactions, and its extensibility and elasticity is crucial for this role (Houser et al., 2010; Helms et al., 2012).

1.5 Fibrinogen and Cardiovascular Disease

As fibrinogen is an acute phase protein, the plasma levels are observed to increase during states of infection and inflammation. Whether the increased fibrinogen level itself is a risk for cardiovascular disease or a resultant effect of the inflammatory state from the underlying pathology is still unclear. There have been several studies that have observed elevated fibrinogen levels in patients with cardiovascular disease and studies that have not. Furthermore, the impact of fibrinogen in acute phases of CVD such as study of collected thrombi and plasma samples from patients is further discussed in sections 1.5.1 and 1.5.2.

In a meta-analysis study comprising 154,211 participants covering 31 prospective studies it was found that there were moderately strong associations between plasma fibrinogen level and the risks of coronary heart disease and stroke in healthy middle-aged adults (Fibrinogen Studies Collaboration et al., 2005). In a later study of 2,288 participants having investigations for coronary angiography with angina-like chest pain, higher fibrinogen levels were linked with the presence and severity of new-onset coronary atherosclerosis (Zhang et al., 2014). In a study of 13,195 participants undergoing angiography diagnosed coronary artery disease, fibrinogen was found to independently correlate with mortality rates (Ndrepepa et al., 2013). A single centred study of 2,126 participants with and without coronary artery disease found that fibrinogen was directly associated with the presence of MI and a short-term predictor of mortality (Acevedo et al., 2002). In a study of 77,608 participants from the Danish population, the association between elevated fibrinogen level between DVT and DVT with PE was investigated (Klovaite et al., 2013). The study found that elevated fibrinogen levels associated with increased risk of PE with DVT but not with DVT alone. The link with elevated fibrinogen and risk in cardiovascular disease has been observed in various ethnicities highlighting the universal benefit of measuring fibrinogen levels (Kaptoge et al., 2007; Shojaie et al., 2009; Zhang et al., 2014). However, there have been a number of studies that have not observed associations between fibrinogen levels and CVD. A study of 4,685 patients with MI and 3,460 participants without coronary disease where genotyping and

fibrinogen concentration was studied (Keavney et al., 2006). In addition, the study also did meta-analysis into fibrinogen β-chain genotypes (12,220 participants with coronary disease and 18,716 controls), the study concluded that the long-term impact in fibrinogen concentrations and fibrinogen is not a principal factor of coronary disease risk. A multi-ethnic meta-analysis GWAS of 91,323 individuals showed no causal relationship between CAD, stroke VTE and circulating fibrinogen levels (Sabater-Lleal et al., 2013). In agreement with this study a Mendelian randomization study using the CHARGE consortium concluded that the effect of fibrinogen on CVD is likely to be small (Ward-Caviness et al., 2019)

Interestingly, a transgenic mouse was made with elevated fibrinogen levels, however these mice had no increase in mortality or morbidity compared to littermates (1 year old) (Gulledge et al., 2001). Additionally, the fibrinogen level in the transgenic and WT littermates increased from 2 months to 12 months which agrees with observations in humans (Aizhong et al., 1998). The histologic investigations of the lung, liver, kidney, and spleen in the mice with elevated fibrinogen were no different from WT littermates. These transgenic mice were further studied to see if elevated fibrinogen had an effect initiation and early progression of atherosclerotic lesions due to atherogenic diet (Gulledge et al., 2003). Aortic sections from transgenic mice and WT mice on either atherogenic diet or chow were compared, and no difference was observed after 8-12 months on number or size of lesions for fibrinogen level or genotype. However, the atherogenic diet can initiate inflammation in the gut and therefore increase the level of fibrinogen. The WT mice on an atherogenic diet did have increased levels of fibrinogen over 8 months compared to the level of the transgenic mice on the same diet. Again, this study demonstrates the difficulty of separating fibrinogen driven inflammatory response and higher circulating levels of fibrinogen. To further investigate the relationship of hyperfibrinogenaemia and thrombosis, mice were injected with human fibrinogen to increase the circulating level. These mice were then subjected to either arterial or venous thrombosis models where an occlusive thrombi was formed sooner (Machlus et al., 2011). The authors found an increased fibrin content in the clots, increased clot strength and fibrinolysis resistance. These results indicate that elevated fibrinogen levels effect thrombosis and increased levels influence clot behaviour.

Elevated levels of D-dimer are used as a biomarker for DVT and following surgery. Increased levels have also been observed in large vessel occlusion in acute ischemic stroke, stroke recurrence, and poor functional outcome (Adam et al., 2009; Wang et al., 2016; Zhang et al., 2019; Lin et al., 2020; Ramos-Pachón et al., 2021). Whether the increased D-dimer levels are due to normal fibrinolysis of elevated fibrinogen levels or elevated fibrinolysis in cardiovascular disease, and whether such characteristics change with disease progression,

is unclear. In addition to fibrinogen levels, clot composition and structural aspects of fibrin can influence how easily clots can be lysed.

1.5.1 Arterial Thrombosis

Investigations into arterial thrombi have shown that thrombus composition is variable, and that the composition of thrombi is heterogeneous. Thrombi undergo structural alterations as they age, which may influence the effectiveness of treatment and long-term mortality. A study into composition changes of thrombi from patients with ST-elevation myocardial infarction (STEMI) showed that more platelets were observed earlier on in thrombus development but over time fibrin fibre contribution increased (<3 hours vs 6-12 hours) (Silvain et al., 2011). A study of uncomplicated STEMI (98 patients) and STEMI with sudden cardiac death patients (23 patients), showed no difference in clot composition (Silvain et al., 2017). Comparable to the previous study, there was an alteration in fibrin and platelet thrombus composition with increased fibrin network and reduced platelet content in thrombi with ischemic times of <3 hours compared to >6 hours. A study into long term mortality of patients with STEMI who received thrombus aspiration during primary percutaneous coronary intervention showed that presence of an older thrombus was a predictor of long-term mortality (Kramer et al., 2008). Another study analysed patients with acute STEMI who received percutaneous intracoronary thrombectomy during primary angioplasty, where the thrombi were collected and studied (Rittersma et al., 2005). The thrombi were classified as fresh (<1 day), lytic thrombus (1-5 days) and organised thrombus (>5 days). The authors concluded that in 50 % of patients with acute STEMI, thrombi were days to weeks old indicating that there is a variable period of thrombus formation before onset of symptoms in patients. These data agrees with observations in young adults who died suddenly, and when their heart and coronary arteries were studied there was evidence for plaque instability days to weeks before the acute incident (Henriques de Gouveia et al., 2002). Additionally, a study of stasis-induced venous thrombosis in rabbits using supersonic shear-wave imaging to measure the hardening of blood clots *in vivo* followed by *ex-vivo* mechanical characterisation (Mfoumou et al., 2014) showed that thrombus hardening occurred with age indicating that changes in fibrin network may impact the effectiveness of treatment.

The composition of thrombi can be studied to improve patient outcome. Thrombi collected and studied to determine their composition in the TIDE study from patients with STEMI (uncomplicated and sudden cardiac death) showed no difference in thrombus composition but fibrin fibres had the highest content, followed by platelets, RBC and leukocytes (Silvain et al., 2017). Another earlier study into thrombus formation showed that the main

component of the thrombus was fibrin fibres (60 %), then platelets and RBCs (Silvain et al., 2011). Thrombus composition appears similar between the TIDE study and a study of 40 patients with STEMI (Sadowski et al., 2014). A study examining thrombus composition in arterial and venous thrombosis as well as pulmonary emboli (PE) (Chernysh, et al., 2020a) showed that fibrin was a dominant feature across all locations of thrombi (51 % arterial vs 36 % venous vs 31 % PE), with the next highest component being platelets in arterial thrombi and RBCs/polyhedrocytes in venous thrombosis and PE. In addition to thrombus compositions, the authors described various fibrin structures (single fibres, bundles, and sponge) and RBC morphology (biconcave, echinocytes, compressed – polyhedrocytes, intermediate and balloon-like) highlighting the complex nature of thrombi. Interestingly, there was a higher percentage of fibrin bundles in arterial (23 %) compared to venous thrombi (17 %) and PE (10 %), while no difference was observed in sponge structures, and single fibres were the greatest in PE.

Acute treatment for ischaemic stroke may involve intravenous t-PA, but t-PA has a narrow therapeutic window and the treatment carries a risk of intracranial haemorrhage (Albers and Olivot, 2007). Recanalisation of vessels is further achieved by thrombectomy which can be used on a larger number of patients and has a longer treatment window (>6 hours vs thrombolysis >4.5 hours). Additionally, the mechanical removal of the thrombi allows for the study of clot composition. (Jolugbo and Ariëns, 2021). Furthermore, clot composition can influence mechanical characteristics and therefore how easily it is removed (Chueh et al., 2011). Structural analysis of 188 thrombi collected following endovascular treatment showed that thrombi have two main areas, RBC-rich and platelet-rich (Staessens et al., 2021). The RBC-rich areas showed thin fibrin fibres, whereas the platelet-rich areas demonstrated a dense fibrin network, which was aligned with vWF, with leukocytes and DNA surrounding the platelet-rich areas. One study suggested that fibrin-rich clots with reduced RBC content were more resistant to removal by thrombectomy and more retrieval attempts were required (Gunning et al., 2018).

In another study of patients following endovascular thrombectomy, retrieved thrombi from acute ischemic stroke were studied by *ex-vivo* thrombolysis assay, immunohistology analysis and subset by scanning electron microscopy (Di Meglio et al., 2019). This study showed a dense surface shell with a heterogenous core which was more resistant to t-PA mediated thrombolysis, and there was also an accumulation of platelets in the thrombus shell. An earlier study comparing thrombus features in stroke subtypes (6 undetermined, 22 diagnosed with cardioembolism and 8 with atherothrombosis) following mechanical thrombectomy (Ahn et al., 2016) showed that in arteriogenic thrombi RBCs were the most

abundant component followed by fibrin, platelets, and white blood cells (WBC), whereas in cardiogenic thrombi, fibrin was the most abundant then RBC, platelets, and WBC. Furthermore, the authors observed that in the arteriogenic thrombi, RBCs were located to the centre of the clot, and there was a thin outer covering composed of platelets and fibrin. In addition to the fibrin shell/film observed in patients with acute ischaemic strokes, a study of 47 STEMI patients found fibrin film in 7/47 thrombi analysed by scanning electron microscopy (Silvain et al., 2011; Zabczyk et al., 2019) demonstrating the conditions for formation of the film is possible across various conditions.

As fibrin is a key contributor to the thrombus there have been many studies into fibrin clot structure in plasma to determine how structure effects function in CVD. A study examining the fibrin clot properties by permeation, turbidimetric studies for structure and fibrinolysis from 45 acute ischemic stroke patients with 45 age and sex matched healthy controls (Undas, et al., 2010a) showed that clots from patients had reduced network porosity, were less susceptible to fibrinolysis and showed thicker fibres with a more compact clot. A recent study comparing clot properties of 23 patients with acute phase MI and 24 healthy individuals (Siniarski et al., 2021). Found that patient's clots were denser, less permeable and lysed more slowly compared to the healthy controls. Additionally, analysis by protofibril packing and microscopy confirmed the turbidimetric data. A study composed of 33 patients with coronary arterial diseases (CAD) and 33 healthy individuals to observe if the physical properties of fibrin are an independent correlator with premature CAD showed that patients with premature CAD produced stiffer clots, with a fibrin network of shorter and thinner fibres that were more resistant to fibrinolysis (Collet et al., 2006). A study of patients with acute coronary syndromes and patients with stable angina (40 in each group) were compared for clot structural and functional properties (Undas et al., 2008); reduced clot permeability, quicker polymerisation and prolonged fibrinolysis were observed in the acute coronary compared with the stable group.

Fibrinogen can acquire a number of post-translational modifications (oxidation, glycation, phosphorylation etc) and these influence its structure and function (De Vries et al., 2019). Patients with type 2 diabetes mellitus have increased risk of CAD, and circulating fibrinogen becomes glycated which can interfere with polymerisation (Undas and Ariëns, 2011). Studies into fibrin clot structure of patients with type 2 diabetes mellitus showed a denser clot structure with reduced pores which are more resistant to fibrinolysis (Dunn et al., 2005; Dunn et al., 2006; Bochenek et al., 2013), and also showed that these changes were associated with the level of protein glycation.

A consistent observation in many of the studies into fibrin clot properties using plasma, is that clots from patients with CVD are more resistant to fibrinolysis. The prospective PLATO biomarker study of 4,354 participants with acute coronary syndrome observed that a 50 % increase in clot lysis time was associated with a 36 % increase in risk of having a cardiovascular related death within 12 months (Sumaya et al., 2018). Additionally, a prospective observational study of 496 participants with STEMI, showed that endogenous fibrinolysis was impaired in high cardiovascular risk patients, despite dual treatment of antiplatelet therapy and primary percutaneous coronary intervention (Farag et al., 2019).

Furthermore, patients with acute ischemic stroke or transient ischemic attack showed reduced clot contraction (Tutwiler et al., 2016). When the platelets were further investigated there was a reduced count and platelets were found to be pre-activated, therefore showing reduced capacity to normally respond to thrombin ('tired' platelets). In addition, higher fibrinogen levels and reduced platelet count can impede clot contraction (Tutwiler et al., 2016). Another study of thrombi collected from patients with cerebral thrombi observed that the majority of RBCs were polyhedral therefore indicating the presence of clot contraction (Khismatullin et al., 2020). These authors observed that thrombi content correlated with stroke severity, and that fibrin bundles as well as platelet aggregates and high polyhedral RBC content were more typical in severe cases. The porosity, composition, age and compactness of the ischaemic stroke thrombi may impact effectiveness of current treatment options, which is an important area for future studies.

1.5.2 Venous Thrombosis

Venous thromboembolism covers DVT and PE; DVT typically occurs in the legs and is the main manifestation of venous thrombosis. The risk of death following a VTE in patients is increased up to 8 years after the original episode (Wolberg et al., 2015). Furthermore, the long-term complication of DVT is known as post-thrombotic syndrome (PTS), were patients have reduced quality of life caused by pain, cramps and ulceration of the affected limb (Bouman et al., 2016).

Investigations into thrombus of the venous system are more limited compared to arterial thrombosis however, the clots collected have been described as RBC rich and have been referred to as red clots and composed of mainly fibrin and RBC (Alkarithi et al., 2021). A PE collected following an autopsy was studied by scanning electron microscopy and the clot structure was found to be composed of layers of fibrin and platelets alternating with layers of RBC (Undas, et al 2010b). A study of a 7cm thrombus collected following embolectomy imaged by scanning electron microscopy showed that it was composed mainly of RBC, with limited platelet aggregates and white cells (Mazur et al., 2013). In addition, the fibrin

network observed was randomly arranged. The thrombi removed from the lobar and segmental pulmonary arteries showed an incremental increase in fibrin density and platelet aggregates. A study of two emboli from different patients were studied for mechanical and structural properties, which showed that the emboli were heterogeneous with one of the emboli having higher fibrin to RBC ratio and the other having a similar amount of fibrin as RBCs (Chernysh et al., 2020b). Furthermore, compression of the emboli caused fibre bundles and density to increase, whereas porosity decreased with the fibres being aligned. There were changes to the RBC structure with RBCs changing from biconcave to polyhedrocyte. A study comparing thrombi collected from STEMI (45 patients), venous thrombi (25 patients) and PE (10 autopsy) showed higher amounts of polyhedrocytes in the venous and PE thrombi compared to STEMI (Chernysh et al., 2020a). The RBC component was the highest in the venous thrombi (63 %) compared to 48 % in the PE and 17 % in the arterial thrombi whereas the fibrin observed was quite similar for the thrombi (arterial 43 %, venous 35 % and PE 41 %).

Studies into the maturation of thrombi of the venous system are few and far between. A murine study found that venous thrombi formed in the inferior vena cava undergo clot contraction between 2 and 4 weeks (Lee et al., 2015). Also, between 2- and 4-weeks thrombi undergo remodelling with fibrin content being replaced with collagen, infiltration of macrophages and neutrophils and increasing stiffness. Another murine study examined the effects of thrombolysis on aged thrombi formed by ferric chloride injury to the femoral vein and showed that fibrinolysis was limited in aged venous thrombi (Stein-Merlob et al., 2015). In the aged thrombi there was reduced access of the fibrinolytic enzymes to fibrin, resulting in the reduction of success of external fibrinolysis.

A study of 140 autopsy samples where the cause of death was from PE included a dissection of the deep veins to uncover the point of venous embolism as well as the age of thrombi (Fineschi et al., 2009). The majority of the PE originated from within the deep crural veins (74.8 %) then femoral veins (20.7 %) and then iliac veins (4.5 %). The majority of DVT were between 2-8 weeks old (50 %); there were 34. 3 % cases between 1-7 days and 15.7 % were over >2 months old. Another study of thrombi collected following catheter-based thrombectomy (7 DVT and 10 PE cases) were evaluated for their age by histological features (Silver et al., 2021). The thrombi were classified as stage 1 (0-1 day with fibrin, platelets, and RBCs), stage 2 (1-3 days old, acute thrombi no cellular organisation but inflammatory cells), stage 3 (4-7 days old thrombi exhibiting cellular growth with smooth muscle and endothelial cells) and stage 4 (> 7days, thrombi exhibited healing). Most of the PE were in stage 2 and the majority of DVT were in stage 3 and 4. Interestingly, the majority of DVT were classified

>stage 3 (6/7 cases) but the onset of symptoms in these patients was between 1-14 days (3/7 case older than 4 days). In contrast, the onset of symptoms in the PE cases was 1-21 days (4/10 over 7 days) with many thrombi classified as stage 2. This highlights that there is a period of asymptomatic DVT development before symptoms are observed by the patients. Studies of clots made with plasma from patients with VTE have generally observed reduced porosity and extended fibrinolysis and furthermore, DVT and PE appear differ in permeability. A large study of patients with VTE (100), their first-degree relatives (100) and 100 asymptomatic subjects found that VTE patients showed lower clot permeability, reduced compaction, prolonged fibrinolysis and higher clot absorbency compared to asymptomatic subjects (Undas et al., 2009). Furthermore, PE patients' clots were more permeable, less compact, and lysed easier compared to VTE. Relatives showed similar features to the VTE group. A study of 35 patients with DVT and 40 with PE showed that PE patients had faster lysis times but no difference in maximum optical density (OD) (Martinez et al., 2014). The differences observed in fibrinolysis were not due to levels of plasminogen or FXIIIa cross-linking. Scanning electron microscopy showed PE patients had lower fibre density compared to DVT patients. Viscoelastic investigations found that PE patients established viscoelastic properties sooner than DVT patients but had similar final G' and G". A case-control study of patients with DVT (24 patients with PTS and 28 patients without PTS) and healthy controls (22 participants) found that patients with recurrent VTE compared to without recurrence had lower maximum turbidity and lower permeability (Bouman et al., 2016). No difference was observed with fibrinolysis or by laser-scanning confocal microscopy. A study of 320 participants aimed to undercover if abnormal clot properties can predict recurrent DVT. Enrolled in this study were 77 patients that had recurrent DVT and 231 that did not (Cieslik et al., 2018). Clot properties were evaluated after 3 months of anticoagulant treatment. Recurrent DVT plasma samples clotted faster, with denser networks, prolonged fibrinolysis, and higher maximum OD. Prolonged clot lysis time and reduced Ks predicted recurrent DVT. In a study of mechanical properties of recurrent (11 patients) and non-recurrent VTE (33 patients), the recurrent VTE group had nearly two fold less elastic and viscous moduli (Baker et al., 2019). No difference was observed between the two groups for clot structure or fibrinolysis.

Clot contraction is critical for haemostasis, wound healing and to re-establish blood flow following vascular obstruction by a thrombi. Several studies highlighted that clot contraction is impaired in venous thrombosis. A study of 3 PE clots collected following autopsy observed in two samples (collected 7 and 15 hours after death) showed compressed RBC (polyhedral in shape) indicating that clots had undergone contraction, and further evidence of clot

contraction was observed by accumulation of fibrin at the periphery (Litvinov et al., 2018). This observation of clot contraction in thrombi agrees with later studies (Peshkova et al., 2018; Chernysh et al., 2020a). A further study into clot contraction and VTE observed a reduced rate of contraction in VTE patients compared to healthy controls, and the contraction was further impaired in patients with PE, potentially explaining that less compacted thrombi are susceptible to embolise (Peshkova et al., 2018). A study in VTE patients and healthy controls showed that platelets were morphologically more activated in VTE patients and showed less activation markers in response to activation. A study comparing clot contraction of patients following brain surgery who developed a post-operative DVT (23) compared with those who did not (55) found that clot contraction in those that developed DVT was reduced 1 day after surgery (Evtugina et al., 2020). Suppression of clot contraction was still observed 5-7 days post-surgery; however, no difference was observed in the two patients' groups pre-surgery. These data suggest that clot contraction might be used to predict DVT outcome.

1.6 Fibrinogen and COVID-19

At the end of 2019 a prolonged global pandemic called COVID-19 started, which was caused by the SARS-CoV-2 virus. The respiratory illness has a mortality in hospitalised patients between 11.5-13 %, and although most patients may be asymptomatic or have mild symptoms (80 %), around 10 % of patients develop acute respiratory distress syndrome (ARDS) (Tang et al., 2020; Klok et al., 2020; Wool and Miller, 2021). Similarly to related coronavirus outbreaks caused by severe acute respiratory syndrome coronavirus-1 (SARS-CoV-1) and Middle East Respiratory Syndrome Coronavirus (MERS-CoV), significant thrombotic events have been observed in patients with COVID-19 and on autopsy (Giannis et al., 2020). The incidence of venous thrombotic events was increased in patients with COVID-19 who were treated in intensive care unit (ICU) compared to those (26 %) treated on wards (5.8 %) (Middeldorp et al., 2020). Furthermore, this study found that with longer duration within the ICU, the incidence of venous thrombotic increased (7 days 26 % increasing to 59 % at 21 days). In agreement with this, a previous single cohort study of 81 patients with COVID-19 in ICU observed a 25 % incidence of VTE (Cui et al., 2020). A study comparing patients with COVID-19 ARDS and non-COVID-19 ARDS found a higher number of thrombotic complications (11.7 % compared to 4.8 %) and PE (11.7 % compared to 2.1 %) in the COVID-19 patients (Helms et al., 2020).

There are ICU specific risk factors that increase the risk of VTE, such as mechanical ventilation, catheterisation, and sedation. A study into the VTE risk from mechanical ventilation in patients in ICU by thoracic computed tomography scans (Minet et al., 2012).

The scans showed that in 18.7 % of patients PE was observed, of those patients there was no clinical suspicion of PE in 61 %, and DVT in 19.8 %. The study did not observe any difference in the length of stay.

Together these studies highlight that while the risk of VTE is increased by ICU treatment, there is a further increased risk of VTE associated with COVID-19. It is thought that the interplay between inflammation, complement activation and coagulation cascade is responsible for the disseminated intravascular coagulation observed in patients with COVID-19 (Page and Ariëns, 2021). There is evidence that the PE observed within the lungs do not always originate from an associated DVT. A study observed two-thirds of patients who had a PE had no associated DVT (Minet et al., 2012). A study of lung tissue examined by histology of patients with fatal COVID-19 showed presence of fibrinous thrombi in small pulmonary arterioles in 8 of 10 cases, which was occurred in both damaged and preserved lung parenchyma (Dolhnikoff et al., 2020). A multi-institutional cohort study of 68 lung autopsies observed large vessel thrombi in 42 % of cases, while platelet and/or fibrin microthrombi were present at least focally in 84 % of these cases (Borczuk et al., 2020).

An early observation in hospitalised COVID-19 patients was the presence of very high D-dimer levels associating with poor outcome. A study which compared D-dimer levels in surviving patients and non-surviving patients of COVID-19 over three time points observed that all non-surviving patients had higher D-dimer levels at all time points (Lodigiani et al., 2020). Furthermore, the D-dimer levels in both patient cohorts increased greatly after 7 days in ICU compared to those patients on general wards. In agreement with the previous study, D-dimer levels were found to increase with severity of COVID-19 (Litvinov et al., 2021). A systematic review of 6 studies totalling 1,355 hospitalised patients found that elevated D-dimer was associated with the risk of mortality in COVID-19 patients (Sakka et al., 2020). Interestingly, a prospective multicentre study which compared patients with COVID-19 ARDS (77 patients) and non-COVID-19 ARDS (145 patients) observed significantly lower D-dimer levels in the COVID-19 ARDS group (Helms et al., 2020). Compared to other studies however, they did not compare D-dimer levels and patient survival.

Research into clot structure and COVID-19 is in its infancy. A study into fibrin clot structure of plasma samples from patients with ARDS from influenza, COVID-19 (moderate and severe) and healthy donors observed altered clot structure in severe COVID-19 patients (Wygrecka et al., 2022). Turbidimetric studies observed an increase in the duration of the lag phase for patients with COVID-19, however there was a further extension observed in the influenza patients. The maximum turbidity was highest for COVID-19 patients which could potentially be due to increased fibrinogen levels in these patients (8 g/L) compared to

the influenza patients (4 g/L). The range of fibrinogen levels were between 4.0-9.0 g/L for the COVID-19 patients and 3.2-9.0 g/L influenza patients. Hospitalised patients (63) with influenza H1N1, had fibrinogen level measured on admission (4.9±0.9 g/L) and discharge (3.8±0.8 g/L) (Milosevic et al., 2013). Another study of patients (22) with H5N1 found that fibrinogen levels ranged between 1.3-5.2 g/L (Soepandi et al., 2010). Potentially, ARDS caused by influenza does not result in the same elevation of fibrinogen concentration as COVID-19.

Microscopy of clots from COVID-19 patients showed increased fibre density compared to healthy donors and influenza patients, potentially due to the higher fibrinogen levels (Wygrecka et al., 2022). LSCM showed unusual clot architecture for all groups. Fibrinolysis was extended the most in patients with COVID-19, additionally t-PA, PAI-1 and TAFI concentrations were elevated in these patients (Wygrecka et al., 2022). A study comparing critically ill patients with COVID-19 and sepsis (COVID-19 unrelated), showed altered clot structure by microscopy in the COVID-19 patients, with denser structures and shorter fibres (Brubaker et al., 2022). Furthermore, patients with COVID-19 had reduced porosity which agreed with the microscopy analysis and previous observations of fibrinolysis resistance. A further study in 255 patients with moderate or severe COVID-19 by thrombodynamics and clot contraction (Litvinov et al., 2021) showed hypercoagulability in three quarters of patients with COVID-19, increased mechanical strength and impaired clot contraction kinetics due to combination of moderate thrombocytopenia and platelet dysfunction, which was more evident in the severe cases. Highlighting the important relation between platelets and fibrin in clot contractions and an imbalance between either can impair clot contraction.

1.7 Investigations in to the αC-region

1.7.1 Patient Studies

Patient cases with mutations in the fibrinogen αC-region provide key insights into the structure and function relationships of this region. Congenital mutations within the chains of fibrinogen can result in changes in fibrinogen expression, function, or both. Affected individuals are referred to as afibrinogenemic when lacking detectable circulating fibrinogen, hypofibrinogenemic when there is lower than normal circulating levels of fibrinogen, dysfibrinogenaemic when the fibrinogen is functionally abnormal but with normal levels, or finally hypodysfibrinogenemia when the fibrinogen is abnormal and at low circulating levels (Fish and Neerman-Arbez, 2012). Mutations found in patients are listed in Table 1 for αC-connector and Table 2 for the αC-domain.

Table 1 Reported Patient Cases of Alterations within the αC-connector

Change: fs is for frameshift, del is for deletion. Status: reported expression of gene in patient, A is afibrinogenemia, H is hypofibrinogenemia, and D is dysfibrinogenaemia. Gene expression: hom is for homozygotes and het is for heterozygous gene expression. Clinical symptoms are stated as either bleeding (B), thrombosis (T), recurrent miscarriage (RM) or asymptomatic (AS). For fibrinogen concentration by Clauss or antigen N.D is not determined and N.S is not stated. % Loss of WT α-chain does not include any non-WT residues. Normal range for fibrinogen 1.5-4 g/L

Change	Case	Status	Gene Expression	Clinical Symptom	Clauss mg/mL	Antigen mg/mL	% Loss of WT α-chain	Residues Inserted	Reference
Aα(221)Gln>stop	Egyptian	A	Hom	B	N.D	N.D	64	0	Abdel Wahab et al., 2010
Aα(229)Trp>stop	Iran	A	Hom	B	<0.05	< 0.02	62	0	Monaldini et al., 2007
Aα(243_244)Glu>Asp fs-stop	Morocco	A	Hom	B	N.D	N.D	60	158	Robert-Ebadi H et al. 2009
Aα(252)Arg>Stop	Zaghouan	A	Hom	B	N.D	N.D	59	0	Amri et al., 2016
Aα(260)Thr>Pro fs-stop	France	A	Het	B	N.S	N.S	57	141	Angles-Cano E et al. 2007
Aα(268)>Gln-Glu-Pro-stop	Otago	H	Hom	B & RM	0.06	N.D	56	3	Ridgway et al., 1997
Aα(270)Pro>Thr	South Italy	D	Het	AS	0.6	2.5	0	0	Santacroce et al., 2006
Aα(272)ins39aa	Champagne-au-Mont-d-Or	D	Het	T	2.7	2.1	0	39	Hanss et al., 2003

Change	Case	Status	Gene Expression	Clinical Symptom	Clauss mg/mL	Antigen mg/mL	% Loss of WT α-chain	Residues Inserted	Reference
Aα(277)Asp> fs-stop	India BL-564	H	Hom	B	0	0	54	59	Sumitha et al., 2013
Aα(276)Trp>stop	Latina P3	H	Hom	B	0.2	0.5	55	0	Asselta, et al., 2015a
Aα(315)Trp>Stop	Turkey	A	Hom	B & T	0	N.D	0	0	Simsek et al., 2008
Aα(323)Gly>Glu fs-stop	Mahdia (Siblings)	H	Het	B	0.2	1.70	52	79	Amri et al., 2017
Aα(327)Asn>Thr fs-stop	Germany	A	Hom	B	N.D	N.D	46	75	Neerman-Arbez and de Moerloose, 2007
Aα(328)Gln>Stop	Keokuk	H	Het	B, T & RM	0.3	0.5	46	0	Lefebvre et al., 2004
Aα(328)Gln>Pro	Seoul II	D	Het	T	<0.5	2.3	0	0	Park et al., 2006
Aα(333)Pro-del fs-stop	United States	A	Het	Unknown	N.D	N.D	45	69	Neerman-Arbez et al., 2000
Aα(373)Trp>stop	Italy	H	Hom	B	Unclotable	1.1	39	0	Castaman et al., 2015
Aα(381)Ser>Phe	Austin	D	Het	B	0.3	N.D	0	0	Brennan et al., 2015

Table 2 Reported Patient Cases of Alterations within the αC-domain

Change: fs is for frameshift, del is for deletion. Status: reported expression of gene in patient, A is afibrinogenemia, H is hypofibrinogenemia, and D is dysfibrinogenaemia. Gene expression: hom is for homozygotes and het is for heterozygous gene expression. Clinical symptoms are stated as either bleeding (B), thrombosis (T), recurrent miscarriage (RM) or asymptomatic (AS). For fibrinogen concentration by Clauss or antigen N.D is not determined and N.S is not stated. % Loss of WT α-chain does not include any non-WT residues. Normal range for fibrinogen 1.5-4 g/L

Change	Case	Status	Gene Expression	Clinical Symptom	Clauss (mg/mL)	Antigen (mg/mL)	% Loss of WT α-chain	Residues Inserted	Reference
Aα(434)Ser>Asn	Caracas II	D	Het	AS	N.D	N.D	0	1	Maekawa et al., 1991
Aα(439)Arg>Cys	Bordeaux	D	Het	T	2.1	2	0	1	Hanss et al., 2008
Aα(446)Thr>fs -stop	India BL-376	A	Hom	AS	0	0	27	17	Sumitha et al., 2013
Aα(452)Gly>Trp-Ser-stop	Milano III	HD	Hom	T	0.2	2.6	26	2	Furlan et al., 1994
		HD	Het	B	1.1	1.9			Asselta et al., 2015a
Aα(453)Pro>Cys-stop	Nieuwegein	D	Hom	AS	1.7	N.D	26	1	Collen et al., 2001
		D	Het	B&T	1.4	3.1			Tajdar et al., 2018
Aα(461)Lys>stop	Marburg	HD	Hom	B&T	<0.3	0.6	25	0	Koopman et al 1992

Change	Case	Status	Gene Expression	Clinical Symptom	Clauss (mg/mL)	Antigen (mg/mL)	% Loss of WT α-chain	Residues Inserted	Reference
Aα(465)Thr>del-fs stop	Wilmington	D	Het	B	1.2	2	24	12	Brennan et al., 2006
Aα(467)Glu>stop	Caracas I	D	Het	B	2.4 & 2.8	N.D	0	0	Marchi et al., 2004
Aα(467)Glu>stop	Guarenas	D	Het	B	2.8	N.D	0	0	Marchi et al., 2006
Aα(472)Cys>Ser	Sumida	D	Het	AS	ND	1.33	0	1	Ikeda et al., 2015
Aα(475)Ala>Met-fs-stop	Lincoln	D	Het	B	1.9	N.D	23	4	Ridgway et al., 1996
Aα(494)His>del-fs-stop	Perth	D	Het	B	1.8	N.D	20	23	Homer et al., 2003
		D		T	N.D	2.3 & 1.9			Westbury et al., 2013
Aα(494)His>Pro-fs-stop	Mannheim V	D	Het	RM	1.8	3	20	24	Dempfle et al., 2009
Aα(500)Phe>Ser-fs-stop	San Giovanni Rotondo	D	Het	AS	0.7	2.3	18	18	Margaglione et al., 2001

Change	Case	Status	Gene Expression	Clinical Symptom	Clauss (mg/mL)	Antigen (mg/mL)	% Loss of WT α-chain	Residues Inserted	Reference
Aα(532)Ser>Cys	Caracas V	D	Het	T	N.D	N.D	0	1	Marchi et al., 2000
Aα(554)Arg>Cys	Dusart	D	Het	T	N.S	N.S	0	1	Koopman et al., 1993
	Chapel Hill III			T	2.8	N.D			Carrell et al., 1983
	Nashville (11 family members)			T & A	1.8-3.8	1.9-4.2			Tarumi et al., 2000
	Scandinavia (5 family members)			T	1.8-2.4	2.7-3.5			Ramanathan et al., 2013
	Dallas			T	1.1	2.8			Shen et al., 2014
	South Italy			T	0.9	1.8			Santacroce et al., 2006
Aα(559)>fs	Grand Lyon	HD	Het	B	N.D	1.1	8	72	Hanss et al., 2005

Change	Case	Status	Gene Expression	Clinical Symptom	Clauss (mg/mL)	Antigen (mg/mL)	% Loss of WT α-chain	Residues Inserted	Reference
Aα(587)Thr>His-fs	South Syria (13 family members)	A	Hom	B, T & RM	0-1.2	0-1.7	4	32	Levrat et al., 2011
		HD	Het	AS	1.2-2-1	1.2-2			

A common observation for both mutations within the αC-connector and αC-region is the reduction in fibrinogen levels measured via the Clauss method which is commonly referred to as functional fibrinogen compared to the quantification measurement by antibodies through enzyme-linked immunosorbent assay (ELISA). As the Clauss method relies on fibrinogen concentration as well as clot function such as mechanical ability to measure fibrinogen levels in plasma, these data are difficult to interpret as they could be influenced by either impaired fibrinogen level or clot mechanics. The reduced fibrinogen levels observed in many of the dysfibrinogenaemia's measured by Clauss within the αC-connector and αC-region highlight that although the fibrinogen can be present in normal levels by antigen, the circulating fibrinogen has dysfunctional qualities including mechanical weakness (Madhia, Seoul II, Milano and Nieuwegein) (Furlan et al., 1994; Park et al., 2006; Amri et al., 2017; Tajdar et al., 2018).

Several recombinant fibrinogens have been produced with the same mutations observed in patients with Fibrinogen Sumida (Aα472), Seoul II (Aα328) and Egyptian (Aα221); Sumida and Seoul II were produced in CHO cells and Egyptian in COS-7 cells (Park et al., 2006; Abdel Wahab et al., 2010; Ikeda et al., 2015). The recombinant fibrinogen was functionally like the homozygous mutation found in the patient. No characterisation studies were performed with Fibrinogen Egyptian (Abdel Wahab et al., 2010). Fibrinogen Sumida (Aα472Cys>Ser) produced clots with thinner fibres with increased fibre density, impaired lateral aggregation of protofibrils but no difference was observed in fibrinolysis (Ikeda et al., 2015). The study did not investigate either plasma or purified fibrinogen from the patient with Fibrinogen Sumida to observe if the recombinant fibrinogen differed in phenotype. The patient with fibrinogen Seoul II (Aα328Gln>Pro) had an MI at 43 and again after 8 years. The mutation was observed in the patient's mother and son who were also heterozygous and their plasma was purified and studied (Park et al., 2006). The recombinant and plasma purified fibrinogen Seoul II showed reduced maximum OD and fibre diameter. No difference was observed in the lag phase for the recombinant fibrinogen but was extended in the plasma purified fibrinogen. Delayed fibrinolysis was observed in plasma purified fibrinogen but was not studied in the recombinant fibrinogen (Park et al., 2006; Park et al., 2013). Although the two fibrinogens were not directly studied together there are several similarities indicating that the study of recombinant fibrinogen of patient cases is beneficial and can provide insight to the patient phenotype.

The majority of thrombotic events observed in patients with dysfibrinogenaemia are of the venous system (DVT and PE), with recurrent DVT being common (Fibrinogen Bordeaux (Aα439), Milano (Aα452) and Caracus V (Aα434) (Furlan et al., 1994; Marchi et al., 2000;

Hanss et al., 2008). Additionally, these events can occur at a young age, which was particularly evident in the families with Aα(554)Arg>Cys mutation that has been studied over a number of years (Wada and Lord, 1994; Tarumi et al., 2000; Ramanathan et al., 2013; Shen et al., 2014). Plasma studies of patients with these mutations have shown a clot structure composed of thinner fibres, reduced OD, and defective fibrinolysis (Soria et al., 1983; Koopman et al., 1993; Ramanathan et al., 2013). Furthermore plasma clots made with Bordeaux fibrinogen showed extended fibrinolysis as well as reduced maximum OD (Fernández-Cadenas et al., 2016). Fibrinogen Bordeaux has a Aα439Arg>Cys mutation and alike Aα(554)Arg>Cys there is an unpaired cysteine within the fibrinogen protein both mutations show fibrinogen:albumin binding.

Investigations into a family with Fibrinogen Perth who had thrombotic events, showed whole blood clots with increased visco-elastic strength and delayed fibrinolysis (Westbury et al., 2013). Purified studies showed that the clots were composed of thinner fibres with a denser architecture. Interestingly, the same mutation was observed in another patient who had bleeding events but no reported thrombosis and alike the above study, reduced maximum OD was observed but fibrinolysis by external fibrinolysis was similar (Homer et al., 2003).

Cases of thrombosis in patients with αC-connector mutations are less frequent, a patient with Fibrinogen Champagne au Mont d'Or (elongation of the αC-connector), developed a DVT and PE at the age of 31 and suffered from recurrent thrombosis, and family members with the same mutation also experienced DVT (Hanss et al., 2003). A patient with Fibrinogen Keokuk had thrombotic events following surgery at the age of 43. Treatment with cryoprecipitate potentially caused thrombotic events as family members with the mutation experienced no thrombotic episodes. Moreover, at later surgeries where no cryoprecipitate was given, no thrombotic episodes or bleeding were observed (Lefebvre et al., 2004). A similar thrombotic episode was observed in a patient with Fibrinogen Marburg following treatment for haemorrhage after caesarean section (Koopman et al., 1992). However, this evidence remains largely anecdotal and further studies are needed to establish safety profiles of cryoprecipitate in patients with dysfibrinogenaemia. Interestingly, a patient with afibrinogenemia (Fibrinogen Turkey (Aα315)) had early thrombotic events of venous and arterial system (Simsek et al., 2008). Mirroring the cases observed in the αC-connector, the observation of thrombosis was at an early age.

The challenge with investigations of the patients with dysfibrinogenemia are that patients are not always homozygous for the mutation, there may be substantial variation in fibrinogen levels, the ratio of incorporation of aberrant fibrinogen within the fibre network

may vary, and there could be additional residues which are not usually present in the normal chain.

1.7.2 Murine *Fga$^{270/270}$*

A murine model has recently been established with a truncated Aα-chain terminating at residue 270, which is analogous to fibrinogen Otago (Ridgway et al., 1997; Hur et al., 2021). This murine model allows for the exploration of the αC-region *in-vivo*, *ex-vivo* as well as *in-vitro* plasma and purified studies. Fibrinogen Otago is the first truncation of the αC-region which does not result in afibrinogenemia (Table 1), which is potentially why the truncation point was chosen for this model. *FGA$^{270/270}$* shared many similarities to fibrinogen Otago such as reduced fibrinogen levels, prolonged thrombin time and alike Otago there were challenges during pregnancy with miscarriages, and additionally many mice died during pregnancy or shortly afterwards of postpartum haemorrhage (Ridgway et al., 1997; Hur et al., 2021).

Due to the challenges of comparing models with unequal fibrinogen levels (*FGA$^{WT/WT}$* vs *FGA$^{270/270}$*), and consequently dissecting if the observations were due to reduced fibrinogen levels or altered fibrinogen, authors used small interfering RNAs (siRNA) to knockdown the *FGA$^{WT/WT}$*. The knockdown mice had similar fibrinogen level to *FGA$^{270/270}$* (Hur et al., 2021). *In-vivo* bleeding models showed no difference bleeding between *FGA$^{270/270}$* compared to *FGA$^{WT/WT}$* or siRNA knockdown.

No thrombi were observed in *FGA$^{270/270}$* during ligation of the inferior vena cava. Furthermore, 2/6 mice with *FGA$^{WT/WT}$* knockdown developed a thrombus in contrast to the *FGA$^{WT/WT}$* and *FGA$^{WT/270}$* where all mice developed thrombi after 24 hours. The authors concluded that this protection against thrombosis was due to a combination of hypofibrinogenemia and loss of αC-region.

In vitro aggregation studies with platelet rich plasma showed similar activation with ADP and protease-activating receptor 4 (PAR4) between *FGA$^{WT/WT}$*, *FGA$^{WT/270}$* and *FGA$^{270/270}$*, but faster disaggregation was observed with ADP activation in *FGA$^{270/270}$*. The platelet aggregation profile was similar in the *FGA$^{WT/WT}$* knockdown. The authors concluded that the changes in platelet adhesion and aggregation were not due to membrane expression, however they studied membrane expression in unstimulated platelets only and did not use the *FGA$^{WT/WT}$* knockdown.

Interestingly, *in vitro* plasma studies showed a spread of clotting times for the thrombin time and prothrombin time for *FGA$^{270/270}$*, with some of the mice not clotting after 5 minutes. The authors produced two lines; it is not stated if the variability in clotting times was due to the slight differences between the two lines. Purified and plasma studies for turbidimetric assays

showed reduced maximum OD for FibAα^{270} compared to FibAα^{WT} and additionally no fibrinolysis was observed in FibAα^{270}. In plasmin generation studies, plasmin generation was undetectable for *FGA$^{270/270}$*, whereas the *FGA$^{WT/WT}$* knockdown had reduced plasmin peak and endogenous plasmin potential, but lag time and time to peak where like *FGA$^{WT/WT}$.* It would have been interesting if D-dimer assay was performed alongside the IVC ligation assay to observe if there was hyperfibrinolysis occurring.

These results are interesting when comparing *in vivo* and *in vitro* studies, where the *in vitro* studies show delayed clotting using standard coagulation assays and no fibrinolysis, but these findings are not replicated in *in vivo* bleeding assays.

1.7.3 Fragments and Fibrinogen Digests

In the circulation there are different molecular weight forms of fibrinogen (HMW, LMW, LMW'), which were studied to observe the influence on polymerisation (Holm et al., 1985). The authors found that thrombin clotting time was increased with a stepwise reduction in fibrinogen molecular weight, but no difference was observed in FpA cleavage. Furthermore, polymerisation studies with fibrin monomers of the various forms showed an elongated lag phase and reduced maximum OD (Holm et al., 1985).

Following the observations of the different forms of fibrinogen, proteolytic digestions of fibrinogen were made known as fragment X. Fragment X is produced by the limited proteolysis of fibrinogen by plasmin, and the resultant effect of this limited proteolysis is the removal of a large proportion of the αC-region. The amount of αC-region loss can vary (20,000-40,000 Da), however, resulting in a fibrinogen molecular weight between 240,000-285,000 Da (Nieuwenhuizen and Gravesen, 1981; Erickson and Fowler, 1983; Sato and Weisel, 1990; Sato and Swadesh, 1993). Additionally, there the Bβ-chain (Bβ58) can also be partially digested, particularly when longer periods of digestion are used (Nieuwenhuizen and Gravesen, 1981).

Studies into polymerisation with fragment X have shown that the absence of the αC-region resulted in impaired polymerisation (higher maximum OD and elongated lag phase) (Sato and Swadesh, 1993; Gorkun et al., 1994). Additionally, scanning electron microscopy showed increased fibre diameter with further loss of the αC-region (Gorkun et al., 1994). Investigations with fragment X' (260 kDa) which has less heterogeneity than observed in standard preparations of fragment X, and SDS-PAGE (Sodium Dodecyl Sulphate–Polyacrylamide Gel Electrophoresis) gel showed reduced Aα-chain bands visible between 39-25 kDa whereas the γ-chain and most of the βb-chain were intact. Clots produced with fragment X' had less fibre branching than WT fibrinogen (Weisel and Papsun, 1987).

As fragment X is a product of fibrinogen digestion, it has been used to gain further knowledge of fibrinolysis. Fragment X fibrin showed increased glu-plasminogen binding to its structure than either fibrinogen or fibrin (Weisel et al., 1994). Additionally, investigations into fibrinolysis with fragment X showed a concentration-dependent reduction in lysis time with the inclusion of higher concentrations of fragment X into the clot (Schaefer et al., 2006). Furthermore, the authors showed that increased rates of fibrinolysis were due in part to enhanced rates of plasmin generation. Investigations into mechanical behaviour of fragment X showed that clots only had 1 % rigidity compared to WT fibrinogen by time dependence rigidity and it was not due to reduced clotability of the fibrinogen protein (Shen et al., 1977). Fragments of the αC-region expressed in *E.coil* have been used to investigate their role in fibrin assembly. Through the study of fragments, it was observed that the αC-domains undergo conformational changes and self-associate into αC-polymers. This interaction occurs in the N-terminal subdomain of the αC-domains (Tsurupa et al., 2009; Tsurupa et al., 2012). The C-terminal subdomains were able to interact with the αC-connectors (Tsurupa et al., 2012). Together, these observations demonstrate that αC-polymers are oriented to allow effective interaction which is further supported by FXIIIa-mediated cross-linking.

The study of proteolytic fibrinogen digestion products and recombinant fragments of the αC-region demonstrated that the αC-domains associate with the central E-region in fibrinogen and are released upon FpB cleavage (Erickson and Fowler, 1983; Veklich et al., 1993; Litvinov et al., 2007; Protopopova et al., 2017) (Erickson and Fowler 1983)

1.7.4 Recombinant Fibrinogen

This thesis is based on studies with human recombinant fibrinogen. Several recombinant fibrinogens with mutations to the αC-region have been produced previously; which include truncations (α251), point mutations (AαQ328P, AαQ366P) and region substitutions (αC-region human for chicken) (Gorkun et al., 1998; Collet et al., 2005; Ping et al., 2011; Park et al., 2013). These proteins have been used previously to provide insight into clot structure, polymerisation, and function as well as clarity to the complex findings observed in patients with dysfibrinogenemia and heterogeneous fibrinogen preparations.

1.7.4.1 α251

A recombinant fibrinogen truncated in the α-chain at α251 was previously produced using a CHO cell expression system (Binnie et al., 1993; Lord et al., 1993). Fibrinogen α251 is similar to fragment X (generated by limited proteolysis of fibrinogen) but without any degradation of the N-terminus of the β-chain which was common in preparation of fragment X or variation in size and termination of the αC-region (Gorkun et al., 1998). In the produced

fibrinogen, the α-chain size was reduced to 28 kDa (WT is 66 kDa) and the size of the fibrinogen protein to 265 kDa (WT is 340 kDa).

Investigations into fibrinopeptide release showed no difference in FpA cleavage between WT and α251 but there was slower cleavage of FpB observed in α251. Polymerisation was studied in fibrin monomers and fibrinogen by turbidimetric analysis and was like WT but α251 had a lower maximum OD. However, there was slower lateral aggregation observed for α251 and considerably lower maximum OD with lower concentration of NaCl for fibrin monomer polymerisation compared to WT (Gorkun et al., 1998).

Later investigations into α251 focused on a combination of structural observations by microscopy and functional characteristics. These investigations showed reduced formation of γ-γ band for α251 and no disappearance of the α-chain or the appearance higher molecular weight polymers (Collet et al., 2005). Microscopy of α251 showed a higher density network with increased branching and reduced fibre diameter, and permeation confirmed the denser fibrin network. Similar to fragment X, α251 showed reduced clot stiffness and permeation, and could not be studied without the addition of FXIIIa (Shen et al., 1977; Collet et al., 2005). Investigations into fibrinolysis showed faster lysis in α251 compared to WT, alike previous investigations with fragment X (Collet et al., 2005; Schaefer et al., 2006). However, some of the observations differed from fragment X, which might be due to heterozygosity of fragment X species used, loss of N-terminal of the β-chain or fibrinogen species.

1.7.4.2 α-chain FXIII Cross-linking Sites

Three recombinant fibrinogen proteins have been previously produced with point mutations in the α-chain; AaQ328P, AaQ366P and double point mutation AaQ328,366P (Park et al., 2013). The mutation AaQ328P is observed in Fibrinogen Seoul II (Park et al., 2006). Alike the patient cases, the authors found that all point mutations influenced the polymerisation with reduced maximum OD and thinner fibres compared to WT. AaQ328,366P showed the most extensive alterations compared to WT in scanning election microscopy and turbidimetric studies. Fibrinolysis was not investigated in the recombinant study but the patient case showed a delayed start of fibrinolysis by turbidimetric analysis and the patient had a MI at the age of 43 (Park et al., 2006). Investigations into cross-linking showed that AaQ328,366P had the greatest impact on cross-linking as more α-monomers remained for each time point but α-chain cross-linking was not prevented which mirrored the patient observations. The point mutation into proline within αC-connector might influence self-association of the αC-polymers as it may alter the structure of part of the tandem repeat, as prolines can form kinks (von Heijne, 1991).

1.7.4.3 Substitution

A recombinant human fibrinogen with the αC-region of chicken was produced, which included the human α-chain sequence up residue Aα197, followed by residues which would be found in the chicken αC-region (Aα199-491) (Ping et al., 2011). The chicken αC-region lacks the tandem repeats present in the human αC-region, but does share sequence homology in the disulphide-linked β-hairpin within the globular αC-domain (Weissbach and Grieninger, 1990).

Although there was no difference in fibrinopeptide cleavage, the human:chicken hybrid showed altered polymerisation with limited increase in OD compared to WT human fibrinogen. There was no microscopy performed on clots made with recombinant fibrinogen proteins but the inclusion of a limited amount of human:chicken hybrid fibrinogen with WT human fibrinogen impacted polymerisation (Ping et al., 2011). The inclusion of WT chicken fibrinogen within the assays would have been valuable to observe if the assays were sensitive to the chicken fibrinogen polymerisation. Previously it had been reported that there was increased clotting times in plasma from chickens using thrombin from different species. Additionally, chicken thrombin was suspectable to slight variations in pH or the use of saline and these factors influence clotting times (Bigland and Triantaphyllopoulos, 1961). Indicating there may be intricate different in coagulation systems of difference species.

Dysfibrinogenemia Champagne-au-Mont-d'Or has an insertion of 39 residues after residue 268 within the tandem repeat section of the αC-connector and extends the tandem repeat motif a further 3 times (Hanss et al., 2003). In standard coagulation tests, clotting times were extended with fibrinogen Champagne-au-Mont-d'Or and the patient suffered a DVT at the age of 38. Together these findings indicate the important role the αC-connector has in normal fibrinogen polymerisation.

1.7.5 Polymorphism

There is one polymorphism within the αC-connector at residue Aα312, where a threonine is substituted for an alanine. This polymorphism is more abundant in African (43.3 %) and East Asian (43.2 %) populations (Baumann and Henschen, 1993; Sovova et al., 2021). Investigations into the structural and functional aspects of this polymorphism have found that clots made with Aα312A fibrinogen showed thicker fibres, more α-α cross-links and increased stiffness (Standeven et al., 2003).

Patient studies have indicated that the polymorphism may be associated with a number of CVD such as VTE (LITE study of 506 cases vs 1012 controls), two studies on thromboembolic pulmonary hypertension (214 cases vs 200 controls and 101 cases vs 108 controls), DVT and

PE (Carter et al., 2000; Rasmussen-Torvik et al., 2007; Suntharalingam et al., 2008; Li et al., 2013).

The polymorphism was not associated with MI and there was a decreased the risk of stroke in multicentred RATIO study on pulmonary thromboembolism (102 cases vs 108 controls) (Siegerink et al., 2009; Li et al., 2013). Another patient study showed no association with stroke or stroke subtypes but they did observe interaction between the polymorphism and atrial fibrillation in relation to poststroke mortality (Carter et al., 1999).

1.7.6 Interactions with binding partners

There are many sites in the αC-region that are involved in protein-protein interaction, which provide clot stability, resistance, or susceptibility to fibrinolysis. The αC-region contains most of the sites involved in FXIIIa cross-linking; the αC-connector contains the glutamines whereas most of the lysine donor sites are located within the αC-domain. Investigations into the reactivity of the glutamines between αC233-425 (Q237, Q328 and Q366) showed that Q237 was the most reactive, but there no was dependency for certain sites to be preferentially cross-linked first (Mouapi et al., 2016). FXIIIa α-chain cross-linking increases clot stiffness and elasticity (Standeven et al., 2007; Helms et al., 2012; Duval et al., 2014). There was no difference in external fibrinolysis between FXIIIa cross-linked clots made with recombinant WT and γQ398N/Q399N/K406R (which has normal α-chain cross-linking) fibrinogens, in agreement with a major role for α- and not γ-chain cross-linking in resistance to fibrinolysis. This was further confirmed for internal fibrinolysis with the same recombinant fibrinogen (Duval et al., 2014). The cross-linking of α_2-antiplasmin by FXIIIa to the Aα303 residue within the αC-connector critically provides fibrinolysis resistance to the fibrin clot (Sakata and Aoki, 1982; Fraser et al., 2011; Pechlivani et al., 2021). The retention of RBC into clots is FXIIIa dependent, which is also mediated by fibrin α-chain cross-linking (Aleman et al., 2014; Byrnes et al., 2015).

Recently, it has been shown that GPVI expressed on platelets, which is known as the major signalling receptor for collagen, can also bind fibrin (Mammadova-Bach et al., 2015; Alshehri et al., 2015). Further investigations have shown that the αC-region is responsible for binding to the GPVI receptor (Xu et al., 2021). GVPI can influence thrombus formation and has a role in pathogenesis of ischaemic stroke and potentially venous thrombosis (Xu et al., 2016; Perrella et al., 2021).

1.8 Fibrinogen γ’

A splice variant of the γ-chain called fibrinogen γ’ was first described in 1972, as two fibrinogen peaks were observed by ion-exchange chromatography. Further investigation by

electrophoresis found two γ-chains in the second fibrinogen peak (Mosesson et al., 1972). At the same time, similar findings of γ-chain variation were made by other groups, and the variant was referred to as γ', γB or γ57.5 (Francis et al., 1980; Fornace et al., 1984; Peerschke et al., 1986). The γ'-chain is observed in circulation at about 11 % of the total circulating fibrinogen (Macrae et al., 2016) and due to the additional residues in the γ' variant it has a higher molecular weight.

1.8.1 Splicing Mechanism

The principal γ-chain is known as γA and is composed of 10 exons and 9 introns which terminate after 411 residues (Weisel and Litvinov, 2017). The two γ-chains are identical for the first 407 residues, with the final four residues of γA (AGDV) absent in γ'. These final four residues along with the 3' noncoding sequence are encoded by exon 10, the mature mRNA for the γA-chain is completed by the removal of the 9th intron following processing and polyadenylation by a downstream signal of exon 10 (Chung and Davie, 1984; Cilia La Corte et al., 2011). The γ'-chain arises by an alternative processing and polyadenylation site within the 9th intron, which results in alternative C-terminal sequence composed of 20 residues (408-427 VRPEHPAETEYDSLYPEDDL) (Chung and Davie, 1984). There is a high number of negatively charged residues within the γ'-chain sequence, and the two tyrosine residues are sulphated adding further negative charge (Farrell et al., 1991).

The presence of γ'-chain has not been observed in megakaryocytes or platelets. Fibrinogen found in the platelet α-granules has been reported to come from the circulating plasma pool, suggesting selective uptake of γA through integrin $\alpha_{IIB}\beta_3$ engagement which is absent in γ' (Haidaris et al., 1989). Further investigations into tissue specific expression in rats observed that γ'-chain was expressed only in the liver where γA-chain was expressed in the liver, lung, brain and marrow (Haidaris and Courtney, 1990).

Several genetic elements have been associated with the regulation of fibrinogen γ' levels, which are included in haplotype FGG-H2 tagged by single nucleotide polymorphisms (SNP) 10034 C>T and FGG-H3 by SNP 9340 T> C (Uitte de Willige et al., 2005). SNP 10034 C>T is associated with reduced γA/γ' and SNP 9340 T> C increased γA/γ' plasma levels (Uitte De Willige et al., 2007; Mannila et al., 2007; Nowak-Götte et al., 2009).

1.8.2 Fibrinogen γ’ and Thrombosis

In view of the observations of increased fibrinogen levels in patients with CVD, many studies have investigated if fibrinogen γ’ levels could be used as a biomarker for CVD. However, like increased fibrinogen levels observed in CVD, it is not certain if any changes in fibrinogen or fibrinogen γ’ are due to inflammatory responses related to CVD. A summary of these studies into γ’ levels in various CVD diseases is shown in Table 3. There appear to be contrasting associations with γ’ levels and thrombosis, highlighting the intricate relationship. Arterial thrombosis is associated with elevated γ’ levels (Lovely et al., 2002; Mannila et al., 2007). Whereas studies into venous thrombosis have observed associations with reduced levels as well as no change in γ’ levels (Uitte de Willige et al., 2005; Smalberg et al., 2013; Maners et al., 2020). Differences in the studies could be due to subtle differences in VT conditions. In addition to the differences in flow between the arterial and venous systems, the formation of thrombi in arterial and venous systems differ which may explain the differing of γ’ levels associations to CVD phenotypes.

Furthermore, fibrinogen γ' has been shown to reduce thrombin-mediated activation of co-factors FVIII and FV and to increase activated protein C sensitivity in plasma (Lovely et al., 2007; Omarova et al., 2013; Omarova et al., 2014), further complicating the relationship of γ’ with thrombosis.

Table 3 Clinical Studies of Fibrinogen γ' Levels and Thrombosis

Abbreviations: Study type: GWAS - genome-wide association study, Patient Cohort: ARIC - Atherosclerosis Risk in Communities, CHS - Cardiovascular Health Study, CVD – cardiovascular diseases, CAD - coronary artery disease, DVT – deep vein thrombosis, IPH - intraplaque haemorrhage, LRNC- plaque ulceration and lipid-rich necrotic core, TIA - transient ischemic attack, PAH- peripheral artery disease, VTE - Venous thromboembolism, HF – heart failure, A – atherosclerosis, TMA - thrombotic microangiopathy, UAP - unstable angina pectoris, IS - ischemic stroke and PE - pulmonary embolism.

Authors (year)	Study Type	Patient Cohort	Study Conclusion	CVD	Associated
Lovely et al., 2002	Case-control	91 patients with CAD (average age 62) and 42 controls (average age 59)	Fibrinogen γA/γ' levels were higher in CAD patients, independent of total fibrinogen levels	CAD	Yes ↑ levels
Uitte de Willige et al., 2005	Case-control	474 patients with DVT and 474 controls (average age 45 both groups)	Genetic variation in FGG-H2 influences thrombotic risk through htSNP 10034C/T, reducing γ' levels	DVT	Yes ↓ levels
Mosesson et al., 2007	Case-control	45 patients with thrombotic microangiopathy and 87 controls (average age 50 both groups)	Total fibrinogen γ' and fibrinogen γ' /total fibrinogen ratios were reduced compared to control group	TMA	Yes ↓ levels

Authors (year)	Study Type	Patient Cohort	Study Conclusion	CVD	Associated
Mannila et al., 2007	Case-control	387 patients post infraction and 367 controls	Higher plasma fibrinogen γ' concentration in patients, no difference in fibrinogen γ' /total fibrinogen ratios compared to control	MI	Yes ↑ levels
Cheung et al., 2008	Case-control	Patients 124 (47 patients in convalescent and 114 patients in acute phase) and 125 controls (average age 56 for both)	Fibrinogen γ'/total fibrinogen ratio is associated with ischemic stroke, especially in the acute phase of the disease. In addition, FGG-H3 haplotype appears to be protective against ischemic stroke.	Stroke	Yes ↑ γ' ratio (acute phase) ↓ γ' ratio in convalescent phase
Cheung et al., 2009	Case-control	Patients with IS (53), PE (non-acute phase 13 and acute phase 16) and Unstable angina pectoris (stabilised 130 and refractory 72) and 173 controls	Elevated γ' ratio in patients with IS, PE and unstable angina pectoris compared with controls. Higher fibrinogen γ' levels observed in patients as well.	IS, PE & UAP	Yes ↑ levels and ratio

Authors (year)	Study Type	Patient Cohort	Study Conclusion	CVD	Associated
van den Herik et al., 2011	Case-control	200 patients with ischaemic stroke and 156 controls (average age 62 and 59 respectively)	γ'/total fibrinogen ratio is associated with unfavourable outcome in patients with IS. γ'/total fibrinogen ratio and increased γ' levels observed in patients	IS	Yes ↑ levels and ratio
Lovely et al., 2011	GWAS	2,879 patients with no history CAD and 421 with prior history (average age 61)	Increased γ' levels associated with prevalence of CVD.	CVD	Yes ↑ levels
Pieters et al., 2013	Case-control	Prospective Urban and Rural Epidemiology of 2010 healthy participants	Plasma γ' modifies plasma clot structure and fibrinolysis. Increased ratio of γ'/total fibrinogen and γ' levels associated with CVD risk factors.	CVD	Yes ↑ levels
Lovely et al., 2013	Randomized controlled	15 children with obesity (average age 15.8) and 6 without (average age 16)	Association between fibrinogen γ' concentration and other risk factors for CVD, including total fibrinogen.	CVD	Yes ↑ levels

Authors (year)	Study Type	Patient Cohort	Study Conclusion	CVD	Associated
Smalberg et al., 2013	Case-control	106 patients with portal vein thrombosis and 103 controls	Ratio of fibrinogen γ' levels/total fibrinogen were lower in PVT compared to controls and both groups had similar γ' levels.	PVT	Yes ↓ γ' ratio
Appiah et al., 2015	Prospective Study	10, 601 participants ARIC free of CVD (average 60 years)	Higher levels of γ' fibrinogen was positively associated with PAH, HF and CVD deaths. Association was not specific to γ' but a general contribution of inflammation to CVD.	CVD	Not specific to γ'
Folsom et al., 2016	Prospective, Multicentre	16,234 participants from ARIC and CHS study (median follow up 17 and 9 years respectively)	No associations between γ' concentration or ratio and incidence of VTE either overall or in a subgroup	VTE	No
Appiah et al., 2016	Prospective	3219 patients in CHD study mean age 74 (1992-1993) and followed to 2013 for CVD incident (CHD, ischemic stroke, PAD, HF and CVD deaths)	No association between plasma γ' levels and CHD, ischemic stroke, PAD, HF	CVD	No

Authors (year)	Study Type	Patient Cohort	Study Conclusion	CVD	Associated
Schreiner et al., 2017	Prospective, Multicentre	6847 51-70 years old Atherosclerotic clinical & community surveillance	γ' levels not independently associated with carotid-intima-media far wall thickness when controlling for total fibrinogen	A	No
van Dijk et al., 2019	Prospective, Multicentre	182 patients (average age 67) with recent TIA or ischemic stroke	Fibrinogen γ' levels are inversely associated with IPH and LRNC volume. Results independent of inflammation.	Stroke	Yes ↓ levels
Maners et al., 2020	Mendelian Randomization of multiple GWAS	Participants of MEGASTROKE, CHARGE (haemostasis and inflammation), ARIC and INVENT consortium and studies	Higher genetically determined fibrinogen γ' levels were associated with a lower risk of VTE, any ischemic stroke, cardioembolic stroke, and large artery stroke.	VTE and Stroke	Yes

1.8.3 *In-vivo* and *Ex-vivo* Studies

As mice do not produce γ', investigations using murine models are limited. A murine study inserted the human γ'-chain (residues 408-427) onto the murine γ-chain C-terminus (Mosesson et al., 2009). This hybrid insertion of the γ'-chain reduced the circulating level of fibrinogen in plasma. Scanning electron microscopy of clots showed thinnest fibres and densest clot in the γ'-chain homozygous mice, with the WT mice having thicker fibres, while heterozygous mice clot structure was in between the two. The mice were investigated for the function of γ'-chain in heterozygous mice in venous thrombosis by transient electrolytic injury producing a non-occlusive femoral vein thrombus. No difference was observed between the WT and heterozygous mice. However, mice with factor V Leiden following injury had the largest thrombus volume, which was reduced in heterozygous mice for factor V Leiden and γ'-chain, suggesting that the γ'-chain can modify the thrombotic risk.

A reduction of fibrinogen-rich thrombi was reported in a study of arteriovenous shunt thrombosis model on baboons (Lovely et al., 2007). However, the study used two baboons treated with peptide infusion of γ'408-427 peptide compared to 8 control baboons. Additionally, the thrombosis model did not mirror the process of endothelial damage and exposure of sub-endothelium observed in arterial thrombosis. Therefore, it is difficult to make conclusions on the effects of γ' *in vivo*.

The effects of γ' on arterial thrombosis were studied using C57BL/6 mice which were infused with either human γA/γA or γA/γ'. There was an increase in fibrin formation rate in γA/γA compared to γA/γ' infused animals, and γA/γA showed shortened time to carotid artery occlusion (Walton et al., 2014). Furthermore, γA/γ' infused animals showed lower levels of plasma thrombin-antithrombin complexes following injury, which was not observed in γA/γA, indicating the binding of γA/γ' to thrombin *in vivo*. Together, the data suggested that elevated levels of γA/γA promoted arterial thrombosis but not γA/γ' fibrinogen.

A recent study into the effects of flow and stasis on various γ' ratios on clot structure (Macrae et al., 2021) showed that in static conditions, increased γ' resulted in reduced maximum OD and increased time to 50 % lysis, which was observed in both purified and plasma samples. There was a stepwise reduction in average rate of clotting in purified studies with increasing percentage of γ', however this difference was absent in plasmas with increasing percentage of γ'. A stepwise increase percentage of γ' showed a stepwise increase in clot density by microscopy and decrease in porosity. Under flow at arterial and venous rates, increasing percentage of γ' in plasma showed increased fibrin deposition rate, with

more fibrin deposition producing larger clots at both arterial and venous flows. These data suggest that γ' has prothrombotic effects on clot structure and under flow.

The apparently conflicting data on γ' and thrombosis in the literature indicate that the effects of γ' on disease may be dependent on the type of vasculature (venous or arterial), presence of other genetic variants (FV Leiden), levels of shear stress, or other factors. However, its physiological effects are still apparent and are discussed further below.

1.8.4 *In vitro* Studies

1.8.4.1 Plasma Purified Studies

There have been numerous studies investigating the γ'-chain, and these studies have used either commercially purified fibrinogen or pooled plasma and then further purified fibrinogen to separate the two γ-chain splice variants.

A study into fibrinolysis resistance examined the influence of increased fibrinogen levels and the influence of γA/γ', the study showed that increased fibrinogen levels resulted in resistance to internal fibrinolysis (Falls and Farrell, 1997). Furthermore, the study observed that fibrinolysis rates were similar between purified γA/γA and γA/γ' without the inclusion of FXIIIa but with the addition of FXIIIa there was increased fibrinolytic resistance observed in in γA/γ' compared to γA/γA. In addition, γA/γ' showed a reduced rate of clotting. The authors concluded that the resistance to fibrinolysis in γA/γ' is due to FXIIIa, as with inhibition of FXIIIa, fibrinolysis rates became similar to that of γA/γA. A D-dimer agglutination assay showed more cross-linked fibrin for γA/γ' and plasma studies γA/γ' showed increased fibrinolytic resistance (Falls and Farrell, 1997).

A study by Cooper et al, compared the two forms of fibrinogen and found a similar lag phase but reduced maximum OD for γA/γ' compared to γA/γA clots (Cooper et al., 2003). The Fp release was similar for FpA but the release of FpB was slower in γA/γ' compared to γA/γA. This study also analysed unfractionated fibrinogen in turbidimetric investigations which showed a shorter lag phase but similar maximum OD as γA/γA clots, with a similar number of branch points. In scanning electron microscopy, the fibre diameter was significantly reduced for γA/γ' fibrin compared with either γA/γA or unfractionated fibrinogen clots.

Another study into γA/γA and γA/γ' on the other hand showed similar diameter of γA/γA and γA/γ' fibres in scanning electron microscopy (Siebenlist et al., 2005). However, clots formed via fibrinogen, γA/γ' exhibited a finer fibre network with extensive branching, indicating that the release of Fp could be involved. When Fp release was investigated, both Fp were released more rapidly in γA/γA than γA/γ'. Further investigations showed that the FpA release by thrombin was slower in γA/γ' due to allosteric changes within the catalytic

site of thrombin following γ'-chain binding to thrombin exosite 2. Cross-linking of the γ-chain was initially slower in γA/γ' but following time points showed no difference in the rate of cross-linking. However, α-chain cross-linking was slower and less extensive in γA/γ'. Purified thromboelastography studies showed a higher maximum amplitude in γA/γ' at lower thrombin concentrations only and exhibited longer fibrinolysis times.

A study by Allan et al, into the mechanisms of γ'-chain and clot structure showed thinner fibres in γA/γ' compared to WT in microscopy and turbidimetric studies (Allan et al., 2012). Furthermore, fibre bundles were observed in scanning electron microscopy of γA/γ' clots, combined with a less uniform clot structure with large pores extending through 50 µm by LSCM for γA/γ'. Reduced α-α crosslinks but normal γ-γ crosslinks were observed in γA/γ' clots, which agrees with the earlier study by Siebenlist et al. Viscoelastic studies by magnetic micro-rheometer γA/γ' showed reduced clot stiffness with and without FXIIIa, and increased viscosity suggesting γA/γ' clots are less resistant to deformation compared to γA/γA. Protofibril arrangement was studied by AFM and longer oligomers were observed in γA/γA and these oligomers were in looser associations compared to γA/γ', in addition, γA/γ' protofibrils gelled earlier than γA/γA. Turbidimetric studies of thrombin and reptilase initiated clot indicated that effects of γA/γ' on clot structure were independent of thrombin (Allan et al., 2012).

A study into fibrinolysis resistance and the γ'-chain found that fibrinolysis was delayed with thrombin but a similar lysis profile was observed when clotting was initiated with batroxobin which only cleavages FpA (Kim et al., 2014b). The author also observed slower thrombin mediated FpB release in γA/γ', which then resulted in delayed plasminogen binding and activation giving rise to increased resistance to fibrinolysis.

Thus, the presence of the γ'-chain appears to result in changes in its interactions with thrombin, plasminogen and FXIIIa, and because of these interactions there is resistance to fibrinolysis, slower Fp release and alterations to cross-linking. In addition, the γ'-chain influences protofibril formation potentially due to the electrostatic repulsion.

In support of this, a study examining protofibril packing between γA/γA and γA/γ' fibrin found a reduced number of protofibrils packed per average fibrin fibre for γA/γ' (Domingues et al., 2016). Furthermore, ROTEM analysis of fibrinogen-deficient plasma supplemented with either γA/γA and γA/γ' initiated with two different thrombin concentrations showed reduced maximum clot firmness at the higher thrombin concentration for γA/γA, but a consistently lower maximum clot firmness was observed for both thrombin concentrations for γA/γ'. The study shows the influence of γ'-chain on intrafibrillar structure of fibres and how this affects clot mechanics.

1.8.4.2 Recombinant Studies

An initial recombinant study into γ'-chain produced γ'/γ' and γA/γA in BHK cells (Collet et al., 2004). Structural investigations by microscopy (scanning electron and laser-scanning confocal microscopy) showed no difference between the recombinant fibrinogens in fibre density, diameter, or porosity by permeation. Fibrinolysis was studied via LSCM microscopy and γ'/γ' was slower than γA/γA. Mechanical investigations showed that γ'/γ' was stiffer compared γA/γA but the difference was only observed with the addition of FXIIIa.

A later study produced three recombinant fibrinogens in CHO cells (γA/γA, γA/γ', γ'/γ') (Gersh et al., 2009b). In the turbidimetric assay, polymerisation was studied at three $CaCl_2$ concentrations, the lag phase was only significantly different at the lowest $CaCl_2$ concentration with γ'/γ' compared to γA/γA. The maximum rate and maximum OD were reduced for both γA/γ' and γ'/γ', with the homodimer having the slowest rate and lowest maximum OD. The investigations into Fp release saw no difference in FpA release between any of the recombinant fibrinogen proteins however, FpB was faster for γ'/γ' compared to γA/γA and γA/γ'. Scanning electron microscopy showed numerous fibres ends, although they were observed with all three recombinant fibrinogens, they were mostly seen with γA/γ', followed by γ'/γ'. However, fibre ends were not observed in the recombinant study into γ'/γ' or the WT (Collet et al., 2004). The presence of fibre ends is rare observation especially in γA/γA and as the assay was performed under purified conditions the fibrinolytic enzymes are absent. Potentially experimental set up resulted in the production of fibre ends. Fibre diameter measurements of the recombinant fibrins showed that γ'/γ' produced thinner fibres compared to γA/γA in contrast γA/γ' had thicker fibres (Gersh et al., 2009b). Furthermore, the clot architecture observed for γ'/γ' exhibited a structure which was tightly packed with small pores and increased branching. Although small pores were observed in γ'/γ' clots, large pores and bundles were observed at low magnification and this was similar to γA/γ' clots (Gersh et al., 2009b).

Recombinant studies are able to mitigate any FXIIIa contamination as FXIII is co-purified with plasma purified fibrinogen γA/γ', but absent in recombinant fibrinogen, and thus the addition of an inhibitor is not required for recombinant studies (Falls and Farrell, 1997). As with the plasma purified fibrinogen, recombinant γ'-chain fibrinogens altered clot structure and increased fibrinolysis resistance. However, the differences in Fp release and clot mechanics were not exactly mirrored in the recombinant proteins, which could be due to differences in post-transcriptional modifications or experimental conditions.

1.8.5 Other Clot Structure Players

1.8.5.1 Thrombin

The concentration of thrombin used to initiate clotting can influence the fibrin network, with high thrombin concentrations producing a dense, highly branched, thin fibrin fibre network. In contrast, clots formed with low thrombin concentrations are porous, with limited branches and thicker fibrin fibres (Blombäck et al., 1994; Wolberg et al., 2003; Wolberg, 2007; Domingues et al., 2016).

In addition to the catalytic triad, thrombin contains two exosites (I and II) (Troisi et al., 2021). The γ'-chain has been shown to bind to exosite II on thrombin and the two tyrosine's at γ'418 and 422 provide maximum binding (Lovely et al., 2003). A crystal structure of thrombin with γ' peptide showed that there was widespread interaction between the two players, and that they interact via electrostatic interactions with residues of exosite II site on thrombin and hydrophobic interactions in close proximity to the Na^+ binding site (Pineda et al., 2007). Furthermore, the binding of γ' to exosite II is at a higher affinity than exosite I interaction with fibrinogen, while the highest affinity is observed when both sites are occupied by the fibrinogen γ' sequence and E-region respectively (Pospisil et al., 2003).

The binding of γ' to exosite II competitively inhibits the binding of anti-thrombin-heparin, therefore preventing the inhibition of thrombin (Pineda et al., 2007; Fredenburgh et al., 2008).

1.8.5.2 FXIII

Purification of fibrinogen to separate the different γ-chains, found that $FXIIIA_2B_2$ co-purifies with γA/γ' and it has been suggested that the γA/γ' may bind to the B-subunit of FXIII (Mosesson and Finlayson, 1963; Siebenlist et al., 1996). Furthermore, the binding of $FXIIIA_2B_2$ was apparently 20-fold stronger for γA/γ' compared to γA/γA (Moaddel et al., 2000). An experiment where the activation peptide of FXIII was used as indicator of activation observed faster activation for γA/γA compared to γA/γ' (Siebenlist et al., 2005). Further experiments using Atroxin which cleaves only FpA, showed no difference in acceleratory rates suggesting the differences are due to thrombin binding to γ' sequence. Additionally, a later study using recombinant fibrinogen (γA/γA and γ'/γ') studied $FXIIIA_2B_2$ binding by immobilisation on ELISA plate and observed no difference in affinity of fibrinogen/FXIII binding for either fibrinogen types, suggesting that the C-terminal of the γ-chain is not essential for binding $FXIIIA_2B_2$ (Gersh and Lord, 2006). Potentially differences could be due to experimental differences of immobilised fibrinogen compared to soluble fibrinogen as

immobilised fibrinogen can have a different conformation. Furthermore, surface plasmon resonance has shown that FXIIIa and $FXIIIA_2B_2$ bind to the αC-region (Smith et al., 2011). Following this observation there have been several studies into the role of FXIII cross-linking in fibrinogen with the γ'-chain. There was a slower rate of $FXIIIA_2B_2$ mediated cross-linking of γA/γ' compared to γA/γA, but cross-linking was mediated by addition of $CaCl_2$ only (Siebenlist et al., 2001). A later study measuring the rate of D-dimer formation initially there was a slower rate for γA/γ' in formation of cross-linking (first minute) but overall no difference was observed in the rate or extent of cross-linking (Siebenlist et al., 2005). Additionally, the authors observed no difference in rates of γ-chain cross-linking between γA/γA and γA/γ' fibrinogen or fibrin. Authors found that thrombin mediated FXIII activation was slower in the presence of γA/γ', and the suggestion was due to γ'-chain inducing allosteric changes at the catalytic site although the kinetics of peptide release were not determined. A further study also reported similar cross-linking between γA/γA and γA/γ' (Allan et al., 2012). Interestingly, the studies by Allan et al and Siebenlist et al both showed reduced α-chain cross-linking in γA/γ' fibrinogen. A further note is that the association of $FXIIIA_2B_2$ in circulation with fibrinogen is of high affinity (K_d 10^{-8} M), and therefore all the circulating $FXIIIA_2B_2$ is bound to fibrinogen (Greenberg and Shuman, 1982). The cross-linking studies have not pre-incubated $FXIIIA_2B$ with the fibrinogen, moreover it might be of interest to study if there are alterations in initial or overall cross-linking between γA/γA and γA/γ' *in vivo*.

1.8.5.3 Platelets

A major interaction site between fibrinogen and platelets is through the platelet integrin $\alpha_{IIB}\beta_3$ (glycoprotein IIb-IIIa) (Farrell et al., 1992). The integrin interacts with fibrinogen through the γ-chain C-terminal residues γ408-411, residues AGDV, however these residues are absent in the γ'-chain variant. Platelet aggregation is mediated by fibrinogen binding to activated $\alpha_{IIB}\beta_3$ (Bennett, 2006). The γ'-chain variant was shown to reduce thrombin-induced platelet aggregation (Lancellotti et al., 2008).

A recombinant study compared three fibrinogen variants, two with alterations to the RGD sites in the α-chain (RGD to RGE at α97 or α574) and γ'-chain homodimer, with WT fibrinogen (Farrell et al., 1992). ADP mediated platelet aggregation for either α97 or α574 mirrored the WT, whereas the γ'-chain homodimer exhibited limited aggregation.

A number of reported dysfibrinogenaemias with mutations in the C-terminal end of the γ-chain have been reported (e.g. Fibrinogen Montreal (γ407), Hershey IV (γ411) and Tsukuba (γ408)) (Sheen et al., 2006; Flood et al., 2008; Mukai et al., 2016). No functional studies were performed on Fibrinogen Tsukuba and Fibrinogen Montreal, and both had other mutations

in the α-chain. Fibrinogen and platelet investigations were performed with purified fibrinogen Hershey IV, which showed little difference in platelet aggregation by ADP (Flood et al., 2008). This could potentially be due to fibrinogen being heterozygous for the mutation, suggesting that there may have been sufficient γA present to support normal platelet aggregation. Synthetic dodecapeptides with either residues for normal γ-chain or Hershey IV were used to study the influence of the mutation without the presence of the normal γ-chain. Less inhibition was observed in platelet aggregation with the dodecapeptides with Hershey IV residues. Furthermore, reduced fibrinogen $\alpha_{IIB}\beta_3$ binding was also observed in the aberrant fibrinogen. Although bleeding was reported in patients with Fibrinogen Montreal and Hershey IV, they also had other mutations present.

In agreement with earlier studies, a recombinant fibrinogen homozygous in γ'-chain produced in CHO cells was unable to support platelet aggregation, however there was no difference in clot contraction between WT and γ'/γ' (Rooney et al., 1996). This observation was mirrored in a murine model γΔ5/γΔ5 which lacks the final 5 residues of the γ-chain (QAGDV). Furthermore, the mouse model showed sustained blood loss following surgical challenge (Holmbäck et al., 1996). Clot contraction of triple mutated fibrinogen (AαD97E, AαD574E and γ407), showed a delay in clot contraction using platelets from patient with afibrinogenemia (Rooney et al., 1998). A study examining the relationship of fibrin compared to fibrinogen with $\alpha_{IIB}\beta_{3,}$ showed that γ'/γ' displayed higher binding strength for $\alpha_{IIB}\beta_3$ as fibrin (Litvinov et al., 2016). Furthermore, the conversion to fibrin reveals cryptic binding sites in fibrinogen, two α-chain RGD sites and γ316-322, additionally there may be other sites involved in platelet mediated clot contraction (Remijn et al., 2002; Remijn et al., 2003). Furthermore, inhibitors to $\alpha_{IIB}\beta_3$ are less effective for fibrin than fibrinogen potentially due to alternative interaction sites for fibrin compared to fibrinogen (Litvinov et al., 2016). Multiple binding sites within the α_{IIB} β-propeller domain have been shown bind to fibrin highlighting that there is various sites of interaction for fibrin (Podolnikova et al., 2014). A study into the mechanobiology of platelet contraction showed that inhibition of $\alpha_{IIB}\beta_3$ by abciximab had a greater inhibitory effect on clot contraction dynamics than the suppression of myosin IIA by blebbistatin (Kim et al., 2017), thus confirming the importance of the relationship between $\alpha_{IIB}\beta_3$ and fibrin(ogen) for platelet function.

1.8.5.4 RBC

Fibrinogen has been shown to bind to RBCs by AFM. The receptor for this interaction is not known but appears to be related to $\alpha_{IIB}\beta_3$ due to inhibition in binding observed with eptifibatide, and interactions with the RGD sequences on the fibrinogen Aα95-97 (Carvalho et al., 2010; Carvalho et al., 2018).

A study comparing γA/γA and γA/γ' clots with RBCs, found reduced clot porosity, reduced fibre diameter for γA/γ' and increased fibrinolytic resistance with the addition of RBC (Guedes et al., 2018a). The presence of RBCs increased clot stiffness for γA/γ' but not γA/γA and furthermore, there was more work required to detach RBC-RBC interactions for γA/γ' but not γA/γA fibrinogen.

Further investigations into the relationship between the γ'-chain and RBC used recombinant fibrinogens γA/γA and γ'/γ' and showed higher force required to break the attachment of γ'/γ' and receptor on RBC and there was higher frequency of binding for γ'/γ' compared to γA/γA fibrinogen (Guedes et al., 2018b). Also, γ'/γ' clots containing RBCs were more viscous than γA/γA and the inclusion of RBCs altered the viscoelastic properties of both types of clots. The addition of RBCs did not influence fibre diameter of γ'/γ' clots in agreement with plasma purified γA/γ' observations (Guedes et al., 2018a). However, γ'/γ' clots showed larger fibre diameter than γA/γA. Like the study with plasma purified fibrinogen, scanning electron microscopy images showed an increased number of thinner fibres close to the RBC surface. Comparable to the fibrinolysis investigations with γA/γ', the fibrinolysis rate was reduced in γ'/γ' clots that contained RBCs, and the way the clots lysed was also less uniform.

1.9 Hypothesis and Aims

1.9.1 Hypothesis

The fibrinogen αC-region and γ'-chain show unique effects on clot structure and function that impact thrombosis.

1.9.2 General Aims

This thesis aimed to explore the roles of the αC-region subdomains (αC-domain and αC-connector) and γ'-chain (multiple truncations to γ'-chain) in purified, plasma and whole blood *ex-vivo* assays, as well as state-of-the-art biophysical, cellular, and *in vitro* models, using recombinant fibrinogens with new truncations to both chains.

Specific Aims**:**

- Produce and purify new recombinant truncations of the αC-region and γ'-chain of fibrinogen.
- Characterise the recombinant truncated fibrinogens through structural investigations by turbidimetric assay and different types of microscopies.
- Characterise the recombinant truncated fibrinogens by functional investigations into viscoelastic and fibrinolysis properties using micro-rheology and turbidimetric/microscopic methods respectively.

- Investigate the role of recombinant truncated fibrinogens in whole blood via *ex-vivo* studies including ROTEM and clot contraction methodologies

Chapter 2 General Methods

2.1 Generation of pMLP γ'

The construction of pMLP γ', was established through the combination of complementary DNA (cDNA) from two plasmids, pMLP γA and pMLP D-domain γ' (plasmid maps displayed in appendix 11.4 Figure 63). The plasmids pMLP γA and pMLP D-domain γ' were a kind gift from Dr Susan Lord (University of North Carolina at Chapel Hill) and established by Dr Shirley Uitte de Willige member of the Ariëns lab respectively. The pMLP γA carries the cDNA of the predominant γ-chain and the pMLP D-domain γ' contains the γ'-chain C-terminus and then only the D-domain of the γA. Using restriction sites within the plasmid the C-terminal region of pMLP, γA was removed and replaced with C-terminus of pMLP D-domain γ'.

2.1.1 Restriction Digest

The composition of the restriction digest contained either 2 µg of pMLP D-domain γ' or pMLP γA and was digested by 3 µL of XbaI and 2 µL of BstXI in 1x buffer 3 (New England Biolabs; Hitchin, UK) in a final reaction volume of 50 µL. The digestion mixture was incubated at 37 °C for 1 hour and 20 minutes, followed by separation on a 1 % agarose gel ran in TAE buffer (Tris, acetic acid and ethylenediaminetetraacetic acid (EDTA)). The agarose gel was prepared with agarose tablets (Bioline Reagents; London, UK) dissolved in a TAE buffer. The buffer composition was 40 mM tris base (VWR International; Pennsylvania, USA), 20 mM acetic acid (Sigma-Aldrich; Missouri, USA), 1 mM EDTA (VWR International) pH 8.3). Two microlitres of 0.5625 µg/mL ethidium bromide (Sigma-Aldrich) was added to the agarose gel to visualise the digested fragments. The separated fragments were visualised on a TFX-35M UV-Transilluminator (ThermoFisher Scientific; Massachusetts, USA) and bands for the insert at 797 base pairs (pMLP D-domain domain γ') and vector at 4880 base pairs (pMLP γA) were isolated. The fragments were extracted from the agarose gel using the Wizard® SV Gel and PCR (Polymerase Chain Reaction) Clean-Up System (Promega; Wisconsin, USA) following the manufacturer's instructions, and fragments were eluted into double-distilled water (ddH_2O). The eluted DNA was quantified on a NanoDrop 1000 spectrophotometer (ThermoFisher Scientific), where 2 µL was loaded on the spectrophotometer and quantified.

2.1.2 Ligation

The two purified digested fragments pMLP γA (vector) and the pMLP D-domain γ' (insert) were ligated together by T4 DNA ligase. This assembly was achieved with a ratio of 1:1 of vector (100 ng) to insert (17.55 ng) in a 1x ligase buffer using 0.4 µL of T4 DNA ligase

(Promega) in a final reaction volume of 20 µL. The mixture was incubated overnight at 4 °C to achieve the ligation.

2.1.3 Transformation

Escherichia coli (*E.coli)* competent cells, DH5α (ThermoFisher Scientific) were transformed with the ligated plasmid mixture. To a pre-cooled tube on ice, 50 µL of DH5α cells and 2 µL of the ligation mixture were added and then incubated for 30 minutes. After incubation, the cells were heat shocked at 42 °C for 45 seconds before returning to ice for a further 2 minutes. Five hundred micro litres of SOC medium (ThermoFisher Scientific) were added to the heat shocked cells and incubated at 37 °C on a shaker (G-25 Incubator Shaker, New Brunswick Scientific, New Jersey, USA) at 225 rpm for 1 hour. After incubation, the mixture was plated out on Lysogeny Broth plates ((LB), 1 % v/w tryptone (Fisher Scientific; New Hampshire, USA), 0.5 % v/w yeast extract (Fisher Scientific) and 1 % v/w sodium chloride (NaCl, Fisher Scientific) and autoclaved) and incubated for 16 hours at 37 °C. LB plates were supplemented with 100 µg/mL ampicillin (Sigma-Aldrich) when prepared.

2.1.4 Small Scale Isolation of Plasmid

Following transformation, colonies were selected and grown in 5 mL of LB broth containing 100 µg/mL of ampicillin, on a shaker at 225 rpm (G-25 Incubator Shaker) at 37 °C for 16 hours. A master plate of each of the colonies was prepared before overnight culture by making a small streak on a LB agar plate containing 100 µg/mL of ampicillin before the colony was inserted in the broth. The following morning the plasmid was extracted by QIAprep Spin Miniprep Kit (Qiagen; Hilden, Germany) as directed by manufacturer's instructions and the plasmid was eluted in ddH_2O. The DNA was quantified as described in 2.1.1

2.1.5 Large Scale Isolation of Plasmid

A starter culture was established for the desired plasmid by using the master plate. A streak of cells was used to inoculate 5 mL of LB broth containing ampicillin (100 µg/mL) and incubated in a shaker at 225 rpm at 37 °C for 3 hours. This was followed by a further addition of 200 mL of LB broth and ampicillin, and the culture was returned to the shaker for an additional 16 hours. The plasmid was isolated the following morning by the PureYield™ Plasmid Maxiprep System (Promega) as instructed by the manufacture and eluted in ddH_2O. The DNA was quantified as previously described in 2.1.1.

2.1.6 Sequence Verification

A two-step process was used to establish plasmid integrity and that the desired change had occurred. The initial sequencing confirmed if the desired base changes (site directed

mutagenesis) or digestion insert (establishing plasmid pMLP γ') had occurred, as only part of the plasmid was sequenced, checking only the area around the site of change. Further sequencing was performed after the large-scale maxi prep where the entire cDNA sequence was verified for any additional unwanted alterations. The plasmids were sequenced by MRC PPU DNA Sequencing and Services (University of Dundee; Dundee, Scotland), see appendix 11.1 for the list of primers used. The sequences were aligned to the expected cDNA fibrinogen chain using Serial Cloner 2.6.1 (Serial Basics) to determine homology.

2.2 Site Directed Mutagenesis

Following the generation of pMLP γ', the plasmid was used to create the γ'-chain truncations (16,12,8,4,0) and for the α-chain truncations the plasmid pMLP Aα was used, this was kindly gifted by Dr Susan Lord. Mutagenesis of the cDNA sequence was used to established stop codons at the desired point using the QuikChange II Site-Directed Mutagenesis Kit (Aligiant; California, USA). The mutagenesis primers contained either 1, 2 or 3 base changes to create a stop codon in the cDNA sequence at the desired location. The mutagenesis primer sequences for all the truncations are listed in appendix 11.2.

The mutagenesis reaction mix was composed in x1 reaction buffer and contained 20 ng of plasmid either pMLP Aα or pMLP γ', 125 ng of the desired forward and reverse mutation primers, 1 µL of Deoxyribonucleoside Triphosphate (dNTP) mix and 1 µL of PfuUltra high-fidelity DNA polymerase was added per reaction. The total reaction volume was 50 µL and was achieved with the addition of ddH2O.

Table 4 Mutagenesis Thermal Cycle for α- and γ- chain Truncations

Temperature (°C)	α-chain Truncations	γ-chain Truncations	Cycles
95	30 seconds	30 seconds	1
95 - denaturation	30 seconds	30 seconds	16
55 - annealing	1 minute	1 minute	
68 - elongation	6 minutes and 30 seconds	5 minutes and 40 seconds	
4	2 minute	2 minute	1

The thermal cycling parameters used for mutagenesis is described in Table 4. The two plasmids had a different length in the duration of the elongation step due to the length of the Aα cDNA being longer than the γ' cDNA. Following thermal cycling, 1 µL of Dpn1 (New England Biolabs; Ipswich, UK) was added to each tube and incubated at 37 °C for 1 hour, to digest the parentally methylated plasmid therefore preventing transformation in competent cells. The Dpn1 treated plasmid was transformed in 50 µL XL-1 Blue cells as described in

2.1.3. Five isolated colonies for each truncation were grown as described in section 2.1.4 and verified by sequencing as mentioned in section 2.1.6. One colony for each of the truncations was grown up for large scale isolation as described in 2.1.5 and then sequenced again as described in 2.1.6.

2.3 Cell Culture

2.3.1 Routine Cell Culture

Optimal cell growth of the Chinese hamster ovarian (CHO) cells was achieved by maintaining the cells three times a week. If cells were under 80 % confluent, spent medium was aspirated and fresh growth medium (Dulbecco's Modified Eagle Medium (DMEM)/F12 (Thermo Fisher Scientific), 5 % foetal calf serum (FCS, Labtech; East Sussex, UK) and 5 % Nu Serum IV (Corning; New York, USA)) was applied. A confluence greater than 80 %, cells were split by aspirating the medium and briefly washing the cells with 0.1 % EDTA in phosphate buffer saline (PBS, 2.7 mM potassium chloride and 137 mM sodium chloride pH 7.4, Sigma-Aldrich), followed by overlaying with 0.25 % trypsin-EDTA (Sigma-Aldrich) until the cells detached. The trypsin was inhibited by the serum in the fresh growth medium, and the cells were plated at the required densities. All cell culture was performed in a BioMat 2 Class 2 Microbiological Safety Cabinet (CAS; Manchester, UK) and the cells were incubated at 5 % CO_2 at 37 °C in an MCO-20AIC incubator (Sanyo; Middlesex UK).

2.3.2 Thawing

Cells were rapidly thawed from storage in liquid nitrogen and added to 9 mL of pre-warmed growth medium and centrifuged at 350 g for 4 minutes (Rotina 35, Hettich; Salford, UK). The supernatant was aspirated, and the pellet was gently resuspended in growth medium. The cells were seeded as required and incubated as described in section 2.3.1.

2.3.3 Freezing

Cells were lifted as mentioned in 2.3.1 and centrifuged at 350 g for 4 minutes (Rotina 350). Supernatant was aspirated, and cells were resuspended in freezing mix (90 % FCS and 10 % dimethyl sulfoxide (DMSO, Sigma-Aldrich), filter sterilized through a 0.2 µm syringe filter (Pall; Portsmouth, UK) and aliquoted into freezing vials (Nunc; Thermo Fisher Scientific). Vials were stored in a Mr Frosty (Nalgene; Thermo Fisher Scientific) for 24 hours at -80 °C before transferring to liquid nitrogen.

2.3.4 Calcium Phosphate Transfection

For the expression of recombinant fibrinogen, the CHO cells require the presence of all 3 chains of fibrinogen (α, β and γ). CHO-βγ cells carrying the β- and γ-chain or CHO-αβ

containing the α- and β-chain were used for transfection as well as CHO-αβγ which expressed all the fibrinogen chains producing the recombinant WT fibrinogen. These various CHO cells were kindly gifted by Dr Susan Lord (Binnie et al., 1993; Lord et al., 1993).

For the α-chain truncations, CHO-βγ cells were transfected with a truncated α-chain to produce either α390 or α220. For the various γ'-chain truncations and γ' homodimer, CHO-αβ cells were transfected with the respective γ' plasmid. The day before the transfection, a confluent 10 cm dish (Corning; High Wickham, UK) of CHO cells were passaged 1:10 as per 2.3.1 into three 10 cm dishes. Two hours before the transfection, the culture medium was replenished with fresh growth medium. Two DNA concentrations were used for the transfection (10 μg and 20 μg), a second plasmid (pMSV-His) was also transfected at a ratio of 1:10 to the pMLP plasmid. The plasmid pMSV-His confers resistance to L-histindol which was used as a selection marker to select for transfected clones. The plasmids were added to 2.5 M calcium chloride ($CaCl_2$, Sigma-Aldrich) and the calcium/DNA mixture was then added dropwise to a bubbling 2xHEBS buffer (50 mM hepes (Sigma-Aldrich), 280 mM NaCl and 1.48 mM sodium phosphate dibasic (Sigma-Aldrich) pH 7.05). This mixture was incubated for 30 minutes at room temperature, then the mixture was added dropwise over the cells. Dishes were then returned to the incubator for 4 hours. After incubation the medium was removed, and the cells were treated with 2 mL 10 % glycerol for 3 minutes to enhance transfection efficiency. After glycerol treatment, the cells were washed 3 times with PBS before the addition of fresh growth medium. A control plate of CHO cells was glycerol shocked and used as a selection control. The cells were incubated at 37 °C and 5 % CO_2 for 48 hours. All the truncations were generated by calcium phosphate transfection.

2.3.5 Clone Selection

Forty-eight hours after transfection, the cells were passaged as described in 2.3.1 and seeded to a range of densities (1:50, 1:100, 1:150, 1:200 and 1:400) in a 10 cm dish, to allow the establishment of single cell colonies. The following day the medium was aspirated and changed to selection medium (growth medium supplemented with 800 μM L-histidinol (Sigma-Aldrich)). Every few days the medium was changed and replenished with fresh selection medium, and plates were viewed regularly for the appearance of single cell colonies. Once the single cell clones appeared, medium was aspirated and 24 distinct clones per transfection condition were isolated by cloning rings, by adding a few drops of 0.25 % trypsin-EDTA to each ring. Once detached, cells were transferred to a 24 well plate (Corning) containing 500 μL selection medium and incubated at 5 % CO_2 at 37 °C. The plate was viewed daily, and once cells achieved 70 % confluency or one week had passed, medium was harvested, and cells were passaged into 6 cm dishes (Corning). The harvested medium was

tested for the presence of fibrinogen by enzyme-linked immunosorbent assay (ELISA) 2.4. The highest expressing clones were further investigated by passaging into two 10 cm dishes and culturing until confluent, the medium of one dish was changed to serum free medium (SFM) and dishes were returned to the incubator for 1 week. The remaining dish was lifted and frozen as described in 2.3.3. After a week, the medium was harvested and assessed for fibrinogen expression by ELISA.

2.3.6 Expression of Recombinant Fibrinogen

The fibrinogen expressing clone for each truncation was thawed as described in 2.3.2 and passaged until there were 40 confluent 10 cm dishes. Two dishes were passaged per 850 cm^2 roller bottle (Corning) in growth medium, medium was changed until cells had covered the surface of the roller bottle. Bottles were maintained in a Jencons incubator at 37 °C on a R2P 2.0 Roller Apparatus (Wheaton; Millville, USA). The roller bottle surface area was increased by the addition of 1 g of cytodex microcarrier beads (Sigma-Aldrich) per bottle. The beads were added to PBS and autoclaved before use. Prior to the addition of the beads into the roller bottle the PBS was removed and the beads were washed twice with DMEM/F12 medium before changing to growth medium and then inserted into roller bottles. Bottles were returned to the incubator for a further two days to allow the cells to proliferate over the beads. After two days, the medium was removed from the bottles and 50 mL of SFM was slowly rotated around the bottle and then discarded. One hundred millilitres of SFM medium were added to the bottles and incubated overnight, to remove any further trace of fibrinogen from the serum. The following morning the SFM was removed and 200 mL of ITS medium (DMEM/F12 supplemented with 1 % antibiotic antimycotic solution (Sigma-Aldrich), 4 µg/mL aprotinin (Sigma-Aldrich, prepared in ddH_2O), and 5 µg/mL insulin, 5 µg/mL transferrin and 5 ng/mL sodium selenite (ITS prepared in ddH_2O, Roche; Basel, Switzerland) was added to each roller bottle. For the next 6-8 weeks, 100 mL of medium was collected from each bottle three times/week and replenished with 100 mL of fresh ITS medium. One hundred and fifty microliters of 150 µM phenylmethylsulfonyl fluoride (PMSF, prepared in isopropanol Sigma-Aldrich) was added to every 100 mL of medium collected. Before the addition of the PMSF, 1 mL of the pooled harvested medium was removed to monitor expression levels over the course of the production cycle. The recombinant WT fibrinogen was expressed in the same way as truncated and homodimer fibrinogens.

2.4 Fibrinogen Enzyme-linked Immunosorbent Assay

At multiple stages of clone selection and expression, a sandwich ELISA was performed to investigate the secreted fibrinogen levels in the medium. A F96 Maxisorp Immuno plate (Nunc) was coated with 100 µL per well with polyclonal rabbit anti-human fibrinogen antibody at 1:4000 (Dako; Cheshire, UK) prepared in 100 mM sodium carbonate buffer pH 9.6 (Sigma-Aldrich) and incubated at room temperature for 1 hour. After 1 hour, the contents of the plate were removed and 300 µL per well of blocking buffer (PBS with the addition of 3 % Bovine Serum Albumin (BSA; Cell Signalling Technologies; Danvers, USA) and 0.05 % Tween 20 (Sigma-Aldrich) at pH 7.4) was added to the plate and incubated overnight at 4 °C. The following morning, the contents of the plate were emptied, and the wells were washed once with 300 µL of washing buffer (10 mM PBS with 0.05 % Tween 20 at pH 7.4) before the addition of the samples and standards. Standards and harvested medium were prepared in duplicate in dilution buffer (10 mM phosphate buffer with 1 % BSA and 0.05 % Tween 20 at pH 7.4) and were added at 100 µL per well. A standard curve was prepared by serial dilutions of commercially sourced fibrinogen (1000 ng/mL – 15 ng/mL) which had been purified by IF-1 affinity chromatography as described in 2.6.2.

Depending on the stage of clone selection or expression, the harvested medium was loaded on the plate either neat or diluted in dilution buffer. Two wells of dilution buffer were used as a blank. The plate was incubated for 2 hours at room temperature on an orbital shaker (Stuart; Staffordshire, UK). Following incubation, the content of the plate was removed, and the plate was washed 3 times with 300 µL of washing buffer per well before the addition of 100 µL per well of detecting buffer (1:1000 sheep anti-human fibrinogen horseradish peroxidase linked antibody (Enzyme Research Laboratory; Swansea, UK) prepared in dilution buffer). The plate was further incubated for 1 hour on an orbital shaker. After incubation, the plate was washed 3 times with 300 µL of washing buffer per well, then a 100 µL of development buffer (50 mM dibasic sodium phosphate (Sigma-Aldrich) and 25 mM citric acid (Sigma-Aldrich) at pH 5.0) supplemented with 0.04 % hydrogen peroxide (Sigma-Aldrich) and 6 mg of O-phenylenediamine (Sigma-Aldrich) was added per well and the plate was incubated for 5 minutes. The reaction was stopped by the addition of 200 µL per well of sulphuric acid (3 M sulphuric acid (Sigma-Aldrich)). The plate was read at 490 nm on a PowerWave HT Microplate Spectrophotometer (Bio-Tek; Swindon, UK). The concentration of fibrinogen in the harvested medium was calculated using the equation from a linear line of best fit generated on graph of the log concentration (x) of the standards plotted against their absorbance (y) and rearranging the equation for a straight line to find the concentration of the secreted fibrinogen (x). The equation and rearranged equation are

shown in Equation 1. The inverse log was calculated from the log concentration to give the concentration of the fibrinogen in the medium.

A

$$y = mx + c$$

B

$$x = \frac{y - c}{m}$$

Equation 1 Equation used for Calculating the Concentration of Fibrinogen
x is the concentration, y is the absorbance, m is the slope and c is the intercept.

2.5 Purification of Recombinant Fibrinogen

2.5.1 Ammonium Sulphate Precipitation

The first step in the two-step purification was using ammonium sulphate to decrease the solubility, resulting in the precipitation of the recombinant fibrinogen which was then collected through centrifugation.

The harvested medium was defrosted and 90 mL of protease inhibitor cocktail 1 (20 mM MES hydrate (Sigma-Aldrich), 5 mM 6-Aminohexanoic acid (Sigma-Aldrich), 5 mM benzamidine (Sigma-Aldrich), 100 µM PMSF, 1 µM pepstatin (prepared in methanol) and 1 µM leupeptin (prepared ddH_2O) Sigma-Aldrich) was added to 3 L of defrosted medium. The defrosted medium was gently stirred at 4 °C while saturated ammonium sulphate (VWR International) was filtered through a folded 320 mm Whatman filter paper (VWR International) above and slowly added to reach 40 % saturation in the solution. After all the ammonium sulphate had been filtered and added, the medium was removed from the stirrer and incubated overnight at 4 °C. The following morning the precipitated medium was centrifuged at 14,500 x *g* for 45 minutes without brakes at 4 °C in an Avanti J-265 XPI (Beckman Coulter; California, USA). After centrifugation the supernatant was gently removed, and the pellet was resuspended in protease inhibitor cocktail 2 (333 mM NaCl, 222 mM Tris, 111 µM PMSF, 5 µM pepstatin, 5 µM leupeptin, 1 mM EDTA, 11 U/mL trypsin inhibitor (Sigma-Aldrich), 5 mM benzamidine, 5 mM 6-Aminohexanoic acid) and incubated for 30 minutes on ice. After incubation the mixture was further centrifuged at 43,000 x *g* for 30 minutes at 4 °C in an Avanti J-265 XPI, the supernatant was collected and stored in 5 mL aliquots at -80 °C.

2.5.2 IF-1 Affinity Chromatography

The second purification step for the recombinant fibrinogen utilised affinity chromatography exploiting the calcium ion-dependent monoclonal antibody clone IF-1 against fibrinogen (Kamiya BioMedical; Seattle, USA) (Takebe et al., 1995).

The IF-1 antibody binds to the D-domain of the recombinant fibrinogen in a calcium dependant manner, allowing the fibrinogen to be separated from any contaminants. EDTA in the elution buffer disrupts the interaction between the fibrinogen and Ca^{2+} allowing the fibrinogen to be eluted from the column and therefore collected. The antibody was covalently coupled to cyanogen-bromide activated Sepharose 4B (Sigma-Aldrich) and packed in a XK16/20 column (GE Healthcare; Hatfield, UK). The IF1 antibody within the column has the capacity to bind 5 mg of fibrinogen. Recombinant fibrinogen was defrosted and incubated with 10 mM $CaCl_2$ for 10 minutes before loading onto a 10 mL loop attached to an AKTA Avant 25 (GE Healthcare). The recombinant fibrinogen was loaded onto the column in a single column volume (CV = 7.439 mL) of equilibration buffer (20 mM Tris, 300 mM NaCl and 1 mM $CaCl_2$ at pH 7.4). Non-specifically bound contaminants were removed by two wash steps, the initial step utilising high salt and the following step using a reduced pH. The column was first washed with wash buffer 1 (20 mM Tris, 1 M NaCl, 1 mM $CaCl_2$ at pH 7.4) for 5 CV followed by wash buffer 2 (50 mM Sodium Acetate (Sigma-Aldrich), 300 mM NaCl and 1 mM $CaCl_2$ at pH 6) for an additional 5 CV. The fibrinogen was removed from the column with 7 CV of elution buffer (20mM tris, 300 mM NaCl and 5 mM EDTA at pH 7.4). The eluted fibrinogen was collected in 2 mL aliquots. The fractions collected from the peak were pooled and stored at -80 °C. Following elution, the column was equilibrated with 5 CV of equilibration buffer to remove elution buffer and allow binding for subsequent runs. Between different recombinant fibrinogen runs the column was regenerated by 1 CV equilibration buffer and then 5 CV of regeneration buffer E (20 mM tris, 300 mM NaCl and 50 mM EDTA pH 7.4) following by a further 5 CV of regeneration buffer G (10 mM glycine pH 2.8), and finally the column was equilibrated with 10 CV of equilibration buffer. The flow rate remained constant at 1.300 mL/minute for runs, sample loading and regeneration.

2.5.3 Concentration

For each batch of recombinant fibrinogen, the frozen fractions from chromatography were defrosted, pooled then concentrated. Fibrinogen was concentrated to achieve a final volume between 1-4 mL using concentrator tubes with a polyethersulfone membrane with a molecular weight cut off at 100 kDa (ThermoFisher Scientific) at 4 °C at 4460 x *g* (Rotanta 460 (Hettich)).

2.5.4 Dialysis

For the experimental characterisation the removal of the EDTA from the recombinant fibrinogens buffer was required. The first dialysis step was for 1 hour in dialysis buffer (50 mM tris and 100 mM NaCl at pH 7.4). After the first hour, the buffer was changed for fresh dialysis buffer, and then the recombinant fibrinogens were dialysed overnight. The following morning the buffer was changed again for fresh dialysis buffer and incubated for 1 hour. For all the steps the recombinant fibrinogens were dialysed on a stirrer at 4 °C in D-Tube™ Dialyzer (Merck-Millipore; Watford, UK). The concentration of protein was determined by a bicinchoninic acid (BCA) assay (2.5.5), and samples were stored in aliquots at -80 °C.

2.5.5 Bicinchoninic Acid Assay

In a 96 well plate (ThermoFisher Scientific), the recombinant fibrinogen was diluted 1:10 in ddH_2O. Standards were composed of serial dilutions of BSA 1000 µg/mL (1000, 800, 600, 400 and 200 µg/mL (Sigma-Aldrich) in ddH_2O, 25 µL of each standard was inserted per well. Twenty-five microliters of ddH_2O were used for a blank. All standards, blank and recombinant fibrinogen were loaded in duplicate and 200 µL of a ratio of (50:1) of bicinchoninic acid to copper II sulphate solution (Sigma-Aldrich) was added per well and incubated at 37 °C for 30 minutes. Following incubation, the plate was read at 562 nm on a PowerWave microplate spectrophotometer. The concentration of the recombinant fibrinogen was established by the rearranging the equation for a straight line as shown in Equation 1 to obtain the unknown concentration of recombinant fibrinogen.

2.6 Purification Commercial Sourced Protein

2.6.1 FXIII Purification

Commercially sourced FXIII (Zedira; Darmstadt, Germany) was purified through a Hiload 16/600 Superdex 200 pg (GE Healthcare) with a column volume of 120.6 mL to remove contaminating albumin and glucose. The $FXIIIA_2B_2$ was dissolved in 1 mL ddH_2O and loaded in to a 2 mL loop attached to a AKTA Avant 25. The column was equilibrated with 0.1 CV of equilibration buffer (20 mM hepes (Sigma-Aldrich), 150 mM NaCl at pH 7.4) at 1 mL/minute. Following equilibration, the sample loop was emptied with 4 mL of equilibration buffer at 0.5 mL/minute. The elution of the samples was over 1.5 CV at a flow rate of 0.5 mL/minute with equilibration buffer. Eluted samples were collected in 1.6 mL factions at 4°C.

The fractions were quantified by BCA assay (2.5.5) and 0.5 µg of each fraction was prepared for non-denaturing SDS-PAGE analysis as described in 2.8.2 The protocol was modified as the samples were not heat denatured and the sample reducing agent was not included. The

fractions that contained no contaminating material were pooled, aliquoted and stored at -80°C.

2.6.2 Purification of Plasma Fibrinogen

The commercially sourced, plasminogen depleted, fibrinogen (Merck; Feltham, UK), was first purified by IF-1 affinity chromatography as described in 2.5.2 and then further purified by anion exchange chromatography through a DE-52 column, (CV-23.562 mL) to separate γA/γA from γA/γ'. Before loading onto the column, 30 mg of fibrinogen was first dialysed into buffer A (39 mM tris, 6.5 mM H_3PO_4 (Sigma-Aldrich), 0.5 mM PMSF, 1 mM benzamidine, 5 mM 6-Aminohexanoic acid at pH 8.6). The fibrinogen was incubated with buffer A for 1 hour before the buffer was changed for fresh buffer A and further incubated overnight. The solution was changed the following morning for fresh buffer A and dialysed for a final 1 hour. All dialysis steps were performed at 4 °C and samples were dialysed in a D-Tube™ Dialyzer with gentle stirring. The fibrinogen was loaded onto a 5 mL loop attached to a AKTA Avant 25, the column was equilibrated with 2 CV (1CV=23.562 mL) of buffer A at 2 mL/minute. The sample was injected, and the column was washed with 5 CV of buffer A at 2 mL/minute. The sample was eluted over a gradient of buffer A to buffer B from 0-100 % (0.5 M tris, 6.5 M H_3PO_4 (Sigma-Aldrich), 0.5 mM PMSF, 1 mM benzamidine, 5 mM 6-Aminohexanoic acid pH 4.2). The elution started with 5 % buffer B at 2 mL/minute, and there was a gradual increase in buffer B for each step is shown in Table 5. Once at 100 % there was a further 5 CV of buffer B and the column was equilibrated with 5 CV of buffer A, both steps occurring at 2 mL/minute. Samples were collected in 3.5 mL fraction at 4°C, concentrated and dialysed as described in 2.5.3 and 2.5.4. The fractions were analysed by SDS-PAGE for presence of γA- and γA/γ'-chain as described in 2.8.2 and corresponding fractions were pooled and stored at -80°C.

Table 5 Summary of Elution Steps for Separation of γA/γA and γA/γ' from DE-52 Column

Buffer B (%)	Length (CV)
5	3.16
10	3.63
15	1.59
20	1.13
25	0.70
30	0.70
40	0.58
50	0.46
60	0.40
70	0.35
80	0.29
90	0.25
100	0.16

2.7 Quantitative PCR

To monitor the expression of the three chains in the two α-chain truncations over the course of the fibrinogen expression, α390 and α220 were seeded into nine, 10 cm dishes as described in 2.3.1. The dishes were medium changed once a week and each week one dish was harvested for mRNA with the first dish harvested following the overnight incubation in SFM. The mRNA was harvested and extracted using the RNeasy Kit (Qiagen) following the manufacturer's instructions. The extraction of mRNA, reverse transcription and subsequent quantitative (q) PCR was performed by Dr Kingsley Simpson. The concentration of the extracted and reverse transcribed cDNA was quantified on a DS-11 FX+ spectrophotometer (DeNovix; Wilmington, USA).

For the qPCR reactions, 1x SYBR green I master mix (Roche), 500 nM primer pairs and 20 ng of cDNA were prepared in a total volume of 10 µL. Primers and sequences used are shown in table 11.3. Using a Roche Lightcycler 480, samples were subjected to 10 minutes at 95 ^{o}C followed by 40 cycles of 10 seconds at 95 ^{o}C, and 30 seconds at 60 ^{o}C. After each cycle, a fluorescence measurement was taken per sample and used to calculate the crossing point (or Ct) for each sample. Samples were carried out in duplicate and the averaged Ct values were normalised to the housekeeper transcripts *Gnb1* and *Fkbp1a*. The normalised Ct values were transformed into absolute amounts of transcript (relative to the stationary housekeepers) using the 2^{-dct} method.

2.8 Initial Characterisation of Recombinant Fibrinogen

2.8.1 Native Polyacrylamide Gel Electrophoresis

Investigations using native polyacrylamide gel electrophoresis (PAGE) into the recombinant fibrinogens were to establish if there were more than one homogeneous species present within the batch and whether there was a reduction in the fibrinogen size for the truncated α-chain truncations. Using the NativePAGE system from ThermoFisher Scientific 1 µg of recombinant fibrinogen was added to 1x sample buffer and loaded onto a NativePAGE Novex 3-12 % Bis-Tris protein gel. The gel was run at first at 150 V for 60 minutes followed by an increase in voltage to 250 V for a further 60 minutes. The gel was fixed in a solution of 40 % methanol (Sigma-Aldrich) and 10 % acetic acid (Sigma-Aldrich) and heated for 45 seconds, then incubated on a shaker for 30 minutes, followed by staining with 0.02 % Coomassie Brilliant Blue R-250 dye (ThermoFisher Scientific) prepared in 30 % methanol and 10 % acetic acid, heated for 45 seconds, and incubated for an additional 30 minutes. The gel was destained with 8 % acetic acid (Sigma-Aldrich), heated again for 45 seconds and left to destain for 2 hours followed by imaging on a G:Box (Syngene; Cambridge, UK).

2.8.2 Sodium Dodecyl Sulphate Polyacrylamide Gel Electrophoresis

The integrity of the purified recombinant fibrinogen was established through sodium dodecyl sulphate-polyacrylamide gel electrophoresis (SDS-PAGE). Recombinant fibrinogen (2.5 µg) was added to 1x LDS sample buffer and 1x sample reducing agent, the final volume of 25 µL was reached by the addition of ddH_2O. The mixture was denatured at 95 °C for 10 minutes, and then placed on ice for 2 minutes before loading on a NuPAGE Novex 4-12 % Bis-Tris gel with a 5 µL molecular weight ladder (Bio-Rad laboratories Ltd; Deeside, UK). The tank was filled with 1 x NuPAGE MES SDS running buffer and ran at 160 Volts, until there was suitable separation of the ladders. The gel was removed from the cassette and briefly washed with ddH_2O and stained with Instant Blue (Sigma-Aldrich) for 2 hours. The gel was washed twice with ddH_2O for 30 minutes each before imaging on G:Box.

2.8.3 Clotability

To quantify the proportion of recombinant fibrinogens that was able to clot in each batch, a clotability assay was performed. The method was adapted from Ajjan et al., 2008. A final concentration of 0.5 mg/mL (1.47 µM) fibrinogen was prepared in Tris Buffered Saline (TBS (50 mM tris and 100 mM NaCl at pH 7.5)). Clotting was initiated with a final concentration of 0.1 U/mL human plasma purified thrombin (Merck Chemicals Ltd; stock concentration of thrombin (250 U/mL) was prepared in ddH_2O and aliquots were stored at -80°C) and 5 mM

$CaCl_2$ and then incubated at 37 °C for 2 hours. Following the incubation, the clots were centrifuged for 1 hour at 14,000 x *g*. The supernatant containing any unclotted fibrin(ogen) was removed and was quantified on the DS-11 FX+ spectrophotometer. The assay was done in triplicate, TBS was used as a blank for the before measurements (non-activated) and a mixture of 0.1 U/mL thrombin and 5 mM CaC_2 in TBS was used as a blank for the after reading (supernatant). The clotabillity was determined by equation shown in Equation 2.

$$Clotability\ \% = \left(\frac{(average\ non\text{-}activated\ at\ \ A280 - average\ A280\ of\ the\ supernatant)}{average\ non\text{-}activated\ at\ \ A280} \right) x\ 100$$

Equation 2 Equation used to Determine Recombinant Fibrinogen Clotability

2.9 Purified Characterisation of truncations

2.9.1 Fibrin Clot Formation

Fibrin polymerisation using the recombinant fibrinogen was studied by turbidimetric analysis. In a 384 well flat bottom plate (Greiner Bio-One Ltd; Stonehouse, UK), a final concentration of 0.5 mg/mL (1.47 µM) recombinant fibrinogen was diluted in TBS. An activation mix of 5 mM $CaCl_2$ and 0.1 U/mL thrombin diluted in TBS was prepared and used to initiate clotting. The addition of the activation mix to the plate was done by one vertical column at a time, leaving a 10 second gap between each lane. The plate was read at 340 nm for every 12 seconds for up to 2 hours at 37 °C on a PowerWave microplate spectrophotometer (Bio-Tek, Vermont, USA). The assay was repeated at least 3 times. For the γ'-chain truncations and γ'-chain homodimer, polymerisation was investigated in the absence or presence of FXIII which was included at a final concentration of 3.6 µg/mL and loaded at the same time as the recombinant fibrinogen.

2.9.1.1 Fibrin Clot Formation Analysis

The kinetic data collected during the assay was analysed in Microsoft Excel, where the first value was used to zero all the subsequent values and therefore the curve generated started at 0. The data was further analysed using a spreadsheet designed by Dr Fraser Macrae member of the Ariën's Lab, where the lag phase, vMAX, average rate of clotting, maximum optical density (OD), time to 50 % clotting and maximum OD was calculated. These parameters are highlighted in Figure 6.

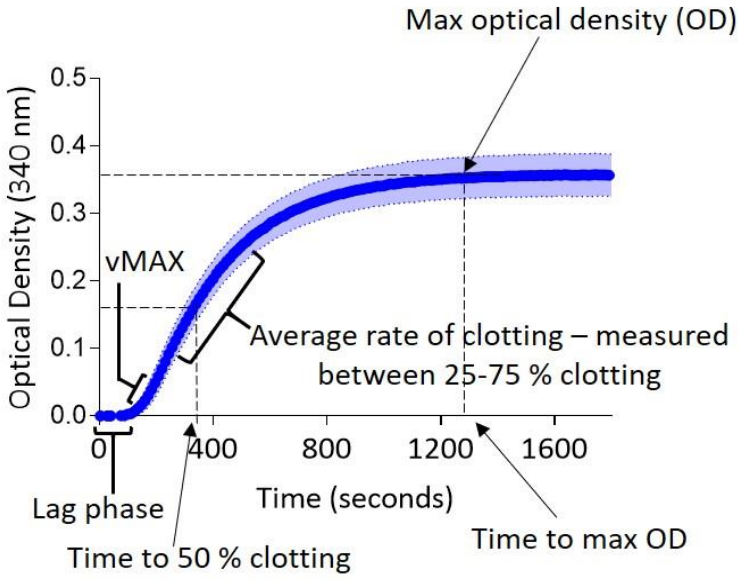

Figure 6 Parameters Studied in Fibrin Clot Formation

Parameters calculated during analysis of collected data from turbidimetric assay. Analysis of data was done in a spreadsheet designed by Dr Fraser Macrae.

2.9.2 Atomic Force Microscopy

Atomic force microscopy (AFM) was used to investigate early fibrin protofibril growth over time for the α-chain truncations. The AFM experiment and analysis in OriginLab was done by Dr Stephen Baker a member of the Ariëns lab. The surface used in the experiments was a recently cleaved mica treated for 5 minutes with 50 µL of 2 mM $NiCl_2$. Following treatment, the mica surface was rinsed with ddH_2O and dried with nitrogen gas. The activation mix to initiate fibrin polymerisation was composed of 0.05 U/mL thrombin and 2 mM $CaCl_2$, and the activation mix was added to 0.02 mg/mL (59 nM) fibrinogen in TBS. As fibrin polymerisation occurs rapidly, the samples were diluted so polymer formation could be examined at 10, 20, and 30 minutes. After each timepoint, polymerisation was stopped by diluting the polymerising mixture 3 times with TBS, after which 3 µL of the diluted mixture was immediately added to the surface of pre-treated mica for 10 seconds. Following this,

150 µL of deionised water was then placed onto the mixture on the mica surface for 10 seconds and then was dried by nitrogen gas. The polymerisation timepoints were imaged using a Nanoscope IV Dimension 3100 AFM (Bruker; Santa Barbara, USA) using the tapping mode at a scan rate of 0.8 Hz. Measurements were done in air using silicon cantilevers (TESPA-V2, Bruker) with an average radius of 7 nm. For each timepoint, five images were taken, and each time-point was repeated 3-4 times. Processing of images was carried out using NanoScope Analysis software. Images were standard flattened by the software and no resolution enhancement was done. ImageJ (Rasband, W.S., ImageJ, U. S. National Institutes of Health, Bethesda, Maryland, USA) was used to measure polymer lengths and statistical analysis was performed using OriginLab software (OriginLab Corporation; Northampton, MA, USA) and GraphPad Prism 8 (La Jolla, CA, USA).

2.9.3 Laser Scanning Confocal Microscopy

2.9.3.1 Fluorescent Labelling of Recombinant Fibrinogen

For the visualisation of the recombinant fibrinogen during laser scanning microscopy (LSCM) experiments, the recombinant fibrinogen was labelled with Alexa Fluor 488®, using the protein labelling kit from Molecular Probes (ThermoFisher Scientific). The proteins were amine coupled to the fluorescent label. One hundred micrograms of each recombinant fibrinogen were labelled. The fibrinogen was first dialysed into PBS (pH 7.4) as there was incompatibility with the kit and proteins were in Tris buffers. The fibrinogen was labelled as directed by the manufacturer's instructions. The degree of labelling of each recombinant fibrinogen was quantified by Nanodrop NB-1000 and calculated as shown in Equation 3. Once labelled, the fibrinogens were aliquoted and stored at –80 °C protected from light.

$$Degree\ of\ labelling = \frac{(A_{280}\ x\ 10) - ((A_{494}\ x10)x\ 0.11)}{1.51}$$

Equation 3 Calculation used to Determine Degree of Labelling of Recombinant Fibrinogen

A_{280} and A_{494} is the amount of absorbance detected at 280 nm and 494 nm respectively. 0.11 is the corrected factor value of labelling given by Thermofisher Scientific. 1.51 is molar extinction coefficient for fibrinogen. Molar coefficient of 1.74 and 1.66 used for α390 and α220 respectively.

2.9.3.2 Polymerisation and Influence of Fluorescent Label

To establish if the labelled corresponding fibrinogen influenced polymerisation and clot structure, a turbidimetric assay was performed comparing labelled and unlabelled fibrinogen. The assay was performed as described in 2.9.1 with the labelled comparison containing 0.025 mg/mL (0.074 μM) of corresponding labelled fibrinogen and 0.475 mg/mL (1.40 μM) fibrinogen, so the final concentration of fibrinogen was maintained at 0.5 mg/mL (1.47 μM).

2.9.3.3 Clot Structure by Laser Scanning Confocal Microscopy

The clot architecture of α- and γ'-chains truncation and γ'-chain homodimer was studied through LSCM, clots were formed in a VI flow, uncoated sterile μ-slide (Thistle Scientific; Glasgow, UK). A final concentration of 0.475 mg/mL (1.4 μM) fibrinogen prepared in TBS with the corresponding Alex Fluor 488® at a final concentration of 0.025 mg/mL (0.074 μM). Clotting was initiated by the addition of 0.1 U/mL thrombin and 5 mM $CaCl_2$ and the mixture was immediately transferred to the slide. Clots were left to form in a humidity chamber for 1 hour before taking a z-stack on a LSM880 inverted laser scanning confocal microscope (Zeiss; Cambridge, UK) using a x40 magnification oil objective. The z-stack was composed of 29 slices every 0.7 μm over 20.3 μm and taken in the middle of the clot. Random areas of the clot were imaged and at least 3 images were taken from each clot and the experiment was repeated at least 3 times. The average number of fibres count was calculated in ImageJ using an in-house macro designed by Dr Fraser Macrae. The γ'-chains truncation and γ'-chain homodimer were investigated with and without the presence of FXIII at final concentration of 3.6 μg/mL.

2.9.3.4 Influence of Thrombin on Clot Structure

Investigations into the effects of thrombin and γ'-chain homodimer on clot structure used a range of concentrations of thrombin. The clots were prepared and imaged as described in 2.9.3.3 and various thrombin activation mixes were prepared to achieve the desired range of final thrombin concentrations of 0.01, 0.05, 0.1, 0.5 and 1 U/mL.

2.9.3.5 Recombinant Fibrinogen Spiked with Fluorescent Labelled WT

To test whether the observations made with the γ'-chains truncation and γ'-chain homodimer were due to protein differences and not the fluorescent label, clots were examined using the fluorescently labelled WT at a final concentration of 0.025 mg/mL (0.074

μM). The fibrinogen concentration, activation mix, and visualisation of clots was as described in 2.9.3.3.

2.9.3.6 Recombinant WT Spiked with α-chain Truncations

To confirm that the observations made in the α-chains truncation were not due to the fluorescent label, WT clots were prepared with increasing percentage of either α390 or α220 (0, 25, 50, 75, 90 and 95 %). Fluorescently labelled WT was used for visualisation and was maintained at 0.025 mg/mL (0.074 μM/ 5 %) in all percentage variations and the final concentration of fibrinogen was maintained at 0.475 mg/mL (1.4 μM). The activation mix and visualisation of clots was as described in 2.9.3.3.

2.9.3.7 Fibrinolysis by Laser Scanning Confocal Microscopy

Following the imaging of the clots by LSCM, the clots were lysed by the addition of 20 μL lysis mix (plasminogen 0.4 μM and t-PA 6 nM in TBS) inserted to one side of the Ibidi μ-slide. The slide was held vertically for 1 minute to allow the lysis mix to infiltrate the fibrin network and the slide was imaged after 14 minutes. The lysed clot was imaged on a LSM880 inverted laser scanning confocal microscope using a x40 magnification oil objective. Following the 15 minutes incubation, the lysis front was located a combination of z-stack and time-series was initiated. The z-stack was over 20.3 μm and composed of 8 slices taken at the middle of the clot. The experiment was repeated on at least 3 occasions.

2.9.4 Clot Structure by Scanning Electron Microscopy

Recombinant fibrinogen (α-chain experiments 2.94 μM and γ'-chain experiments 1.47 μM) was clotted with 1 U/mL thrombin and 5 mM $CaCl_2$ and incubated in a humidity chamber for 2 hours. After incubation, the clots were washed three times, each wash was for 20 minutes in 0.05 M sodium cacodylate buffer pH 7.4 (Sigma-Aldrich) and fixed overnight in 2 % glutaraldehyde (Sigma-Aldrich) prepared in 0.05 M sodium cacodylate buffer. Then the following morning the fixed clots were washed a further three times with the sodium cacodylate buffer, with each wash for 20 minutes. The fixed clots were dehydrated with increasing percentage of acetone (30, 50, 70, 80, 80, 95 and 100) (Fisher Scientific). The clots were then subjected to critical-point drying and sputter-coating with 5 mm iridium using a High-Resolution Sputter Coater (Agar Scientific; Essex, UK) and carbon painted stubs, before imaging on a SU8230 Ultra-High-Resolution Scanning Electron Microscope (Hitachi; Tokyo, Japan). The critical point drying, and sample mounting was done by Mr Martin Fuller. Each clot was prepared at least 3 times and imaged across multiple random areas over a range of magnifications (x2,000, x5,000, x10,000, x20,000 and x50,000). Fibre diameter was

calculated in ImageJ using the images taken at x20,000, fibres were measured at over three points and an average was calculated, and 15 fibres were counted for each clot.

2.9.5 Fibrinolysis Assay

2.9.5.1 α-chain

2.9.5.1.1 External Fibrinolysis

For fibrinolysis experiments with the α-chain truncations, clots were formed as described in 2.9.1 after 2 hours, and a lysis mix of 1 nM t-PA and 0.24 μM glu-plasminogen was gently layered on top of the formed clot and clot lysis was monitored. Wells were read every 12 seconds for 4 hours at 37 °C at 340 nm on a PowerWave plate reader. The assay was repeated 4 times.

2.9.5.1.2 Internal Fibrinolysis with α_2-antiplasmin

Recombinant α-chain fibrinogen and WT were investigated to assess the impact of α_2-antiplasmin on fibrinolysis. In a 384 well flat bottom plate, a final concentration of 0.25 mg/mL (0.735 μM) recombinant fibrinogen was diluted in TBS. Four lysis mixes were prepared in TBS for the conditions investigated; in all conditions a final concentration of 0.24 μM glu-plasminogen was used. Lysis mix one only contained plasminogen; lysis mix two had the addition of $FXIIIA_2B_2$ at a final concentration of 1.8 μg/mL. Lysis mix three contained α_2-antiplasmin (Enzyme Research Laboratories) at a final concentration of 5.8 μg/mL and lysis mix 4 contained both α_2-antiplasmin and $FXIIIA_2B_2$ at the concentration stated above. Clotting was initiated by the addition of 5 mM $CaCl_2$, and 0.1 U/mL thrombin diluted in TBS, t-PA was also added to this mixture at a final concentration of 100 pM. The concentration of α_2-antiplasmin was based on Reed et al., 2017. The addition of the activation mix to the plate was performed as previously stated in 2.9.1. The plate was read at 340 nm for every 12 seconds for up to 8 hours at 30 °C on a PowerWave microplate spectrophotometer. The assay was repeated at least 3 times.

2.9.5.2 γ-chain

2.9.5.2.1 Internal Fibrinolysis

The fibrinolysis properties of the recombinant fibrinogens; WT, γ'-chain truncations and γ'-chain homodimer were investigated by turbidimetric analysis. In a 384 well flat-bottomed plate, a final concentration of 0.5 mg/mL recombinant fibrinogen diluted in TBS. Before the addition of the activation mix to the recombinant fibrinogen, glu-plasminogen at a final concentration of 0.24 μM was added to each well. For the γ'-chain truncations and γ'-chain

homodimer, polymerisation was investigated in the absence or presence of FXIII (final concentration 3.6 µg/mL). A final concentration of 100 pM t-PA was included in the activation mix (5 mM $CaCl_2$ and 0.1 U/mL thrombin diluted in TBS). The addition of the activation mix to the plate was carried out by pipetting the activation mix into the plate a vertical row at time leaving a 10 second gap between each lane. The plate was read at 340 nm for every 12 seconds for 4 hours at 37 °C on a PowerWave microplate spectrophotometer. The assay was repeated at least 3 times.

2.9.5.3 Fibrinolysis Analysis

The kinetic data collected during the various fibrinolysis assays was analysed in Microsoft Excel. For the α-chain external lysis, the minimum value was subtracted from all the readings and then the first value was normalised to 100 % and the subsequent values were calculated as a percentage of the first value therefore generating a curve starting at 100 %. In the fibrinolysis experiments by external lysis, the max OD value was obtained, and as per external lysis the minimum value was subtracted from all the readings, the first value was normalised to be 100 % and the subsequent values were calculated as a percentage of the first value. For internal and external fibrinolysis, the data was further analysed using a spreadsheet designed by Dr Fraser Macrae, where the average rate of lysis and time to 50 % lysis and max OD was calculated. These parameters are highlighted in Figure 7.

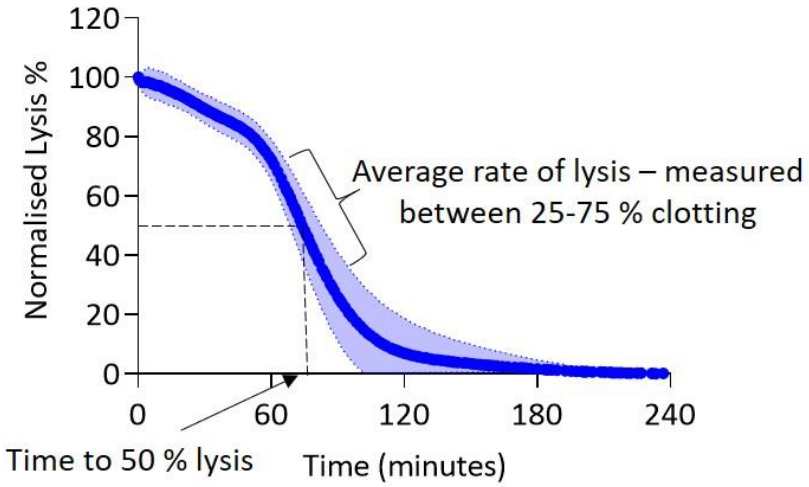

Figure 7 Parameters Calculated for Fibrinolysis

Representation of parameters calculated for external and internal fibrinolysis experiment. The data was normalised and time to 50 % lysis and average rate of lysis was calculated.

2.9.6 Micro-rheology using Magnetic Tweezers

2.9.6.1.1 Equipment Set-up

The study of the clots viscoelastic properties was achieved through magnetic tweezers. The equipment was built and designed by Dr Robert Harrand (Harrand, 2007). The instrument is composed of an inverted microscope, an iron frame containing four electromagnetics and an amplifier which generates the magnetic field. The sample sits across the objective in a holder and is in the centre of the electromagnets. The equipment has four magnetic poles named up, down, left, and right and are situated on a stage. Each pole is connected to an individual BOP 20-5M amplifier (Kepco, Inc; New York, USA), which provided the voltage to produce the magnetic field. The microscope is an Olympus IX-71 inverted microscope with a CCD camera (Olympus, UK), and is situated underneath the stage. The lens used to visualise the magnetic beads in the fibrin clot is a 40x ultra long working distance air objective, the images are measured at 25 Hz and processed by a PXI-8186 which software able to track movement (National Instruments; Texas, USA). To limit vibrations, microscope and magnetic poles are placed on a vibration reduction optical table

2.9.6.1.2 Sample Preparation

The recombinant fibrin clots were prepared in TBS with 0.5 mg/mL (1.47 μM) of fibrinogen, paramagnetic beads (4.5 μm) diluted at 1:250 (v:v) (Dynabeads M-450 Epoxy, Invitrogen, Paisley, UK) and either with or without 3.6 μg/mL of $FXIIIA_2B_2$. Clotting was initiated by a final concentration of 5 mM $CaCl_2$ and 0.1 U/mL thrombin after which the mixture was rapidly transferred to square capillary tubes (50 mm length and 0.5 diameter; CM Scientific, Bradford, UK). The ends of the capillary tube were sealed with petroleum jelly to prevent clot dehydration. The capillary tubes were gently rolled for 15 minutes to allow the paramagnetic beads to be captured in the forming fibrin matrix and not sediment to one side of the capillary tube, following rotation the clot was incubated overnight in a humidity chamber. All samples were prepared at least in triplicate.

2.9.6.1.3 Measurements

The following morning measurements were taken on the formed clot, using the “right” electromagnet and the deformation of the clots was measured for 10 minutes and up to 10 beads were measured per clot. The force applied was either 20 pN (α220 with FXIII), 40 pN (without FXIII) or 60 pN (with FXIII). LabVIEW 7.1 software was used to locate and track the magnetic beads; beads that where either close to the capillary wall or close to another bead were not selected. Dr Stephen Baker assisted with sample measurements.

2.9.6.1.4 Analysis

The analysis of data generated is processed in GraphPad Prism 8, MATLAB (MathWorks; Natick, MA, USA) and an excel spreadsheet designed by Dr Cédric Duval member of the Ariën's lab and Dr Stephen Baker. The data was exported in a .txt file from the PXI-8186 and contained the X and Y position of the bead, force applied, and the direction of the force.

The relationship between the time dependent displacement of the bead during the measurement period of 10 minutes is related to the time dependant compliance J (t), the equation is shown in Equation 4 (Allan, 2012).

$$J(t) = \frac{6\pi a x(t)}{F}$$

Equation 4 Time Dependent Compliance is Related to the Time Dependent Particle Displacement

J(t) is the time dependent compliance, a is the radius of the paramagnetic bead, x(t) is for time dependent particle displacement and F is the amplitude of the step for the force applied.

The compliance fitting of the experimental data using Equation 5 was unable to be used in GraphPad Prism therefore an approximation was used, the equation of which is shown in Equation 6. This equation was derived by Dr Marco Domingues member of the Ariën's lab.

$$J\,(t) = Jo + \sum_{1}^{n} A_n\, e^{(\frac{-t}{\tau_n})}$$

Equation 5 Compliance Fitting

J(t) is the time dependent compliance and Fitting parameters represented by J_o, τ_n and A_n. n is varied to achieve the best fit for the data.

$$Y = \frac{1}{Ko}\left(1 - \frac{K_1}{Ko + k_1}\right) e^{-x/\tau} + \frac{x}{viscosity}$$

Equation 6 Compliance Fitting Equation used in GraphPad Prism

Fitting parameters represented by K_o, k_1, viscosity and τ, x is time and Y=J(t) from Equation 4

The above equations described how to convert the time dependent compliance to frequency dependent moduli. Once Equation 4 and Equation 6 were solved, G' (storage modulus or clot stiffness) and G" (loss modulus or clot viscosity) could be extracted using Equation 7.

$$G^{*}(\omega) = G'(\omega) + iG''(\omega)$$

Equation 7 The Equation used to Solve G' and G"

For comparison, G' and G'' are determined at frequencies of 0.1, 1 and 10 Hz which were selected as they were at points where deformation events occurred once force was applied on to the fibrin clots. These deformation events corresponded to network, individual fibre, and internal fibre structures (molecular level), respectively. Tan delta, described as G"/G', was used to calculate the overall viscoelastic properties of the fibrin clots

2.9.7 Cross-linking

This method was used to examine alterations in α-chain FXIIIa cross-linking for clots made with the α-chain truncated fibrinogens. The reaction mixture composed of 5 µg of recombinant fibrinogen variants or WT and 15 µg/mL FXIIIA_2B_2 in TBS, which was mixed with 0.1 U/mL thrombin and 5 mM $CaCl_2$ to activate clotting. The reaction was stopped at 0, 2, 15, 30, 60, and 120 minutes after initiation with a stop solution containing 1x sample reducing buffer and 1x LDS sample buffer in TBS, then denatured at 95 °C for 10 minutes and incubated on ice till all time points were complete. The samples were run on a 4-12 % NuPAGE Bis-Tris gel, using the NuPAGE system as described in 2.8.2 and run at 160 Volts until adequate separation of the bands. Gels were stained with InstantBlue™ and imaged on a G:Box. Using ImageJ, the densitometry of the bands for α-, β- and γ-chain were measured. As the β-chain does not get cross-linked and therefore its migration is unchanged, the disappearance of crosslinked α-and γ-chain was measured relative to the β-chain.

2.10 Plasma Studies

2.10.1 Plasma Turbidimetric Investigations

2.10.1.1 Thrombin Initiated Turbidity

To understand the influence plasma has on the γ'-chain truncations and γ' homodimer, turbidimetric assays were performed with fibrinogen deficient plasma (Enzyme Research Laboratories). The fibrinogen deficient plasma composed 50 % of the reaction mix and was supplemented with 0.5 mg/mL (1.47 µM) recombinant fibrinogen and incubated at 37 °C for either 0, 5 or 60 minutes before inserting the solution into a 384 well plate and adding the activation mix. The activation mix was composed of 0.1 U/mL thrombin and 10 mM $CaCl_2$ (final concentrations). The loading of the activation mix in the wells was as stated in 2.9.1. The plate was read at 340 nm for every 12 seconds for 1 hours at 37 °C on a PowerWave

microplate spectrophotometer. The assay was repeated on at least 3 occasions. The experiment was analysed as described in section 2.9.1.1.

2.10.1.2 Tissue Factor Initiated Turbidity

Following the observations in the thrombin-initiated, fibrinogen-deficient plasma supplemented with γ'-chain truncations and γ' homodimer, the experiment was repeated to study the influence of tissue factor-initiated clotting. The assay was performed as stated in 2.9.1, with the activation mix composed of 30 pM of tissue factor and 10 mM $CaCl_2$ (final concentrations) instead of thrombin. The plasma was incubated for 1 hour with the recombinant fibrinogen before clotting was initiated and assay was repeated on 4 occasions. The experiment was analysed as described in section 2.9.1.1.

2.10.1.3 Afibrinogenemia Plasma

Further investigations into the influence of plasma on the γ'-chain truncations and γ' homodimer was performed with plasma from patients with afibrinogenemia reconstituted with recombinant fibrinogen variants. The plasma samples from patients with afibrinogenemia were kindly gifted by Dr Alessandro Cassini from the University of Geneva. The assay was performed as stated in 2.9.1 with the samples only incubating with the plasma for 1 hour. Each repeat was done in plasma from a different patient with afibrinogenemia and assay was repeated 3 times. The experiment was analysed as described in section 2.9.1.1.

2.10.1.4 Laser Scanning Confocal Microscopy

Structural investigations to understand influence of plasma on γ'-chain truncations and γ' homodimer was performed by using LSCM. Plasma deficient fibrinogen was used at 50 % of the final volume or fibrinogen was diluted only in TBS. Recombinant fibrinogen was added at a final concentration of 0.475 mg/mL and the corresponding recombinant Alexa Fluor 488® labelled fibrinogen was added at 0.025 mg/mL. The Alexa Fluor 488® labelling of the recombinant fibrinogen is described in section 2.9.3.1. The plasma and fibrinogen were incubated together at 37 °C for 1 hour before an activation of 0.1 U/mL thrombin and 10 mM $CaCl_2$ was used to initiate clotting, and 30 µL was transferred to a µ-slide V1 0.4 uncoated #1.5 polymer coverslip. The clots were left to form in a humidity chamber for 1 hour before viewing on a LSM880 inverted laser scanning confocal microscope, using a x40 magnification oil objective. Six random areas of the middle of the clot were imaged by a z-stack, composed of 29 slices of 0.7 µm over 20.3 µm. Clots were analysed as described in 2.9.3.3. Clots were prepared on 3 separate occasions.

2.11 *Ex-vivo* Experiments

2.11.1 FGA$^{-/-}$ Mice

All breeding, husbandry and bleeding of mice was done by Dr Cédric Duval. The mice were kept in individually ventilated cages, at 21 °C with 50-70 % humidity, 12/12 hours light/dark cycle and on standard ad libitum diet. The background of the *FGA*$^{-/-}$ mice (Suh et al., 1995), was C57BL/6, the fibrinogen deficiency was generated by crossing male *FGA*$^{-/-}$ with female *FGA*$^{+/-}$ mice, and genotypes were determined using real-time PCR (Transnetyx; Cordova, USA). All procedures were performed in agreement with accepted standards of humane animal care, approved by the ethical review committee of the University of Leeds, and conducted under license from the United Kingdom Home Office (P144DD0D6, Professor Stephen Wheatcroft).

2.11.2 Clot Contraction

To study the behaviour of the WT, γ'- and α-chain truncations, and γ'/γ' in whole blood, a clot contraction assay was performed using whole blood from *FGA*$^{-/-}$ mice. The method for clot retraction was adapted from (Aleman et al., 2014). Micro test tubes (Alpha Laboratories Ltd; Eastleigh, UK) were coated with Sigmacote (Sigma-Aldrich) for 10 minutes and then washed twice with ddH_2O and left overnight to dry. The following day whole blood was collected from *FGA*$^{-/-}$ mice into a 10 % v/v 109 mM trisodium citrate (Sigma-Aldrich) solution. The blood was diluted 1 in 3 in TBS to a final volume of 300 µL, then 0.5 mg/mL (1.47 µM) of recombinant fibrinogen was added to each glass tube. Fifteen microliters were removed for initial counts of red blood cell (RBC) and platelet numbers. Fifteen microliters of activation mix was added to the tubes, composed of tissue factor (Stago; Reading, UK) and $CaCl_2$ (1 pM and 10 mM final concentrations respectively). Two control tubes were prepared containing only diluted whole blood. To one of the two tubes 15 µL activation mix was added and to the other TBS to return the final volume to 300 µL following the removal of 15 µL for RBC and platelet incorporation assay. The tubes were incubated at 37 °C and an imaged for clot retraction at 0, 15, 30, 60, 90, and 120 minutes. After 120 minutes the clot was removed from the tube and weighed. The supernatant surrounding the contracted clot was collected to measure RBC and platelet numbers, which are inversely related to the cells incorporated into the clot. Clot contraction was measured between 60- and 120-minutes using ImageJ. The assay was repeated three times.

2.11.2.1 Platelet Incorporation by Flow Cytometry

Analysis of Platelet numbers by flow cytometry was performed by Dr Matthew Hindle member of Professor Khalid Naseem's group. To quantify the platelet incorporation into the

contracted clots, aliquots for flow cytometry were collected from non-activated samples before the addition of activation mix and activated samples after 120 minutes. Samples were diluted 1 in 10 in modified Tyrodes buffer (150 mM NaCl, 5 mM HEPES (Sigma-Aldrich), 0.55 mM $NaH2PO_4$ (Sigma-Aldrich), 7 mM $NaHCO_3$ (Sigma-Aldrich), 2.7 mM KCl (Sigma-Aldrich), 0.5 mM $MgCl_2$ (Sigma-Aldrich), 5.6 mM glucose (Sigma-Aldrich) at pH 7.4) and then stained with 5 µg/mL anti-CD41-AF488 clone MWReg30 (α-chain) and CD41-APC700 clone MWReg30 (γ'-chain studies) (BioLegend; London, UK) for 15 minutes. Following incubation, the sample was further diluted (1:100 in PBS). CD41 is marker integrin $\alpha_{IIB}\beta_3$, which is composed of two subunits αIIb (CD41) and β3, this integrin binds to fibrinogen via the γ-chain (Farrell et al., 1992). Samples were applied to a CytoFLEX RUO flow cytometer (Beckman Coulter) at a flow rate of 10 µL/minute for 2.5 minutes where CD41 positive events were acquired and relative events/µL were compared using CytExpert (2.1; Beckman Coulter).

2.11.2.2 Red Blood Cell Incorporation

Red blood cell incorporation into the contracted clot was analysed by measuring the haemoglobin in haemolysed samples from non-activated samples and the supernatant from activated samples collected after 120 minutes. Samples were diluted (1 in 100 and 1 in 200) in ddH_2O and incubated for 30 minutes to allow haemolysis and sample absorbance was read at 415 nm on a PowerWave HT Microplate. RBC incorporation in the clot was calculated as shown in Equation 8.

$$RBC\ incorporation\ (\%) = \left(\frac{(average\ non\text{-}activated - average\ of\ the\ activated)}{average\ non-activated} \right) x\ 100$$

Equation 8 Equation used to Calculate Red Blood Cell Incorporation into Blood Clots

2.11.3 Rotational Thromboelastometry

Investigations into whole blood clot formation and clot firmness for clots made with α-chain, γ'-chain truncations and γ' homodimer fibrinogens were performed using a ROTEM Delta (Werfen Limited, Warrington, UK). In all assays, clotting was initiated through the extrinsic pathway, with tissue factor used as the agonist. Investigation into the γ'-chain used EXTEM and FIBTEM tests and for the α-chain investigations EXTEM and APTEM were used. Additionally, the EXTEM test with the addition of t-PA (final concentration of 5 nM) was used to examine fibrinolysis of γ'-chain. The EXTEM test is influenced by fibrinogen, platelets, and the extrinsic coagulation factors. Whereas FIBTEM allows investigation of fibrinogen function, as the platelet function is inhibited by cytochalasin D which inhibits actin

polymerisation therefore blocking the platelet effect on clot formation. APTEM test allows investigation of hyperfibrinolysis within the clot, with the EXTEM test as the base of the assay and with the addition of aprotinin to prevent fibrinolysis. *FGA*$^{-/-}$ mice were bled as described in 2.11.1, the collected blood was combined with the recombinant fibrinogen at a final concentration of 0.5 mg/mL (1.47 µM) for EXTEM and APTEM and 1 mg/mL for FIBTEM. The ROTEM® Cup and Pin mini system was used for all the assays. The cup was prepared containing the relevant substrate for the test, for EXTEM (7 µL of EXTEM and 7 µL STARTEM), APTEM (7 µL of EXTEM and 7 µL APTEM) and for FIBTEM (7 µL of EXTEM and 7 µL of FIBTEM). The recombinant fibrinogen was added to 91 µL of whole blood and 105 µL of the mixture was transferred to the cup and the assay was immediately started. Data was collected over the course of 1 hour, and all assays were repeated 3 times. *FGA*$^{-/-}$ whole blood without addition of recombinant fibrinogen was performed for each test to confirm that there was no fibrinogen in the whole blood to influence the assay. The clot contents of the cups were collected afterwards for scanning electron microscopy (SEM) analysis.

2.11.3.1 Measurement Parameters

The parameters generated on the ROTEM used in analysis for α- and γ'-chain truncations and γ'-chain homodimer were clotting time (seconds), maximum clot firmness (mm), shear elastic modulus (G) (EXTEM, APTEM, FIBTEM) and with the addition of t-PA to EXTEM assay, lysis time (seconds) and lysis on set time (seconds). Clotting time is the time from the test start until an amplitude of 2 mm is reached. Maximum clot firmness is the maximum amplitude reached by the sample. Shear elastic modulus is calculated by equation shown in Equation 9. The lysis on set time is the time from clotting time to the start of significant lysis, the significant lysis is defined as a decrease of the maximum clot firmness amplitude by 15 %. Lysis time is the time from clotting time, until the clot firmness is decreased to 10 % of maximum clot firmness during fibrinolysis. ROTEM assay software provided no values for shear elastic modulus in EXTEM investigations into γ'-chain.

$$G = \frac{5000MCF}{(100 - MCF)}$$

Equation 9 Equation used to Calculate Shear Elastic Modulus in ROTEM Assay

Maximum clot firmness is defined as MCF in equation.

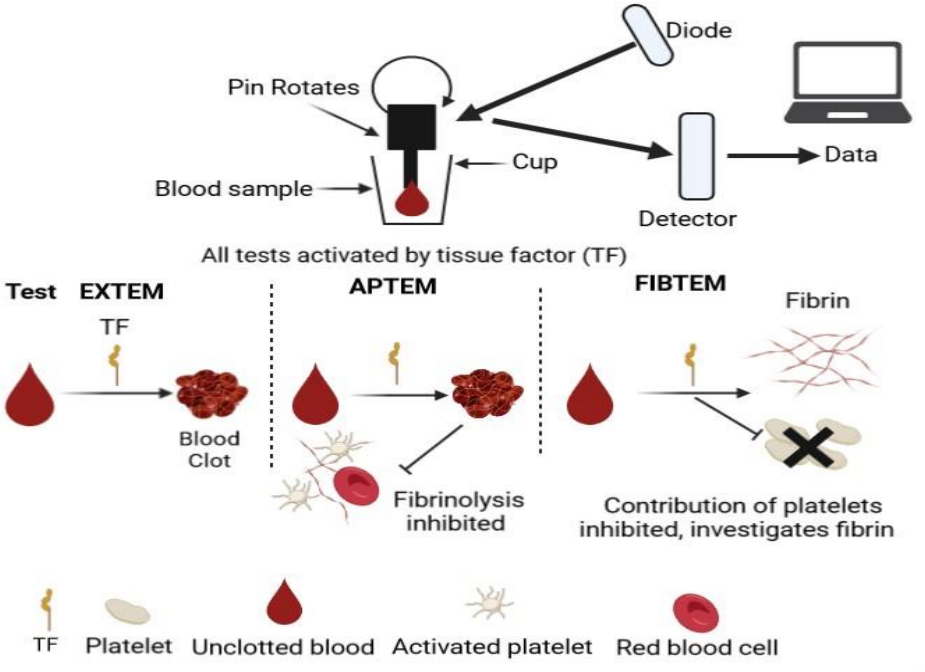

Figure 8 Schematic of ROTEM method and Tests used

The pin rotates with the blood sample, and when the blood clots there is increased resistance for the pin's movement within the cup. The three tests used for investigation of clotting are all initiated by extrinsic pathway. EXTEM is the standard, APTEM includes a fibrinolysis inhibitor and is thus used to investigate fibrinolysis potential and FIBTEM includes a platelet inhibitor and is thus used to study the contribution of fibrin. Image created in Biorender.

2.11.3.2 Scanning Electron Microscopy

The clots were harvested after ROTEM analysis and were transferred to 0.5 mL tubes. Numerous holes were made on the lid and to the body of the tube, to allow permeation of glutaraldehyde solution. The harvested clots were fixed overnight in 2.5 % glutaraldehyde prepared in 0.9 % NaCl (VWR International). The following morning, clots were washed 3 times with fresh 0.05 M sodium cacodylate for 40 minutes each. The clots were then dehydrated with increasing percentage of acetone (30, 50, 70, 80, 90, 95 and 100) for 15 minutes, followed by 2 further washes in 100 % acetone. The clots were critical-point dried, coated, and imaged as described in 2.9.4.

2.11.4 Platelet Fibrinogen Interactions

The interaction between recombinant fibrinogen and platelets was investigated using flow cytometry. *FGA*$^{-/-}$ whole blood was supplemented with recombinant fibrinogen (WT, α390, α220, γ'/γ' or γ'0) or plasma purified γAγ'. Fibrinogen γ'/γ', γ'0 and γAγ' were used as

controls as both γ'/γ' and γ'0 lack the C-terminal AGDV residues, and γAγ' contains the AGDV site at one half of the fibrinogen molecule. The AGDV residues are known to bind to the platelet integrin $\alpha_{IIB}\beta_3$ (Farrell et al., 1992). To maintain a physiological setting and interactions, the ratio of platelet number and fibrinogen concentration was kept constant. The experiment was performed and analysed by Dr Lih Cheah a member of Professor Khalid Naseem's group.

The various fibrinogens (15 µg) were diluted in modified Tyrodes buffer. An antibody staining cocktail of 60 µg/mL anti-fibrinogen FITC (Agilent Technologies; Cheadle, UK), 10 µg/mL CD62P-PE (clone RMO-1), 5 µg/mL CD63-APC (clone NVG-2), 5 µg/mL CD41-AF700 (clone MWReg30) (BioLegend) was prepared. The cocktail mix contained a marker against fibrinogen, two markers for platelet activation (surface expression of α-granule secretion (CD62P/P-Selectin) and lysosomal glycoprotein from dense granules (CD63)) and a marker for integrin $\alpha_{IIB}\beta_3$, which is composed of two subunits αIIb (CD41) and β3. The antibody staining cocktail was added to the fibrinogen followed by one of the various agonists PAR4 (200 µM) or ADP (1 or 10 µM) or no agonist for basal activity of platelets. Five micro-litres of whole blood collected in 10 % v/v 109 mM trisodium citrate from *FGA*$^{-/-}$ mice was added to cocktail/fibrinogen mixed and then rapidly agitated and incubated 20 minutes in the dark. After incubation the samples were fixed 1 % paraformaldehyde in PBS.

There were two types of isotype negative controls used, isotype controls (either IgE-PE (clone MOPC-173) and IgG-APC (clone RTK 2758)) which are primary antibodies but do not have specificity to the target and used to differentiate from non-specific background signal, and EDTA (10 mM). The $\alpha_{IIB}\beta_3$ integrin is calcium dependant therefore the EDTA control can chelate the calcium and prevent binding of fibrinogen. The fixed samples were run on a 2-laser 4-detector CytoFLEX RUO flow cytometer, using a combination of CD41 positive signal and characteristic SSC/FFC profiles to gate the platelets. For each sample, 10,000 positive events were recorded, and the assay was repeated 3 times. The analysis was performed using CytExpert (2.1) to obtain the median fluorescence intensity (MFI) values and to calculate percentage positive cells based on 2 % gates on the background fluorescence of the controls.

2.12 Statistical Analysis

Initial data preparation was performed in Microsoft excel and then data was exported for production of graphs and statistical analysis in GraphPad Prism 8 (La Jolla, CA, USA). Data was tested for normality before statistical analysis by one- or two-way ANOVA or Kruskal-Wallis test, followed by post-hoc test of Dunnett, Dunn, or Šídák multiple comparison test or Gieisser-Greenhouse correction with Dunnett multiple comparison test. In all data sets,

the results were compared to the WT or pre-treatment sample (clot contraction assay, RBC and platelet incorporation). The statistical tests used for each experiment is detailed in the respective figure legend with the number of experiments. The error bars are shown as ± standard deviation in all experiments except for early fibrin polymers length which are shown as ± interquartile range. A *p* value below 0.05 was considered as statistically significant.

Chapter 3 Generation and Expression of Recombinant Fibrinogen

3.1 Introduction

To investigate characteristics of the fibrinogen αC-region and the role of the fibrinogen γ'-chain in this thesis, a number of truncations were made to either the α- or γ'-chain, respectively. This chapter describes how these truncations were designed, produced, and purified.

Production of variant recombinant fibrinogens has previously been used to investigate different features of fibrinogen such as polymerisation (Gorkun et al., 1998), protein-protein and protein-cell interactions (Farrell et al., 1992; Farrell and Al-Mondhiry, 1997; Duval et al., 2014; Litvinov et al., 2016) as well as function (Collet et al., 2005; Standeven et al., 2007). Many of these investigations have produced recombinant fibrinogen by expression in CHO cells (Gorkun et al., 1998; Collet et al., 2005; Duval et al., 2014). An early expression system of human fibrinogen was set up by Lord et al. in *E. coli* containing the individual chains, with the α-chain expressed first followed by the β-chain and then the γ-chain (Lord, 1985; Bolyard and Lord, 1988; Bolyard and Lord, 1989).

Over the years, three different cell types have been used for the expression of recombinant human fibrinogen, namely baby hamster kidney (BHK), COS-1 (CV-1 in origin and carrying the SV40 genetic material), and CHO cells. The above cell types are all mammalian cells that have been used to express fibrinogen. As fibrinogen is a large multichain protein with multiple post-translational modifications (PTM), it is not suited to be produced in bacterial, as PTM occur in relatively low number of bacterial proteins and have low levels of modification (Macek et al., 2019). Fibrinogen has been expressed in yeast using the *Pichia pastoris* strain SMD1168 as the WT strain (GTS115) resulted in degradation of the fibrinogen, in addition there were differences in PTM of produced fibrinogen compared to plasma but it was biologically active (Tojo et al., 2008).

The first system that produced biologically fully active recombinant fibrinogen was reported in BHK cells (Farrell et al., 1991). Recombinant fibrinogen was produced by transfecting the BHK cells using calcium phosphate followed by glycerol shock treatment, with the fibrinogen α- and γ-chain cDNA encoded on a pAG-1 plasmid and the β-chain on a pBD-1 plasmid. The recombinant fibrinogen was assessed alongside fibrinogen naturally secreted by HepG2 (hepatoblastoma) cells (López-Terrada et al., 2009). No difference in protein activity as

investigated by clotting and cross-linking assays, or the size of the fibrinogens on SDS-PAGE, were observed when comparing these fibrinogens.

A subsequently published CHO transfection method also used calcium phosphate followed by glycerol shock treatment to transfect the cells (Binnie et al., 1993; Lord et al., 1993). In contrast to the method described by Farrell et al., 1991, the cDNA encoding the fibrinogen chains was placed on separate plasmids; pMLP Aα, pMLP Bβ and pMLP γ. The initial transfection with pMLP Aα and pMLP γ made use of co-transfection with an additional pRSV neo plasmid for selecting transfected cells. The cells with the highest levels of both α- and γ-chain expression were then co-transfected with pMLP Bβ and pMSV-His to produce recombinant fibrinogen. The recombinant fibrinogen produced was assessed for size and clotting properties and compared to plasma purified fibrinogen showing no difference. In contrast to the expression in the BHK and CHO cells, COS-1 cells have been transiently transfected with the three plasmids at the same time via calcium phosphate followed by glycerol shock (Hartwig and Danishefsky, 1991). Even though the focus of this publication was on fibrinogen assembly, the authors nevertheless showed that the recombinant fibrinogen produced by the COS-1 cells could form the expected fibrin clots. Secreted and clottable fibrinogen was also produced in COS-1 cells by Roy et al 1990; in which stable fibrinogen expression constructs were established.

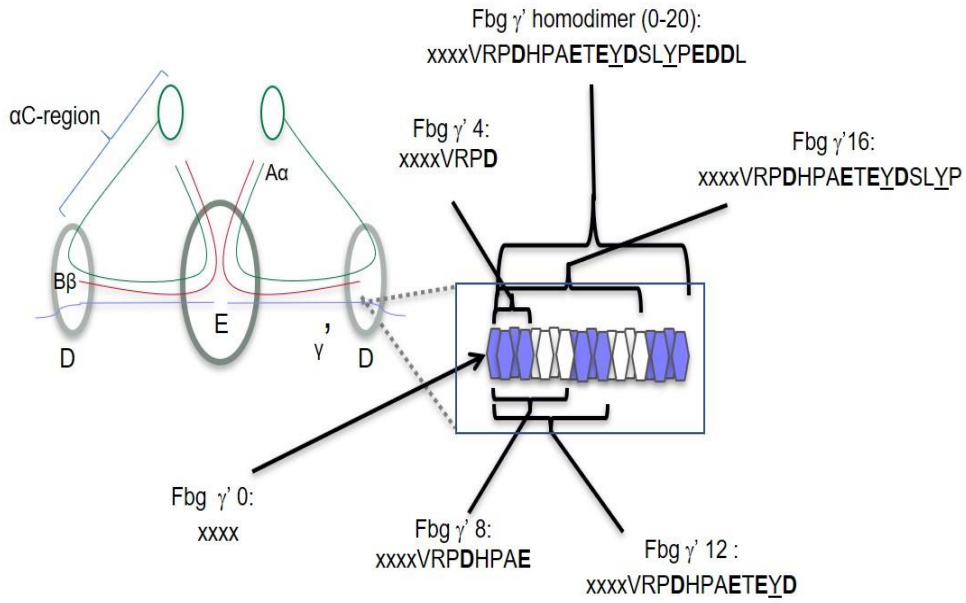

Figure 9 Schematic of Fibrinogen (Fbg) γ', Highlighting the γ'-chain and the γ'-chain Truncations Produced in CHO cells.

Each truncation of the γ'-chain is four residues shorter, with γ'0 containing neither the γ'-chain residues nor the final four residues of γA. Amino acid residues shown in bold are negatively charged and residues underlined are known to be sulphated.

The recombinant variants developed and described in this thesis basically followed the method, used the plasmids and the CHO-fibrinogen WT cells described in Binnie et al., 1993; and Lord et al., 1993. All the recombinant fibrinogens expressed were homozygous for the truncations. For the investigation in to the γ'-chain, 5 truncations were established as well as a γ' homodimer, these truncations are shown in Figure 9. The truncations are termed γ'16, γ'12, γ'8, γ'4 and γ'0. γ'16 is the longest of the truncations containing 16 out of the 20 residues which constitute the γ' extension, while the other truncations are each 4 residues shorter, with γ'0 being the shortest. γ'0 has neither the γ' extension nor the final 4 residues of the prevalent γA chain (AGDV) as these are lost in the splicing to produce γ'.

For the investigations into the αC-subdomains, two truncations were generated in the α-chain cDNA, termed α390 and α220. In α390 fibrinogen, the αC-domain was removed while preserving the αC-connector, whereas α220 fibrinogen was truncated at the start of the αC-region, therefore both the αC-domain and αC-connecter are deleted in this latter variant. Figure 10 shows a schematic of the representative fibrinogens produced by recombinant expression (WT, α390 and α220) and comparing the α-chains of the WT and α-truncations, highlighting important interaction sites with other functional protein partners.

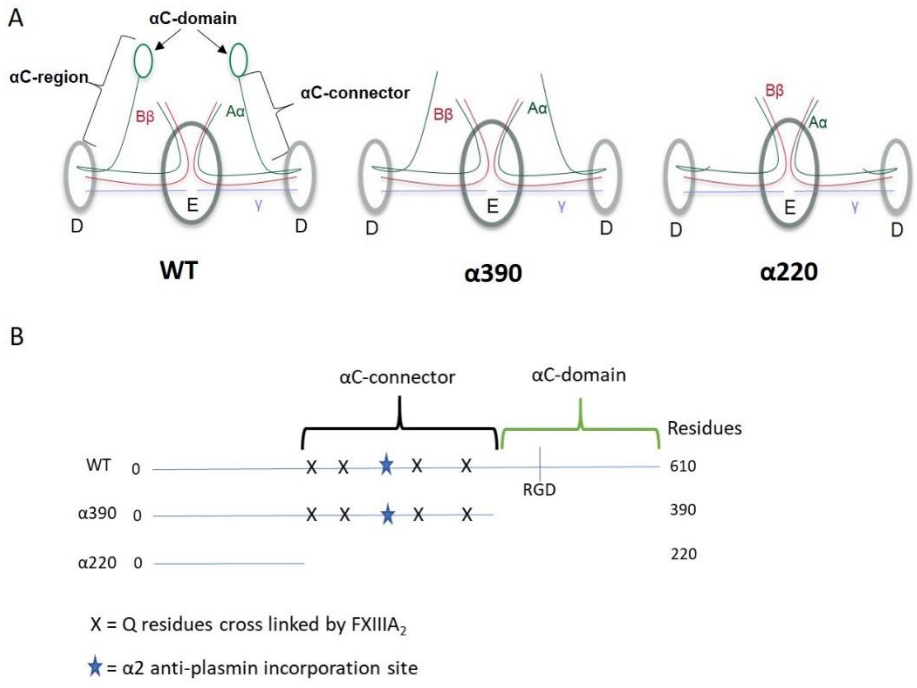

Figure 10 Schematic of α-chain Truncations α390 and α220 Compared to WT

Diagram of WT Fibrinogen (left), α390 (centre) and α220 (right) revealing the loss of the α-chain in each of the truncations (A). Representation of the α-chain highlighting the αC-domain, αC-connector, difference in length, loss of $FXIIIA_2$ glutamines (Q) cross-linking site and α2 anti-plasmin incorporation site (B).

3.1.1 Aims

The main aim of this chapter was to produce and purify specific recombinant fibrinogens with mutations of the α-chain and γ'-chain using CHO cells.

3.2 Results

3.2.1 Establishing pMLP γ'

To establish the pMLP γ' plasmid, a restriction digestion was performed on two plasmids; a pMLP D-domain γ' plasmid created by Dr Shirley Uitte de Willige and the pMLP γA plasmid kindly given by Dr Susan Lord using the restriction enzymes Xbal and Bst XL. The acquisition of γ'-chain was achieved by removing the C-terminal end of the γ'-chain protein from the pMLP D-domain γ' plasmid and ligating it into the pMLP γA plasmid, following the removal of the γA sequence. The restriction sites and plasmids sequence are shown in appendix 11.4, Figure 65 and Figure 66. The extracted γ' was ligated into the pMLP γA plasmid by T4 ligase, transformed into DH5α cells and grown on LB ampicillin plates. The plasmids were extracted and sequenced for the expected cDNA of fibrinogen γ', and no alterations were found in the nucleotide sequence. Figure 11 shows the protein sequence for pMLP γ' aligned to the expected protein sequence, the γ' sequence is highlighted in orange.

```
FGG'      MSWSLHPRNLILYFYALLFLSSTCVAYVATRDNCCILDERFGSYCPTTCGIADFLSTYQT
pMLP γ'   MSWSLHPRNLILYFYALLFLSSTCVAYVATRDNCCILDERFGSYCPTTCGIADFLSTYQT
          ************************************************************
FBG'      KVDKDLQSLEDILHQVENKTSEVKQLIKAIQLTYNPDESSKPNMIDAATLKSRKMLEEIM
pMLP γ'   KVDKDLQSLEDILHQVENKTSEVKQLIKAIQLTYNPDESSKPNMIDAATLKSRKMLEEIM
          ************************************************************
FBG'      KYEASILTHDSSIRYLQEIYNSNNQKIVNLKEKVAQLEAQCQEPCKDTVQIHDITGKDCQ
pMLP γ'   KYEASILTHDSSIRYLQEIYNSNNQKIVNLKEKVAQLEAQCQEPCKDTVQIHDITGKDCQ
          ************************************************************
FBG'      DIANKGAKQSGLYFIKPLKANQQFLVYCEIDGSGNGWTVFQKRLDGSVDFKKNWIQYKEG
pMLP γ'   DIANKGAKQSGLYFIKPLKANQQFLVYCEIDGSGNGWTVFQKRLDGSVDFKKNWIQYKEG
          ************************************************************
FGG'      FGHLSPTGTTEFWLGNEKIHLISTQSAIPYALRVELEDWNGRTSTADYAMFKVGPEADKY
pMLP γ'   FGHLSPTGTTEFWLGNEKIHLISTQSAIPYALRVELEDWNGRTSTADYAMFKVGPEADKY
          ************************************************************
FGG'      RLTYAYFAGGDAGDAFDGFDFGDDPSDKFFTSHNGMQFSTWDNDNDKFEGNCAEQDGSGW
pMLP γ'   RLTYAYFAGGDAGDAFDGFDFGDDPSDKFFTSHNGMQFSTWDNDNDKFEGNCAEQDGSGW
          ************************************************************
FGG'      WMNKCHAGHLNGVYYQGGTYSKASTPNGYDNGIIWATWKTRWYSMKKTTMKIIPFNRLTI
pMLP γ'   WMNKCHAGHLNGVYYQGGTYSKASTPNGYDNGIIWATWKTRWYSMKKTTMKIIPFNRLTI
          ************************************************************
FGG'      GEGQQHHLGGAKQVRPEHPAETEYDSLYPEDDL
pMLP γ'   GEGQQHHLGGAKQVRPEHPAETEYDSLYPEDDL
          *********************************
```

Figure 11 Sequence Alignment Between FGG' and pMLP γ'

The amino acid sequence alignment showed no alterations compared to FGG'. The γ' amino acid sequence is highlighted in orange, the signal peptide lost in the mature protein is highlighted in red and matched residues are shown by *.

3.2.2 Generation of Truncated Plasmid for the α- and γ'- chain

To achieve the desired truncations in the sequence, primers were designed to establish stop codons at the desired locations in either pMLP γ' and pMLP Aα for the 5 γ'- or 2 α-chain truncations respectively. Following site directed mutagenesis, Dpn1 was added to each tube to digest the methylated parent plasmid to prevent transformation with the original template. The Dpn1 treated plasmids were transformed in XL-1 Blue competent cells, and then plated on ampicillin containing LB plates. The following morning the clones were picked, and the plasmids were extracted and sequenced for the desired changes. Clones harbouring the desired changes were selected for large scale plasmid extraction and the cDNA sequence was verified again before transfection into CHO cells. Figure 12 shows the sequence of pMLP γ'16; no unwanted changes to amino acid sequence were incorporated and the desired stop codon for truncation was present. Sequence alignment for the remaining truncations is shown in appendix 11.6, as with pMLP γ'16, there were no unwanted alterations in amino acid sequences for each construct and the stop codon was always located at the desired position.

```
FGG'          MSWSLHPRNLILYFYALLFLSSTCVAYVATRDNCCILDERFGSYCPTTCGIADFLSTYQT
pMLP γ'16     MSWSLHPRNLILYFYALLFLSSTCVAYVATRDNCCILDERFGSYCPTTCGIADFLSTYQT
              ************************************************************
FGG'          KVDKDLQSLEDILHQVENKTSEVKQLIKAIQLTYNPDESSKPNMIDAATLKSRKMLEEIM
pMLP γ'16     KVDKDLQSLEDILHQVENKTSEVKQLIKAIQLTYNPDESSKPNMIDAATLKSRKMLEEIM
              ************************************************************
FGG'          KYEASILTHDSSIRYLQEIYNSNNQKIVNLKEKVAQLEAQCQEPCKDTVQIHDITGKDCQ
pMLP γ'16     KYEASILTHDSSIRYLQEIYNSNNQKIVNLKEKVAQLEAQCQEPCKDTVQIHDITGKDCQ
              ************************************************************
FGG'          DIANKGAKQSGLYFIKPLKANQQFLVYCEIDGSGNGWTVFQKRLDGSVDFKKNWIQYKEG
pMLP γ'16     DIANKGAKQSGLYFIKPLKANQQFLVYCEIDGSGNGWTVFQKRLDGSVDFKKNWIQYKEG
              ************************************************************
FGG'          FGHLSPTGTTEFWLGNEKIHLISTQSAIPYALRVELEDWNGRTSTADYAMFKVGPEADKY
pMLP γ'16     FGHLSPTGTTEFWLGNEKIHLISTQSAIPYALRVELEDWNGRTSTADYAMFKVGPEADKY
              ************************************************************
FGG'          RLTYAYFAGGDAGDAFDGFDFGDDPSDKFFTSHNGMQFSTWDNDNDKFEGNCAEQDGSGW
pMLP γ'16     RLTYAYFAGGDAGDAFDGFDFGDDPSDKFFTSHNGMQFSTWDNDNDKFEGNCAEQDGSGW
              ************************************************************
FGG'          WMNKCHAGHLNGVYYQGGTYSKASTPNGYDNGIIWATWKTRWYSMKKTTMKIIPFNRLTI
pMLP γ'16     WMNKCHAGHLNGVYYQGGTYSKASTPNGYDNGIIWATWKTRWYSMKKTTMKIIPFNRLTI
              ************************************************************
FGG'          GEGQQHHLGGAKQVRPEHPAETEYDSLYPEDDL
pMLP γ'16     GEGQQHHLGGAKQVRPEHPAETEYDSLYP----
              ****************************
```

Figure 12 Sequence Alignment of pMLP γ'16 Compared to Reference

The amino acid sequence alignment showed no difference in sequence compared to reference, until the desired loss of the final four residues to establish pMLP γ'16. The γ' amino acid sequence is highlighted in orange, the signal peptide lost in the mature protein is highlighted in red and matched residues are shown by *.

3.2.3 Generation of Clones Expressing Variants of Fibrinogen

The clones for the fibrinogen variants were transfected, employing calcium phosphate, into CHO cells containing either the β- and γ-chains for the α truncations or the α- and β-chains for the γ' variants. Since the pMLP plasmid contains the adenovirus major late promoter but does not carry a mammalian selection marker, a pMSV-His plasmid was co-transfected which encodes resistance to L-histidinol. Two concentrations of pMLP plasmid were used for transfection and the transfection efficiency was increased by glycerol shock of the cells. The control plate was also glycerol shocked and used as a selection control. The cells were incubated for 48 hours before seeding in-order to select single cell colonies. The following day, the medium was changed to contain L-histidinol. Twenty-four resistant single cell clones were picked, and a two-step method was employed for clone selection, the initial step with medium containing serum followed by a second step without serum, as during large-scale expression cells are without serum for period of 6-8 weeks.

3.2.3.1 Initial Fibrinogen Expression in Clones

The picked single cell colonies were grown in a 24 well plate and the medium was harvested either once the well became confluent or after 1 week. The harvested medium was tested for fibrinogen expression by ELISA. Table 6, Table 7 and Table 8 show the concentration of fibrinogen in the medium of the clones for the γ' transfections at 10µg, 20µg and α-chain transfections respectively. The clones which were taken forward for further investigation in serum free medium are highlighted. The criteria for selection were a combination of high level of expression and cell confluence

3.2.3.2 Fibrinogen Expression in Serum Free Medium

To confirm that the clones will secrete fibrinogen in the conditions used for large-scale expression, the selected clones from the initial assessment were grown to confluence and the growth medium was change to SFM. Clones were tested in SFM as the production stage the cells are maintained in the same roller bottle in SFM for up to 8 weeks therefore in is important to confirm that clones will still express in SFM. In addition, there are low levels of bovine fibrinogen in the serum (FBS), and this would contaminate the produced recombinant fibrinogen and likely be co-purified with the produced fibrinogen.

The cells were incubated for 1 week before medium was harvested to assess the levels of expression by ELISA. Table 9 and Table 10 show the γ'- and α-chain variants expression levels respectively, clones chosen for high-level expression are highlighted. CHO cells have a population doubling time of 24 hours (DSMZ ACC110 https://www.dsmz.de/dsmz), therefore a cut off 1 week was used to collect medium. A balance was attained between fibrinogen expression per cell and population growth time as large number of cells was needed to seed and colonises the roller bottles.

Table 6 Initial Investigation into Fibrinogen Expression of CHO Cells Expressing γ'/γ' and γ'-chain Truncations Transfected with 10 µg of Respective cDNA

Clones highlighted (green) were selected for further investigation. No cells were observed in blank wells. Cells were picked between day 1 and 7.

10 µg	γ'			γ'16			γ'12			γ'8			γ'4			γ'0		
	ng/mL	Confluency %	Picked (Day)	ng/mL	Confluency %	Picked (Day)	ng/mL	Confluency %	Picked (Day)	ng/mL	Confluency %	Picked (Day)	ng/mL	Confluency %	Picked (Day)	ng/mL	Confluency %	Picked (Day)
1	13.0	20	7	99.7	85	6	2.6	70	2	10.5	65	7	37.2	50	7	29.2	40	6
2	22.2	30	7	19.8	80	4			-			-	10.1	50	5	7.7	50	6
3	21.4	65	4	51.0	70	6	153.6	100	5	8.8	85	6	151.2	100	2	65.3	70	6
4	14.6	70	3	38.1	40	6			-	22.8	85	6			-	9.8	75	5
5	28.5	35	7	8.9	65	5	57.4	90	7	6.6	100	6			-	41.9	70	4
6	39.7	70	4	54.0	70	5	3.4	60	2	13.2	70	7			-	18.2	75	5
7	24.9	70	4			-	4.6	100	5	24.3	60	6	12.4	70	5	10.9	80	5
8	46.8	75	4	29.9	70	5	59.9	80	2			-	6.9	100	5			-
9	81.0	75	3	76.3	80	5	45.4	100	5	18.9	90	6	11.8	60	7	45.2	75	5
10	16.7	100	7	29.1	80	5	34.1	80	5	14.1	60	6			-			-
11	16.6	70	4	52.8	90	4	26.7	60	5	42.2	45	7	12.1	50	7	6.7	80	5
12	19.1	100	7	13.7	70	5			-	9.1	90	4	113.6	100	2	14.7	75	5
13			-	27.5	80	5			-	3.2	70	2	12.7	75	5	8.5	85	5
14	77.5	100	7	125.9	80	5	38.9	80	5	7.8	100	2			-	52.1	70	4
15	114.4	40	7	22.9	70	4	4.4	30	5	81.3	100	2	6.8	70	5	8.1	65	6
16	212.1	60	7	16.6	70	4	27.1	70	7	9.5	60	2	36.7	100	7	61.1	80	6
17	23.2	100	7	9.1	70	4			-	41.1	80	6	6.7	70	5	9.9	80	6
18	214.4	55	4	11.3	75	4			-	53.5	45	7	9.3	70	5	8.4	85	6
19	105.7	90	3	18.2	90	5	2.8	100	2	22.3	70	4	9.6	20	7	16.8	55	6
20	195.2	100	7	9.4	70	5			-	109.2	100	7			-	7.4	75	5
21	15.1	100	7	86.5	80	5	7.2	70	7	16.8	90	2				72.1	80	5
22	162.1	90	7	10.4	70	6			-	84.5	100	2	6.7	100	2	7.5	75	5
23			-	112.7	75	5	10.4	100	5	6.8	80	6			-	17.5	80	5
24			-	9.1	60	6			-			-	6.6	70	5	144.7	70	5

Table 7 Initial Investigation into Fibrinogen Expression of CHO Cells Expressing γ'/γ' and γ'-chain Truncations Transfected with 20 µg of Respective cDNA

Clones highlighted (green) were selected for further investigation. No cells were observed in blank wells. Cells were picked between day 1 and 7.

20 µg	γ'			γ'16			γ'12			γ'8			γ'4			γ'0		
	ng/mL	Confluency %	Picked (Day)	ng/mL	Confluency %	Picked (Day)	ng/mL	Confluency %	Picked (Day)	ng/mL	Confluency %	Picked (Day)	ng/mL	Confluency %	Picked (Day)	ng/mL	Confluency %	Picked (Day)
1	248.8	100	7	73.9	80	5	82.0	100	5	2.8	80	2			-	10.7	80	5
2	48.8	70	3	88.1	100	5	12.7	100	5	3.2	100	5	114.6	60.00	7	68.1	70	6
3	207.4	100	7	26.4	90	5	83.5	100	5	33.0	100	5	95.2	80.00	7			-
4	204.3	100	7	14.7	90	5	3.4	20	5	3.3	90	5			-			-
5	28.8	90	3	58.8	70	6	2.8	100	7	2.9	100	5	79.4	100.00	2			-
6	40.8	80	3	32.1	70	6	13.1	75	5	3.1	100	5	60.5	50.00	7	9.2	80	4
7	51.0	60	4	164.7	90	6	7.9	75	5	5.5	35	7	118.7	50.00	5	27.9	40	6
8	176.4	100	4	78.2	50	6	6.8	75	5	56.2	100	5	38.3	70.00	7	80.8	80	5
9	41.3	70	6	104.8	80	5	12.1	100	7	3.3	70	2	10.5	70.00	7	29.6	70	6
10	126.8	90	7	71.6	65	5	18.3	35	5	3.6	70	5	50.7	65.00	2	188.5	70	5
11	18.3	70	7	24.8	70	4	123.9	60	6	3.6	70	5	9.1	100.00	5	12.1	85	5
12	20.1	40	7	95.7	80	5	17.5	50	6	22.4	90	5	110.3	85.00	5	10.5	70	4
13	67.8	80	7	13.2	50	4	32.2	95	5	7.3	20	7	10.0	100.00	5	68.4	80	5
14	196.8	100	7	36.3	80	5	10.8	70	7			-	69.8	100.00	7			-
15			-			-	43.5	95	5			-	36.2	80.00	7	68.6	75	5
16			-	20.1	70	5			-			-	12.1	80.00	5	29.1	80	5
17	200.6	100	7	112.2	80	5	134.6	90	2	2.8	10	2	28.1	70.00	7	14.8	80	4
18	52.0	60	7	60.6	70	4	12.3	90	5	8.2	100	5	155.1	75.00	7	93.4	80	5
19	23.0	50	7	160.8	80	5	5.6	60	2	13.4	100	7			-	29.8	75	6
20	13.0	100	7	64.5	80	4	4.2	60	2	3.6	90	2	73.1	85.00	2	27.8	70	4
21			-			-	3.0	70	5	51.0	100	2	64.6	100.00	5	41.7	80	5
22	51.9	60	4	130.6	80	5	3.9	100	5	3.9	100	5	47.3	75.00	7	17.4	75	6
23	69.7	70	3	61.2	70	4	4.0	50	5	63.3	100	5	40.3	75.00	7	32.3	70	6
24	101.0	80	4			-	94.6	100	5	21.6	100	5	150.5	75.00	7	38.6	70	6

Table 8 Initial Investigation into CHO cells Expressing Fibrinogen with α-chain Truncations

Clones highlighted (green) were picked for further investigation. No cells were observed in blank wells. Cells were picked between day 1 and 7.

10 µg	α220			α390			20 µg	α220			α390		
Clone	ng/mL	Confluency %	Picked (Day)	ng/mL	Confluency %	Picked (Day)	Clone	ng/mL	Confluency %	Picked (Day)	ng/mL	Confluency %	Picked (Day)
1	2.3	30	6	11.8	100	4	1	0.55	100	7	7.3	100	7
2	3.5	100	7	4.6	100	4	2	0.46	80	7	4.9	60	6
3	2.3	85	6	4.4	100	4	3	0.48	60	7	5.9	100	7
4	2.7	100	7	4.4	100	4	4	0.76	80	7	5.0	70	6
5	2.2	90	6	4.8	90	4	5	0.52	100	7	6.8	90	7
6	2.3	70	7	4.6	65	6	6	0.46	90	6	7.9	100	7
7	2.2	100	7	21.4	100	6	7	0.49	55	7	7.7	100	7
8	2.2	100	7	6.2	100	6	8	0.45	40	7	5.6	100	7
9	2.2	100	7	5.6	100	6	9	0.48	40	7	5.3	100	7
10	2.3	30	7	19.0	100	6	10	0.46	100	6	6.8	100	6
11	2.3	100	7	11.8	100	6	11	0.46	35	6	5.2	100	7
12	2.3	100	7	5.5	100	4	12	0.48	100	6	5.6	100	7
13	2.2	100	7	5.0	70	4	13	0.48	80	7	5.1	100	7
14	2.2	100	7	4.8	100	4	14	0.53	100	7	7.8	100	6
15	2.3	75	7	4.7	100	4	15	0.45	50	7	5.2	100	7
16	2.2	20	7	4.6	100	4	16	0.46	60	7	5.5	90	7
17	2.3	70	7	4.6	100	4	17	0.63	80	7	5.4	100	7
18	2.6	100	7	5.4	100	4	18	0.49	70	7	5.3	100	7
19	2.4	70	6	4.9	100	6	19	0.46	100	7	5.0	70	6
20	2.6	100	7	5.7	100	6	20	0.47	40	7	5.7	100	7
21	2.5	100	7	8.0	100	4	21	0.48	60	7	5.0	100	7
22	2.4	100	7	5.5	80	6	22	0.47	100	7	5.6	100	7
23	2.4	90	7	7.2	90	6	23	0.47	30	7	5.4	100	7
24				4.8	90	6	24	0.64	55	7	5.1	100	7

Table 9 Fibrinogen Expression in Serum-free Medium of CHO Cells Expressing Fibrinogen with γ'/γ' and γ'-chain Truncations

Clones highlighted (green) selected for large-scale expression.

Transfected amount	γ'		γ'16		γ'12		γ'8		γ'4		γ'0	
	Clone	ng/mL	Clone	ng/mL	Clone	ng/mL	Clone	ng/mL	Clone	ng/mL	Clone	ng/mL
10 µg	8	189.5	1	155.3	3	246.5	4	14.01	3	372.3	3	84.2
	9	191.8	3	160.7	5	227.4	7	171.80	7	55.9	5	79.0
	14	113.3	4	111.5	8	234.3	9	92.27	9	49.2	9	39.0
	15	225.0	6	132.3	9	201.5	11	110.27	11	151.8	14	118.2
	16	164.7	8	90.2	10	224.5	15	62.38	12	296.1	16	66.5
	18	139.7	9	96.8	11	358.2	18	236.75	13	201.4	21	96.4
	19	187.5	10	111.9	14	97.4	17	212.47	16	195.0	24	90.8
	20	192.8	11	106.8			19	202.11				
	22	182.0	14	110.6			20	166.75				
			19	104.5			21	180.87				
			21	124.7			22	186.07				
			23	131.4								
20 µg	1	174.8	1	155.9	1	359.4	3	112.9	2	183.2	2	113.9
	3	189.5	2	152.4	3	191.9	8	165.6	3	205.9	8	130.8
	4	173.5	7	176.3	10	205.5	12	103.4	5	297.0	10	147.6
	8	137.1	8	175.7	11	254.7	21	144.5	6	136.5	13	121.9
	10	110.6	9	219.6	13	345.6	23	158.5	7	287.1	15	111.5
	14	175.8	10	205.5	15	309.1	24	12.6	10	195.9	18	101.5
	17	137.0	12	234.3	17	410.5			12	132.9	21	66.8
	23	174.5	17	228.7	24	258.7			14	120.8	24	102.8
	24	147.1	18	174.1					18	39.2		
			19	234.9					20	254.5		
			20	175.4					21	235.8		
			22	141.9					24	264.7		
			23	183.8								

Table 10 Fibrinogen Expression in Serum-free Medium of CHO Cells Expressing αC-region Truncations

Transfected amount	α390		α220	
	Clone	ng/mL	Clone	ng/mL
10 μg	1	54.7	2	11.8
	7	36.9	4	8.7
	8	57	10	4.7
	9	73.3	18	7.4
	10	102.7	19	8.1
	11	70.8	20	7.7
	20	32.1	21	6.9
	21	20.7	22	7.3
	23	22.4	23	7.3
20 μg	1	27.5	4	11.6
	5	17.8	17	72.7
	6	12.7	24	15.4
	7	17.3		
	10	20.2		
	14	7.2		

3.2.4 Fibrinogen Production Phase

The higher-level expressing clones selected for fibrinogen production were grown in roller bottles to increase yield. Once the cells were confluent, microcarrier beads were inserted into the roller bottles to further increase the surface area. Once the microcarrier beads had been surrounded by the CHO cells, the medium was changed to SFM. The cells were maintained in supplemented SFM for a period of 6-8 weeks and levels of fibrinogen expression were monitored. Medium was collected 3 times a week and replaced with fresh medium. Due to initial experimental results observed in truncations γ'/γ', γ'16, γ'12 and γ'0, it was decided that the truncations γ'8 and γ'4 would not be produced, since there was no difference between the γ'-chain truncations (γ'16 and γ'12) or γ'/γ' and WT in maximum optical density.

3.2.5 Purification of Secreted Fibrinogen

The harvested medium collected from the CHO cells was defrosted and purified in a two-step process, using saturated ammonium sulphate precipitation followed by IF-1 affinity chromatography. The medium was defrosted, and ammonium sulphate was added dropwise to 40 % saturation and incubated overnight at 4°C. The ammonium sulphate concentrates the collected fibrinogen in the medium by binding to the water molecules therefore decreasing the solubility of fibrinogen resulting in precipitation. The precipitated fibrinogen was collected by centrifugation and the pellet was resuspended and centrifuged again at a higher speed to remove further contaminants. The fibrinogen containing supernatant was collected and frozen at -80°C.

Figure 13 shows an example chromatogram for the eluted fibrinogen, the bulk of contaminants were eliminated already during column equilibration, before the two wash steps of high salt and reduced pH. However, the two wash steps are required to remove any further trace contaminants binding to fibrinogen at higher affinity. Fibrinogen was displaced from the antibody column by addition of EDTA which chelates calcium and therefore the calcium dependent interaction between the IF-1 antibody and fibrinogen fails, resulting in the elution of fibrinogen from the column. The fractions containing fibrinogen were collected and dialysed, as experimental investigations require the addition of calcium therefore the removal of EDTA in the final fibrinogen preparation was necessary.

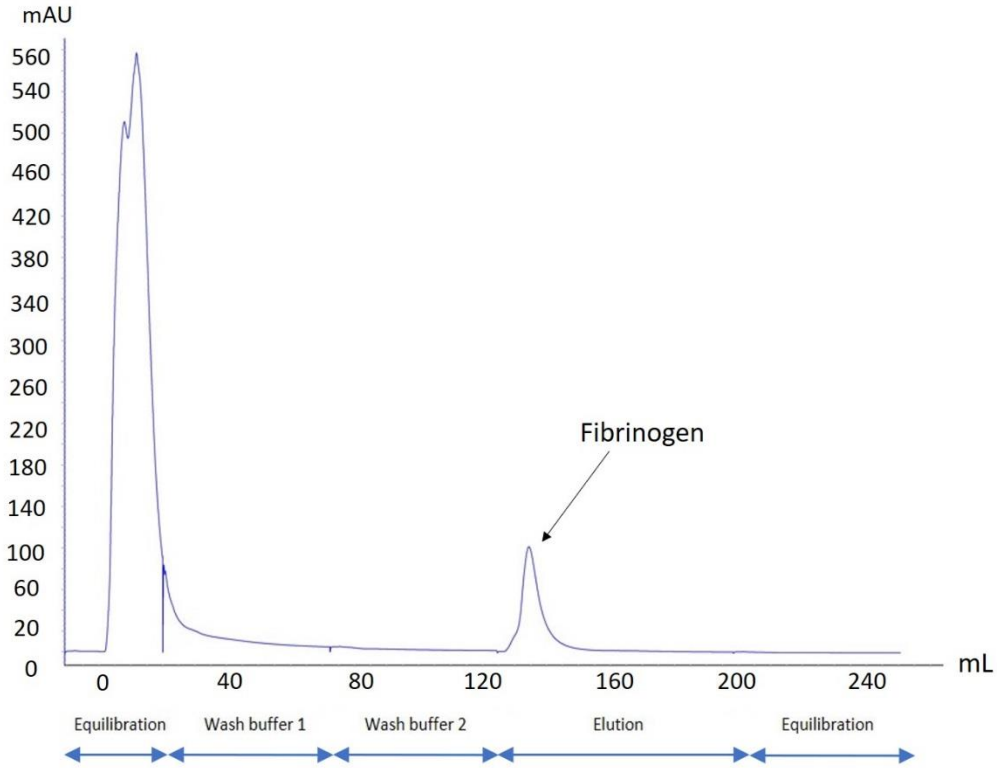

Figure 13 Chromatogram of IF1 Affinity Chromatography of γ'0 Purification

Purification of recombinant fibrinogen by affinity chromatography using the calcium ion-dependent monoclonal antibody clone IF-1. The recombinant fibrinogen was loaded on to the column with single column volume (CV = 7.439 mL) of equilibration buffer (20 mM tris, 300 mM NaCl and 1 mM CaCl2 pH 7.4). Non-specific binding of contaminants was removed by two wash steps, wash buffer 1 (20 mM tris, 1 M NaCl, 1 mM CaCl2 pH 7.4) for 5 CV followed by wash buffer 2 (50 mM Sodium Acetate, 300 mM NaCl and 1 mM CaCl2 pH 6) for 5 CV. The fibrinogen was eluted in 2 mL fractions from the column with 7 CV of elution buffer (20mM tris, 300 mM NaCl and 5 mM EDTA pH 7.4). The stages of the purification are highlight on the x axis of the chromatogram and the elution peak for the fibrinogen collected is highlighted by the arrow.

3.2.6 Yield

The yield of the purified recombinant fibrinogen and duration of production is shown in Table 11. The two αC-region truncations produced considerably less protein than the γ'-chain variants, with γ'12 variant having the highest yield.

Table 11 Yield of Fibrinogen Variants

Variants	No. of Weeks of Production	Medium Collected (L)	Yield per Harvested Medium (mg/L)	Purified Fibrinogen (mg)
γ'0	8	54	0.51	28.0
γ'12	6	48	1.71	82.4
γ'16	8	54	0.25	13.4
γ'/γ'	6	48	0.52	25.1
α390	8	54	0.10	5.5
α220	8	54	0.03	1.6

3.2.7 Investigation into the Individual Chain's Expression of the αC-region Truncations

To investigate the reduced yields observed with the fibrinogen α-chain truncations variants further, a real-time PCR assay was performed by Dr Kingsley Simpson, to observe the levels of the 3 fibrinogen chains over the period of fibrinogen expression. Cells expressing either α390 or α220 fibrinogen were grown in a petri dish in serum free medium and mRNA was harvested each week. The cells were maintained for a series of weeks in the same dish before collection of RNA. As such, fewer cells would be harvested for each successive collection. This variation was controlled for by only reverse transcribing a set amount of mRNA and then expression was normalised to the amount of the housekeeper gene present in the same sample.

The individual gene amount of the fibrinogen chains is expressed relative to the housekeeper genes Gnb1 and FbpK1a. The expression of these housekeeper genes has been shown to be stable across a number of conditions (Brown et al., 2018). The individual gene expression relative to the housekeeper genes for α390 showed that the transfected α-chain had the highest expression, and that this expression gradually reduced over time (Figure 14A). The expression of the β- and γ-chains was considerably lower but showed a substantial rise in expression at week 2 before reducing again. Furthermore, this rise was mirrored in the expression of the β- and γ-chain for α220, although the increase in γ-chain expression

was not as great as observed with α390 (Figure 14A and B). The α-chain expression in α220 peaked at week 2 and then reduced over time, whereas there was a gradual decline in the α-chain expression in α390. The expression of α-chain in α390 was nearly twice as high at week 2 as observed in α220, and at week 6 the expression in α390 had fallen to the level of highest point of expression of the α-chain observed in the α220.

The secreted fibrinogen concentrations in roller bottle collections for WT, α220 and α390 are shown in Figure 14. The WT fibrinogen was secreted at the highest concentration. As expected α220 showed reduced expression compared with α390 and mirrors the SFM secretion observed during clone selection (Table 11). There was a gradual increase over the weeks of collection for α220 in the roller bottles whereas α390 had a sharp increase between week 1 and 3 before a drop to week 2 expression level at weeks 4-6, followed by an increase for weeks 6-8. As the mRNA was harvested on the final day of the corresponding week's collection there may be a delay observed in the resultant secreted fibrinogen expression.

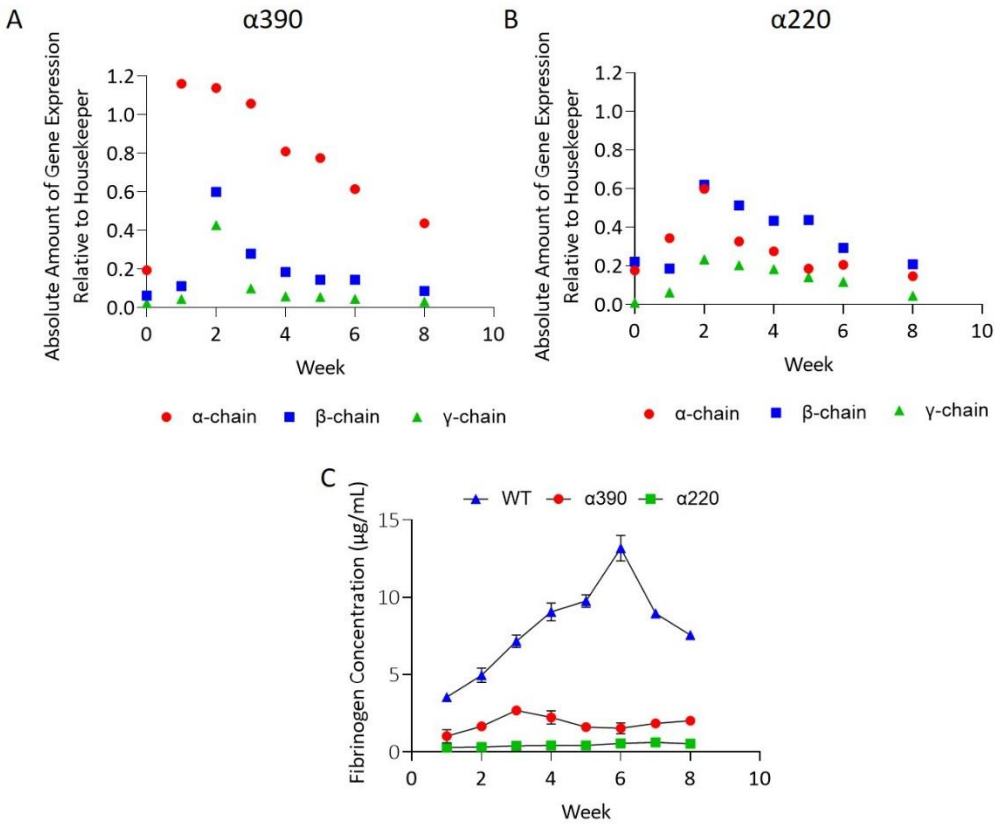

Figure 14 αC-region Truncations Expression of Fibrinogen Chains and Secreted Fibrinogen

The fibrinogen expression of the individual chains by real time PCR over the course of 8 weeks of expression for α390 (A) and α220 (B). The α-chain had the highest expression compared to the other chains for α390. Similar expression was observed for α- and β-chain for α220. The γ-chain showed the lowest expression in both α390 and α220. Housekeeper genes was an average of Gnb1 and FbpK1a. Secreted fibrinogen concentration of WT, α390 and α220 from medium harvested from roller bottles by ELISA over 8 weeks (C). Fibrinogen concentration was highest over the 8 weeks for the WT, with α390 having a greater concentration compared to α220.

3.2.8 Purification of FXIII

The FXIII used in the experiments is commercially sourced $FXIIIA_2B_2$ (Zedira, Darmstadt, Germany) which was then further purified by gel filtration using HiLoad 16/600 Superdex 200 pg column to remove contaminants such as albumin. Figure 15 shows the chromatogram profile, and the corresponding fractions collection on a non-reduced SDS-PAGE gel. The fractions collected were between A5 and D2, these were separated to identify contaminants. $FXIIIA_2B_2$ appeared in fractions between A8 to B5 and contaminants appeared from B4. The fractions pooled were B2 and B3, which were used for experimental work

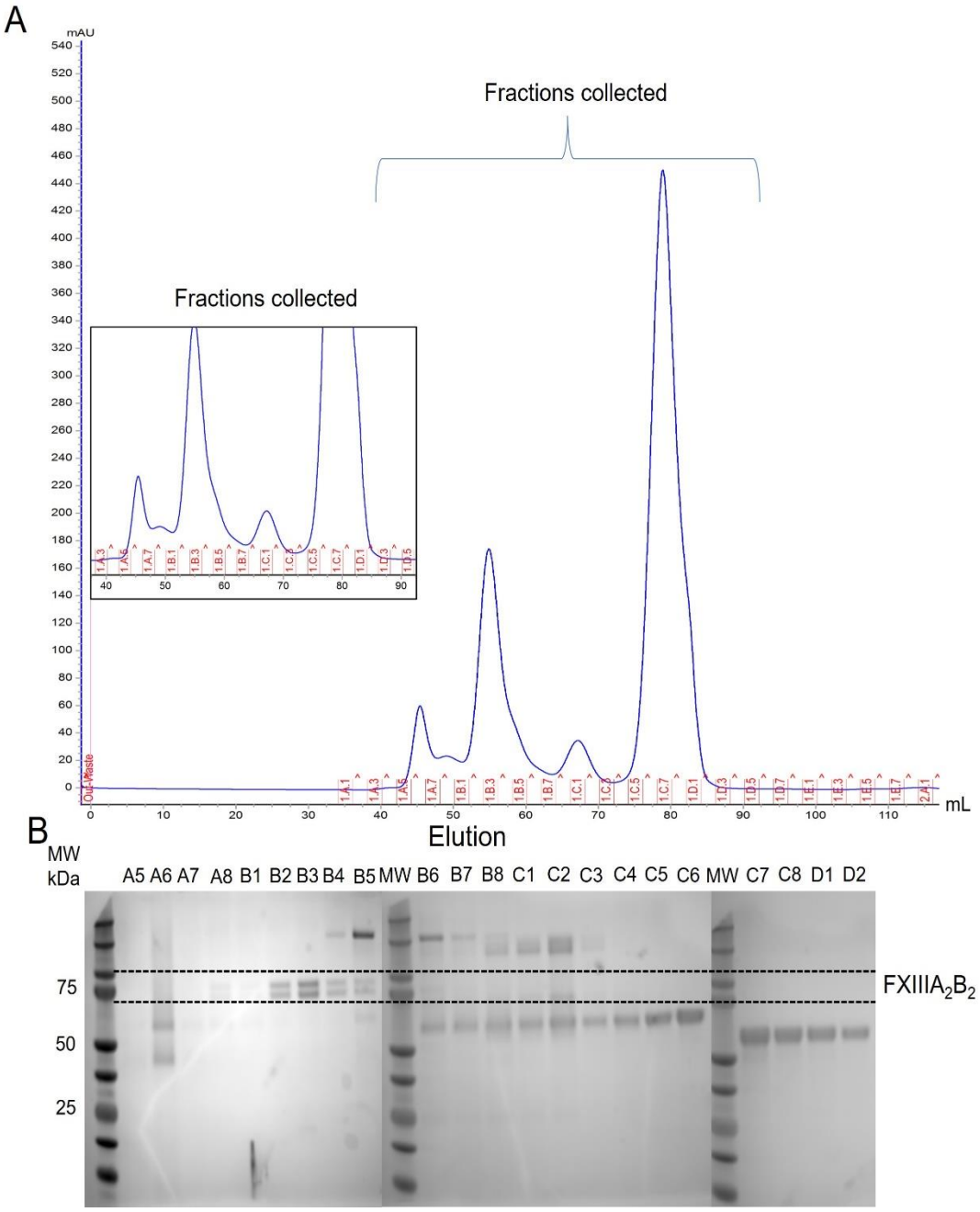

Figure 15 FXIII Purification

Chromatogram profile of $FXIIIA_2B_2$ through HiLoad 16/600 Superdex 200 pg column (A). The $FXIIIA_2B_2$ was dissolved in 1 mL ddH_2O and loaded in to a 2 mL loop and the samples were eluted over 1.5 column volumes (120.637 mL = 1 column volume). The eluted samples were collected in 1.6 mL fractions. Migration of collected fractions on three separate gels by non-denaturing 4-12 % Bis-Tris SDS-PAGE (B). Start of the individual gel is denoted by the molecular weight marker (MW) SDS-PAGE was stained with instant blue and fractions B2 & B3 were selected as contained no contaminates.

.

3.3 Discussion

The focus of this chapter is the production and purification of recombinant fibrinogens variants. A CHO transfection method previously described to establish many other recombinant proteins as well as fibrinogen (Jayapal et al., 2007; Helms et al., 2012; Duval et al., 2020) allowed effective production of two fibrinogen αC-region truncations; α390 and α220 as well as the fibrinogen γ'/γ' and five truncation variants of fibrinogen γ'.

As anticipated, the yield of the two α-chain truncations was much lower compared to the γ'-chains variants. A compilation of fibrinogen abnormalities reported in the human fibrinogen database (GFHT https://site.geht.org/base-fibrinogene/), Table 1 Table 2 demonstrate that the majority of homozygous α-chain mutations result in afibrinogenemia, especially when the α-chain length is shorter than Aα340. Patients with homozygous mutant alleles of the fibrinogen α-chain have circulating levels of fibrinogen that are considerably lower than the normal range (1.5-4.0 g/L) such as Otago at 0.06 g/L (Clauss) and Marburg at <0.25 mg/mL (Clauss) or 0.6 mg/mL (by ELISA) (Koopman et al., 1992; Ridgway et al., 1997). Two patient cases have been reported with truncations either side of α220 both resulting in afibrinogenemia, Arnhem (Aα219) and Egypt (Aα221) (Vlietman et al., 2002; Abdel Wahab et al., 2010). The truncation found in fibrinogen Egypt was transfected into and secreted from COS-7 cells, and as observed with α220, there was a reduced yield compared to the WT (Abdel Wahab et al., 2010). In individuals with heterozygous aberrant fibrinogen alleles, the aberrant fibrinogen was not observed in high concentrations within the circulation. These findings indicate that the aberrant chain does not compete with normal α-chains for the mature fibrinogen and/or that it does not modulate mRNA stability, intra-hepatic assembly, or protein secretion of the normal chain fibrinogen. In the case of the Otago mutation, a heterozygous son had normal clotting times and fibrinogen levels, while fibrinogen Otago was not observed in the plasma. On the other hand, heterozygous family members with fibrinogen Marburg allele showed slightly longer than normal clotting times and reduced fibrinogen levels (1.7 to 2.1 mg/mL), and a reported 10-20% of Marburg fibrinogen was part of the circulating fibrinogen.

There have been relatively few mentions of recombinant fibrinogen yields in the literature, which makes it challenging to compare the yields reported in this thesis. In addition, it is not always clear to what point within the production or purification the yield relates to as the number of cells will impact the yield. CHO cells producing recombinant WT fibrinogen had an expression of 8 µg/mL in a confluent 10 cm dish after 7 days, while in contrast the BHK recombinant fibrinogen were reported to secrete 1.1 $\mu g/mL^{-1}day^{-1}$ in a confluent 24-well plate, while COS-1 cells were stated to secrete an average of 2.08 µg when seeded at 2x10^6

cells (Roy et al., 1991; Farrell et al., 1991; Binnie et al., 1993). Interestingly, in both BHK and COS-7 cell expression systems, production of non-WT fibrinogen showed reduced yields compared to the WT (Farrell et al., 1991; Abdel Wahab et al., 2010). In agreement with these observations in the BHK and COS-7 cells expression systems, this thesis reports reduced expression for both α-chain truncations compared to WT. The range observed in the fibrinogen γ'-chain variants expression could be due to individual differences in α- and β-chain expression in the each of the cells transformed with the truncation variants and the homodimer, therefore impacting on overall expression. Expression of the previously transfected β- and γ-chains in the α-chain truncations was also not consistent. Grosjean et al, showed that high transfectability of cells via calcium phosphate required a high percentage of cells within the S-phase of the cell cycle (Grosjean et al., 2002). Consequently, the success of transfection efficiency depends on where the majority of cells are within the cell cycle during the transfection procedure with the relevant plasmids, which could in part account for differences observed in expression levels for e.g. γ'16 vs γ'12 fibrinogens.

No substantial differences in expression of fibrinogen were observed in the initial ELISA assays of the γ'- and α-chain variants when transfection was performed with either 10 or 20 μg of plasmid. This may be linked to the expression of either αβ-chain or βγ-chain in the γ'-chain variants and α-chain truncations respectively. The real time PCR data of α390 and α220 fibrinogens showed that the γ-chain had the lowest expression compared to the other chains. In addition, CHO cells producing recombinant protein are under high genomic and metabolic demand, this may result in genomic and epigenetic changes resulting in decline in productivity over a production period as observed in the real time PCR results for α390 and α220 (Feichtinger et al., 2016; Tihanyi and Nyitray, 2021).

A number of previous investigations into fibrinogen assembly in HepG2 and stably transfected cells (COS-1 and BHK) indicated that formation of the fibrinogen molecule starts with complexes of βγ with αγ (Hartwig and Danishefsky, 1991; Huang et al., 1993). Furthermore Tamura et al., 2013 suggested that the βγ complex is a by-product of assembly, and produced when the balance of chaperone constituents is interrupted. As observed in the expression levels of the two α-chain truncations, there was low γ-chain mRNA expression. This reduction in abundance of the γ-chain could impact on the rate of assembly and overall accumulating in a reduced yield.

There are several areas where the transfection method or alterations during production could be modified to further improve yield. With the current transfection method, the transfected plasmid carrying the individual cDNA does not include a selection marker, and the selection of positively transfected cells is dependent on the cells accepting a second

selection plasmid. Creating a plasmid encoding an individual chain with a specific selection marker would allow each chain to be selected for independently. An alternative method has been reported with all the fibrinogen chains included on one plasmid in CHO cells using Lipofectamine® 2000 transfection (Hirashima et al., 2016). This method resulted in stable clones expressing 1.1 mg/mL fibrinogen a day. The fibrinogen was then purified through anion and cation exchange chromatography columns. There were limited differences observed in turbidity or SEM but these either had small replicates or data were not shown. Some difference in β- and γ-chains size compared to plasma purified fibrinogen was observed due to alternative carbohydrate post-translational modifications (Hirashima et al., 2016). Interestingly, Hirashima et al, used CHO DG44 cells and in this study recombinant fibrinogen was generated by CHO-K1. A study by Reinhart et al 2019 comparing various CHO subtypes CHO-K1, CHO-S and CHO-DG44 transfected with the same construct demonstrated that CHO-K1 had the highest production rates followed by CHO-DG44 (Reinhart et al., 2019); highlighting the importance of cell subtype on recombinant protein production.

Another way to potentially increase the yield may be to increase the number of glycerol shocks, as this has been shown to increase the efficiency of transfection (Grosjean et al., 2006).

Many of the transfection methods for fibrinogen used equal amounts of cDNA for transfecting the three chains. But since β-chain expression has been suggested to be a rate limiting step (Yu et al., 1983; Farrell et al., 1991; Binnie et al., 1993) it may prove worthwhile to transfect more of this chain. It has also been shown that transfected HepG2 cells overexpressing any of the fibrinogen chains results in higher expression of the other fibrinogen chains, but the β-chain had the highest fold change compared to control cells (Roy et al., 1994). In the recombinant fibrinogen expression system described by Hirashima et al 2016, the plasmid had two γ-chains cDNA encoded, the reason for this is unclear and was not specified by the authors. Transfecting the β-chain at a higher concentration relative to the other chains could result in higher expression and secretion overall.

Slight variations in pH can influence transfection efficacy for calcium phosphate transfections (Felgner, 1990). There are alternative transfection methods that could be used to transfect cells such as FuGENE® (non-liposomal) or Lipofectamine® (Cationic lipid-mediated), that do not have the issues observed with calcium phosphate.

Furthermore, producing recombinant protein at a reduced temperature 30-33 °C has been shown to increase yield compared to 37 °C in CHO cells (Kaufmann et al., 1999; Yoon et al., 2003). Kaufmann et al, showed that culturing cells at 30 °C resulted in growth arrest while cells were mainly in G1 phase of the cycle, which resulted in a 1.7-fold increase in

productivity compared to 37 °C, with a 3.4 times higher yield. Additionally, Yoon et al, found that cell viability remained higher with a decreased release of proteolytic enzymes resulting in a longer culture period at 33 °C compared to 37 °C, with a 2.5-fold increase in yield.

The following chapters will be covering the characterisation of these truncations starting with the initial investigation in fibrinogen integrity followed by purified structural and functional studies. After the analysis of purified recombinant protein, plasma, and whole blood *ex vivo* assays were used to further elucidate the role of these key domains, regions and variants of fibrinogen

Chapter 4 Characterisation of the αC-subregion

4.1 Introduction

This chapter covers the initial characterisation of the two recombinant fibrinogen variants with truncations in the αC-region subregion (α390 and α220) as well as investigations into their influence on clot structure and function. Past research into the fibrinogen αC-region has been through a combination of approaches such as the study of plasma samples from patients with dysfibrinogenaemia related to mutations in the αC-region, fibrinogen fragments generated by partial proteolysis (fragment X), recombinant fragments, recombinant fibrinogen (α251) and murine model (*FGA*$^{270/270}$) (Gorkun et al., 1994; Ridgway et al., 1997; Gorkun et al., 1998; Collet et al., 2005; Hur et al., 2021). Each of these studies had provided further understanding of the αC-region and highlighted its role in polymerisation, mechanical strength, and fibrinolytic sensitivity.

One of the major difficulties in investigations into the αC-region is that any alternations within this region impact the levels of secretion whether this is recombinant production, patient cases or murine models. This has been observed with both recombinant fibrinogen, patient mutations and the murine truncation (*FGA*$^{270/270}$) (Koopman et al., 1992; Ridgway et al., 1997; Abdel Wahab et al., 2010; Hur et al., 2021). In addition, heterozygous patients with αC-region variations show that the circulating level of the variant is not equal to WT, therefore interpretation of its implications can be challenging (Koopman et al., 1992; Ridgway et al., 1997).

Fibrinogen heterozygous mice (*FGA*$^{+/-}$) only show reduced plasma fibrinogen levels of 27 % compared to WT mice therefore they are not an ideal control in comparing models with low fibrinogen levels. In investigations with the *FGA*$^{270/270}$, siRNA was used to knockdown the WT fibrinogen level to 10 % which was similar to the fibrinogen levels in the truncated α-chain (Hur et al., 2021). The combination of using the murine knockdown alongside the α-chain truncation, differences in WT fibrinogen level were overcome and therefore observed effects could be determined to be due to functional consequence of the truncation in the αC-region or caused by the reduction in fibrinogen levels.

The use of recombinant protein production allows for functional comparisons of produced fibrinogens with alterations within the αC-region to WT fibrinogen as the concentration of fibrinogen can be controlled. Several recombinant fibrinogens with mutations in the αC-region, such as a truncation (Aα251), point mutations (AαQ328P, AαQ366P, AαQ328,366P and AαD594E) and region exchange (substitution of the human αC-region with the chicken

αC-region) have been produced in previous studies (Gorkun et al., 1998; Collet et al., 2005; Ping et al., 2011; Park et al., 2013).

However, to date no studies have examined the individual roles of the subregion of the αC-region. The two truncated recombinant fibrinogens produced in this thesis to investigate the subregion were studied for their roles in clot structure by turbidimetric assay, in hydrated (laser-scanning confocal microscopy) and dehydrated (scanning electron microscopy) conditions. Polymerisation was studied by turbidimetric assay and atomic force microscopy. The functional attributes of fibrinolysis were examined using turbidimetric assays and microscopy, and clot mechanics by magnetic tweezers.

4.2 Hypothesis

The subregions of the fibrinogen αC-region have unique roles in the structure and function of fibrin clots.

4.3 Aims

To investigate the roles of the two subregions of the αC-region, i.e. the αC-terminal domain and the αC-connector region, in fibrinogen structure and function.

4.4 Results

4.4.1 Integrity of the Fibrinogen Chains

The purified recombinant fibrinogens were first assessed by native PAGE to confirm that they were one homogenous species. Figure 16A shows there was one band present in each lane for the respective recombinant fibrinogens, confirming presence of only one species for each. As expected, there were differences in migration for the three fibrinogens, whereby α220 had the greatest migration through the gel, followed by α390, while the WT migrated the least. This variation in migration demonstrates the impact on molecular weight caused by the loss of various amounts of the α-chain, as α220 has the largest truncation and therefore is the smallest and migrates furthest through the gel, followed by α390.

To confirm that the difference in migration observed in the native PAGE gel was due to the truncation in the α-chain, a reducing SDS-PAGE gel electrophoresis was performed. The reducing SDS-PAGE gel showed no difference in migration between the β- and γ-chain for either of the truncations compared to WT, indicating there was no truncation in these chains (Figure 16B). In contrast, the α-chain had increased migration for α390 compared to the α-chain for the WT, since the α-chain of α390 migrated to below the γ-chain as shown by the arrow in Figure 16B. The calculated molecular weight for α390 was 42 kDa, which indicated that the α-chain would indeed migrate to just underneath the γ-chain, which has a molecular weight of 47 kDa (Weisel and Litvinov, 2017). As expected, the α-chain for α220 migrated

even further and was in line with the 25 kDa mark within the molecular weight ladder, matching its respective calculated molecular weight. This confirms that the increased migration of the truncations observed in the native PAGE (Figure 16A) was due to reduction in molecular weight of the α-chain and that there were no differences in the sizes of either the β- or γ-chain.

4.4.2 Truncations to the αC-region do not Alter Clotability

Initial functionality of the truncated fibrinogens was investigated by thrombin mediated proteolysis, to uncover if the truncated fibrinogens had reduced clotting capability in comparison to WT. Figure 16C shows the clotability of the recombinant fibrinogens, WT had a clotability of 97±2 %, α390 showed a clotability of 94±2 % and there was a further reduction for α220 to 89±8 %. All the recombinant fibrinogens were able to form clots via thrombin-mediated clotting. The truncations demonstrated that even a significant loss of the α-chain resulted in a slight reduction in clotability compared to WT.

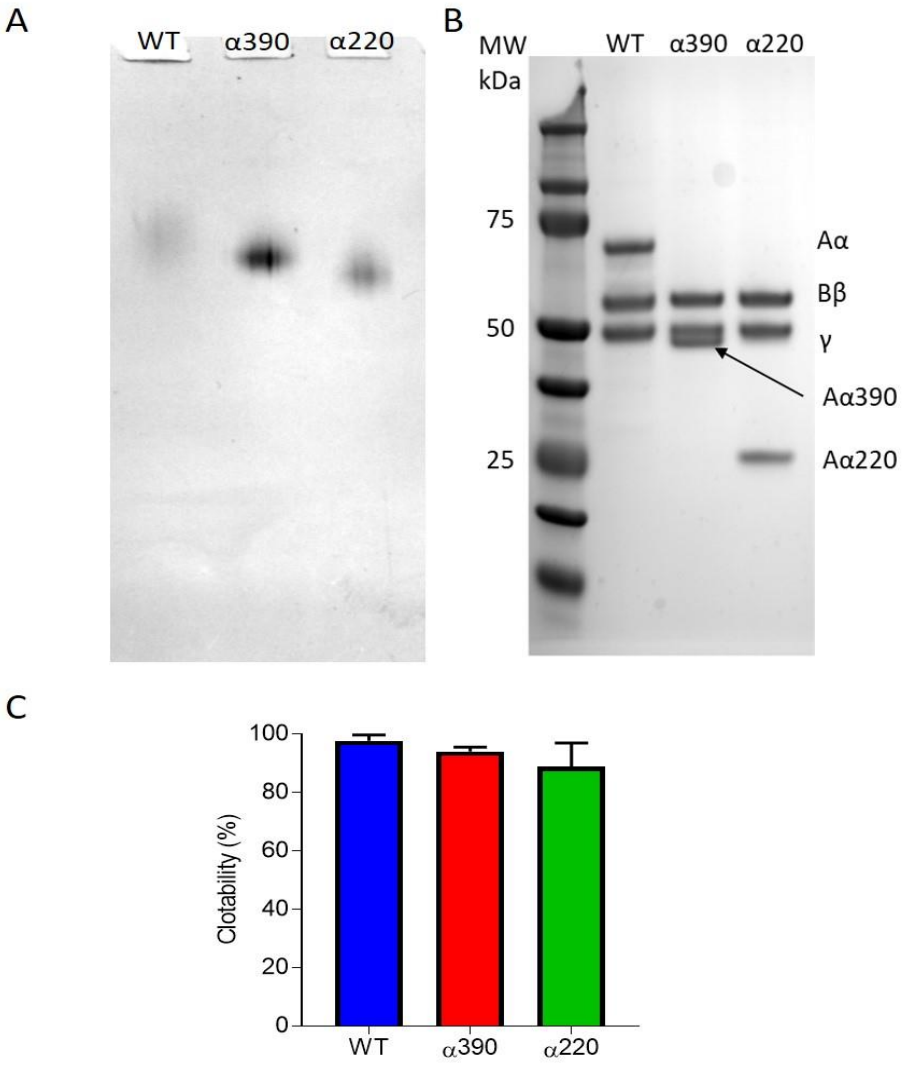

Figure 16 Initial Characterisation of αC-subregions

Native PAGE gel of WT (left), α390 (middle) and α220 (right) (A). Native PAGE gel was stained with 0.02 % Coomassie Brilliant Blue R-250. Reduced SDS-PAGE of WT, α390 and α220 (B). First lane is molecular weight ladder (MW), lane 2 WT, lane 3 α390 and lane 4 α220. SDS-PAGE was stained with Instant Blue Aα-chain for α390 just underneath the γ-chain (highlighted by the arrow) Clotability of the purified recombinant fibrinogen (C). Clotting was initiated with 0.1 U/mL thrombin and 5 mM calcium; Error bars are shown as ± standard deviation, clotability (C) *n*=3.

4.4.3 Structural Impact of the αC-subregions

4.4.3.1 Influence of the αC-subregions on Polymerisation and Fibre Thickness

Initial structural investigations were performed by turbidimetric assay, to understand the impact of the two αC-subregions on polymerisation. The polymerisation of the recombinant fibrinogen was studied by measuring the change in optical density over time. Clotting was initiated by thrombin which cleaves the FpA and then FpB peptides from fibrinogen, converting it to fibrin and allowing the formation of protofibrils and then fibres (Weisel and Litvinov, 2017).

Figure 17A and B show the polymerisation curve for WT (blue), α390 (green) and α220 (red). The polymerisation curves for WT and α220 showed differences in duration of the lag phase, with α220 demonstrating a prolonged lag phase compared to the WT, but both plateaued at similar maximum OD. However, α390 generated a curve with a reduced plateau compared to both the WT and α220 (Figure 17B), in addition to a delay in lag phase. The extension in lag phase observed for the truncations exhibited an increased duration with additional removal of the αC-region (Figure 17A and Figure 18B). The lag phase for α390 was 193±6.2 seconds (p=0.0143) and for α220 it was 227.5±11.4 seconds (p=0.001), while the WT had a lag phase of 159.5±20.4 seconds. There was no difference in maximum OD between the WT (0.359±0.03 OD) and α220 (0.376±0.03 OD), whereas there was a reduction for α390 (0.169±0.04 OD) compared to WT (p<0.0001), which indicates the α390 clot was denser with thinner fibres than the WT (Figure 18A).

The maximum rate of clotting was similar between WT (0.00098±0.00012 δOD/seconds) and α220 (0.00106±0.00014 δOD/seconds), while a reduced rate was seen for α390 (0.00054±0.00013 δOD/seconds) however, this only showed a trend (p=0.0614) (Figure 18C). The average rate of clotting was reduced for α390 (0.00027±4.78x10-5 δOD/seconds) compared to WT (0.00060±7.62x10-5 δOD/seconds p=0.0002) (Figure 12D). No difference for average rate of clotting was seen for α220 (0.00058±4.19x10-5 δOD/seconds) compared to WT (p=0.9413). A delay was observed for α220 (7.54±0.44 minutes) in the time to 50 % clotting when compared to WT (6.2±0.62 minutes p=0.0462), and no difference was found for α390 (6.84±1 minutes) (Figure 18E). After the initial delay in clotting for both truncations, there was no further difference seen in time taken to maximum OD (Figure 18F).

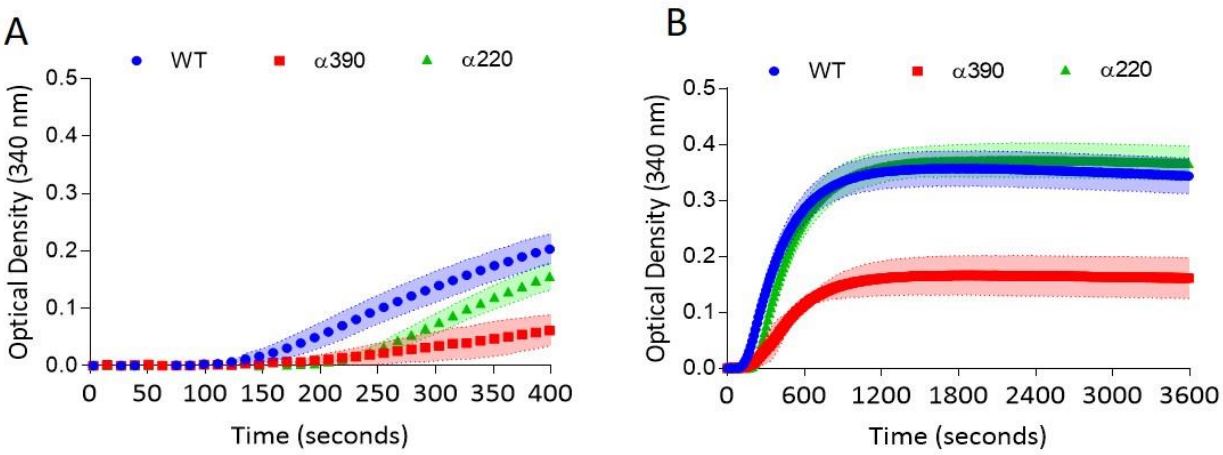

Figure 17 Polymerisation Curves of WT and αC-subregions

Fibrin polymerisation curve of WT, α390 and α220 for the first 400 seconds (A) and over 3600 seconds (B). Clotting was initiated with 0.1 U/mL thrombin and 5 mM calcium; optical density was monitored for 1 hour (3600 seconds). *n*=4.

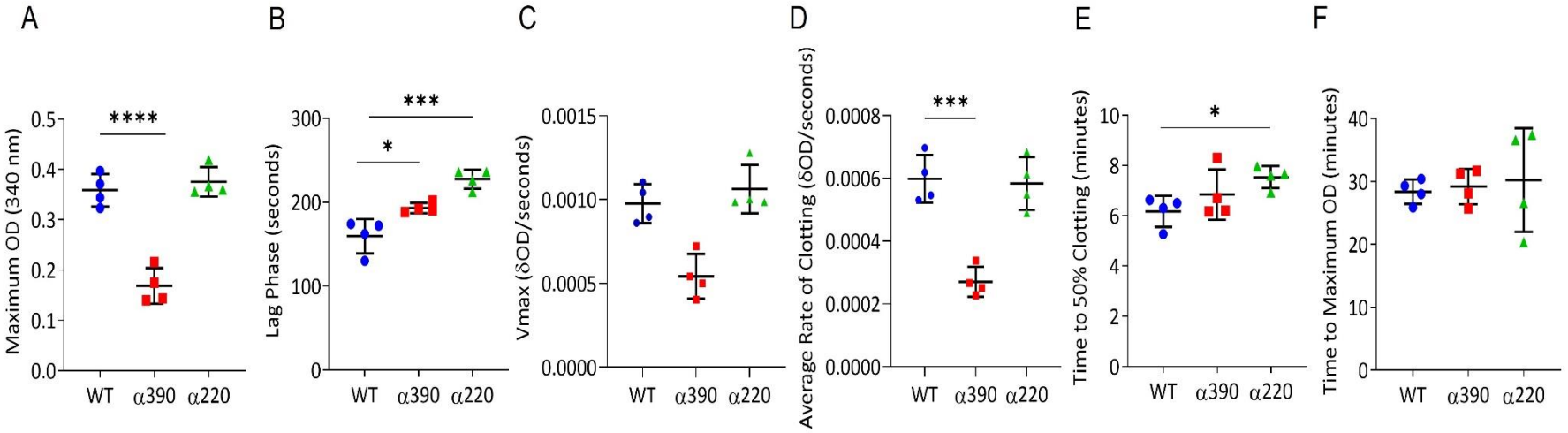

Figure 18 The αC-subregions Alter Polymerisation

Maximum optical density (OD) for WT, α390 and α220 (A). Lag phase for WT, α390 and α220 (B). Vmax of WT, α390 and α220 (C). Average rate of clotting for WT, α390 and α220 (D). Time to 50 % clotting (E) and time to maximum OD (F) for WT, α390 and α220. Results shown as mean ± standard deviation, n=4, *p=0.05, ***p=0.001, ****p<0.0001 by one-way ANOVA with Dunnett's multiple comparison test relative to the WT for graphs A, B, D and E.

4.4.3.2 Fibrin lacking the αC-region shows Limited Polymer Growth

AFM was next used to visualise and study the early stages polymerisation to understand how truncations in the αC-region affect the early events of polymerisation. The AFM experiments shown here were performed by Dr Stephen Baker. To capture the early polymerisation events, the reaction was super-diluted and therefore polymerisation occurred over minutes rather than seconds. Figure 19A shows representative images of early polymerisation of the fibrinogens over time. Over the course of the assay, the polymer length increased for WT and α390, whereas α220 showed limited polymer growth at all time points, emphasised by the final time point where the polymer length of 204±84 nm was similar to the initial time point for both WT (223±94 nm) and α390 (240±103 nm). Figure 19B at 10 minutes showed no difference between the WT and α390, and the average polymer length was 223±94 nm and 240±102 nm respectively. However, α220 exhibited considerably shorter length compared to the WT with 142±56 nm $p<0.0001$. After 20 minutes, there was an increase in polymer lengths for all fibrinogens, however there was no difference in average polymer length observed between the WT (319±263 nm) and α390 (326±245 nm) whereas the α220 was still considerable shorter (173±58 nm) compared to the WT ($p<0.0001$). At 30 minutes, again there was similar growth observed between the WT and α390 with an average polymer length of 372±284 nm and 341±202 nm respectively. As previous time points showed, α220 demonstrated minimal polymer growth compared to WT with an average length of 204±84 nm $p<0.0001$.

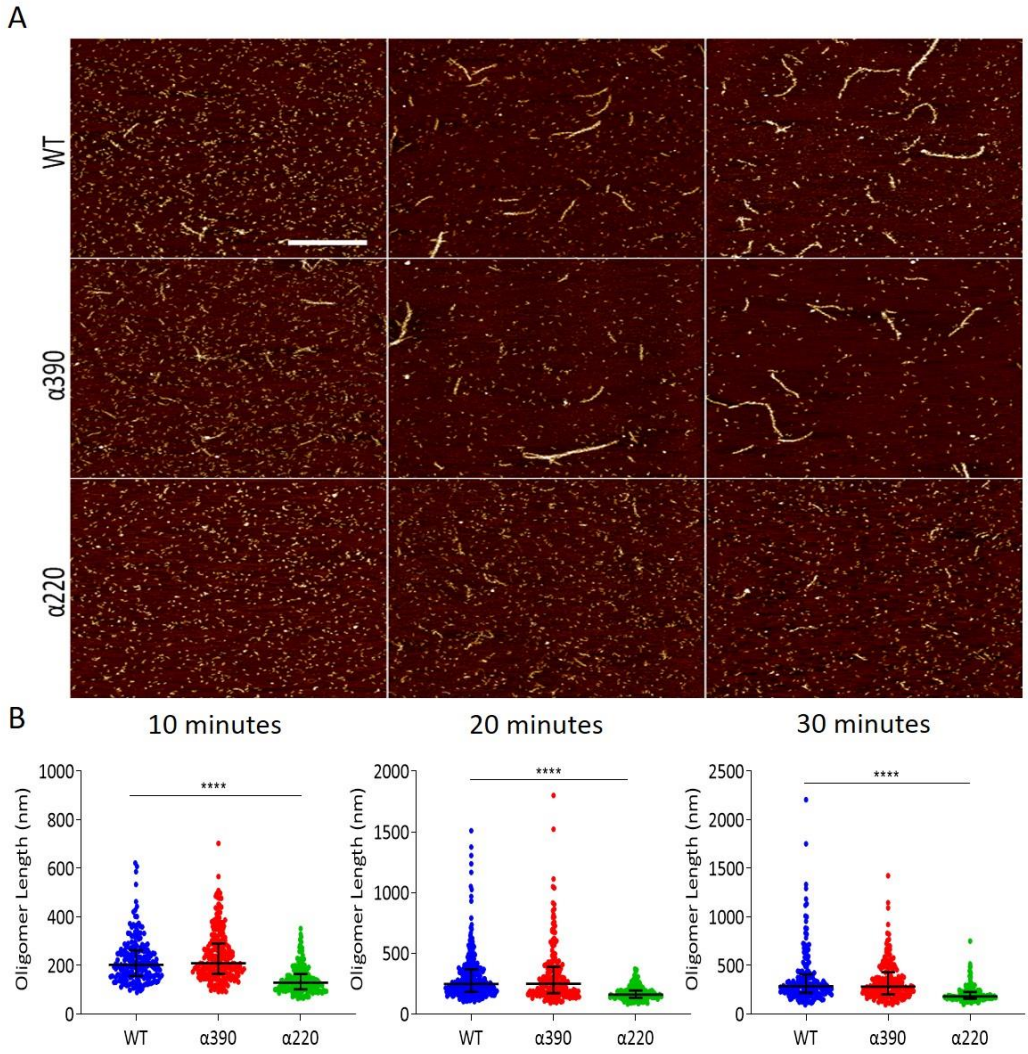

Figure 19 Limited Early Polymerisation Growth for Fibrin Lacking the αC-Region

Representative images on for polymerisation lengths for WT, α390 and α220 at time points 10 (left), 20 (middle) and 30 (right) minutes (A). Images are on atomic force micrographs; scale bar is 1 µm. Average oligomer length at 10 minutes (left), 20 minutes (middle) and 30 minutes (right) (B). Polymerisation was initiated and then stopped at 10, 20, 30 minutes before oligomers were imaged. Results shown as median with interquartile range, n=3, ****p<0.0001 by Kruskal-Wallis test with Dunn's multiple comparison test relative to the WT.

4.4.3.3 Laser-scanning Confocal Microscopy Investigations into Clot Structure

4.4.3.3.1 Fluorescent Labelled Fibrinogen did not Impact Clot Structure

To confirm that the fluorescently labelled fibrinogen required for confocal microscopy did not impact polymerisation and consequently the structure of the fibrin clot, a turbidimetric assay was performed comparing labelled fibrinogen to the unlabelled parent (Figure 20). The amount of labelled fibrinogen included within the assay was equivalent to the final concentration used for the LSCM experiments. All turbidimetric curves were similar for the labelled fibrinogens compared to their respective unlabelled parent and followed the same trend as observed in the initial turbidimetric assay (Figure 20A).

The maximum OD which relates to fibre thickness was similar between unlabelled parent and the respective parent with label (Figure 20B). The unlabelled WT had a maximum OD of 0.371±0.004 OD compared to 0.405±0.004 OD for the labelled fibrinogen. Comparing α390 with labelled α390 fibrinogen, the maximum OD was 0.140±0.006 OD and 0.155±0.009 OD respectively. The maximum OD for α220 was 0.367±0.011 OD compared to 0.362±0.019 OD for labelled α220 fibrinogen.

These results confirm that any differences observed through structural investigations by LSCM are independent of the labelled fibrinogen altering fibrin polymerisation and therefore final clot architecture.

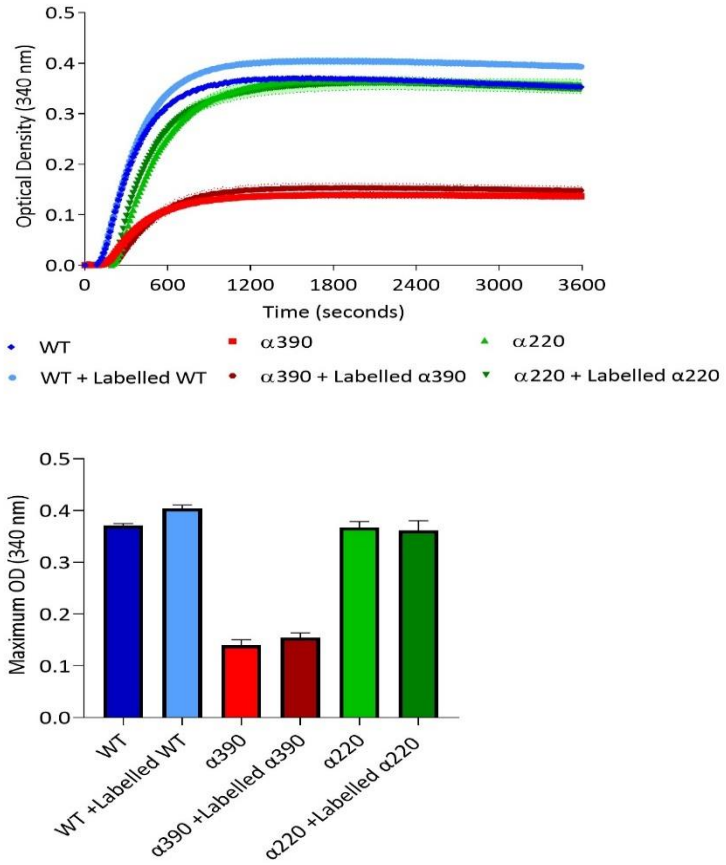

Figure 20 Fluorescently Labelled Fibrinogen did not Alter Fibre Thickness

Turbidity curve showing the polymerisation profile of fibrinogen only (WT (dark blue), α390 (bright red) and α220 (bright green) and fibrinogen with corresponding 5 % fluorescently labelled WT (light blue), α390 (burgundy) and α220 (dark green) (A). Maximum optical density (OD) of fibrinogen only (WT (dark blue), α390 (bright red) and α220 (bright green)) and fibrinogen with corresponding 5 % fluorescently labelled WT (light blue), α390 (burgundy) and α220 (dark green) (B). Clotting was initiated with 0.1 U/mL thrombin and 5 mM calcium and the final concentration of fibrinogen was maintained at 0.5 mg/mL. Error bars are shown as mean ± standard deviation *n*=3 for fibrinogen only and *n*=2 for fibrinogen with 5 % fluorescently labelled fibrinogen.

4.4.3.3.2 Impact of αC-subregions on Clot Architecture

To further investigate the impact of the αC-subregions on clot structure, clots were formed with a corresponding Alexa Fluor® 488 label and imaged by LSCM. Figure 21A shows a vastly different clot structure for both the αC-region subregions compared to the WT. α390 produced a denser clot structure compared to the WT, which agrees with the lower maximum OD observed in the turbidimetric assays (Figure 18A). In contrast, α220 showed no difference in maximum OD compared to the WT but the clot structure was noticeably different, since the clot showed large pores throughout, in addition to compact areas with short, stunted fibres that were highly branched. The fibrin fibre count (Figure 21B) showed no difference between WT (12.97±0.35 fibres/100 μm) and α220 (14.87±2.25 fibres/100 μm) which agreed with the similar maximum OD data from the turbidimetric assays. Also, the fibrin fibre count was greater for α390 clots (19.57±1.63 fibres/100 μm; p=0.0041) compared to the WT, which also agreed with the lower maximum OD data for α390 clots.

To validate that the structural observations observed by LSCM were independent of the fluorescent label, the WT fibrinogen was spiked with increasing percentage of either α390 or α220. For both truncations 5 % WT-labelled Alexa Fluor® 488 was used to visualise the clots.

Figure 22 shows WT clots spiked with α390 increased in clot density the higher the percentage of α390 was incorporated within the clot and this phenotype became dominant from 50 % α390 and above. This observation agrees with the LSCM data of α390 clots labelled with α390-labelled Alexa Fluor® 488, since the α390 truncation produces clots that are denser. WT clots spiked with α220 began to show a noticeable alteration in clot structure at 50 % α220 content, where the clot structure became more porous. At a 75 % α220 content, the fibres were highly branched with stunted fibres. There were porous areas present, but these were smaller than observed at 50 % and 95 % α220. At 95 % α220, the clot was highly porous with stunted fibres that were highly branched, similar to the clots produced with α220-labelled Alexa Fluor® 488. These data demonstrate that the truncated fibrinogens can combine with the WT to form a clot.

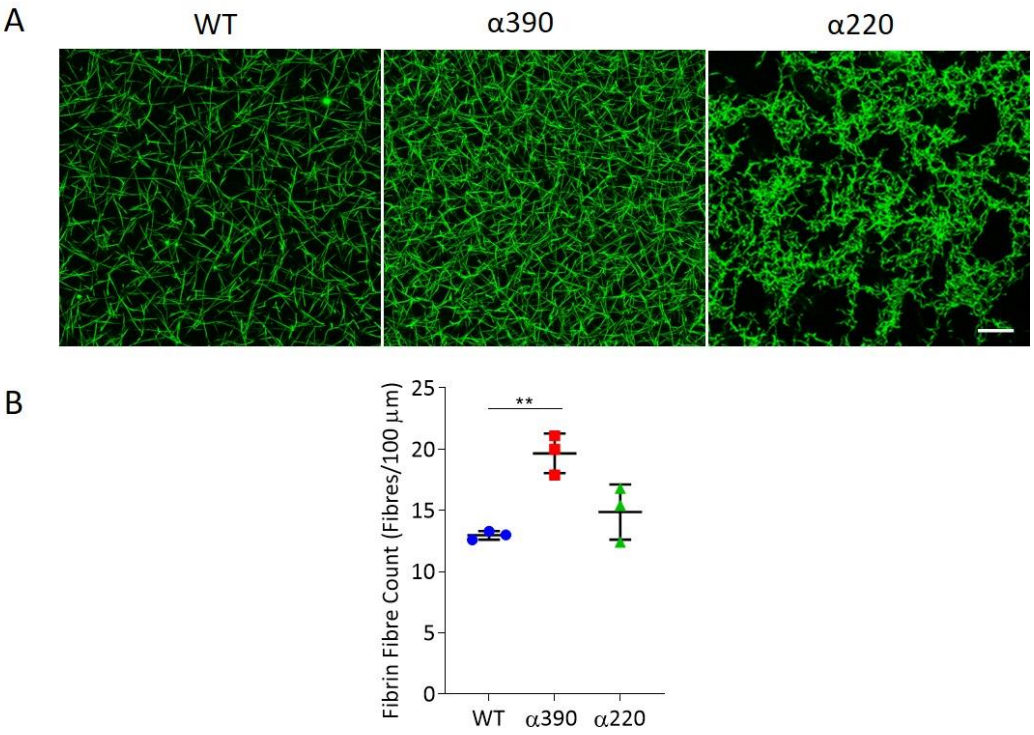

Figure 21 Altered Structure Observed in Clots with Truncations to αC-regions

Representative z stack images of clots composed of fibrin and Alexa-488 labelled fibrin for visualisation; WT (left), α390 (middle) and α220 (right) (A). Images taken on a LSM880 inverted laser scanning confocal microscope, using the x40 objective. Z-stack is over 20.30 µm and composed of 29 slices; scale bar is 20 µm. Fibrin fibre count in clots composed of WT, α390 and α220 (B). Results shown as mean ±standard deviation, *n*=3, ** *p*=0.01 by one-way ANOVA with Dunnett's multiple comparison test relative to the WT.

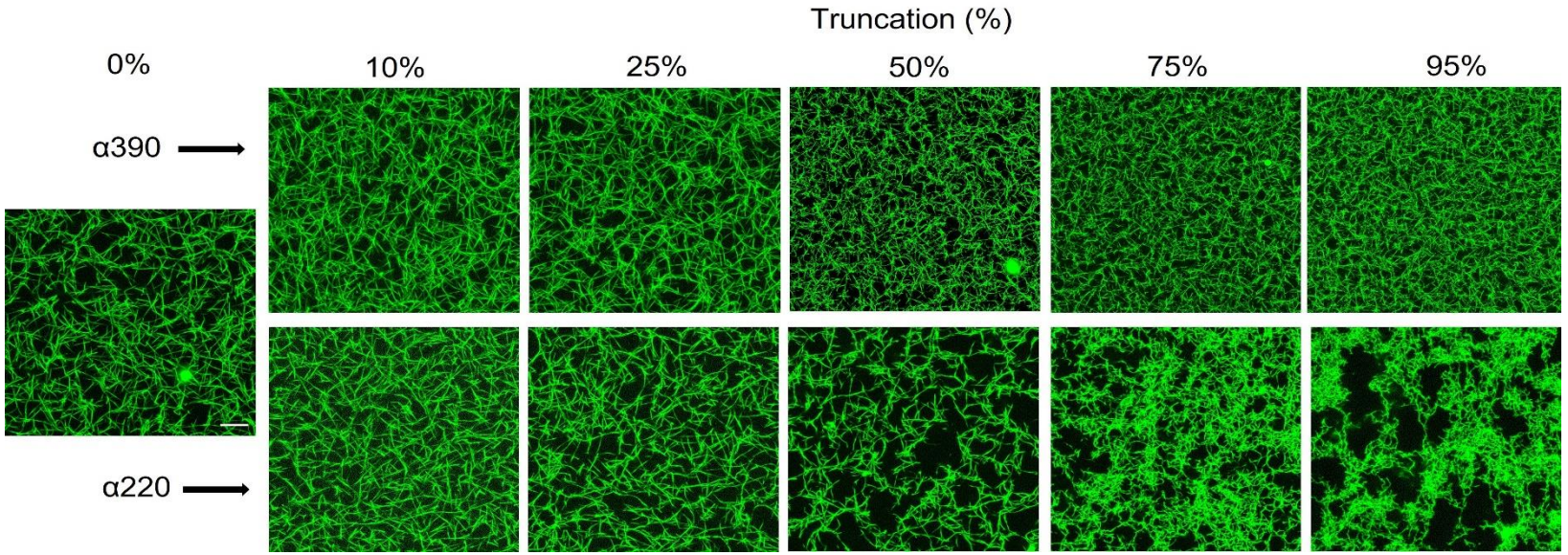

Figure 22 Clots Formed with Increasing Percentage of Truncated αC-region Fibrinogen Gradually Alters WT Clot Structure

Representative z stack image clots composed of WT fibrin with increasing percentage of α390 (top) and α220 (bottom). Clots were visualised with Alexa-488® labelled WT fibrin, maintained at 5 %. Images taken on a LSM880 inverted laser scanning confocal microscope, using the x40 objective, z-stack is over 20.30 µm and composed of 29 slices; scale bar is 20 µm. *n*=3.

4.4.3.4 Reduced Fibre Diameter Observed in Clots Lacking the αC-domain

To gain further structural insights into the impact of the αC-region subregions on clot ultrastructure at the submicrometer and nanometer scales, scanning electron microscopy was performed. This method allows the clots to be studied in much greater magnification than confocal microscopy can. Clots were prepared, fixed, dehydrated, coated, and then imaged on a Hitachi SU8230 Ultra-High-Resolution scanning electron microscope.

Over a range of magnifications, α390 displayed a denser clot structure compared to the WT (Figure 23), α220 clots showed areas where fibres were more compact in between porous areas, which was more notable at the two lower magnifications (x2,000 and x5,000). Interestingly, in addition to porosity, the clot structure for α220 showed numerous fibre ends and these are highlighted by the yellow arrows (Figure 23A) and were seen throughout the clot. In contrast, no fibres ends were observed for either WT or α390.

The average fibre diameter was reduced for α390 (51.7±5.0 nm) compared to WT (79.2±11.7 nm p=0.0059) (Figure 23B), indicating that α390 produces clots with thinner fibres which agrees with the reduced maximum OD observed in the turbidimetric assay.

In contrast, no difference was observed between α220 (86.2±2.3 nm) and the WT, which corresponds with the result from the turbidimetric assay, as both WT and α220 had similar maximum absorbance (Figure 18A).

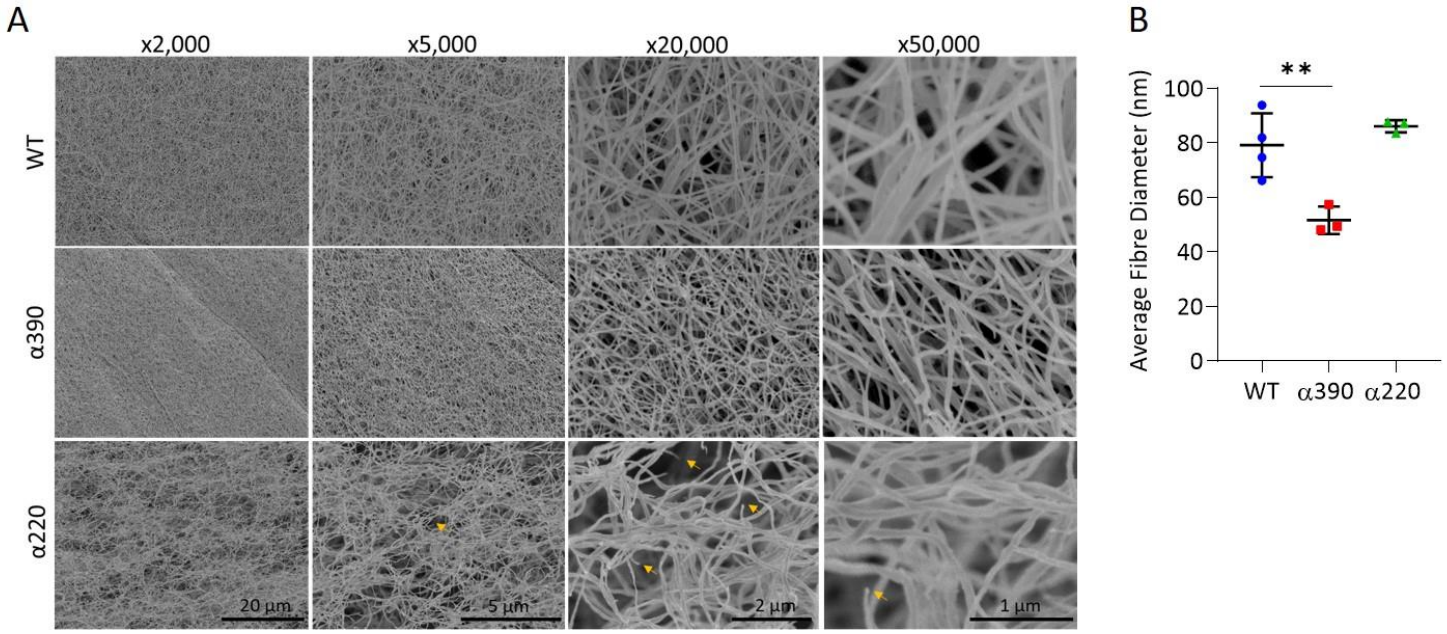

Figure 23 Fibrin Lacking αC-domain had Reduced Fibre Diameter

Representative images of clots composed of WT (top), α390 (middle) or α220 (bottom) by scanning electron microscopy over increasing magnifications of x2,000, x5,000, x20,000 and x50,000 (A). Fibre ends were visible in α220 clots, highlighted by the yellow arrows. Images were taken on a Hitachi SU8230 Ultra-High-Resolution Scanning Electron Microscope. Average fibre diameter for WT, α390 and α220 (B). Fibre diameter was calculated on images at x20,000 magnification. Results shown as mean ±standard deviation, *n*=4 WT and *n*=3 α390 and α220, ***p*=0.01 by one-way ANOVA with Dunnett's multiple comparison test relative to the WT.

4.4.4 Functional Investigations into the αC-subregions

4.4.4.1.1 Rapid External Fibrinolysis Observed in Clots Lacking the αC-region

Initial investigations into fibrinolysis using clots made with fibrinogens truncated in the αC-region subregions were made by observing the fibrinolysis front over time using LSCM. No data could be quantified, however, for α220 using this method as the clot lysed far too rapidly (Figure 24A). There was no defined lysis front due to the highly porous nature of the α220 clot structure observed in Figure 21A. The α220 clot showed multiple areas being lysed simultaneously, therefore fibrinolysis could not be accurately measured. Figure 24B shows an example of the defined lysis front observed for WT and α390 as indicated by the line depicting the lysis front, whereas the images for α220 lysing over time demonstrated that the clot lysed from multiple sides. As WT and α390 clots showed a defined lysis front, fibrinolysis rate could be analysed. No difference was observed in time to 50 % fibrinolysis between WT (4.0±1.4 minutes) and α390 (4.3±1.5 minutes) clots (Figure 24).

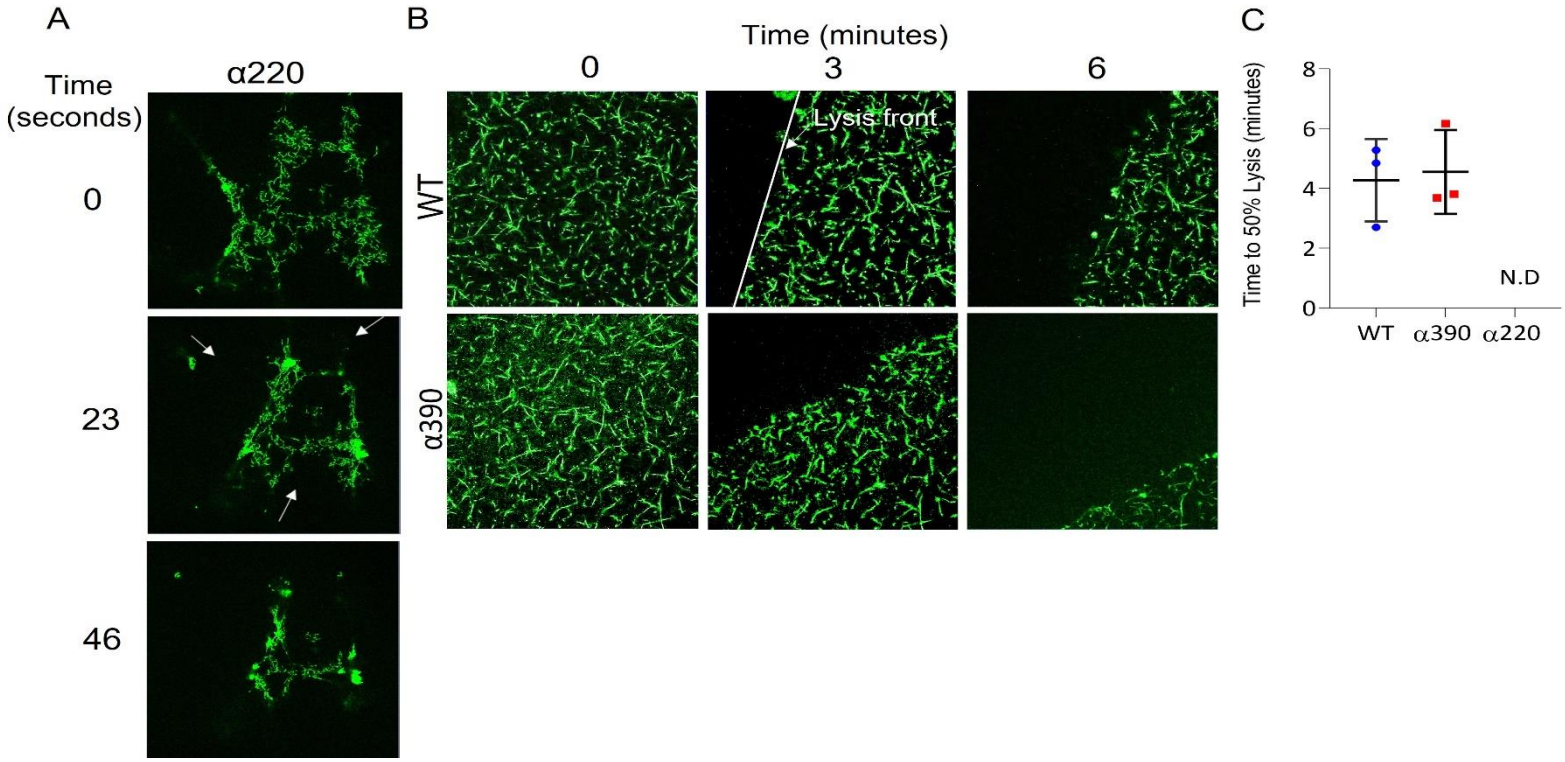

Figure 24 Clots Lacking the αC-region Exhibited Rapid External Fibrinolysis

Representative images of fibrinolysis of α220 (A). Highlighting rapid lysis, with numerous fibrinolysis fronts shown by the arrows. Representative images of fibrinolysis of WT and α390 (B). In contrast to α220, a defined lysis front was observed for WT and α390. Time to 50 % lysis for WT and α390 (C). The time to 50 % lysis was not determined (N.D) for α220. Time series were taken on a LSM880 inverted laser scanning confocal microscope using the x40 objective, and time-series were composed of 8 slice z-stack over 20.30 µm. Clots were visualised with Alexa-488® labelled fibrin matching either the WT or α390 or α220. *n*=3 for WT and α390

4.4.4.1.2 Rapid Internal Fibrinolysis of Clots Lacking the αC-region

Following the initial challenges using microscopy for the characterisation of fibrinolysis for α220, fibrinolysis analysis was achieved through lysing clots in 384 microtiter well plates, and then overlaying the clot with a lysis mix of plasminogen and tPA. Disintegration of the clots was analysed over time using turbidimetry.

The fibrinolysis curve (Figure 25A) exhibited for WT and α390 was comparable, while α220 fibrinolysis profile was extremely rapid. The time to 50 % lysis was similar for WT (73.5±4.8 minutes) and α390 (68.6±8.0 minutes) as was the average rate of lysis (WT -0.025±0.006 δOD/seconds and α390 -0.026±0.013 δOD/seconds). However, α220 lysed significantly faster compared to WT with a time to 50 % lysis of 17.7±3.3 minutes $p<0.0001$, and the average rate of lysis was increased substantially for α220 (-0.068±0.014 δOD/seconds) compared to WT clots ($p=0.0011$) (Figure 25B and C).

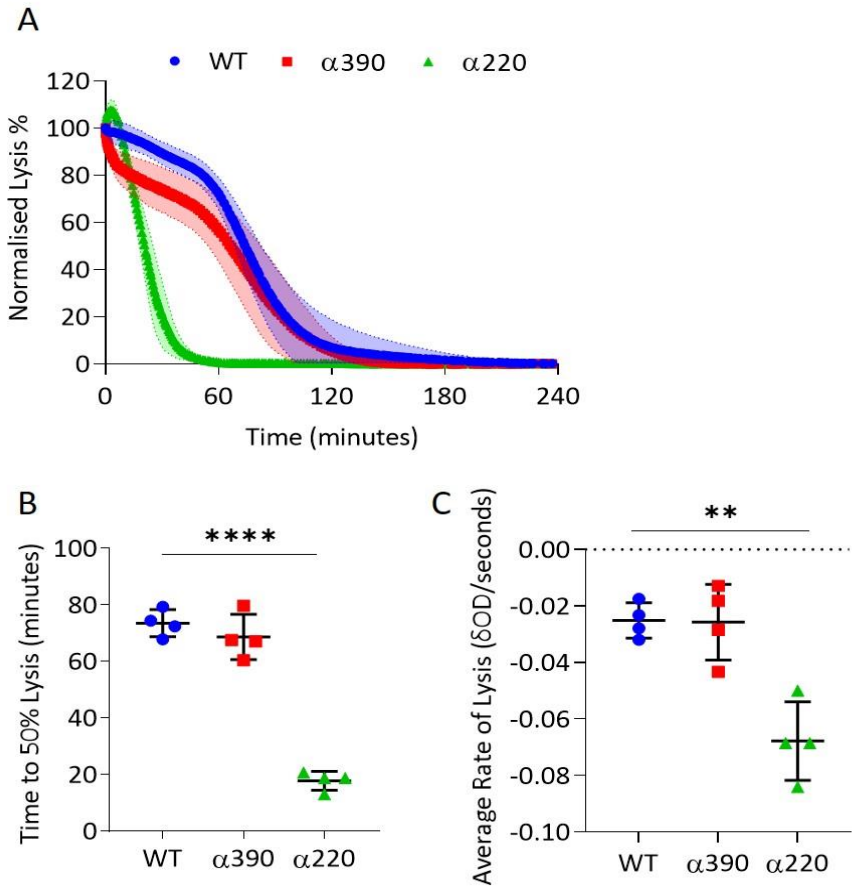

Figure 25 Clots Missing the αC-region showed Sensitivty to Fibrinolysis

Normalised lysis curves for WT, α390 and α220 (A). Time to 50 % lysis for WT, α390 and α220 (B). Average rate of lysis WT, α390 and α220 (C). Fibrinolytic mixture of plasminogen and t-Pa at 0.24 µM and 1 nM respectively were overlayed on a pre-formed clot and lysis was monitored over 4 hours at 340 nm. Results shown as mean ±standard deviation, *n*=4, ***p*=0.01 and *****p*<0.0001 by one-way ANOVA with Dunnett's multiple comparison test relative to the WT.

4.4.4.1.3 Inclusion of α_2-antiplasmin Prolonged Fibrinolysis of WT and α390

The plasmin inhibitor α_2-antiplasmin is incorporated within the clot by FXIIIa. The site of α_2-antiplasmin crosslinking is in the αC-connector at K303 (Mosesson et al., 2008). This residue is missing in fibrinogen truncated at α220 but present in α390 fibrinogen. Investigations into the influence of fibrinolysis in the presence of α_2-antiplasmin were achieved through turbidimetric assay.

As expected, there was an elongation in the time to 50 % lysis with the addition of α_2-antiplasmin. A further extension was observed with the addition of FXIII and the α_2-antiplasmin for WT and α390 fibrin clots (Figure 26). There was a significant increase in time to 50 % lysis between WT clots (20.22±1.4 minutes) and WT with α_2-antiplasmin (84.11±25.5 minutes $p<0.0001$) and a further increase in time when the α_2-antiplasmin (111.5±17.0 minutes $p<0.0001$) was cross-linked into the clot by FXIIIa. α390 clots (23.0±4.5 minutes) showed a significant increase in time to 50 % lysis with the inclusion of α_2-antiplasmin (109.0±1.8 minutes $p<0.0001$), and a further increase in time when the α_2-antiplasmin (143.8±1.8 minutes $p<0.0001$) was cross-linked into the clot by FXIIIa. There was a significant difference between WT with FXIII and the α_2-antiplasmin and α390 with FXIII and the α_2-antiplasmin ($p=0.0127$). Although there was an increase in time to 50 % lysis for α220 clots (15.4±3.5 minutes) after the addition of α_2-antiplasmin (23.5±6.2 minutes) or FXIII and α_2-antiplasmin (33.0±0.8 minutes), this did not reach statistical significance.

The average rate of lysis was reduced for WT, α390 and α220 with the addition of α_2-antiplasmin or FXIII and α_2-antiplasmin, demonstrating the effect α_2-antiplasmin has on inhibiting fibrinolysis (Figure 26B). The average rate of lysis for WT was 0.0006±8.737x10-005 δOD/seconds compared to with α_2-antiplasmin -0.0001063±2.570x10-005 δOD/seconds $p=0.0005$ and with both α_2-antiplasmin and FXIII -7.633x10-005±1.858x10-005 δOD/seconds $p=0.0003$. The average rate of lysis for α390 was -0.0005±5.686e-005 δOD/seconds, compared to -8.200x10-005±2.234x10-005 δOD/seconds ($p=0.0046$) and -6.667x10-005 ±5.033x10-006 δOD/seconds ($p=0.0031$) for α_2-antiplasmin and α_2-antiplasmin with FXIII respectively. The average rate of lysis for α220 (-0.001140±0.0002784 δOD/seconds) did reduce with the addition of α_2-antiplasmin (-0.0004433±0.0001401 δOD/seconds $p=0.0085$) and further reduced with inclusion of FXIII with the α_2-antiplasmin (-0.0003433±7.638x10-005 δOD/seconds $p=0.0007$). There was a significant difference between the WT and α220

both with α_2-antiplasmin p=0.0362. No difference was seen with the addition of FXIII to either WT, α390 and α220 compared to without FXIII for the average rate of lysis.

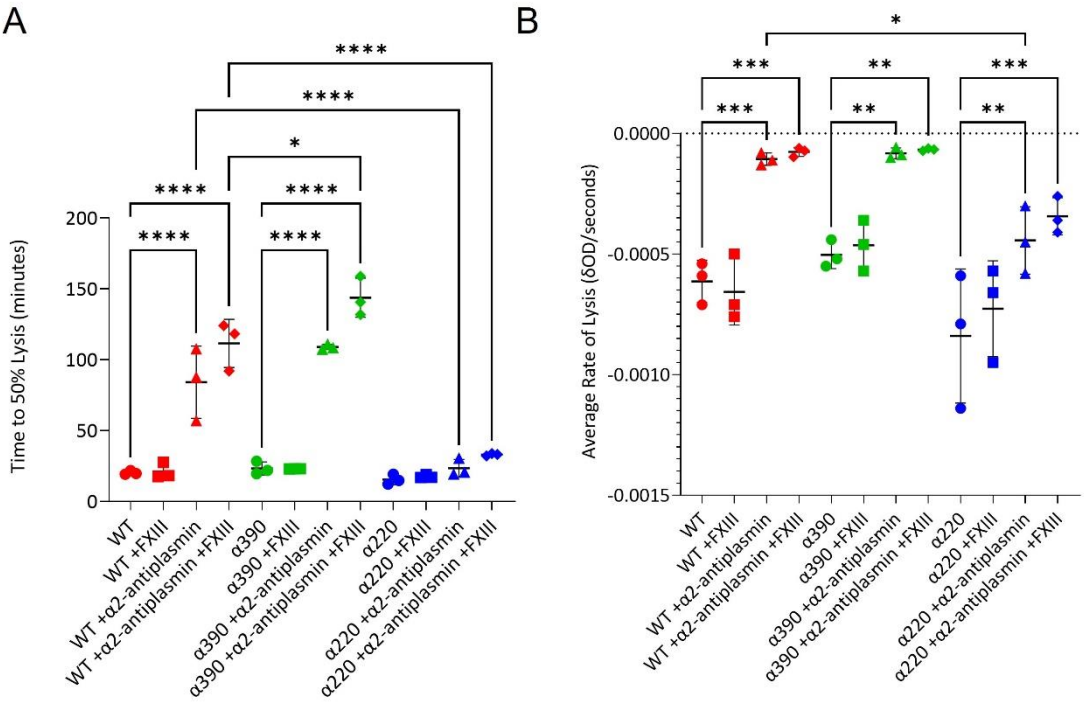

Figure 26 The Inclusion of α2-antiplasmin Increased Fibrinolytic Resistance of WT and α390
Time to 50 % Lysis for WT, α390 and α220 with the fibrinogens only, or with FXIII or α^2-antiplasmin or addition of FXIII and α_2-antiplasmin (A). Average rate of Lysis for WT, α390 and α220 with the fibrinogens only, or with FXIII or α_2-antiplasmin or addition of FXIII and α_2-antiplasmin (B). Results shown as mean ±standard deviation, n=3, *p=0.05, ** p=0.01, ***p=0.001 and ****p<0.0001 by one-way ANOVA with Šídák's multiple comparison test.

4.4.4.2 α-Chain Cross-linking is Reduced, while γ'-Chain Cross-linking Remains Unaffected in Clots with Truncated αC-region

The αC-region has multiple glutamine and lysine residues that are involved in the formation of glutamyl-ε-lysyl isopeptide bonds by FXIIIa (Pisano et al., 1968). Due to the truncations made to the αC-region, there would be alterations in α-chain cross-linking as many of the sites participating in α-chain crosslinking are absent. The αC-domain contains most of the lysine donors and these therefore are absent in both α390 and α220. The glutamines situated within the αC-connector (Q221 and/or Q223, Q237, Q328, and Q366) are present in α390 but subsequently removed in α220 (Mouapi et al., 2016).

In all recombinant fibrinogens there was a noticeable reduction in molecular weight of the α-chains observed after 15 minutes incubation with thrombin and FXIII, indicating the cleavage of FpA (Figure 27). For both truncations, a dual α-chain band of FpA representing cleaved and non-cleaved α-chain was present over the course of the experiment. As observed in the turbidimetric assays, there was an initial delay in clotting compared to the WT for both truncations, which can be seen in the slower disappearance in non-cleaved FpA α-chain and a delay in the appearance of γ-γ dimers (Figure 18B).

As anticipated, there was a delay in α-chain cross-linking for both truncations compared to WT. There was limited change in α-chain crosslinking between 1 and 2 hours for the WT and the truncations, signifying that the majority the cross-linking occurred in the initial stage of clot formation. Furthermore, both truncations had over 60% of the α-chain still uncross-linked at 2 hours whereas all the α-chain monomer had been converted to polymer in the WT clots (Figure 27B). As both truncations demonstrated some α-chain cross-linking and both achieved a similar percentage of cross-linking over the course of the assay, this suggests that there may be further cross-linking occurring beyond the known reported glutamine and lysine residues involved in cross-linking which are absent with the removal of the αC-region. Both truncations displayed normal γ-chain cross-linking (Figure 27C), as observed by the diminishing γ-chain monomer over time and the appearance of the γ-γ dimer observed by in line with the 100 kDa molecular weight marker.

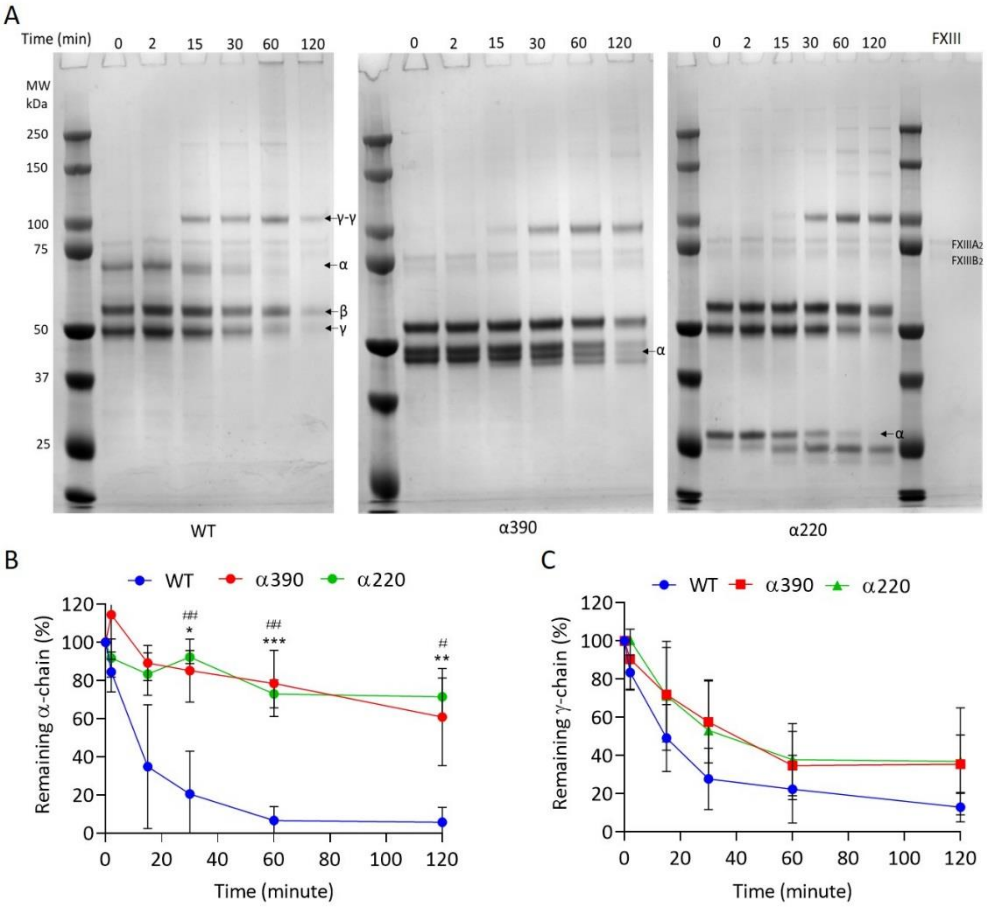

Figure 27 Reduced α-chain Cross-linking and Normal γ-chain Cross-linking in αC-subregion clots

Representative images of SDS-PAGE of FXIII cross-linking of WT, α390 and α220 (A). SDS-PAGE was stained with Instant Blue. Remaining un-crosslinked α-chain in WT, α390 and α220 (B). Remaining un-crosslinked γ-chain in WT, α390 and α220 (C). All fibrinogens showed loss in uncross-linked γ-chain. Results shown as mean ±standard deviation, n=3, */$^{\#}p$=0.05, **/$^{\#\#}$ p=0.01, ***p=0.001 by two-way ANOVA with Geisser-Greenhouse correction with Dunnett's multiple comparison test relative to the WT. * denotes significance for α390 and $^{\#}$ for α220.

4.4.4.3 Fibrin Lacking αC-region showed Reduced Clot Stiffness

Viscoelastic investigations into the αC-subregions were accomplished through micro-rheology using an in-house magnetic tweezers device. Fibrin clots with αC-subdomain truncations were studied in both the absence and presence of FXIII, to investigate clot viscosity/loss modulus (G") and clot stiffness/storage modulus (G'). Once the G" and G' have been calculated, the loss tangent (Tan δ ratio of G"/G') can be calculated which indicates the physical behaviour of a system. A Tan δ above 1 indicates a largely viscous material, while Tan δ < 1 is indicative of a largely elastic material. For a viscoelastic material with Tan δ = 1, the amounts of energy dissipated and stored are equal. Dr Stephen Baker assisted with data collection.

The initial investigations into viscoelastic properties were performed without FXIII (Figure 28). No data was obtained for α220 in the absence of FXIII, as the tracking system was unable to follow the displacement of the incorporated beads within the clot. The frequencies examined for clot viscosity/loss modulus (G") and clot stiffness/storage modulus (G') showed no significant differences between WT and α390 in the absence of FXIII. α390 showed a trend for all G' frequencies to be higher than WT. At 0.1 Hz, the G' for WT was 1.095±0.421 Pa whereas that for α390 was 1.503±0.755 Pa. Both fibrinogen proteins showed an increase in G' at 1 Hz, with WT measuring 1.619±0.396 Pa and α390 2.261±0.769 Pa. At 10 Hz, the G' for WT was 2.596±0.552 Pa and for α390 2.594±1.055 Pa (Figure 28A). The G" at 0.1 Hz was 0.176±0.055 Pa for WT and 0.343±0.041 Pa for α390, at 1 Hz the WT G'' was 0.622±0.181 Pa and for α390 0.363±0.210 Pa. At 10 Hz, the clot viscosity was 0.285±0.130 for WT and 0.184±0.237 for α390 (Figure 28B). The tan δ at all the frequencies showed that both WT and α390 were more elastic than viscous (Figure 28C).

As expected, the addition of FXIII lead to higher levels of clot viscosity/loss modulus (G") and clot stiffness/storage modulus (G'). The G' at 0.1 Hz was significantly reduced for α220 (0.0093±0.0020 Pa) compared to WT (2.4353±0.4987 Pa p=0.0381), and although higher for α390 (3.5473±0.9778 Pa), the latter did not reach significance. At 1 Hz, the G' was higher for α390 (4.1140±1.4793 Pa) compared to WT (2.8584±0.5855 Pa) although again not reaching statistical significance, and there again was a significant reduced G' for α220 (0.0173±0.0057 Pa) compared to WT (p=0.0147). At 10 Hz, the G' was significantly increased for α390 (7.0156±3.0364 Pa) compared to WT (5.5646±0.9624 Pa p=0.0412) as well as α220 (0.0322±0.0106 Pa p<0.0001) (Figure 29A). There was no difference in G" for α390 (0.4473±0.1907 Pa) or α220 (0.0072±0.0094 Pa) compared to WT (0.2025±0.08635 Pa) at

0.1 Hz. Like at 0.1 Hz there was no difference at 1 Hz for α390 (1.4707±0.9210 Pa) or α220 (0.0092±0.0043 Pa) compared to WT (0.9501±0.4802 Pa). At 10 Hz, the G" was significantly different for α220 (0.0145±0.0206 Pa) compared to WT (2.1547±0.6520 Pa p=0.0010), and no difference was observed for α390 (1.7421±0.1.5271 Pa) (Figure 29B). As with the absence of FXIII, the tan δ for WT, α390 and α220 showed that the clots were always more elastic than viscous at all frequencies (Figure 29C). Furthermore, although not significant the higher tan δ observed for α220 indicates that the clots showed reduced stability and are more readily deformable.

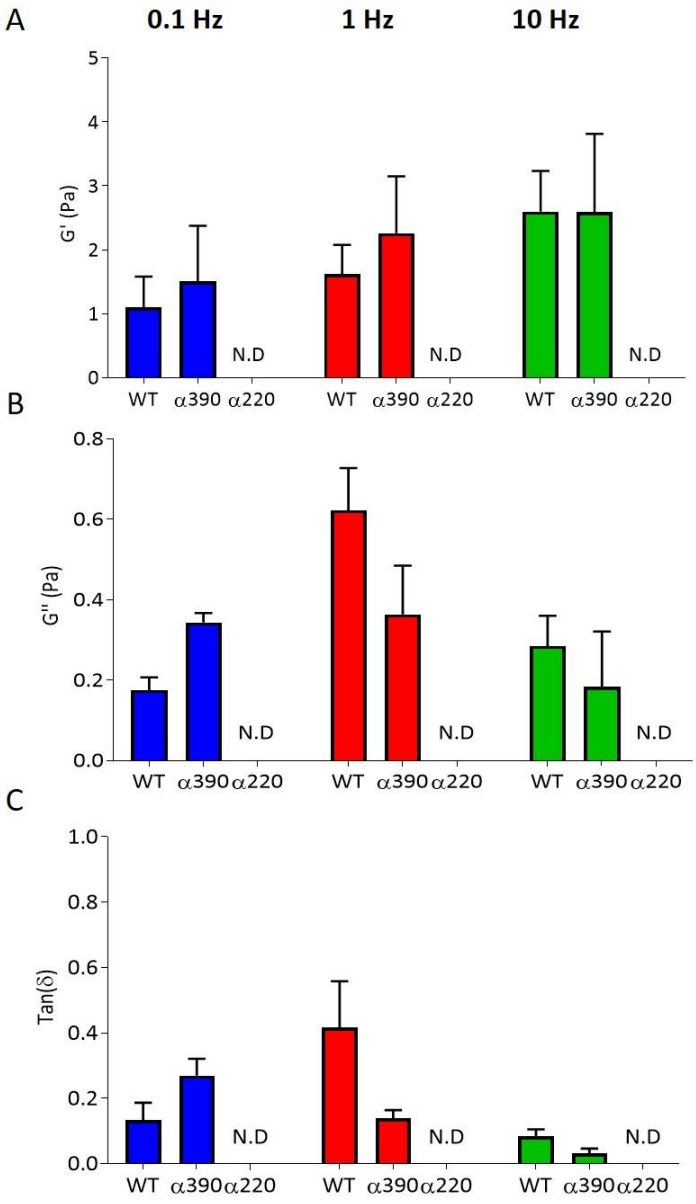

Figure 28 Viscoelastic Investigation into αC-subregions without FXIII

Storage modulus (G') for WT and α390 (A). Loss modulus (G") for WT and α390 (B). The tan δ for WT and α390 (C). No data was generated for α220 (N.D). Results shown as mean ±standard deviation, *n*=4.

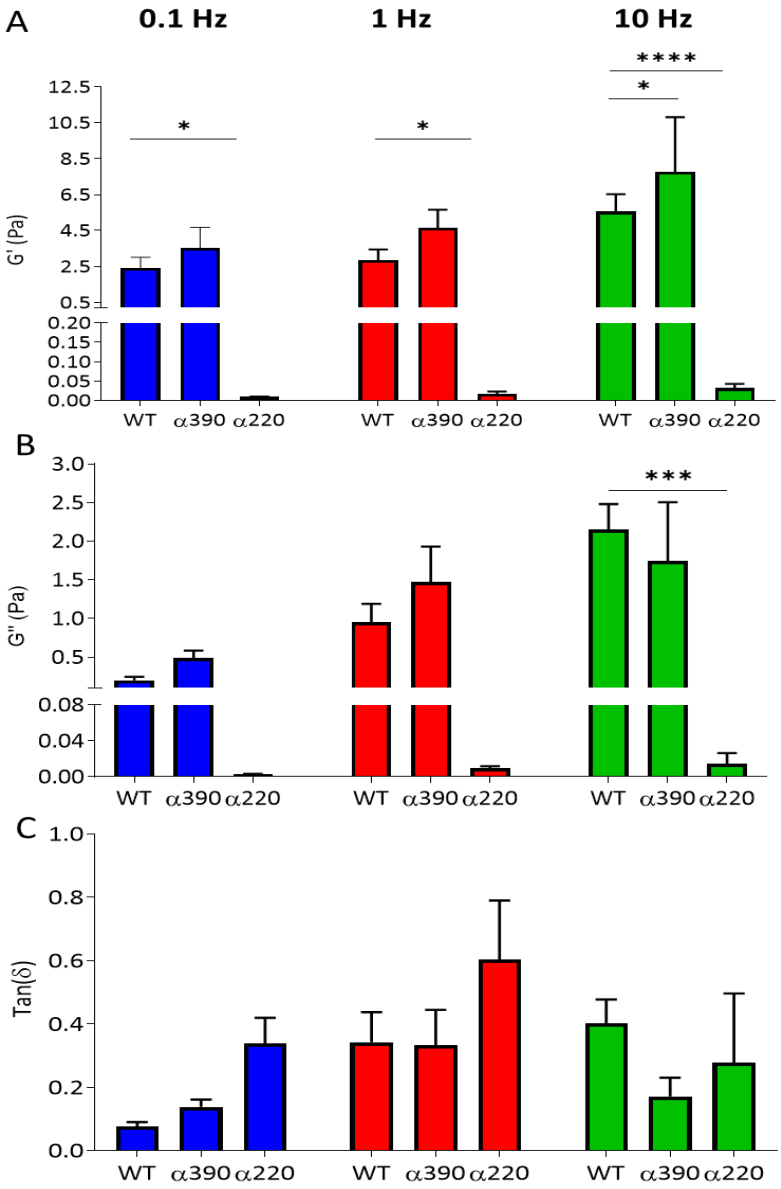

Figure 29 Reduced G' observed for Fibrin Lacking the αC-region

Storage modulus (G') for WT, α390 and α220 clots (A). Loss modulus (G") for WT, α390 and α220 clots (B). The tan δ for WT, α390 and α220 clots (C). Results shown as mean ±standard deviation, *n*=4 WT and α390 and *n*=3 for α220. **p*=0.005, ***p*=0.001 and ****p>0.0001 by two-way ANOVA with Dunnett's multiple comparisons test.

4.5 Discussion

Following initial characterisation of the two recombinant α-chain truncations, further investigations were undertaken to understand their role in fibrin clot structure (turbidimetry, LSCM and SEM) and function (fibrinolysis and mechanics). Both fibrinogen truncations were structurally distinct with regards to the fibrin fibre structure they formed compared to WT, indicating that the αC-region provides critical structural architecture with the αC-connector providing lateral as well as longitudinal fibre growth. In addition to the clot structural alterations observed with the truncations, clots made with fibrinogen lacking only the αC-domain behaved generally more or less like the WT in fibrinolysis and clot mechanics. In contrast, there were vast differences in clot mechanics and fibrinolysis when clots were produced with fibrinogen lacking the entire αC-region.

The initial characterisation confirmed that the recombinant fibrinogens produced in the previous chapter were composed of one homogeneous species. The migration of the α-chains was distinct with α220 migrating the furthest, and the recombinant α-truncations showed the expected difference in size for α-chain for the respective α-truncation. In addition, there was no difference in sizes of the β- and γ-chain compared to the WT, indicating no other changes had occurred. The clotability of the recombinant fibrinogens was similar to the previously published WT, α251 and the α-chain cross-linking point mutations produced by the same CHO cell expression model (98-97 %) (Gorkun et al., 1998; Park et al., 2013).

The removal of the αC-domain (α390) resulted in a clot that was denser and composed of thinner fibres compared to WT, which was observed in both scanning electron microscopy and LSCM. This was comparable to the images of the fibrinogen variant α251, which is 139 residues shorter than α390 (Collet et al., 2005). In contrast, for clots made with α220 fibrinogen, which is closer in length to α251 being only 31 residues shorter, the structure was highly porous with short, stunted fibres. This porous clot structure was not as apparent in scanning electron microscopy as it was in LSCM, possibly due to the sample preparation procedures involved in scanning electron microscopy. However, many fibre ends were visible in scanning electron microscopy of clots composed of α220 fibrin, implying that having only 18 % of the residues of the αC-connector present as observed in α251 can rescue some of the fibre growth capabilities. Furthermore, in previous studies, scanning electron microscopy images of clots made with Fragment X_2, which is produced by proteolytic digestion and in which both C-terminal of the α-chain terminates at residue 219, showed visible fibre ends (Gorkun et al., 1994) which seem similar to what was observed in α220

fibrin. It is unlikely that these visible ends are due to fibrinolysis as the scanning electron microscopy and turbidity samples were prepared as similarly as possible and there was no lysis observed in the turbidimetric assay. The transmission electron microscopy of images of fragment X_2 showed that the fibrin formed large fibre bundles, and that there were sizable pores in between these bundles (Gorkun et al., 1994). These pores within the clot were also observed in their scanning electron microscopy experiments. The observation of areas of densely packed fibres, with large pores throughout seen in Fragment X_2 clots, appear reminiscent of what was observed in the microscopy of clots made from α220 fibrinogen.

The diameter of α251 fibrin fibres was reduced compared to WT in scanning electron microscopy and LSCM, whereas an increased fibre diameter was calculated for fragment X_2 (Gorkun et al., 1998; Collet et al., 2005). Turbidimetric studies with fibrin monomers of fragment X_2 produced a higher maximum OD than WT, in contrast to α251 fibrin monomers had a lower maximum OD compared to WT. When α251 fibrinogen polymerisation was studied, no difference was observed with WT. As with the fibrinogen polymerisation result for α251, α220 showed a maximum OD similar to WT. The apparent differences between fragment X_2, α251 and α220 may be because fragment X_2 was produced with purified bovine fibrinogen compared to recombinant human fibrinogen, or the partial loss of β-chain which is susceptible to proteolytic digestion in the preparation of fragment X_2, in addition to differences in the number of protein purification cycles required to obtain homogeneous fragment populations.

A consistent observation from patient cases with αC-connector mutations are reduced rates of clotting and lower maximum OD are found (Fibrinogen Šumperk II, Mahdia, Keokuk and Seoul II) (Lefebvre et al., 2004; Park et al., 2006; Kotlín et al., 2012; Amri et al., 2017). These results were mirrored in the α390 variant, consistent with an important role of the αC-domain in lateral aggregation. However, clots made from fibrinogen Otago, Fragment X and fibrinogen α251 exhibit a higher or similar maximum OD compared to the control and generally a reduced rate of clotting (Otago and Fragment X's) (Gorkun et al., 1994; Ridgway et al., 1997; Gorkun et al., 1998). Interestingly, scanning electron microscopy of clots made with Fibrinogen Šumperk II showed that the fibres were wider than the control, while Seoul II showed thinner fibres than the control (Park et al., 2006; Kotlín et al., 2012). None of the other cases of aberrant fibrinogens were investigated via microscopy. Similar differences between the data from maximum OD and microscopy may be observed for clots made with α220 and α251 fibrinogens. Although fibre count and diameter were the same for α220 and WT, the clot ultrastructure was vastly distinct, highlighting the importance of multi-technique approaches to study clot architecture.

The point at which longitudinal growth of protofibrils switches to lateral aggregation has been reported to occur at approximate oligomer lengths of 0.6-0.8 µm (Hantgan et al., 1980; Chernysh et al., 2011). Unfortunately, as AFM cannot be performed after protofibrils grow beyond 0.6 µm in length due to network gelation, we were unable to study this phenomenon. Nevertheless, the timepoints used in the AFM demonstrated comparable growth in protofibril length between WT and α390 fibrin, implying normal longitudinal growth for α390. In clear contrast to WT and α390, α220 fibrin showed significantly shorter oligomers for all time points. The α220 protofibrils had only just about reached a similar length at the final timepoint as that for the initial timepoints for WT and α390. Collectively, with the microscopy data showing that the absence of the complete αC-region results in short, stunted fibres with visible fibres ends, these data suggest that α220 fibres are not able to support normal longitudinal fibre growth, which would normally result in a continual network of fibres without visible fibre ends.

In fibrinolysis experiments, clots made with α220 fibrinogen showed very rapid fibrinolysis, highlighting that presence of the αC-connector reduces clot lysis. Interestingly, no difference in fibrinolysis was observed between WT and α390 clots in both intrinsic and extrinsic fibrinolysis experiments, which establishes a critical role for the αC-connector in preventing premature fibrinolysis.

The conversion of fibrinogen to fibrin results in the exposure of cryptic tPA and plasminogen binding sites. One of these sites involves residues γ312-324, which are in the γ-nodule of fibrinogen, and residues Aα148-160 located within the coiled-coil region. These sites are uncovered early on during protofibril formation and disconnection of the β-nodule from the coiled coil respectively (Yakovlev et al., 2000; Medved and Nieuwenhuizen, 2003). It is possible that these sites are already available in α220 fibrinogen prior to the conversion to fibrin, as there is an absence of tethering of the αC-region to the coiled coil and the E-region (Veklich et al., 1993; Litvinov et al., 2007). If these binding sites are available before fibrin conversion, there might be earlier plasmin generation by tPA prior to clot formation. Thus, the combination of the porous clot structure observed for α220 and the potential of more rapid plasmin generation may cause substantially accelerated fibrinolysis.

The incorporation of fragment X into fibrin clots has previously been observed to increase sensitivity to fibrinolysis compared to clots made with normal fibrin alone (Schaefer et al., 2006). The LSCM images for WT clots spiked with either α390 or α220 demonstrated that clot structure was impacted by either becoming more porous or denser for α220 and α390 respectively in clots with more than 50 % truncation content. The fibrinolysis images by LSCM of α220 highlighted that the clot was lysed from multiple points, confirming that the

porous clot structure observed in α220 contributed to the rapid clot lysis as the fibrinolytic enzymes were able to progress more easily within the clot matrix. The incorporation of fragment X into clots showed an increased rate of plasmin formation as well as a greater sensitivity to proteolysis in a previous study (Schaefer et al., 2006). A faster rate of lysis was observed for α220 compared to WT, which agrees with faster lysis rates for clots made with α251 fibrinogen in a previous study (Collet et al., 2005). The presence of active thrombin has been observed in both arterial and venous thrombi (Mutch et al., 2001). Furthermore, recurrent ischaemia or reocclusion after treatment with t-PA has been previously observed after MI (Topol et al., 1989). Therefore, there is a possibility that the fibrin network may form with partially degraded fibrin and non-degraded fibrin mix, which may impact on its stability, and potentially lead to parts of the clots separating and resulting in embolisation elsewhere in the circulation. In addition, it has been shown that in uncross-linked clots there is a lot of structural rearrangement which can occur without any proteolytic digestion, and therefore *in vivo* forming clots could rearrange to include partially degraded fibrin (Chernysh et al., 2012).

Investigations into the effects of α_2-antiplasmin on fibrinolytic resistance of clots in this thesis clearly showed the effectiveness of α_2-antiplasmin in preventing fibrinolysis and reducing the rate of fibrinolysis. Although not a significant difference, there was an extension in time to 50 % fibrinolysis observed for α220 with the addition of α_2-antiplasmin and then a further delay with both FXIII and α_2-antiplasmin. This delay was seen by the reduced rate of lysis in α220 when the α_2-antiplasmin was included. It has been reported that there are two non-covalent high affinity interaction site for α_2-antiplasmin in fibrin, one site in the subdomain of the αC-domain and the other within the D-region, which are cryptic in fibrinogen (Tsurupa et al., 2010). The reduced rate of lysis in α220 could be due to the non-covalent interaction of α_2-antiplasmin in the D-region of α220, or due to the static conditions of the assay, as the α_2-antiplasmin is still present even though it cannot be cross-linked into the α220 fibrin (which lacks α_2-antiplasmin cross-linking site at K303) and therefore inhibit plasmin. There was no difference in fibrinolytic resistance with any of the fibrinogens when only FXIII was included. This observation agrees with a previous study by Fraser et al., 2011, who demonstrated that the fibrinolytic function of FXIIIa is achieved exclusively through the cross-linking of α_2-antiplasmin to the fibrin α-chain. There was an increase in lysis duration by around 50 % for α390 with FXIII and α_2-antiplasmin compared to WT. This may be due to the denser clot structure of α390 fibrin clots, and thus the α_2-antiplasmin may be more trapped in the developing network along with the fibrinolytic factors, inhibiting their abilities. As mentioned above, the static nature of the assay could be

further contributing to the fibrinolytic resistance of the clots made with αC-region truncated fibrinogens. This hypothesis may require further investigation, along with the possible functional role of the α_2-antiplasmin binding site in the D-region of α220 fibrin.

As the entire αC-region is missing in α220, none of the sites involved in α-chain cross-linking are present, whereas α390 only has a number of glutamines involved in cross-linking present within the αC-connector. Previous investigations into α-chain cross-linking with α251 showed no cross-linking of the α-chain and slower γ-chain cross-linking with uncross-linked γ-chain remaining present after 180 minutes (Collet et al., 2005). Unlike α220, there are at least two glutamines (Q221 (and/or 223) and Q237) and two lysine's (K208 and K219) still present in α251 that can be cross-linked by FXIIIa (Cilia La Corte et al., 2011). As with α251, both truncations showed reduced α-chain cross-linking compared to WT with most of the α-chain remaining uncrosslinked at the end of the assay. A trend for a delay in γ-chain cross-linking was also observed with the truncations, but there this was not significant when compared with the WT. In a previous report, α-chain variants AαQ328P, AαQ366P and AαQ328/366P showed delayed α-chain cross-linking compared to WT, but γ-chain cross-linking remained unchanged (Park et al., 2013), in agreement with the findings with α390 and α220 fibrin cross-linking presented in this thesis. Interestingly, purified fibrinogen from a patient with Seoul II (AαQ328P) fibrinogen showed a delay in α-chain cross-linking, but the γ-chain cross-linking was accelerated compared to WT and was concluded within 5 minutes (Park et al., 2006). For the corresponding recombinant variant, the first time point in the cross-linking gel was at 10 minutes and therefore the initial stages of γ-chain cross-linking are not observed. Furthermore, when γ-chain cross-linking sites are absent (in a triple γK406R, γQ398N and γQ399N fibrinogen variant) no γ-chain cross-linking was observed whatsoever, but there was some delay in α-chain cross-linking (Standeven et al., 2007). The murine truncation *FGA*$^{270/270}$, with truncation to the α-chain also had a delay in γ-chain cross-linking compared to WT mice (Hur et al., 2021). Together, these data suggest that changes to either the γ- or α-chain cross-linking sites may impact cross-linking of the other chain (α- and γ-chain respectively).

Clots produced with α220 fibrinogen variant had vastly reduced clot stiffness and were not able to be studied in the magnetic tweezers device without the addition of FXIII. This is likely due to the absence of all the FXIIIa cross-linking sites within the αC-region. In agreement with the lack of clot stiffness for α220 fibrin, studies with α251 fibrin showed that these clots were structurally weaker. Nonetheless, in contrast to α220, the rheology of α251 clots could still be studied both with and without FXIII. However, permeation studies were not possible in the absence of FXIII (Collet et al., 2005). Together, these findings suggest that α251 likely

produced somewhat stiffer clots compared to α220. In previous study, a recombinant γK406R fibrinogen variant produced increased α-γ hybrid cross-links instead of normal γ-γ cross-links and displayed reduced clot stiffness compared to the WT, indicating that any compensatory cross-links formed instead of the dominant α-α or γ-γ-chain do not achieve a similar level of clot stiffness (Standeven et al., 2007). In contrast to the reduced clot stiffness observed in α220 fibrin, α390 clots showed increased G' compared to WT at all frequencies, although this was only significant at 10 Hz. The structural experiments showed that α390 fibrin produced clots that were denser with thinner fibres. As the produced clots were studied the following day, the clots would have had time to fully develop. For clots produced in the presence of FXIII, there would be as complete FXIIIa cross-linking as possible, even though α-chain cross-linking was impaired relative to WT. It is likely that the denser clot structure observed for α390 causes an increase in clot stiffness compared to WT. In support of this, previous studies with magnetic tweezers showed similar clot stiffness in cross-linked WT and γQ398N/Q399N/K406R clots, indicating that α-chain cross-linking is predominant in generating overall clot stiffness (Duval et al., 2014). On the other hand, however, alternative modes of investigation of γQ398N/Q399N/K406R clots using a torsion pendulum device showed there was a reduction in clot stiffness for γQ398N/Q399N/K406R compared to WT (Standeven et al., 2007). This apparent discrepancy could be explained by different lengths of incubation period between clot formation and measurements. For torsion pendulum experiments, the fibrinogens are investigated following a 1-hour incubation, whereas for magnetic tweezers experiments the magnetic pulling is performed in the morning after overnight clot formation. In any case, it is likely that both the α-α and γ-γ fibrin cross-links contribute to overall clot stiffness in tandem, with α-α cross-links contributing at least 60 % and γ-γ cross-links about 40 % to the Young's modulus (Duval et al., 2014).

The clot viscosity was reduced for α220 compared to WT with a significant difference observed at 10 Hz. As for α220, α251 clots showed reduced clot viscosity compared to WT (Collet et al., 2005). The tan δ (ratio of viscous over elastic modulus) for α220 was higher compared to WT and α390 (at both 0.1 Hz and 1 Hz), which indicates a shift to a more viscous nature and therefore more easily deformable clot for α220 fibrin, which would be less able to maintain its integrity. The clot viscosity was unchanged between WT and α390 indicating that loss of the αC-domain at the frequencies investigated did not influence clot mechanical deformation.

Altogether, the main findings from this chapter show that clots formed in the absence of the fibrin αC-connector produced short, stunted fibres with large pores throughout, and that these clots were mechanically very weak and highly susceptible to fibrinolysis. If only the

most C-terminal αC-domain was absent, the clot structure still differed from the WT as the clots are composed of thinner fibres producing a denser clot. The presence of the αC-connector produced clots that were functionally more like WT in both fibrinolysis and mechanics.

4.6 Key Findings

- The fibrinogen αC-connector is critical for normal longitudinal fibrin fibre growth.
- The fibrinogen αC-connector region provides critical mechanical stability in the fibrin clot.
- Fibrinolysis susceptibility is significantly increased for clots made of fibrin that lacks both the αC-connector and αC-domain.

Chapter 5 Investigations of αC-subregions in Whole Blood

5.1 Introduction

Following the initial investigations into the two fibrinogen αC-subregions in Chapter 4, the lack of the αC-connector and αC-domain resulted in clots that were more susceptible to fibrinolysis and had reduced clot stiffness. In contrast, the removal of only the αC-domain produced fibrin clots that were similar in functional aspects (fibrinolysis and clot stiffness) to WT. However, there were differences in clot structure between fibrin missing the αC-domain compared to WT, with thinner fibres and denser clot structure potentially impacting the functional implications of the fibrin clot for α390 clots. Since the initial investigations examined the αC-subregions under purified conditions, this chapter aims to examine the roles of the two fibrinogen subregions in clot formation and function in whole blood.

There have been limited investigations into the role of the fibrinogen αC-region in whole blood or *in vivo*, potentially due to the difficulty of homogenous yields by proteolytic digestion or relative lower yields observed in αC-region alterations of recombinant fibrinogen. Cases of patients with alterations within the αC-region have been used to gain insight into clinical phenotypes. In general, patients with mutations in αC-connector have been observed to show bleeding phenotypes but these can range from mild (Fibrinogen Otago and Italy) to severe (Fibrinogen Latina and Mahdia) (Ridgway et al., 1997; Asselta et al., 2015b; Castaman et al., 2015; Amri et al., 2017). The type of bleeding events, duration and the severity can vary widely, and it is difficult to pinpoint whether the clinical phenotype is due to the reduced fibrinogen levels, which is commonly observed in patients with αC-connector alterations, or due to functional effects. Additionally, in many of the cases where there was at least some fibrinogen expressed (Italy, Champagne-au-Mont-d'Or and Latina), only limited analysis of clinical coagulation assays along with sequencing were performed (Hanss et al., 2003; Asselta et al., 2015a; Castaman et al., 2015). In those studies that performed assays using purified aberrant fibrinogen, the turbidity results have shown prolonged lag phase (Mahdir, Seoul II and Keokuk) (Lefebvre et al., 2004; Park et al., 2006; Amri et al., 2017). Additionally, many of the clinical cases with mutations in the αC-connector reported afibrinogenemia, and therefore no functional studies could be performed. Out of 25 αC-connector variants reported in the human fibrinogen database, 15 were related to afibrinogenemia (GFHT https://site.geht.org/base-fibrinogene/). As the patient case Fibrinogen Otago the murine *FGA*$^{270/270}$ also had hypofibrinogenemia (Hur et al., 2021).

Thrombosis has been associated with some of the clinical cases with mutations in the αC-domain, where there was an unpaired cysteine either due to mutation of an existing cysteine (Marburg and Milano III), or a point mutation introducing a new cysteine (Dusart and Bordeaux) (Koopman et al., 1992; Koopman et al., 1993; Furlan et al., 1994; Fernández-Cadenas et al., 2016). Fibrinogen levels in these cases were not above the normal range as associated with a variety of thrombotic diseases, and therefore the thrombosis in the cases above are likely due to the resultant change in the mutant fibrinogen and its associated impact on clot structure and function (Bridge et al., 2014). Many of the investigations into these mutations have used a limited number of laboratory assays, and investigations in whole blood or plasma assays were limited.

A family with Fibrinogen Perth, in which a frameshift mutation downstream of Aα494 leads to 23 new residues incorporated before a premature termination at residue 517, was observed to be subject to several arterial thrombotic events (Westbury et al., 2013). Fibrinogen from the family members was studied in plasma (turbidimetric) and whole blood (ROTEM) assays. The mutation resulted in fibrin with thinner fibres, which were associated with delayed fibrinolysis (plasma and whole blood assay), reduced plasmin generation, and higher maximum clot firmness. This case of fibrinogen Perth highlights the crucial relationship between fibrinolysis, structure, and mechanics. There was no delay in clot formation rate, lag time or time to maximum OD, but reduced Vmax was found, indicating impaired lateral aggregation. This indicates that the dense network formed with thinner fibres formed more rapidly than the fibrinolytic factors were able to infiltrate, bind and initiate lysis.

As previously mentioned, functional investigations into the roles of the two subregions in whole blood or plasma have thus far been very limited. Using recombinant fibrinogen truncation Aα251, whole blood clot contraction assays demonstrated that RBC retention was mediated by α-chain cross-linking by FXIIIa, as there was limited reduction in clot weight in the absence or presence of the FXIII inhibitor T101 (Byrnes et al., 2015). Whole blood clots formed using Aα251 fibrinogen were heavier in weight compared to the WT and there was no difference in weight after the addition of FXIII, unlike for the control and fibrinogen lacking the γ-chain cross-linking sites. Although the authors did not investigate platelet incorporation and clot contraction over time, the authors suggested that the increase in clot weight was due to the abnormal fibrin network formed. Previously, Aα251 has been shown to be mechanically weak (Collet et al., 2005). Therefore, in addition to the findings with FXIII, a lack of platelet driven contraction likely provides an additional mechanism causing the larger clots for Aα251 fibrinogen. Previously, it has been shown that platelets can generate

contractile forces throughout the cross-linked fibre network, therefore resulting in clot contraction and subsequent reduction of clot size (Lam et al., 2011) .

There have been no studies examining the individual role of the subregions of the fibrinogen αC-region in whole blood. Use of recombinant fibrinogen avoids additional complications from other changes or heterozygosity of fibrinogen chains. Due to the limited yields of the recombinant fibrinogens, no *in vivo* studies were undertaken (e.g. by injecting recombinant fibrinogen in *FGA*$^{-/-}$ mice), but rather assays were performed *ex-vivo* using whole blood or platelets from *FGA*$^{-/-}$ mice, which were supplemented with the recombinant fibrinogens to reduce the amount of fibrinogen needed. The investigations focussed on clot contraction, ROTEM for clot biomechanical properties (whole blood, supplemented with recombinant fibrinogens) and flow cytometry (platelets with recombinant fibrinogens).

5.2 Hypothesis

The fibrinogen αC-region subregions have distinct roles in whole blood clot formation, contraction, and mechanical properties.

5.3 Aims

To investigate the roles of the fibrinogen αC-domain and the αC-connector in whole blood and to further understand their role in the clot formation process.

Secondary Aims:

- Impact of the αC-subregions on clot contraction
- Influence of the αC-subregions on blood cell incorporation in the contracted clot
- Viscoelastic and clot formation studies of the αC-subregions in whole blood

5.4 Results

5.4.1 Clot Contraction was Impaired with the αC-region Missing

Initial investigations into the relationship between the αC-subregion and whole blood involved a clot contraction assay which was performed using citrated whole blood from *FGA*$^{-/-}$ mice combined with either truncated or WT fibrinogen. Clotting was initiated by the addition of tissue factor and $CaCl_2$; a sample of the whole blood and fibrinogen mixture was collected before clot initiation, followed by the supernatant at the final time point after clot contraction for determination of RBC and platelet incorporation within the contracted clot. Two control tubes containing only *FGA*$^{-/-}$ blood were used to confirm if any background clotting was occurring. One of the tubes was to confirm if any clotting was due to interaction with the siliconized coating of the tube and therefore no activation mix was included. The other was to confirm if any contraction was due to the addition of fibrinogen alone, as this tube included the activation mix. Representative images for clot contraction (Figure 30A), show clots forming and contracting over time for both WT and α390, however, for α220 there did not appear to be a clot forming over time. At 2 hours, there was still no visible clot observed in the weighing boat which mirrored the two control tubes. The two control tubes showed no visible clot formation over time and no clot was observed in the weighing boats (Figure 30A), confirming that the observed clot was due to the addition of both fibrinogen and the activation mixture to the *FGA*$^{-/-}$ whole blood. Figure 30B shows clot contraction over time for the truncations and WT. A similar profile was observed for WT and α390, and most of the clot contraction occurred within the first 60 minutes, principally between 30 and 60 minutes (Figure 30A). There was no significant difference observed in clot weight between WT (28.0±4.3 mg) and α390 (25.3±2.1 mg) (Figure 30C).

5.4.1.1 Majority of Platelets were within the Contracted Clot

To study the incorporation of platelets into the contracted clot, flow cytometry was used to compare the platelet count at the start of the assay with the collected supernatant at 2 hours. Flow cytometry was performed by Dr Matthew Hindle.

Figure 31A shows representative forward and side scatter plots of pre-activated sample and post-activated supernatant. The scatter plots for both WT and α390 showed a considerable reduction in the number of platelets from the post-activation supernatant in the contracted clot compared to the pre-activated sample. In the scatter plot for α220, more platelets were observed in the supernatant compared to the WT and α390. The supernatant of the control with the addition of activation mix (activated control) had a similar scatter profile to α220,

and both showed a distinct shift in the profile showing the activation of platelets, which was mirrored in the supernatant of samples from WT and α390. This shift in the scatter was not observed in the supernatant of the non-activated control. The platelet count for the supernatant confirmed that most of the platelets were contained within the contracted clot for WT (pre-activated sample 1901.7±302.2 platelets/µL and post-activation supernatant 17.2±13.4 platelets/µL) and α390 (pre-activated sample 2187.3±712.0 platelets/µL and post-activation supernatant 28.9±29.7 platelets/µL) (Figure 31B).

There was a reduced platelet count in the post-activation supernatant of α220 at 397.5±102.8 platelets/µL compared to pre-activated sample (2156.9±689.7 platelets/µL), even though no visible clot formed. The activated control also showed a reduction in platelet count in the post-activation supernatant 1188.6±276.8 platelets/µL compared to pre-activated sample (2156.2±617.5 platelets/µL). The reduction in platelet counts for activated control and α220 is likely due to a loss of platelets through normal activation, and thus the formation of platelet aggregates that may partly be lost from the post-activation supernatant. In addition, the platelet aggregates were not counted as the flow cytometer was gated for single platelets and as noted above the profile of activated platelets causes an increase in SSC/FITC profile. There was a similar platelet count for the non-activated control between the pre-activated sample (1791.2±127.7 platelets/µL) and post-activation supernatant (1673.3±335.9 platelets/µL), confirming the loss of platelets observed in the activated control is due to the formation of platelet aggregates and these were therefore not counted by the flow cytometer.

5.4.1.2 Incorporation of RBC in Contracted Clot

The incorporation of RBC within the contracted clot was similar for both WT and α390 at 79.4±8.2 % and 78.9±15.3 % respectively (Figure 31C). However, both the control with activation mix and α220 showed a similar and lower incorporation of RBC at 48.3±16.5 % and 42.6±16.6 % respectively, which could be due to the platelet aggregates trapping some of the RBCs.

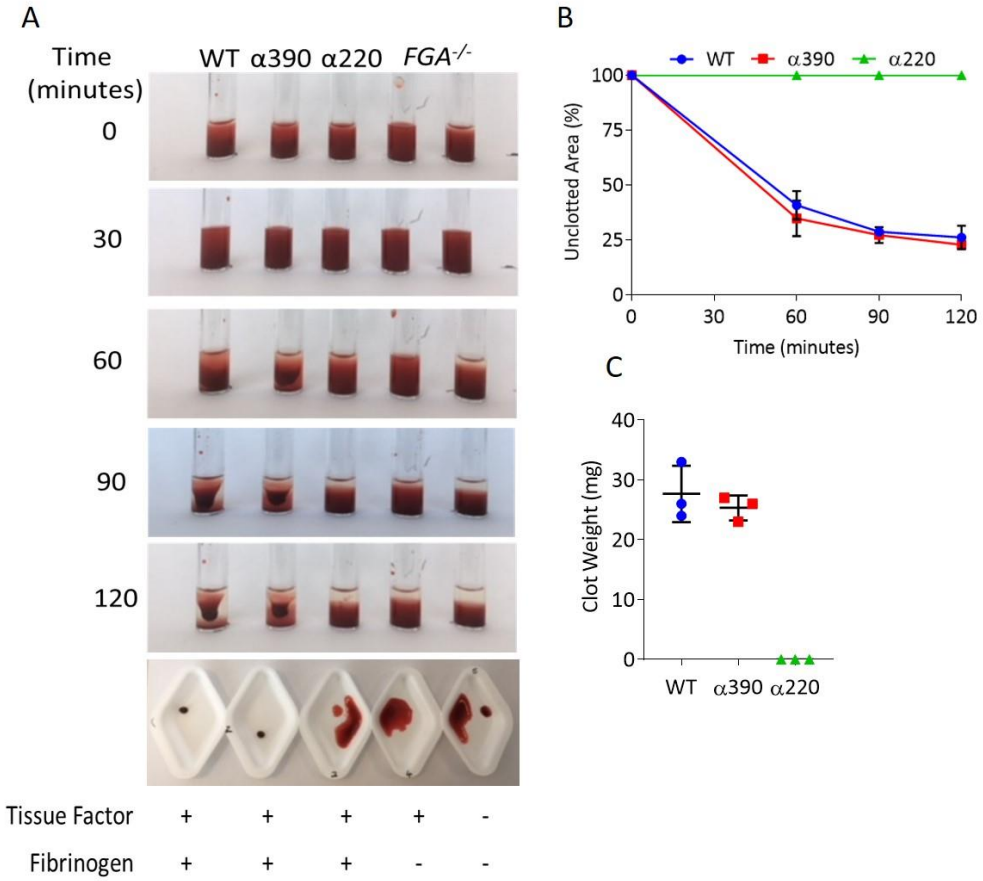

Figure 30 Impaired Clot Contraction for Fibrin Lacking αC-region

Representative images of tissue factor initiated whole blood clot formation and contraction over time of whole blood from *FGA*$^{-/-}$ supplemented with WT, α390, α220 (A). WT and α390 showed a clot forming and contracting, which was not observed for α220 and the two *FGA*$^{-/-}$ controls. Percentage of unclotted area over time for WT, α390, α220 (B). Clot weight of the contracted clot (C). Clot weight was not measured for α220, *n*=3.

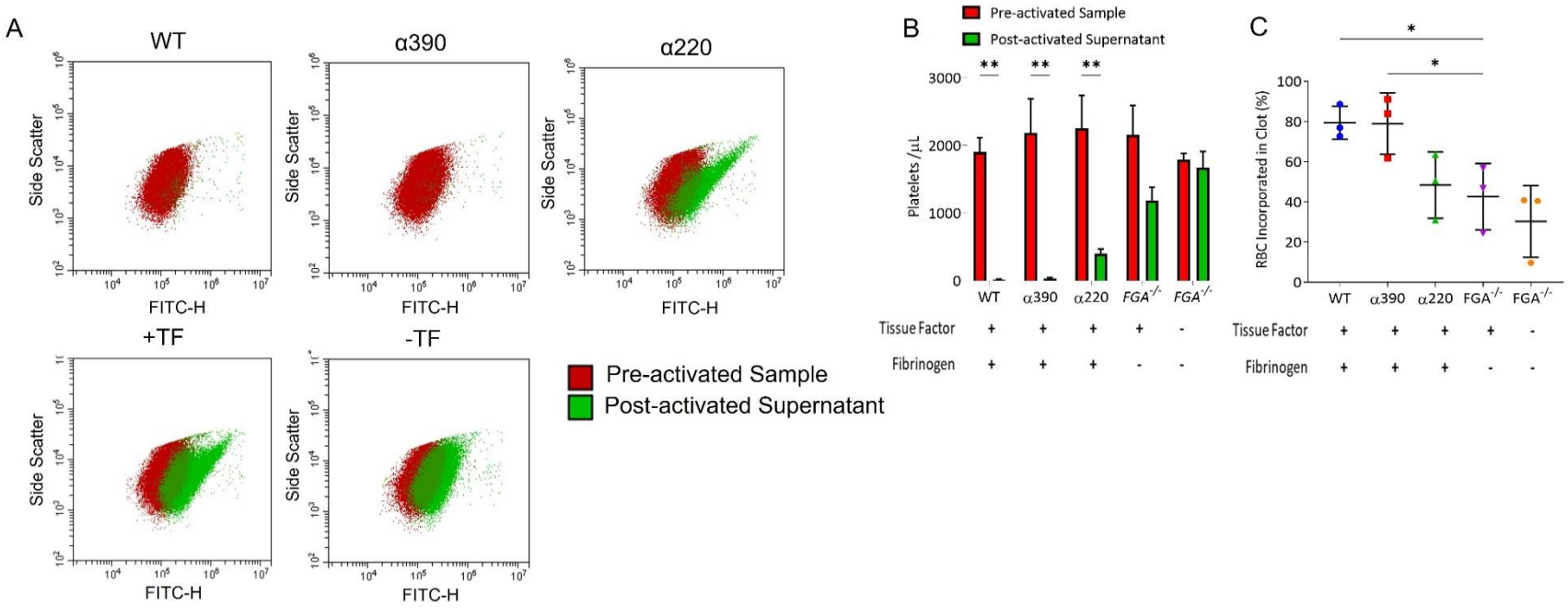

Figure 31 Majority of Platelets and Red Blood Cells were Incorporated within the Clot

Representative FITC-H and side scatter plots for WT, α390, α220 and controls (A). FITC-H is fluorescence measured from antibody CD41-FITC, H denotes the peak of fluorescence pulse, following excitation at 488 nm. Platelets were gated by CD41-AF488 (clone MWReg30). Platelet count in pre-activated and post-activated samples from WT, α390, α220 and controls (B). RBC Incorporation for WT, α390, α220 and controls (C). Results shown as mean ±standard deviation, n=3, *p=0.05 and **p=0.01 by two-way ANOVA with Šídák's multiple comparisons test (B) and one-way ANOVA with Dunnett's multiple comparison test relative to the *FGA*$^{-/-}$ in (C).

5.4.2 The Lack of the αC-region does not Prevent Platelet-Fibrinogen Interaction

Following the results from the clot contraction assay, flow cytometry was used to explore the interaction with the truncations and WT with platelets to investigate if there were alterations in platelet-fibrinogen binding. This experiment was performed by Dr Lih Cheah. The experiment was performed using whole blood from *FGA*$^{-/-}$ mice with the addition of either WT or truncated human fibrinogen. In addition to the αC-region truncated fibrinogens, recombinant fibrinogens γ'/γ' and γ'0 were used, as both lack the integrin-binding C-terminal AGDV motif. In addition, a control with plasma purified fibrinogen γA/γ', which is heterozygous in γ-chain C-terminal, was also included. The platelets were activated by ADP (1 and 10 μM) or PAR4 (200 μM).

The activation of platelets with ADP or PAR4 showed an increase in fibrinogen-positive platelets except for γ'/γ' and γ'0. Using 1 μM ADP, the fibrinogen positive platelets were similar for α390 (89.77±7.96 %), α220 (86.37±10.42 %) and γA/γ' (83.34±13.32 %) to WT (90.45±6.44 %). There was a significant reduction in fibrinogen positive platelets for γ'/γ' (61.66±15.95 % p=0.0248) and γ'0 (61.19±18.61 % p=0.221) compared to WT. As the data with 1 μM ADP, 100 μM ADP showed no difference in fibrinogen positive platelets for α390 (97.70±2.03 %), α220 (96.23±2.96 %) and γA/γ' (94.21±4.93 %) to WT (97.70±1.90 %). Again, there was a significant reduction in the number of fibrinogen positive platelets for γ'/γ' (63.20±15.46 % p=0.007) and γ'0 (64.30±16.09 % p=0.0072) compared to WT. PAR4 activated samples showed the highest percentage of fibrinogen positive platelets and no difference was observed between α390 (99.85±0.10 %), α220 (99.76±0.16 %) and γA/γ' (99.69±0.22 %) and WT (99.89±0.10 %). There was a significant reduction in the number of fibrinogen positive platelets for γ'/γ' (63.73±15.13 % p=0.0032) and γ'0 (73.70±13.80 % p=0.0476) compared to WT (Figure 32A).

At 1 μM ADP, there was no difference in fibrinogen medium fluorescent intensity (MFI) between the various fibrinogens (Figure 32B). Compared to fibrinogen binding with platelets, there was a significant difference in fibrinogen medium fluorescent intensity for α220 (132477.8±43619.1 MFI p=0.0439), γA/γ' (112292.6±46041.0 MFI p=0.003), γ'/γ' (3368.6±2561.4 MFI p<0.0001) and γ'0 (3366.9± 2398.5 MFI p<0.0001) compared to WT (105743.6±47600.4 MFI) using 100 μM ADP. No difference was observed between WT and α390 (108410.3±55704.0 MF). For cells stimulated with 1 μM ADP, as with PAR4, there was a significant difference in fibrinogen medium fluorescent intensity for α220 (132477.8±43619.1 MFI p=0.0133), γA/γ' (112292.6±46041.0 MFI p<0.0001), γ'/γ'

(2913.8±1763.3 MFI p<0.0001) and γ'0 (4494.6±1829.0 MFI p<0.0001) compared to WT (189523.1±69295.3 MFI) using 100 µM ADP. No difference was observed between WT and α390 (193505.9±73173.4 MFI) (Figure 32B). The absence of the αC-domain resulted in no difference in fibrinogen binding with platelets or the intensity of fibrinogen binding per platelet. The absence of the αC-connector as well as αC-domain showed that there was no difference in the number of platelets positive for fibrinogen, but the amount of fibrinogen binding per platelet was reduced. Interestingly, α220 behaved like γA/γ' both for fibrinogen positive platelets and for fibrinogen medium fluorescent intensity. There was limited increase from basal level for γ'/γ' and γ'0 in fibrinogen positive platelets and for fibrinogen medium fluorescent intensity highlighting the importance for the AGDV motif on the γA-chain in fibrinogen binding with platelets.

The markers used to observe platelet activation were CD62P and CD63, which correspond to P-selectin surface expression from α-granule secretion and lysosomal glycoprotein from dense granules respectively. Compared to basal levels, there was a limited increase in CD62P positive platelets and median fluorescent intensity for any of the fibrinogens with ADP (Figure 32C and D). PAR4 showed the largest increase in CD62P positive platelets and median fluorescent intensity. The observation with CD62P was mirrored for CD63 except for PAR4 as only a limited increase was observed.

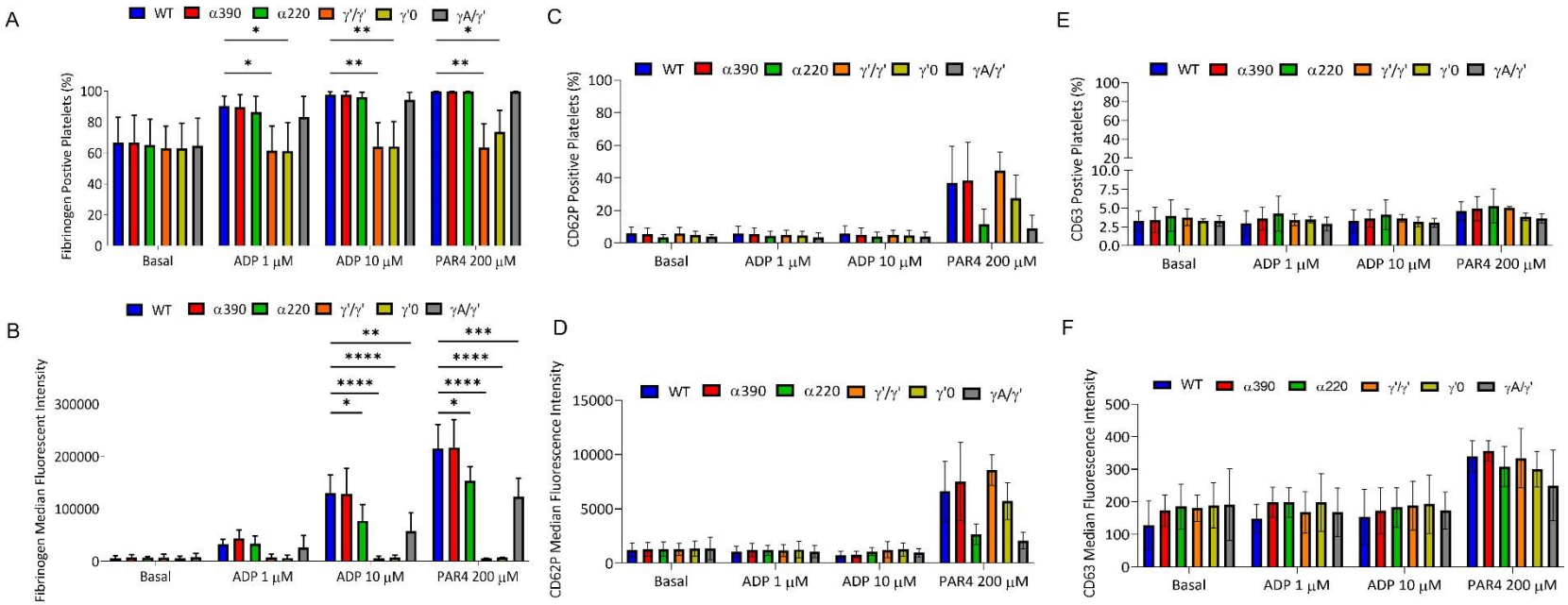

Figure 32 Fibrinogens with αC-region Truncations Can Bind to Platelets

Fibrinogen positive platelets with various fibrinogens and agonists (A). Fibrinogen median fluorescent Intensity with various fibrinogens and agonists (B). Median fluorescent intensity increased with all agonists for WT, α390, α220 and γA/γ'. Positive platelets for CD62 (C) and CD63 (E) with various fibrinogens and agonist. Median fluorescent intensity for CD62(D) and CD63 (F) with various fibrinogens and agonists. Antibodies used for fibrinogen - anti-fibrinogen FITC, P-selectin - CD62P-PE (clone RMO-1), dense granules - CD63-APC (clone NVG-2) and α_{IIB}, - CD41-AF700 (clone MWReg30). Results shown as mean ±standard deviation, *n=3*, **p*=0.05, ***p*=0.01, ****p*=0.001 *****p*>0.0001 by two-way ANOVA with Dunnett's multiple comparison test relative to the WT.

5.4.3 Whole Blood Clot Formation

5.4.3.1 Fibrinogens Lacking the αC-region can Form Clots in Whole Blood

Clot formation did not appear to occur for the α220 fibrinogen sample in the clot contraction experiment using whole blood (Figure 30). Alternatively, it may be that the α220 fibrin clot was so unstable that clot degradation outweighed formation. To discover if clot formation could occur at all with α220 fibrinogen in whole blood, a ROTEM EXTEM assay was performed. In the EXTEM assay, clotting is initiated by tissue factor and the resulting blood clot is influenced by extrinsic coagulation factors, platelets, and fibrinogen.

Figure 33 shows the maximum clot firmness curves over time and all the recombinant fibrinogens showed an increase in clot firmness with WT exhibiting the highest clot firmness. Whole blood from the *FGA*$^{-/-}$ mice, where no fibrinogen was added, showed no increase in clot firmness over time confirming that any change observed in clot firmness would be due to the respective fibrinogen added. In contrast to the WT, both truncations did not maintain clot firmness throughout the course of the assay, this was particularly apparent for α220 where the clot firmness trace returned to baseline within the timeframe of the assay (60 minutes). These data may indicate that premature fibrinolysis could be occurring with clots made with the truncated fibrinogens. The clotting time (Figure 33B), was extended for α220 compared to WT at 425.7±111.4 seconds p=0.0014 and 65.33±16.8 seconds respectively. Also, α390 showed elongated clotting time (110.7±18.5 seconds) compared to WT, but this was not significant (p=0.759). The maximum clot firmness was reduced for both truncations (α390 24.0±8.5 mm p=0.0099 and α220 7.0±2.0 mm p=0.0005) compared to WT (45.3±3.2 mm) (Figure 33C). The shear elastic modulus strength was reduced for α390 (1631±705.6 G) and α220 (359±110.8 G) clots compared to WT (4337±1195 G) (Figure 33D). Altogether, these data confirmed that α220 could form a clot within whole blood, however the clot did not appear to be stable, and exhibited premature fibrinolysis. Premature fibrinolysis also occurred in clots formed by α390.

5.4.3.1.1 Limited Fibrin Observed in Whole Blood Clots Missing αC-region

The clots were collected after ROTEM experiments were prepared for SEM. Figure 34 shows representative images of the clots over three magnifications. WT and α390 clots showed a network of fibrin fibres intermixed with blood cells. In contrast, α220 clots revealed a limited

fibrin fibre network and were mainly composed of blood cells. These data are consistent with the suggestion that rapid, premature fibrinolysis was occurring in the *ex-vivo* whole blood clotting experiments for α220.

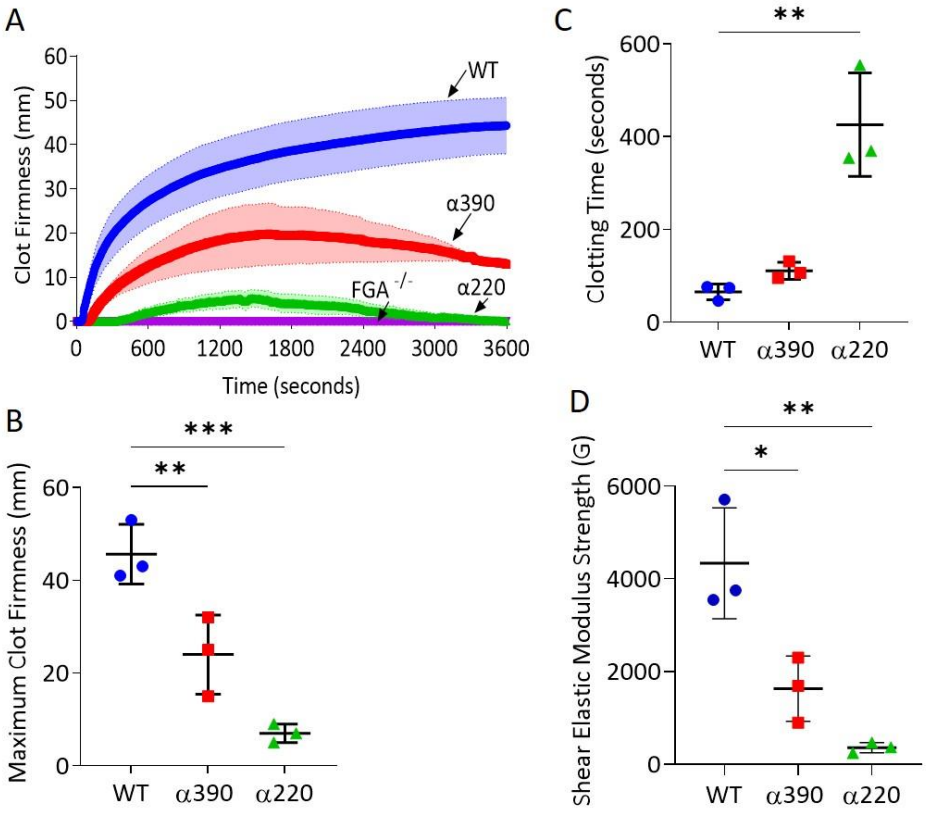

Figure 33 αC-region Truncations Impact Whole Blood Properties

Clot firmness curves for EXTEM with whole blood from *FGA*$^{-/-}$ mice supplemented with WT, α390 or α220 (A). All fibrinogens could form a clot in whole blood. A reduction in clot firmness was observed for α390 and α220. Maximum clot firmness for WT, α390, α220 (B). Both truncations showed a reduced clot firmness. Clotting time for WT, α390, α220 (C). A significant extension in clotting time was observed for α220. Shear elastic modulus strength for WT, α390, α220 (D). Both truncations showed a reduction in shear elastic modulus strength. (D) Results shown as mean ±standard deviation, *n=3*, **p*=0.05, ***p*=0.01 and ****p*=0.001 by one-way ANOVA with Dunnett's multiple comparison test relative to the WT.

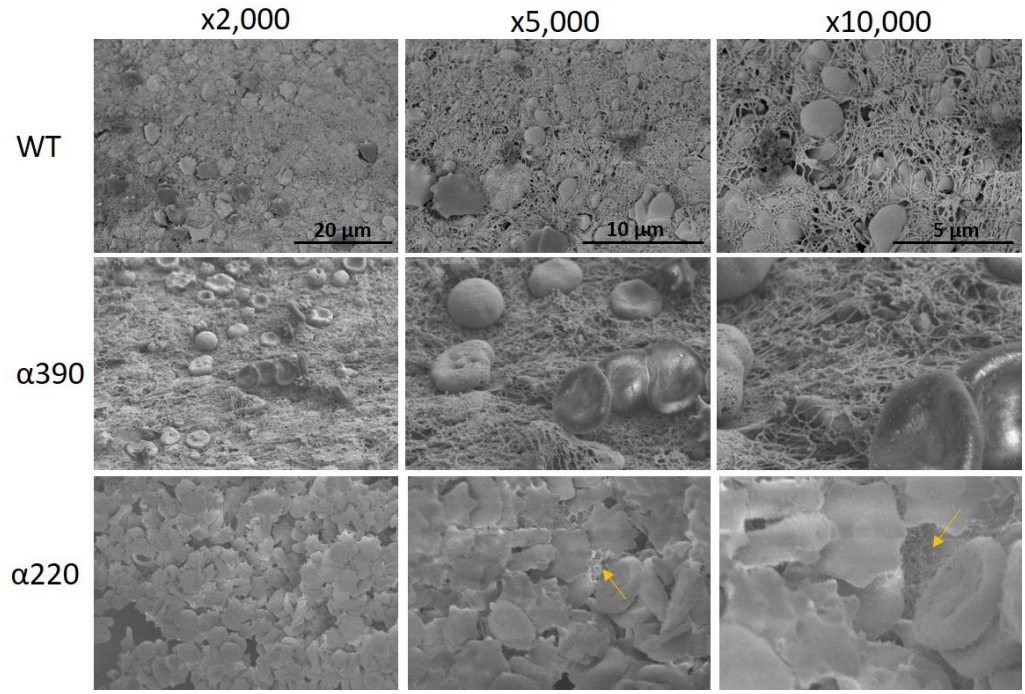

Figure 34 Fibrinogen Lacking the αC-region showed Limited Fibrin in Whole Blood Clots
Representative scanning electron microscopy images at x2,000, x5,000 and x10,000 of whole blood clots from WT (top), α390 (middle) and α220 fibrin (bottom). Clots were collected and fixed with 2.5 % glutaraldehyde after ROTEM EXTEM analysis. Limited fibrin was seen for α220 clots, highlighted by yellow arrows. Images taken on a Hitachi SU8230 Ultra-High-Resolution Scanning Electron Microscope, *n*=3.

5.4.3.2 Inhibition of Fibrinolysis Allows Stabilisation of Fibrinogen αC-subdomains

To comprehend if fibrinolysis or mechanics was the driving factor for the results observed in clot retraction and the EXTEM experiments for α220, ROTEM was performed again using the APTEM setting where fibrinolysis is inhibited by the inclusion of aprotinin. APTEM still instigates clotting through the extrinsic pathway like the EXTEM assay.

Figure 35A shows clot firmness over time but compared to corresponding graph for EXTEM (Figure 33A), there was no reduction in clot firmness overtime for α220, and it did not return to baseline in APTEM. Furthermore, α390 did not display the reduction in clot firmness that was observed in the EXTEM curve over the duration of the APTEM assay. The control whole blood sample from *FGA*$^{-/-}$ did not form a clot in either APTEM or EXTEM.

There was a delay in clotting time for α220 (335.0±106.5 seconds p=0.0141) compared to WT (63.7±8.1 seconds) in APTEM which was also seen from EXTEM. The clotting time for α390 (105.7±15.0 seconds) was increased compared to WT but did not reach significance (Figure 35B). As observed in EXTEM there was a significant reduction in maximum clot firmness for both truncations (α390 31.3±2.1 mm p=0.0012 and α220 15.7±2.5 mm p<0.0001) compared to WT 45.3±3.2 mm (Figure 35C). There was a significant difference in shear elastic modulus strength for α390 (2171±226.7 G) and α220 (910.3±142.0) compared to WT (4317±426.4) (Figure 35D).

5.4.3.3 Fibrin Observed in Clots that Lacked the αC-region when Fibrinolysis was Inhibited

Mirroring the EXTEM investigations, the clots were harvested after the APTEM experiments and prepared for SEM. Figure 36 shows a representative image of clots from the APTEM experiments. Comparable with the EXTEM images, APTEM clots made with WT and α390 fibrinogen showed a clot composed of network of fibrin interspersed by RBC cells, the denser clot structure observed in the purified experiments for α390 did not appear to be as dominant. However, the α220 clots prepared after APTEM with the inhibition of fibrinolysis, were vastly different to EXTEM clots (Figure 34), with substantially more fibrin present throughout the clot. The contrast in visible fibrin fibres seen between the EXTEM and APTEM experiments confirms susceptibility of α220 clots to rapid degradation by fibrinolysis. Interestingly, like the α220 purified clots there were fibre ends visible in the APTEM α220 SEM images.

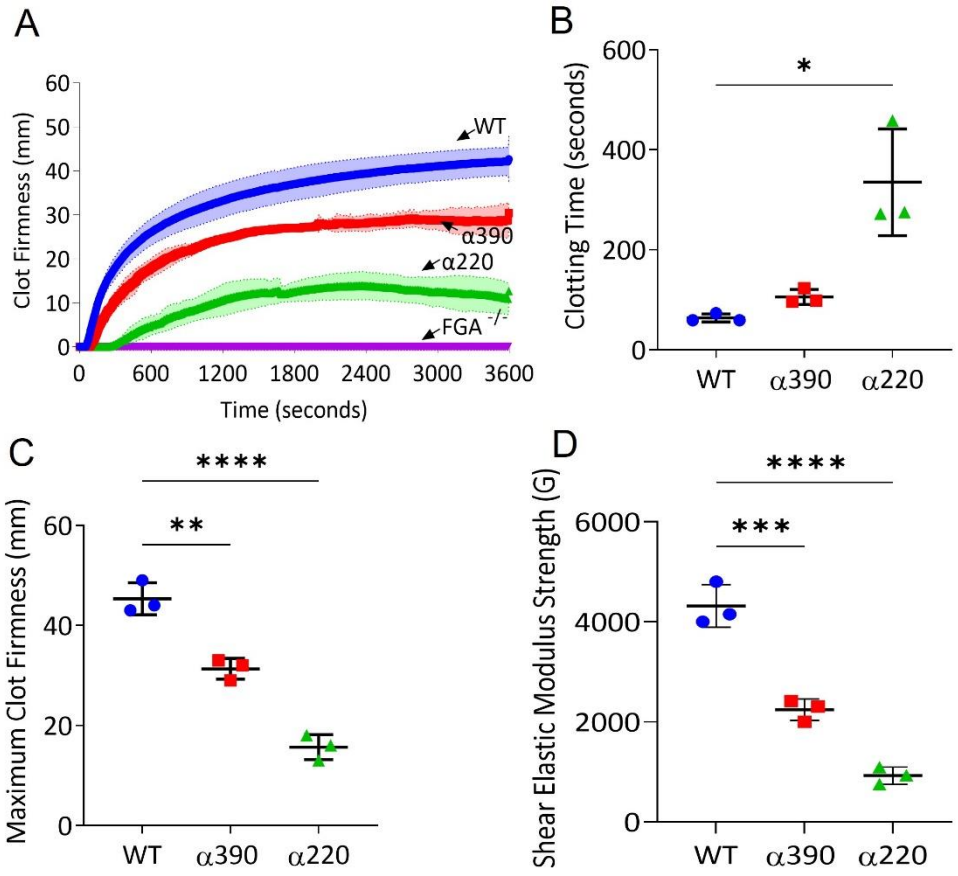

Figure 35 Inhibition of Fibrinolysis Prevented Clot Instability in αC-subregions

Clot firmness curves for APTEM with whole blood from *FGA*$^{-/-}$ mice supplemented with WT, α390 or α220 (A). Clotting time for WT, α390, α220 (B). Maximum clot firmness for WT, α390, α220 (C). Shear elastic modulus strength for WT, α390, α220 (D). Results shown as mean ±standard deviation, *n=3*, **p*=0.05, ***p*=0.01, and *****p*<0.0001 by Kruskal-Wallis test with Dunn's multiple comparisons test (B) and one-way ANOVA with Dunnett's (C& D) multiple comparison test relative to the WT.

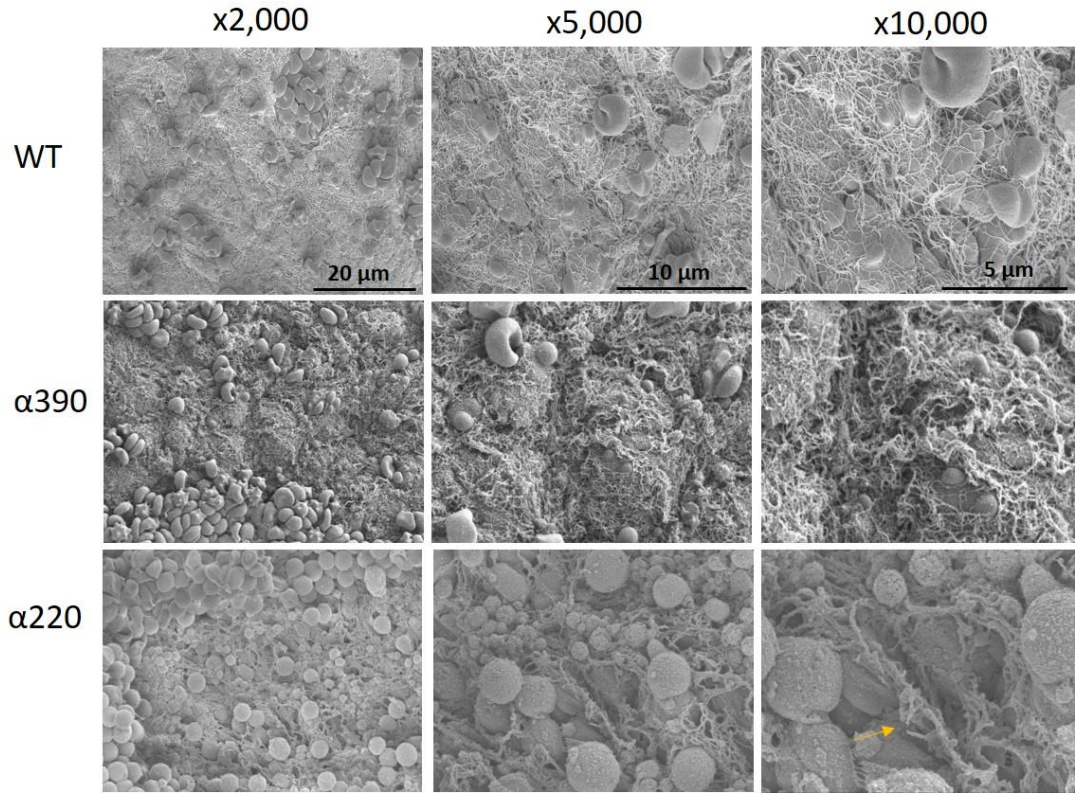

Figure 36 Fibrin Network Observed Following Inhibition of Fibrinolysis in Fibrin Lacking αC-region

Representative scanning electron microscopy images at x2,000, x5,000 and x10,000 of whole blood clots made with WT (top), α390 (middle) and α220 fibrinogen (bottom). Clots were collected and fixed after ROTEM APTEM analysis. Fibre ends where observed for α220 (yellow arrow). Images taken on a Hitachi SU8230 Ultra-High-Resolution Scanning Electron Microscope, *n*=3.

5.5 Discussion

The focus of this chapter was to examine the effects of the αC-subregions within the parameters of whole blood, with experiments undertaken on whole blood clot contraction, fibrinogen platelet interaction and whole blood clot formation studies. The combination of these experimental data and the previous data using *in vitro* conditions reinforce the crucial role the αC-connector has within the αC-region in mechanical stability and prevention of premature fibrinolysis. Although clots prepared with fibrinogen lacking the αC-domain were less firm and showed premature fibrinolysis, this was not as profound as when the entire region was absent.

From the result of the clot contraction assay it was unclear if α220, with the loss of the entire αC-region, was unable to form a clot in whole blood due to the mechanical weakness influencing of platelet driven contraction, sensitivity to lysis, or both. In addition, there could be alterations in fibrinogen/platelet interaction. The loss of the αC-domain with the RGD integrin at Aα572-574 showed no difference in clot contraction, in agreement with the recombinant fibrinogen AαD574E (Rooney et al., 1998). Furthermore, no difference was observed in fibrinogen/platelet binding between WT and α390. There was a similar percentage of fibrinogen positive platelets between WT, α390, α220 and γA/γ' but the latter two have less binding per platelet with PAR4 and higher ADP activation. The two fibrinogens (γ'/γ' and γ'0) lacking the AGDV site were similar to basal levels, showing there was no interaction with these fibrinogen and platelets, in agreement with previous findings (Farrell et al., 1992). Although platelet aggregation was not studied, it has previously been shown that recombinant fibrinogen AαD574E was similar to recombinant WT, whereas recombinant fibrinogens γ'/γ' and γ407 showed limited platelet aggregation (Farrell et al., 1992; Rooney et al., 1996). Potentially the loss of the αC-region could have resulted in minor confirmational changes within the D-region in α220, which may lead to reduced binding per platelet via $\alpha_{IIB}\beta_3$, with the loss of binding being not as significant as with hetero- or homozygosity in the loss of AGDV site. Additionally, clot contraction can occur in fibrin lacking the AGDV site and there is only a difference at the initial stages of clot contraction (Rooney et al., 1996). Platelets have been shown to mechanically sense their environment (Lam et al., 2011). The observations from the magnetic tweezer experiments demonstrated that the α220 had reduced G', compared to WT, therefore during clot contraction the platelets would not be able to apply the same force. Kim et al, observed that during clot contraction, platelets can bend and shorten individual fibrin fibres, thereby remodelling the fibrin fibre network resulting in denser clots with enhanced clot stiffness (Kim et al., 2017).

The initial purified investigations into α220 (Chapter 4) showed that fibrin clot structure was porous with short-stunted fibres, and these features in α220 could potentially cause difficulty during platelet-mediated contraction. In addition, in the purified experiments which investigated fibrinolysis both internal and external fibrinolysis, α220 lysed very rapidly. Tutwiler et al, showed that fibrin degradation products were increased in external fibrinolysis when clot contraction was impaired (Tutwiler et al., 2019). The lack of the αC-region highlights the importance of the inter-linking roles of fibrinolysis and clot mechanics during clot contraction.

FXIIIa cross-linking was shown to retain RBCs within a thrombus (Aleman et al., 2014). Using the recombinant fibrinogen α251, it was shown that α-α crosslinking is essential for the retention of RBCs within the clot (Byrnes et al., 2015). Similar RBC retention and platelet incorporation in the contracted clot was observed between WT and α390 suggesting that having at least some glutamine and lysine residues available in the αC-region allow for normal retention of RBCs and platelets within α390 clots.

Previously, reduced surface expression of P-selectin on platelets has been reported on *FGA*$^{-/-}$ mice and a patient with hypofibrinogenemia when activation was performed with either thrombin and TRAP (Yang et al., 2009). The authors transfused fibrinogen into *FGA*$^{-/-}$ mice and found an increase in P-selectin expression over 4 days. They suggested that the lack of P-selectin was due to a decrease in platelet α-granule.

The initial whole blood investigations by clot contraction showed no clot formation over time for α220 fibrin. As the ROTEM experiments were run for 1 hour they cover the initial phases of the clot contraction assay. The EXTEM assay showed that α220 was able to form a clot within whole blood like WT and α390, but that the formed clot was not maintained over time and subsequently limited fibrin was observed in scanning electron microscopy. This mirrors the observation from the contraction assay as no visible clot was harvested. Furthermore, the images taken at 1 hour showed a clot contracting for WT and α390 but not for α220 samples. In agreement with the *in vitro* data, the *ex-vivo* experiments confirmed that α220 was highly susceptible to fibrinolysis, demonstrating a critical role of the αC-connector in prevention of premature fibrinolysis.

In agreement with the purified micro-rheology experiments for α220, there was reduced firmness observed in whole blood clot formation. Furthermore, the EXTEM and APTEM experiments highlighted the interplay between clot mechanics and fibrinolysis, with both truncations not able to sustain clot firmness during EXTEM analysis, compared to WT. With the inhibition of fibrinolysis in APTEM, clot firmness was maintained in both truncations and the clot firmness was higher than observed in the EXTEM experiment. The purified micro-

rheology experiments generally showed similarity between WT and α390, with and without the addition of FXIII, whereas this similarity was not observed in whole blood ROTEM experiments. This could potentially be due to differences in experimental procedure as in the micro-rheology experiments, clots were left to form overnight while the ROTEM experiments monitor clots in the first hour of formation. In Chapter 4, reduced α-α-chain cross-linking was observed, which covers the window of the ROTEM experiment. This highlights the important role α-α-chain cross-linking has in mechanical stability, in addition to the alterations in clot structure.

The clotting time was reduced for α220 samples in APTEM compared to EXTEM, in addition the maximum clot firmness for α220 had doubled in APTEM to 15.7±2.5 mm compared to that in the EXTEM of 7.0±2.0 mm. These observations suggest that hyperfibrinolysis is occurring, as the inhibition of fibrinolysis in APTEM allowed for the correction of hyperfibrinolysis (McNeil and Kleiman, 2017). Furthermore, the scanning electron images of the clots collected afterwards showed fibrin fibres present throughout the clot. Although not as striking for α220 samples, α390 also exhibited some fibrinolysis in EXTEM and like α220 there was an increase in maximum clot firmness in APTEM compared to EXTEM. These data demonstrate the impact of the αC-domain on fibrinolysis in whole blood. However, no difference was observed between WT and α390 in purified fibrinolysis experiments. This may be due to presence of blood cells or other plasma proteins preventing formation of the denser clot structure observed in scanning electron microscopy and LSCM studies, therefore allowing the penetrations of fibrinolytic enzymes, although this hypothesis will need further investigation.

As discussed in the previous chapter, the hyperfibrinolysis observed in α220 samples could be the result of increased availability of the rate-enhancing residues Aα148-160 that are cryptic in fibrinogen but become exposed in fibrin (Medved and Nieuwenhuizen, 2003). The cryptic sites are exposed early on during protofibril formation and may be related to the disconnection of the β-nodule from the coiled coil (Yakovlev et al., 2000; Medved and Nieuwenhuizen, 2003). As α220 fibrin shows delayed protofibril formation compared to WT, the cryptic binding site within the coiled coil would be exposed. The early exposure of the binding site could be targeted more readily before the fibres were able to form, as fibrinolysis occurs simultaneously. Thus, potentially a situation of hyperfibrinolysis could be created. In addition, the ROTEM measurement for clotting time is defined as from the start of the test until an amplitude of 2 mm is reached, and the duration of clotting time would be extended in the presence of fibrinolysis. During a period of rapid fibrinolysis, the forming clot would take a longer time to reach an amplitude of 2 mm, compared to clots forming

when fibrinolysis was inhibited or less prolific. The duration of clotting time was increased in α220 for EXTEM (425.7±111.4 seconds) compared to APTEM (335.0±106.5 seconds) suggesting that the forming clot had been substantially lysed early on during clot formation. A common phenotype of dysfibrinogenemias within the αC-connector is bleeding. For mutations within the αC-connector, this can range from mild to major bleeding (Ridgway et al., 1997; Kotlín et al., 2012; Castaman et al., 2015; Asselta et al., 2015b; Amri et al., 2017), which agrees with the data on significant clot instability for α390 and α220 presented in this thesis. It could be speculated therefore that for cases of dysfibrinogenemia, maintenance of the αC-region, and specifically the αC-connector, is important for the prevention of unwanted bleeding observed in scenarios such as trauma, childbirth, and the postpartum period. In a previous study, the incorporation of fragment X into fibrin clots resulted in increased susceptibility to fibrinolysis, alongside an increase in the formation rate of plasmin as well as greater sensitivity to proteolysis (Schaefer et al., 2006). In the previous chapter, although fibrinolysis was not specifically investigated, LSCM showed that α390 and α220 could be incorporated into WT clots and influenced clot structure and function in a dose-dependent manner. During incidents of excessive blood loss there could be a mixture of partially degraded fibrin and full-length fibrin molecules incorporated into the developing clot, potentially exacerbating the bleeding phenotype, and further destabilising the clot. In cases of postpartum haemorrhage, increases in D-dimers levels have been observed (Ducloy-Bouthors et al., 2016). The reduction of fibrinogen levels is used as a marker for excessive bleeding, and fibrinogen is the first coagulation factor to fall rapidly in circulating levels during major haemorrhage (Cortet et al., 2012; Levy et al., 2014; Bagoly et al., 2019). Tranexamic acid has been demonstrated to be useful in preventing excess blood loss in trauma, surgery, childbirth and postpartum period, and this has been confirmed in large trials (CRASH-2 and WOMAN), highlighting the importance of preventing of premature fibrinolysis (Roberts et al., 2013; Shakur et al., 2017; Pong et al., 2018).

Furthermore, following thrombolysis in ischaemic stroke, incidents of intracranial haemorrhage associated with low circulating fibrinogen levels and increased levels of fibrin(ogen) degradation products or D-dimers can occur (Bagoly et al., 2019). A study comparing fibrin clot properties from ischaemic stroke patients before and 24 hours after thrombolysis found that clots formed more slowly, were less compact and composed of thinner fibres following treatment (Bembenek et al., 2017). In addition to the structural changes, the clots lysed more rapidly with higher rate of D-dimers after treatment, compared to admission values. Potentially, as the D-dimer levels were not measured in the

plasma samples before the assay, increased fibrin degradation products prior to clot formation may cause structural and functional changes in the developing clot.

The results generated in this, and the previous chapter highlight that the αC-domain and αC-connector have critical and distinct roles in fibrin formation, fibre growth, clot structure and clot stability (Figure 37) in both purified and whole blood systems. The αC-domain is fundamental to lateral aggregation, fibre thickness and clot density, whereas the αC-connector, along with the αC-domain is key for longitudinal fibre growth and the continuation of fibrin fibres. The functional properties of the αC-region demonstrate its importance for mechanical strength and resistance to fibrinolysis, with a stepwise loss in clot firmness and increase in fibrinolysis in α390 and α220 whole blood clots.

5.5.1 Key findings

- The fibrinogen αC-connector is crucial to prevent premature fibrinolysis.
- Both fibrinogen subregions contribute to mechanical stability in whole blood.
-

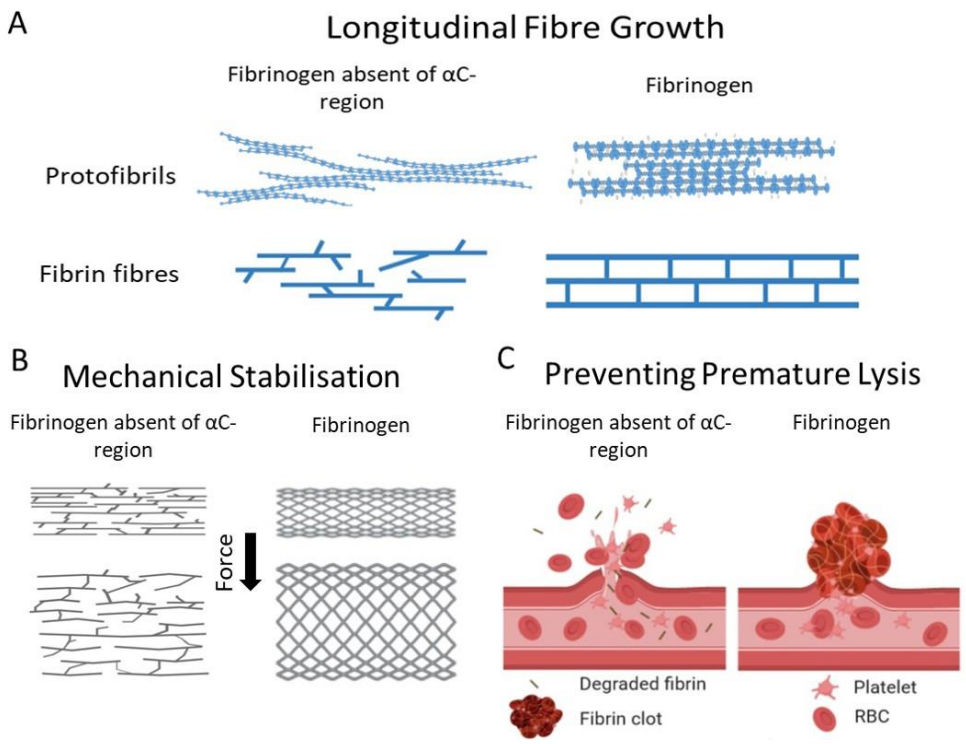

Figure 37 Summary of Key Findings

Absence of the αC-region prevents longitudinal fibre growth (A), reduces mechanical stability (B), and modulates resistance to lysis (C), resulting in premature clot breakdown. Images drawn in Biorender.com and Microsoft PowerPoint and are not to scale.

Chapter 6 Characterisation of Recombinant Fibrinogen γ'-chain Variants

6.1 Introduction

This chapter discusses the characterisation of the recombinant fibrinogens with various truncations to the γ'-chain and a full length γ'-chain homodimer. The truncated γ'-chain variants that were investigated were γ'0, γ'12 and γ'16 which have 0, 12 and 16 residues of the γ'-chain respectively. Furthermore, γ'0 lacks the final four residues of the normal γA-chain.

Previous studies with recombinant and plasma purified containing γ'-chain have shown altered clot structure compared to γA/γA (WT) fibrinogen, with clots composed of thinner fibres producing denser structures (Siebenlist et al., 2005; Gersh et al., 2009b; Allan et al., 2012). Furthermore, there have been several functional studies into the mechanical influence of the γ'-chain. These studies have used various methods to investigate mechanical properties, including ROTEM, TEG, magnetic tweezers, and torsion pendulum. TEG work has found that plasma purified γA/γ' had higher maximum amplitude at 1 and 2 U/mL compared to WT (Siebenlist et al., 2005). Torsion pendulum experiments demonstrated that recombinant γ'/γ' was stiffer than recombinant WT clots but only after the addition of FXIII (Collet et al., 2004). In contrast, viscoelastic properties of clots made from plasma purified γA/γ', studied by magnetic tweezers, showed these to be less stiff and more likely to deform compared to WT clots with and without FXIII (Allan et al., 2012). In agreement with this study, ROTEM analysis found plasma purified γA/γ' had reduced maximum clot firmness compared to WT (Domingues et al., 2016). Interestingly, TEG and ROTEM showed no difference between γA/γ' and γA/γA in either maximum amplitude or maximum clot firmness using 10 or 20 U/mL of thrombin (Siebenlist et al., 2005; Domingues et al., 2016).

Clot resistance to lysis has a role in predisposition to CVD and studies into the role of γ' in clot lysis have been both limited and conflicting. External fibrinolysis studies, using LSCM, found no difference in lysis of recombinant WT and γ'/γ' clots (Collet et al., 2004; Guedes et al., 2018b). Investigations based on internal fibrinolysis found similar fibrinolysis profiles for WT and γA/γ' without FXIII whereas γA/γ' showed more fibrinolysis resistance with the addition of FXIII compared to WT (Falls and Farrell, 1997). Another study observed an increase in time to 50 % lysis by internal fibrinolysis, both in the presence and absence of FXIII, with increasing concentrations of γ'-chain (Macrae et al., 2021). This observation agrees with a delay in fibrinolysis for γA/γ' compared to WT observed by TEG analysis of

purified fibrinogen (Siebenlist et al., 2005). A further study investigated internal fibrinolysis by turbidimetric studies and found that γA/γ' lysed more slowly, due to a delay in activation of plasminogen in γ'-chain containing fibrinogen (Kim et al., 2014b).

Previous studies into γ' chain have used various thrombin, calcium, and fibrinogen concentrations, in addition, some of the plasma purified studies there may have been FXIII contamination which may have influenced the results observed. Furthermore, high thrombin concentrations may overcome any inhibitory effect of γ'-chain on thrombin.

In addition to clot structure and porosity, FXIIIa and thrombin can influence clot behaviour and the γ'-chain co-purifies with FXIII (Siebenlist et al., 1996). Moreover, the γ'-chain has been shown to bind to exosite II on thrombin (Lovely et al., 2003). The majority of observations have shown normal FpA release, but there is slower FpB release in plasma purified γA/γ' (Cooper et al., 2003; Siebenlist et al., 2005; Kim et al., 2014b). Due to the influence of the γ'-chain on other coagulation factors, it can be hard to pin-point the influence directly due to differences in fibrinogen composition or from the impact of other coagulation factors on clot structure and function.

Currently there have been no studies into how many residues of the γ'-chain cause the effects observed in clot structure and function. The truncated γ'-chain (γ'12 and γ'16), γ'-chain homodimer, γ'0 (containing no γ'-chain residues or the final residues of γA) produced in this thesis along with WT are used to investigate how the residues that comprise the γ'-chain influence clot structure and function. Clot structure is investigated by turbidimetric assay, in hydrated (laser-scanning confocal microscopy) and dehydrated (scanning electron microscopy) conditions. The functional aspects of fibrinolysis are analysed by turbidimetric assays and clot mechanics by magnetic tweezers.

6.1.1 Hypothesis

The hypothesis to be tested is that increasing residues of the γ'-chain result in a stepwise change in clot structure and function.

6.1.2 Aims

To understand which constituents of the γ'-chain are responsible for the observations in purified, plasma and patient studies.

Secondary Aims:

- To observe any structural differences using microscopy and turbidimetric assays.
- Study how the γ'-chain and its truncations influence the function of clot mechanics and fibrinolysis by magnetic tweezers (clot mechanics), microscopy and turbidimetric assays (fibrinolysis).

6.2 Results

6.2.1 Integrity of Recombinant Fibrinogens

The purified recombinant fibrinogens were evaluated to confirm that the fibrinogen produced was composed of one homogenous species. Figure 38A the native gel showed that there was one band present in each lane for the respective recombinant fibrinogen, confirming only one species is present for each purified recombinant fibrinogen. There was slightly less migration of the γ'-chain homodimer through the gel matrix compared to the WT as the former is slightly larger.

The composition of fibrinogen protein was examined further by SDS-PAGE analysis. This showed no difference in migration between the Aα- and Bβ-chain for any of the produced fibrinogen proteins compared to WT (Figure 38B). As expected, γ-chain migration showed differences according to the size of the truncation chain. Taken together, the produced fibrinogens showed no changes in the Aα- and Bβ-chain and had the desired changes in the γ-chain.

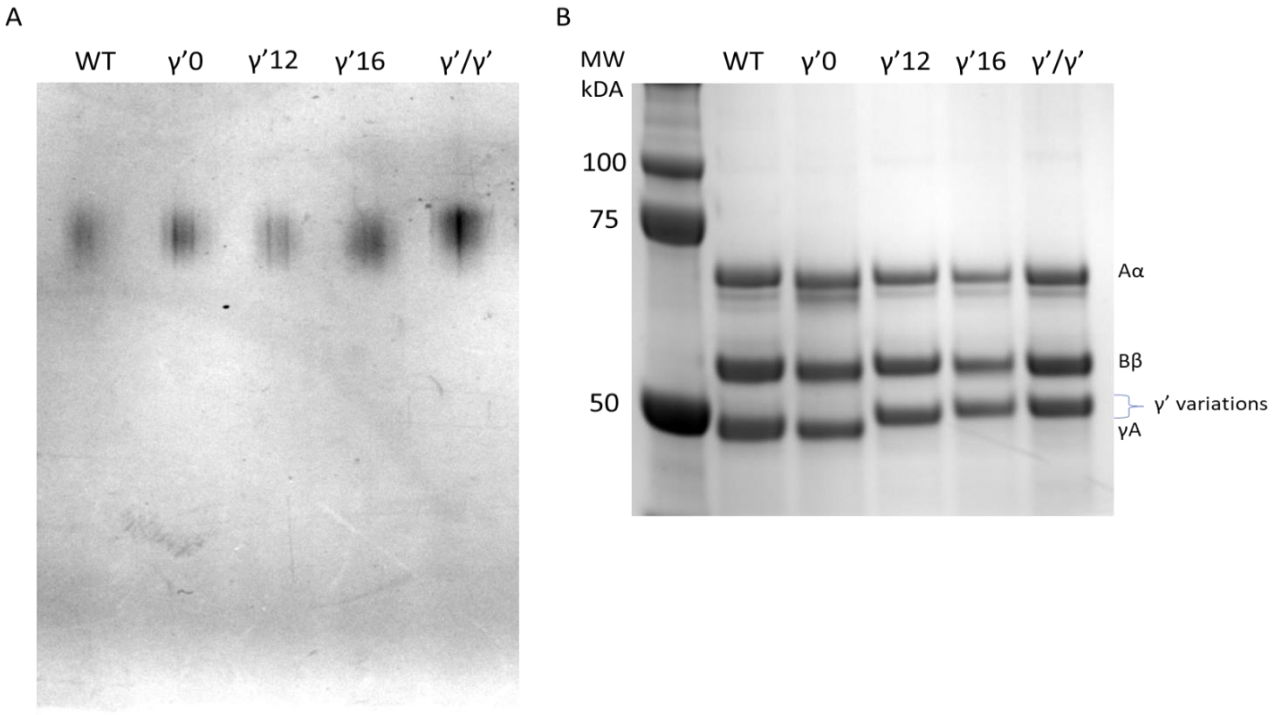

Figure 38 Initial Characterisation of γ′ -chain Variants

Native PAGE gel of WT and γ'-chain variants (A). Native PAGE gel was stained with 0.02 % Coomassie Brilliant Blue R-250. Reduced SDS-PAGE of WT and γ'-chain variants (B). The first lane is the molecular weight marker (MW), and the gel was stained with Instant Blue.

6.2.1.1 γ’ Sequence did not Alter Clotability

Investigations into clotability of the produced and purified recombinant fibrinogen proteins showed no difference to WT (94.0±1.4 %) (Figure 39). Fibrinogen γ’/γ’ had a clotability of 95.7±2.6 %, γ’0 99.7±1.1 %, γ’12 99.7±0.8 % and γ’16 95.6±2.5 %. Thus, all the fibrinogens were able to produce clots through thrombin cleavage.

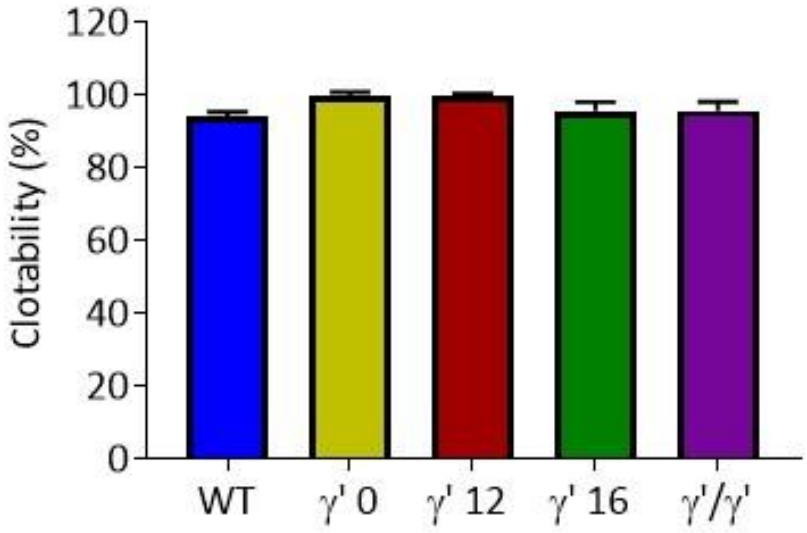

Figure 39 Recombinant γ’-chain Fibrinogen Variants did not Impacted Clotability
Clotting was initiated with 0.1 U/mL thrombin and 5 mM calcium; All fibrinogen proteins had a clotabillity of at least 94 %. Error bars are shown as ±standard deviation *n=3*.

6.2.2 Structural Impact of the γ'-chain

6.2.2.1 Influence of the γ'-chain on Polymerisation

The initial structure investigations were performed by turbidimetric assay, to understand the impact of the γ'-chain and the truncated γ'-chain on fibrin polymerisation. The polymerisation of the recombinant fibrin was examined by measuring the difference in OD over time.

Figure 40A and B and Figure 41A and B show polymerisation curves of the WT and γ'-chain variants in absence and presence of FXIII respectively. Polymerisation curves showed similar maximum OD for γ'12, γ'16 and γ'/γ' and WT, but a reduction was noted for γ'0. No difference was observed in the duration of lag phase without FXIII between the WT γ'-chain variants (Figure 40C). No difference was observed in maximum OD between WT and fibrinogen with γ'-chain residues (Figure 40D). However, γ'0 (0.335±0.012 OD) had a reduced maximum OD compared to WT (0.488±0.065 OD p=0.0041). The average rate of clotting was reduced for all the γ'-chain variants compared to γ'0 0.000740±0.000139 δOD/seconds p=0.0002, γ'12 0.000533±0.000068 δOD/seconds p<0.0001, γ'16 0.000378±0.000085 δOD/seconds p<0.0001, γ'/γ' 0.000384±0.000065 δOD/seconds p<0.0001) to WT (0.001096±0.000047 δOD/seconds) (Figure 40E). There was reduced Vmax observed for γ'16 0.000757±0.000146 δOD/seconds p=0.0044, γ'/γ' 0.000823±0.000163 δOD/seconds p=0.0178) compared to WT (0.001715±0.000138 δOD/seconds). Furthermore, γ'0 and γ'12 with less of the γ'-chain present showed no difference compared to WT.

Investigations with FXIII showed no difference in the duration of lag phase between the WT and γ'-chain variants (Figure 41C). Similar, to the clotting in the absence of FXIII, no difference was observed in maximum OD comparing WT and fibrinogen with γ'-chain residues (Figure 41D). In the presence of FXIII there was still a reduction maximum OD for γ'0 (0.354±0.035 OD) compared to WT (0.488±0.034 OD p=0.0058).

The average rate of clotting was reduced for γ'/γ' 0.000323±0.000072 δOD/seconds) compared to WT (0.000839±0.000189 δOD/seconds p=0.0013) (Figure 41E). No difference in the average rate of clotting with the addition of FXIII was observed for γ'0, γ'12 and γ'16 Reduced Vmax was observed for the truncations containing γ'-chain residues γ'12 (0.001080±0.000225 δOD/seconds p=0.0234), γ'16 (0.000105±0.000121 δOD/seconds p=0.0234), γ'/γ' (0.000746±0.000157 δOD/seconds p=0.0006) compared to WT (0.001526±0.000295 δOD/seconds). No difference was observed between γ'0 (0.00121±0.00025 δOD/seconds) and WT.

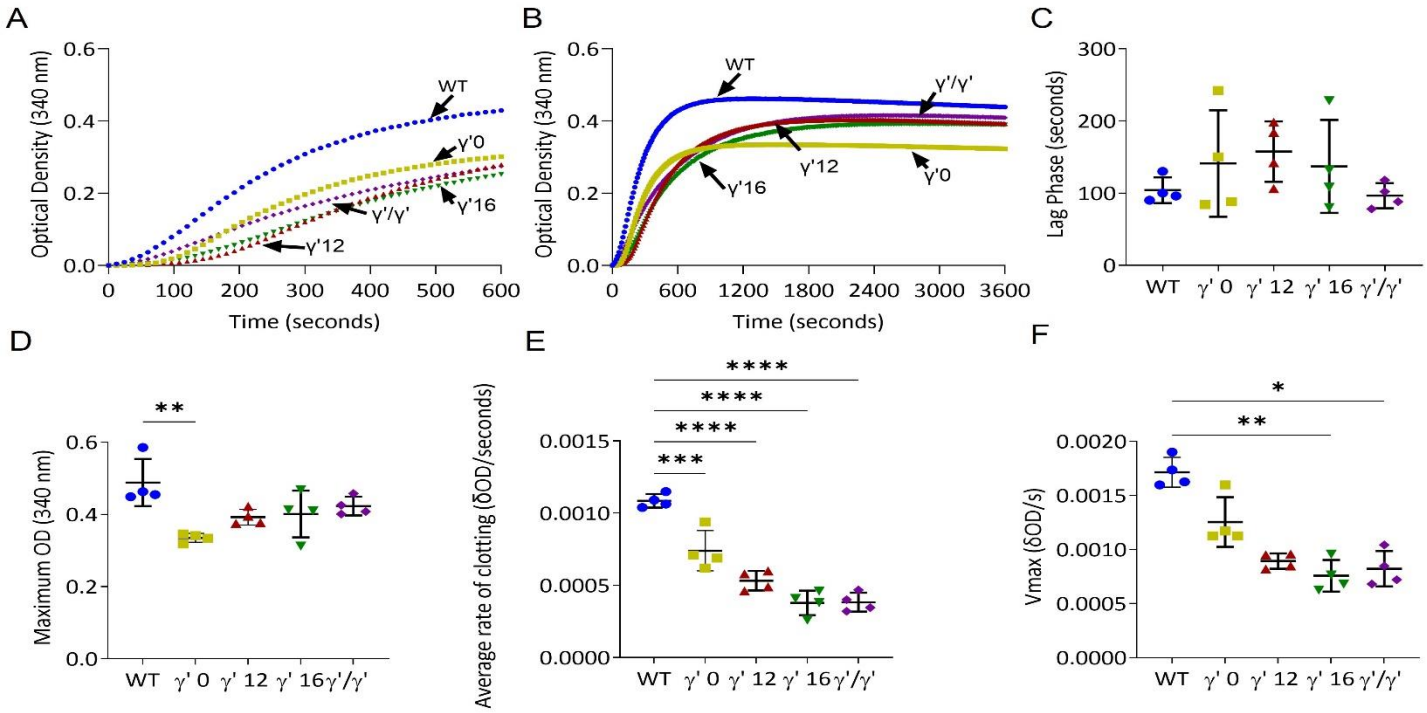

Figure 40 γ'-chain Variants Influenced Rate of Clotting

Polymerisation Curve for WT and γ'-chain variants first 600 seconds (A) and over 3600 seconds (B). Lag phase for WT and γ'-chain variants (C). Maximum optical density (OD) for WT and γ'-chain variants (D). Average rate of clotting for WT and γ'-chain variants (E). Vmax for WT and γ'-chain variants (F). Results shown as mean ± standard deviation, *n=4*, **p*=0.05, ***p*=0.01, ****p*=0.001, *****p*<0.0001 by Kruskal-Wallis test with Dunn's multiple comparisons test (D, F) or one-way ANOVA with Dunnett's multiple comparison test (E) both test relative to the WT. Error bars not shown on A and B.

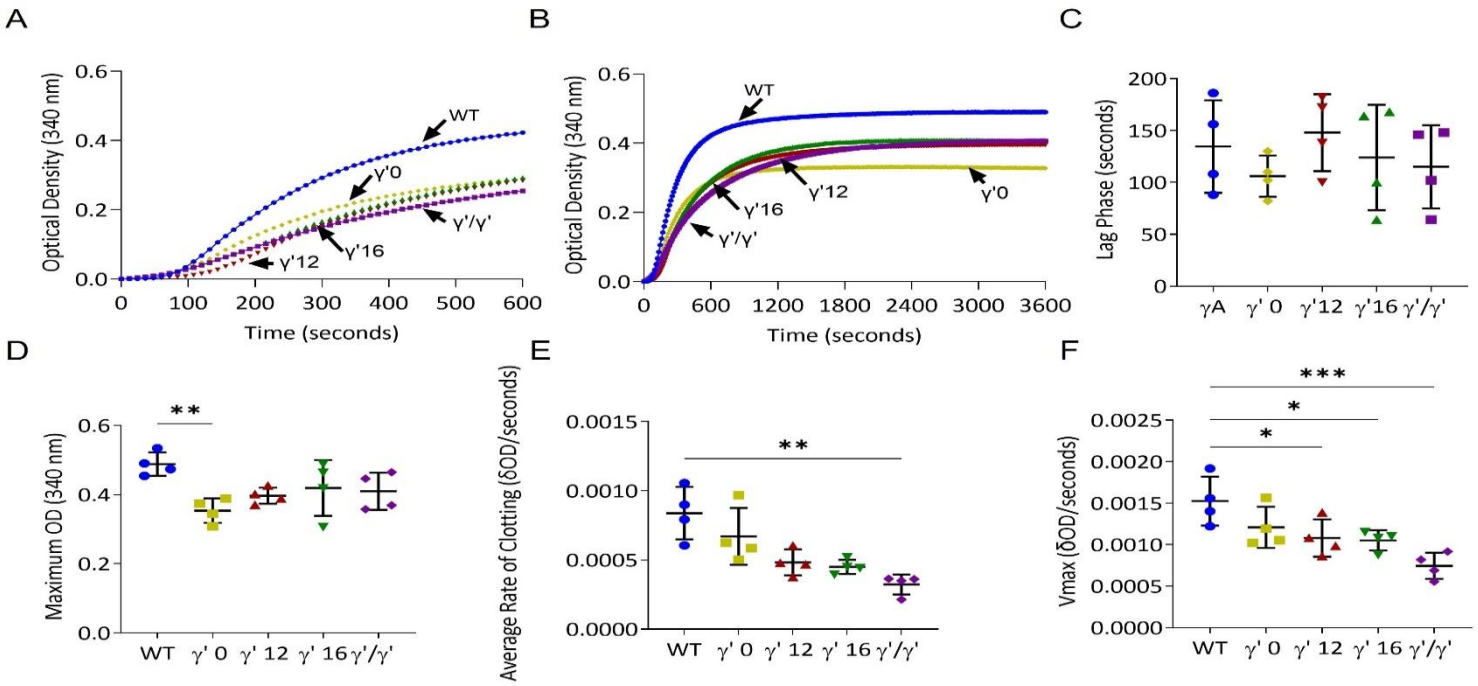

Figure 41 γ'-chain Variants Influenced the Rate of Clotting in the Presence of FXIII

Polymerisation Curve for WT and γ'-chain variants first 600 seconds (A) and over 3600 seconds (B). Lag phase for WT and γ'-chain variants (C). Maximum optical density (OD) for WT and γ'-chain variants (D). Average rate of clotting for WT and γ'-chain variants (E). Vmax for WT and γ'-chain variants (F). Results shown as mean ± standard deviation, *n=4*, **p*=0.05, ***p*=0.01, ****p*=0.001, by one-way ANOVA with Dunnett's multiple comparison test (D, F) or Kruskal-Wallis test with Dunn's multiple comparisons test (E) relative to the WT. Error bars not shown on A and B.

6.2.2.2 Fluorescently Labelled Fibrinogen did not Alter Fibre Thickness

A turbidimetric assay comparing parent fibrinogen protein to the corresponding fibrinogen protein with the addition of the Alexa Fluor® 488 labelled fibrinogen, to determine if the fluorescently labelled fibrinogen used in LSCM impacted polymerisation and consequently the structure of the fibrin clot. The amount of labelled fibrinogen protein included within the assay was equivalent to the final concentration used for the LSCM experiments and the final concentration of fibrinogen was equivalent.

The maximum OD which relates to fibre thickness was similar between unlabelled parent and the respective unlabelled parent (Figure 42). The unlabelled WT had a maximum OD of 0.438±0.042 OD compared to 0.4775±0.021 OD for the labelled fibrinogen. Comparing γ'0 with labelled γ'0 fibrinogen, the maximum OD was 0.345±0.005 OD and 0.328±0.028 OD respectively. The maximum OD for γ'12 was 0.402±0.008 OD compared to 0.396±0.021 OD for labelled γ'12 fibrinogen. The maximum OD for γ'/γ' was 0.439±0.009 OD compared to 0.438±0.043 OD for labelled γ'/γ' fibrinogen. These results confirm that any differences observed through structural investigations by LSCM are independent of the labelled fibrinogen as the labelled did not alter fibrin polymerisation or maximum OD.

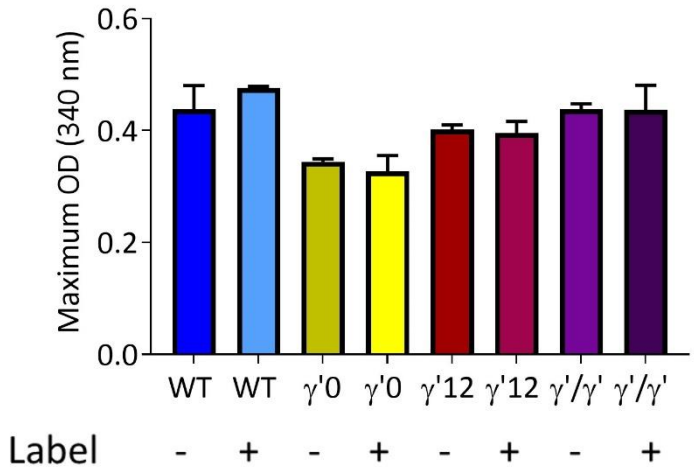

Figure 42 Fibre Thickness was not Altered by Inclusion of Fluorescently Labelled Fibrinogen

Maximum optical density (OD) of fibrinogen only WT (dark blue), γ'0 (mustard), γ'12 (red), γ'/γ' (purple) and fibrinogen with corresponding 5 % fluorescently labelled WT (light blue), γ'0 (yellow), γ'12 (pink), γ'/γ' (dark purple). Clotting was initiated with 0.1 U/mL thrombin and 5 mM calcium and the final concentration of fibrinogen was maintained at 0.5 mg/mL. Error bars are shown as mean ± standard deviation *n=2*.

6.2.2.2.1 Residues of the γ'-chain Impacted Clot Structure

To further investigate the influence of the γ'-chain residues on clot structure, clots were formed with corresponding Alexa Fluor® 488 labelled fibrinogens and imaged by LSCM. Figure 43A shows increased fibre curvature with fibrinogen with γ'-chain residues. Furthermore γ'0 which contains no residues of the γ'-chain, exhibited a straight fibre network which mirrored the WT clot. These observations in fibrin fibre network were observed in the presence and absence of FXIII.

The fibrin fibre count showed no difference between WT (14.1±3.5 fibres/100 μm) and any of the γ'-chain variants (γ'0 16.2±5.8 fibres/100 μm, γ'12 14.9±3.4 fibres/100 μm, γ'16 9.9±2.2 fibres/100 μm and γ'/γ' 12.7±2.5 fibres/100 μm) in the absence of FXIII (Figure 43B). Likewise, there was no difference in fibrin fibre count between WT (16.6±3.1 fibres/100 μm) and any of the γ'-chain variants (γ'0 18.5±4.9 fibres/100 μm, γ'12 16.4±3.8 fibres/100 μm, γ'16 9.9±3.0 fibres/100 μm and γ'/γ' 13.0±2.7 fibres/100 μm) in the presence of FXIII (Figure 43C). This result agrees with the maximum OD data from the turbidimetric assays for clots made with fibrinogen containing γ'-chain residues.

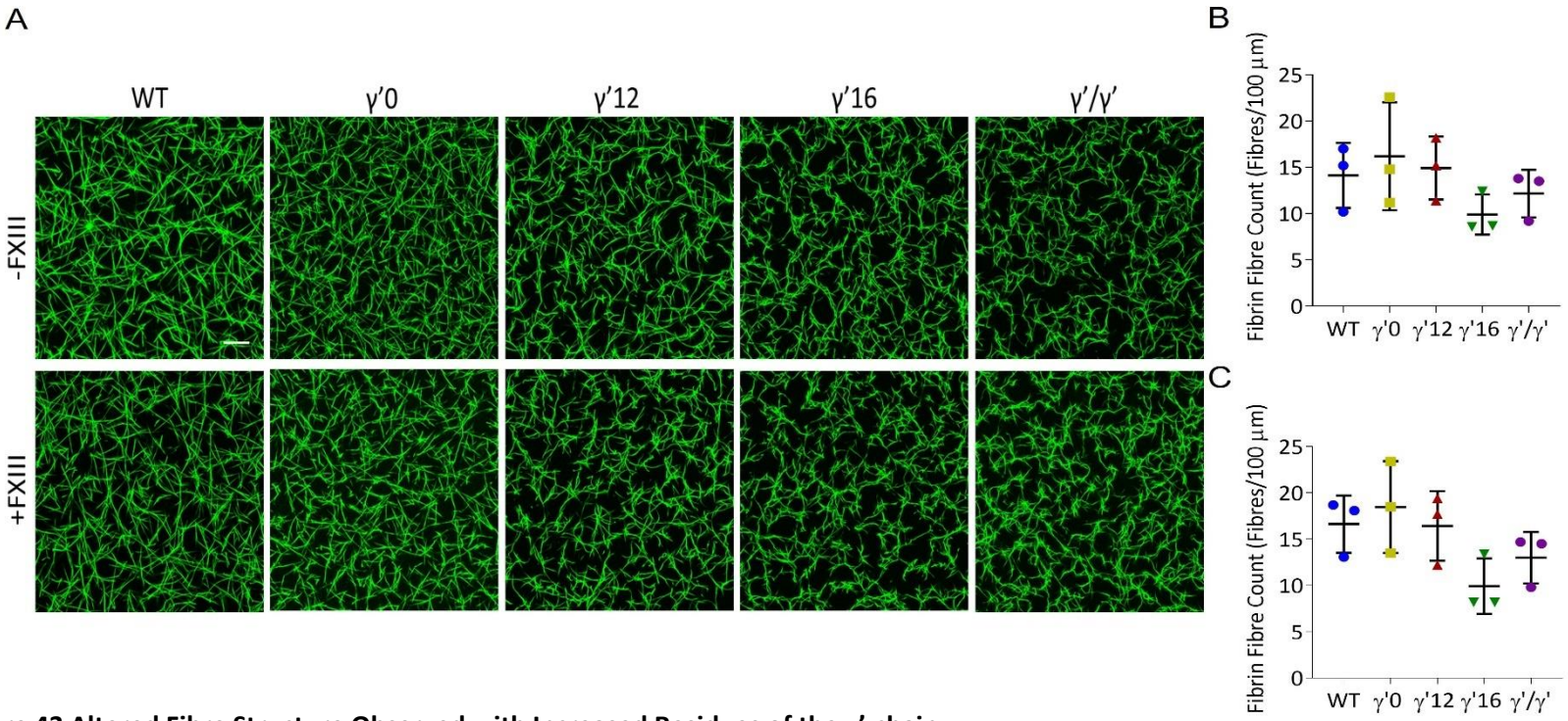

Figure 43 Altered Fibre Structure Observed with Increased Residues of the γ'-chain

Representative z stack images of clots made with Alexa-488 labelled WT and Alexa-488 labelled mutant fibrinogens for visualisation; WT and γ'-chain variants without (top) and with FXIII (bottom) (A). In the absence or presence of FXIII there was an altered structure in fibrin fibres observed in clots made from fibrinogen containing increasing γ'-chain residues. Images taken on a LSM880 inverted laser scanning confocal microscope, using the x40 objective. Z-stack is over 20.30 µm and composed of 29 slices; scale bar is 20 µm. Fibrin fibre count in clots composed of WT and γ'-chain variants absent (B) and presence of FXIII (C). No difference in fibre count was observed between WT and γ'-chain variants. Fibre density was calculated using an in-house macro made in imageJ. Results shown as mean ±standard deviation, *n=3*.

6.2.2.2.2 Fibrin Fibre Curvature was Independent of Fluorescent Label

To establish if the structural curvature observed in clots with increasing extension of the γ'-chain, was due to fluorescent label, clots (WT and γ'-chain variants) were visualised using the fluorescently labelled WT fibrinogen. Figure 44 shows LSCM images of WT and γ'-chain variants. As observed previously with the corresponding fibrinogen, there was fibre curvature observed with fibrin that contained γ'-chain residues. Indicating that the fibrin curvature is not a result of the fluorescent label.

6.2.2.2.3 Fibre Curvature was Independent of Thrombin Concentration

To determine if the structural fibre alterations observed in clots with increasing extension of the γ'-chain was a result of the γ'-chain or an effect of thrombin concentration, clotting was initiated with a range of thrombin concentrations and clot structure of WT and γ'/γ' was compared.

Across increasing thrombin concentrations there was an increase in fibre density for both WT and γ'/γ' (Figure 45), secondary to the fibrin fibres becoming shorter. At all the thrombin concentrations there was a difference in fibre structure between WT and γ'/γ' fibrin with straight fibres observed in WT clots and curved fibres found in the γ'/γ' clots. At the lowest thrombin concentration, the WT exhibited a longer fibre length whereas the curved fibre structure was quite similar at thrombin concentrations 0.01 and 0.05 U/mL in γ'/γ' clots.

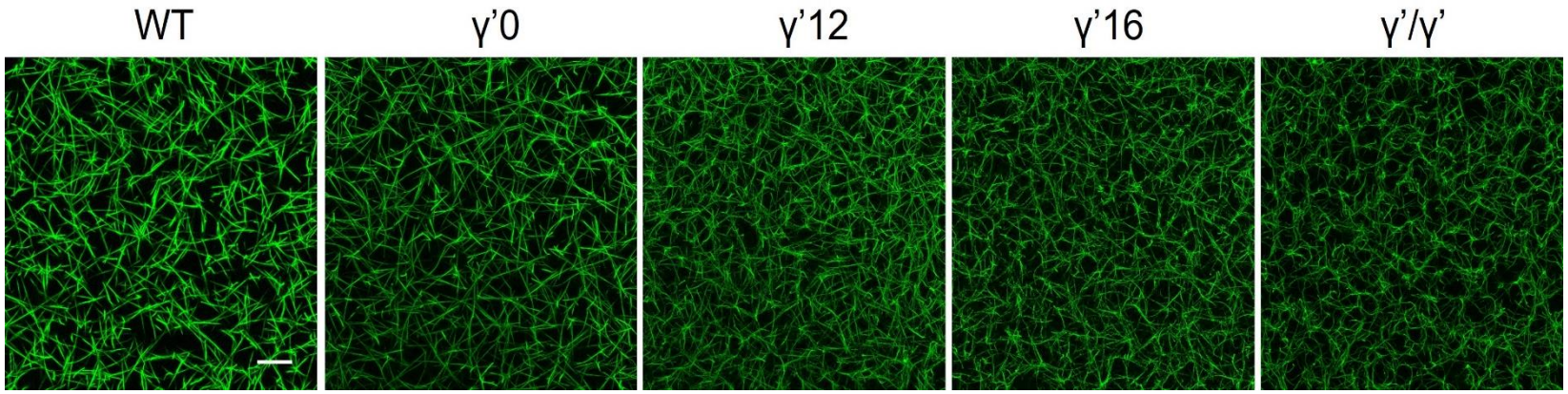

Figure 44 Fibrin Fibre Curvature Independent of Fluorescent Label

Representative z stack images of clots composed WT or γ'-chain variants and visualised with 5 % Alexa-488 labelled WT fibrinogen. The fibrin fibre curvature was observed in clots with γ'-chain residues, indicating the curvature is due to the fibrin variation itself rather than the fluorescent label. Images taken on a LSM880 inverted laser scanning confocal microscope, using the x40 objective. Z-stack is over 20.30 µm and composed of 29 slices; scale bar is 20 µm, *n*=1.

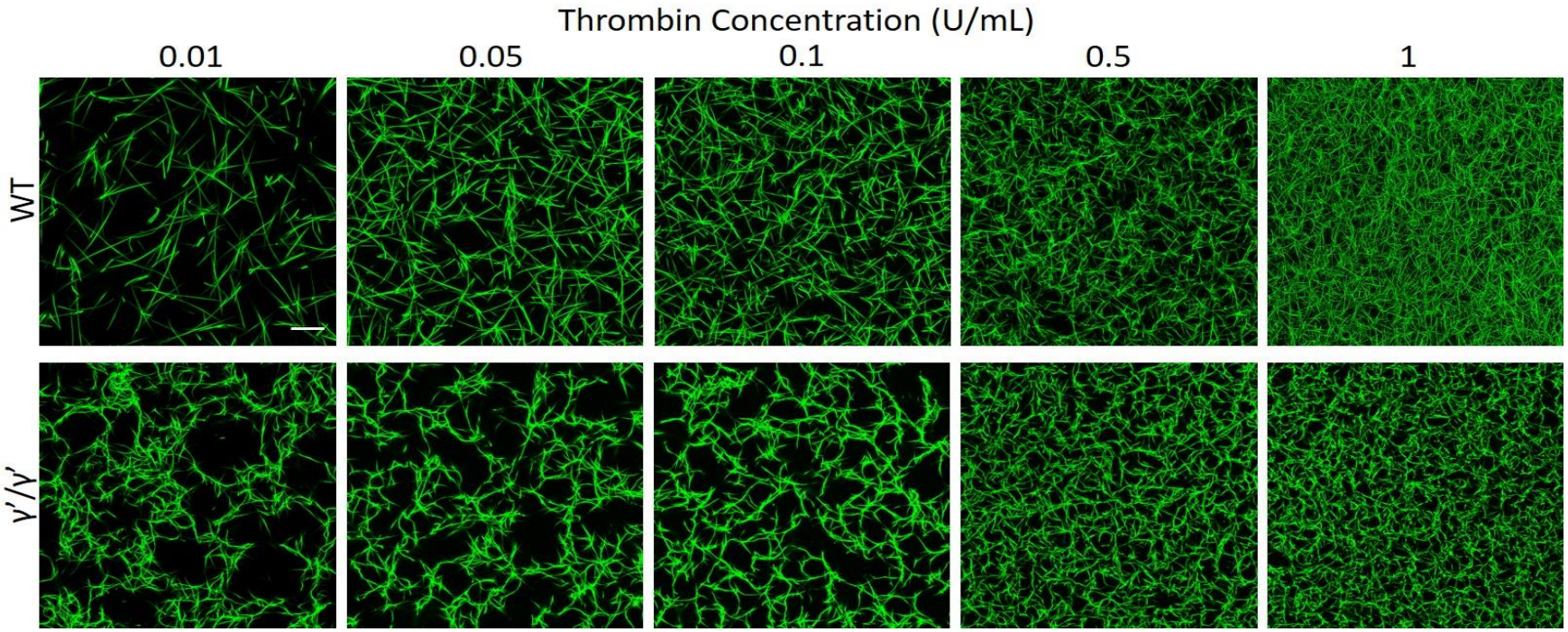

Figure 45 Fibrin γ'/γ' Structure Independent of Thrombin Concentration

Representative z stack images of clots composed of fibrin and Alexa-488 labelled fibrin for visualisation; of clots composed of WT (top) or γ'/γ' (bottom) formed at a range of thrombin concentrations. Clots for both WT and γ'/γ' became denser with shorter fibres at increasing thrombin concentration. However, the fibre curvature observed in γ'/γ', was present at all thrombin concentrations. Images taken on a LSM880 inverted laser scanning confocal microscope, using the x40 objective. Z-stack is over 20.30 µm and composed of 29 slices; scale bar is 20 µm *n*=1.

Reduced Fibre Diameter Observed for γ'/γ' with Addition of FXIII. In agreement with turbidimetric assays, thinner fibre diameter was observed for γ'0 (75.6±9.4 nm) compared to WT (93.3±6.1 nm p=0.7633) Figure 46A and B). No difference was observed in fibre diameter comparing γ'12 (84.9±7.4 nm), γ'16 (77.8±10.6 nm) and γ'/γ' (86.8±9.6 nm) with WT (Figure 40D).

Mirroring the reduced maximum OD observed with the inclusion of FXIII, a thinner diameter was seen for γ'0 (75.3±9.4 nm) compared to WT (93.3±2.3 nm p=0.0005). Additionally, reduced fibre diameter was observed for γ'/γ' (81.4±2.6 nm) compared to WT p=0.0161. No difference was observed in fibre diameter comparing γ'12 (85.8±0.9 nm) and γ'16 (90.7±7.3 nm) to WT, confirming the observations in turbidimetric assays (Figure 41D).

All clots, made in the presence and absence of FXIII showed a spectrum of fibre diameters indicating that there was a variety of fibre diameter within the network.

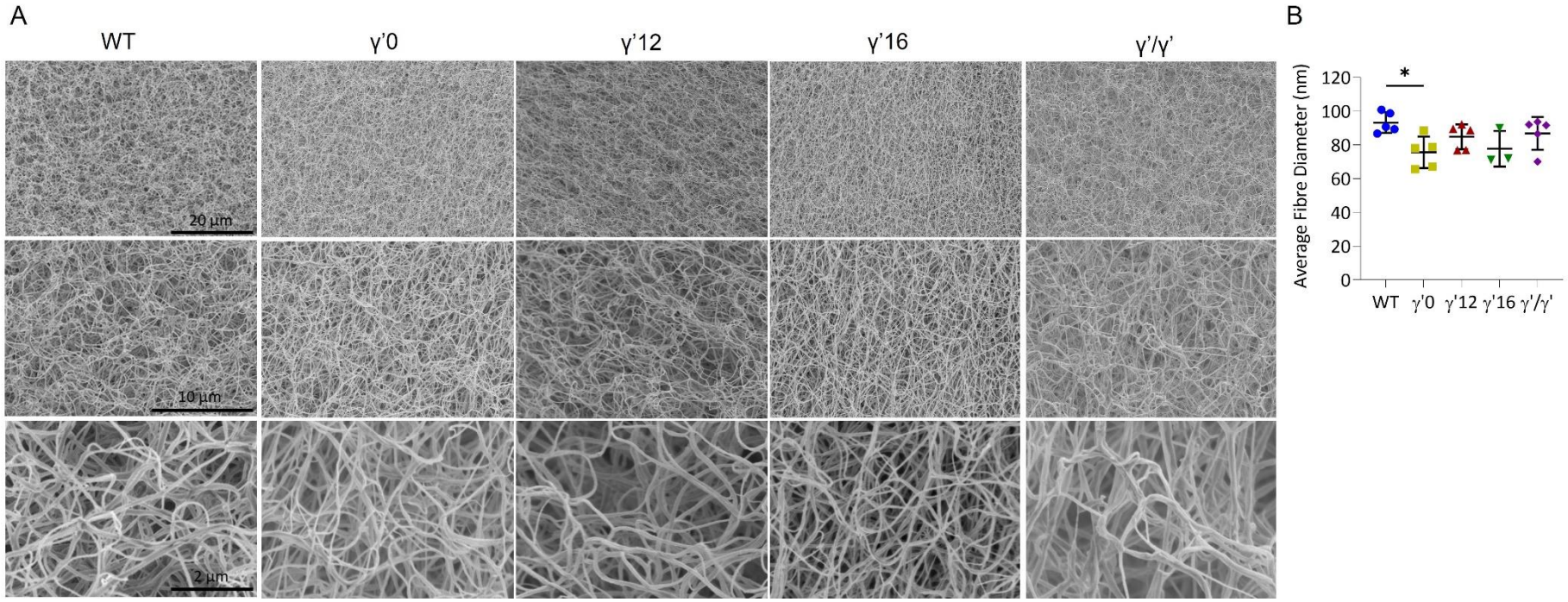

Figure 46 Reduced Fibre Diameter Observed for γ'0

Representative images of clots composed of WT and γ'-chain variants by scanning electron microscopy over increasing magnifications of x2,000, x5,000 and x20,000 (A). Images were taken on a Hitachi SU8230 Ultra-High-Resolution Scanning Electron Microscope. Average fibre diameter for WT and γ'-chain variants (B). Fibre diameter was calculated on images at x20,000 magnification. Results shown as mean ±standard deviation, *n=5* WT, γ'0, γ'12 and γ'/γ', *n=3* γ'16, * *p*=0.05 by Kruskal-Wallis Test with Dunn's multiple comparison test relative to the WT.

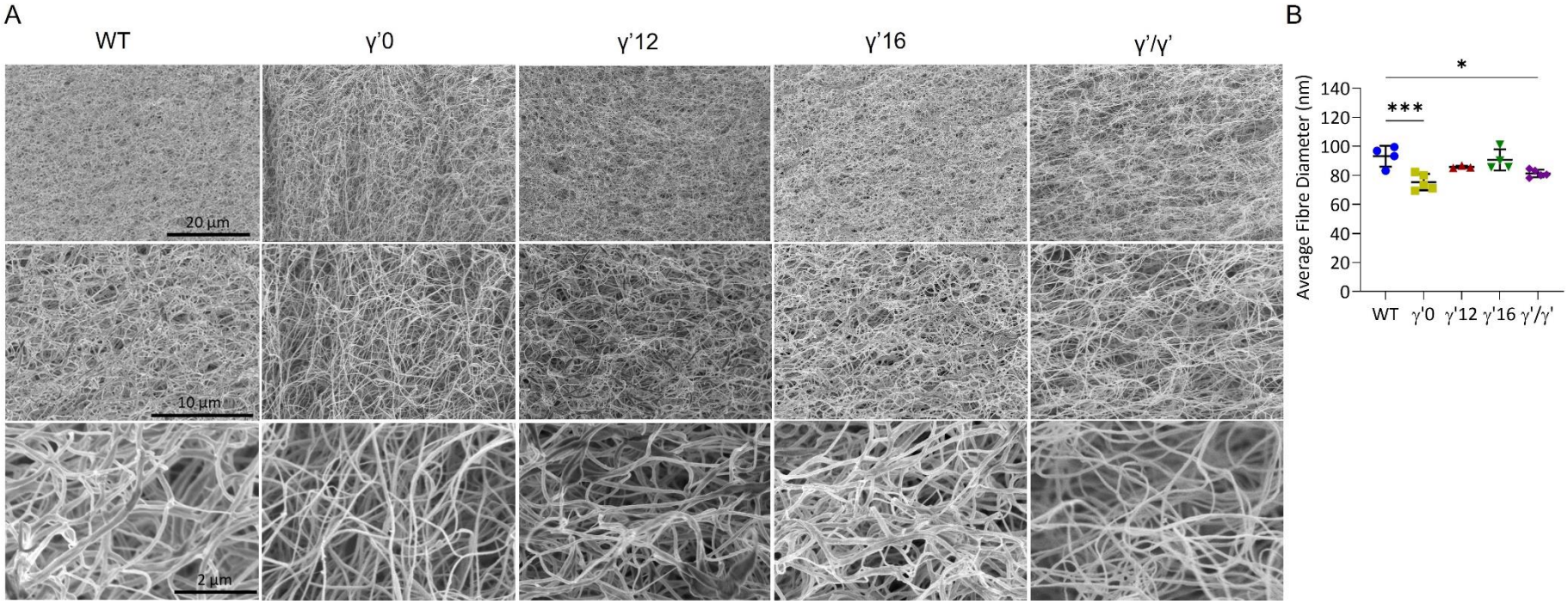

Figure 47 Reduced Fibre Diameter Observed for γ'0 and γ'/γ' with FXIII

Representative images of clots composed of WT and γ'-chain variants in the presence of FXIIIa by scanning electron microscopy over increasing magnifications of x2,000, x5,000 and x20,000 (A). Images were taken on a Hitachi SU8230 Ultra-High-Resolution Scanning Electron Microscope. Average fibre diameter for WT and γ'-chain variants (B). Fibre diameter was calculated on images at x20,000 magnification. Results shown as mean ±standard deviation, *n*=5 γ'0 and γ'/γ', *n*=4 WT and γ'16, *n*=3 γ'12, **p*=0.05 and ****p*=0.001 one-way ANOVA with Dunnett's multiple comparison test relative to the WT.

6.2.3 Functional Impact of the γ'-chain Residues

6.2.3.1 γ'-chain Variants did not Influence Fibrinolysis

To investigate the influence of the γ'-chain residues have on fibrinolysis, internal fibrinolysis was performed, and fibrinolysis was monitored in a turbidimetric assay in the presence or absence of FXIII.

The normalised lysis curves for WT and γ'-chain variants without the addition of FXIII show similar lysis profile (Figure 48A). In agreement with the lysis curves, no difference was observed in time to 50 % lysis between the WT (22.3±5.2 minutes) and the γ'-chain variants (γ'0 25.9±7.9 minutes, γ'12 29.1±8.2 minutes, γ'16 32.1±6.4 minutes and γ'/γ' 28.2±9.1 minutes) in the absence of FXIII (Figure 48B). Similarly, the fibrinolysis profile of the WT and γ'-chain variants without the addition of FXIII, the lysis curve with the addition of FXIII was similar between WT and γ'-chain variants. No difference was observed in time to 50 % lysis or average rate of lysis between the WT γ'-chain (Figure 48B,C,E,F).

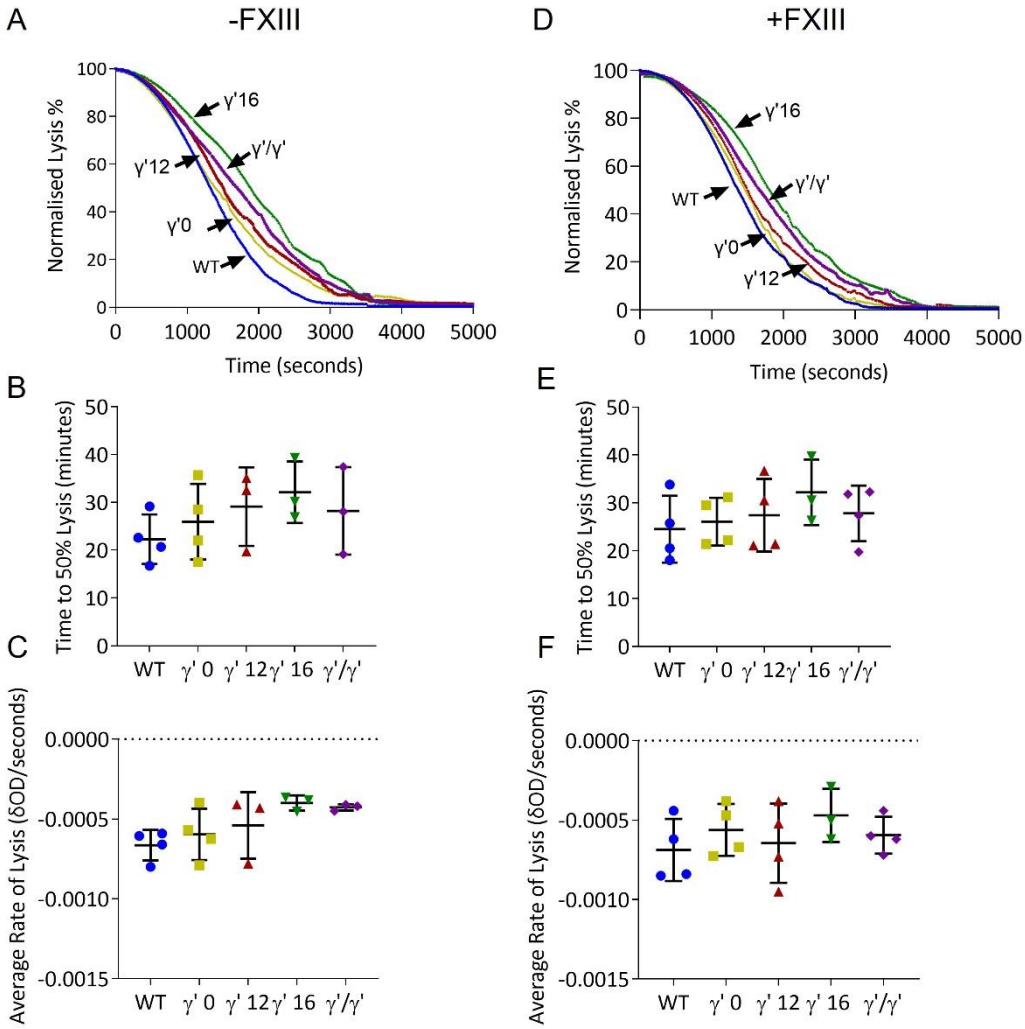

Figure 48 The Presence of γ'-chain did not Impact Fibrinolysis

Normalised lysis curves for WT and γ'-chain variants without FXIII (A) and with FXIII (D). Time to 50 % lysis for WT and γ'-chain variants without FXIII (B) and with FXIII (E). Average rate of lysis for WT and γ'-chain variants without FXIII (C) and with FXIII (F). Clotting was initiated with 5 mM $CaCl_2$, and 0.1 U/mL thrombin and a final concentration of 3.6 µg/mL was used for investigations with FXIII. Fibrinolysis was achieved with glu-plasminogen (0.24 µM) and t-PA (100 pM). Results shown as mean ±standard deviation, *n*=4 WT, γ', γ'12 (with FXIII) and γ'/γ' (with FXIII), *n*=3 γ'15 and γ'12 (without FXIII) and γ'/γ' (without FXIII). Error bars not shown on A and D.

6.2.3.2 The Presence of γ'-chain Residues Influenced Viscoelastic Properties of Fibrin

Viscoelastic investigations into the influence of the γ'-chain residues on clot mechanics was achieved by micro-rheology using an in-house magnetic tweezers device. The viscosity/loss modulus (G") and clot stiffness/storage modulus (G') was calculated for the various fibrin clots and then G" and G' were used to calculate the loss tangent (Tan δ ratio of G"/G'). Dr Stephen Baker assisted with data collection.

At all frequencies, no difference was observed for G' between WT (0.1 Hz at 0.766±0.118 Pa, 1 Hz at 1.448±0.235 Pa and 10 Hz at 0.204±0.060 Pa) and γ'0 (0.1 at Hz 1.178±0.467 Pa, 1 Hz at 1.770±0.477 and 10 Hz at 2.405±0.669 Pa). At 0.1 Hz γ'12 was alike WT (0.664±0.276 Pa p=0.9874), however there was a reduction at 1 Hz 0.947±0.312 Pa p=0.204 and a significant reduction in G' at 10 and 1.349±0.614 Pa (p=0.0149). Both γ'16 and γ'/γ' had reduced G' at 0.1 Hz compared to WT with a 0.406±0.188 Pa p=0.499 and 0.299±0.148 Pa p=0.265 respectively. There was a significantly reduced G' at 1 and 10 Hz for γ'16 (1 Hz at 0.553±0.239 Pa p=0.0067 and 10 Hz 0.606±0.3360 Pa p<0.0001) and γ'/γ' (1 Hz 0.472±0.176 Pa p=0.0029 and 10 Hz 0.496±0.196 Pa p<0.0001) compared to WT (Figure 49A).

Figure 49B shows G" for the WT and γ'-chain variants. No difference was observed for G'' at 0.1 and 10 Hz comparing the variants and WT. However, there was a significant reduction in G" at 1 Hz for γ'12 (0.238±0.136 Pa p=0.0051), γ'16 (0.059±0.061 Pa p<0.0001) and γ'/γ' (0.064±0.032 Pa p=0.0010) compared to WT (0.581±0.266 Pa). No difference was observed between the WT and γ'0 (0.427±0.245 Pa p=0.3719). The tan δ at all the frequencies showed that both WT and γ'-chain variants were more elastic than viscous. The γ'-chain residues appear to have the greatest effect on viscoelastic clot properties at 1 Hz (Figure 49C).

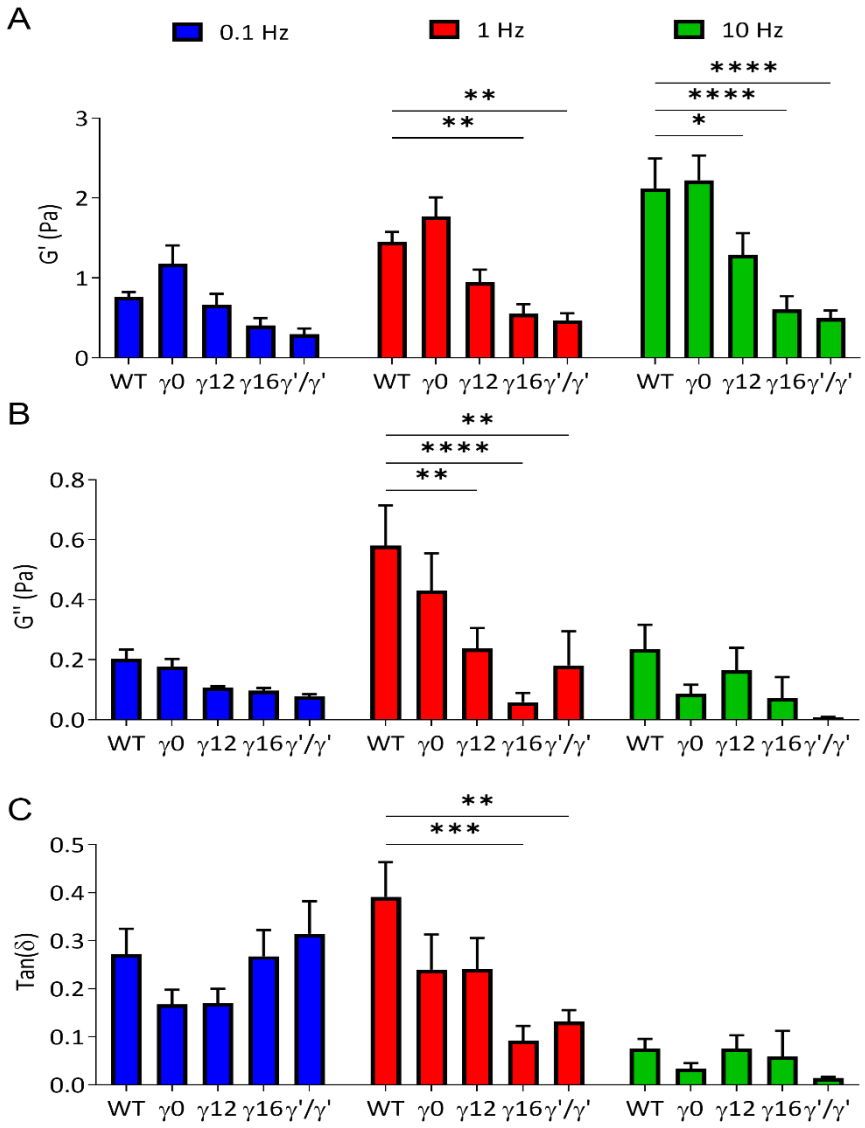

Figure 49 Increased Residues of γ'-chain Influence Viscoelastic Properties of the Fibrin Clot

Storage modulus (G') for WT and γ'-chain variants (A). Loss modulus (G") for WT and γ'-chain variants (B) The tan δ for WT and γ'-chain variants (C). Results shown as mean ±standard deviation, n=4. *p=0.05, **p=0.001, ***p=0.001 and ****p<0.0001 by two-way ANOVA with Dunnett's multiple comparisons test.

6.3 Discussion

The initial characterisation of the γ'-chain variants showed that the presence of the various lengths of γ'-chain did not impact overall clotability (or the ability of fibrin to form a clot). Further studies were undertaken to understand how the composition of the γ'-chain influences fibrin clot structure (turbidimetry, LSCM and SEM) and function (fibrinolysis and mechanics). The γ'-chain variants containing residues of the γ'-chain did not influence fibrin fibre count, maximum OD or fibrinolysis in the presence or absence of FXIII. Reduced fibre diameter was observed for γ'/γ' in scanning electron microscopy in the presence of FXIII. Fibrinogen γ'0 lacking the γ'-chain and the final four residues of γA altogether showed reduced fibrinogen diameter as well as maximum OD with and without FXIII. Additionally, the presence of more than 12 γ'-chain residues resulted in curvature of fibres and alterations in viscoelastic properties with reduced G' and G".

In contrast to previous studies (using plasma purified or recombinant proteins), maximum OD was not significantly reduced for γ'/γ' clots or fibrin made from fibrinogen with γ'-chain containing residues (Cooper et al., 2003; Gersh et al., 2009b; Allan et al., 2012; Macrae et al., 2021). Moreover, LSCM studies found no differences in fibrin fibre count for any of the γ'-chain variants compared WT, which agrees with previous studies with recombinant γ'/γ' and plasma purified without FXIII (Collet et al., 2004; Macrae et al., 2021). However, scanning electron microscopy showed reduced average fibre diameter for γ'0 with and without FXIII. Additionally, γ'/γ' had reduced average fibre diameter in the presence of FXIII. Furthermore, scanning electron microscopy showed that the fibre networks were composed of a range of fibre diameters. Previously, recombinant γA/γ' showed reduced maximum OD compared to WT but scanning electron microscopy showed significantly thicker fibres with a non-uniform fibrin network and a range of fibre diameters (Gersh et al., 2009b). Furthermore, scanning electron microscopy images of plasma purified fibrinogen WT and γA/γ' were composed of mixture of fibre diameters with a predominance towards thinner fibres in the γA/γ' clots (Siebenlist et al., 2005; Allan et al., 2012).

To date none of the studies investigating the γ'-chain have used the same experimental conditions (fibrinogen, thrombin or $CaCl_2$ concentrations), making it more challenging to compare. LSCM comparing WT and γ'/γ' over a range of thrombin concentrations showed how fibre length shortened, and fibre density increased at higher thrombin concentrations. Previous investigation into molecular structure of fibrinogen and the influence of thrombin showed 100 % γ'/γ' had reduced fibre radius, protofibril number and protein density with thrombin concentrations below 0.1 U/mL compared to 100 % γA/γA (Domingues et al.,

2016). Furthermore, ratios of γA/γA:γA/γ' showed differences in protein density, protofibril number at 0.1 U/mL but not at 1 U/mL thrombin. In agreement with previous studies, this study showed that concentration of both thrombin and fibrinogen influences fibrin network structure (Blombäck et al., 1989; Blombäck et al., 1994).

Similarly, to previous studies, reduced rate of clotting was observed in the presence and absence of FXIII with fibrinogen containing γ'-chain residues. Furthermore the more residues are present of the γ'-chain, the slower the rate of clotting becomes (Gersh et al., 2009b; Allan et al., 2012;Kim et al., 2014b; Macrae et al., 2021). This indicates that γ'-chain residues influence the rate of clotting under purified conditions.

The observation of altered fibre structure in the LSCM microscopy in the presence of over 12 γ'-chain residues has also been observed in other studies that have analysed clot structure of γ'-chain containing fibrinogen by LSCM. The studies have been conducted using recombinant or plasma purified fibrinogen (Allan et al., 2012; Guedes et al., 2018a; Guedes 2018b; Macrae et al., 2021). Increased concentrations of thrombin showed a shortening of the fibre curvature and increased fibrin network density. Further studies to observe if this curvature is independent of thrombin would be useful to uncover if this is an attribute of γ'-chain.

Previously studies have indicated that the γ'-chain can influence fibrinolysis, however, this study observed that the γ'/γ' or fibrinogens with truncated γ'-chain did not result in alterations in internal fibrinolysis in the absence or presence of FXIII. A previous study using plasma purified γA/γA and γA/γ' found increased fibrinolysis resistance but only with FXIII and the resistance was due to increased cross-linking in γA/γ' (Falls and Farrell, 1997).

Although both studies investigated fibrinolysis by internal lysis the concentrations used in the Falls and Farrell study fibrinogen (1.25 mg/mL), thrombin (13.2 U/mL) and FXIII (10 µg/mL) are higher than used within in this study. In addition, they used lys-plasminogen compared to glu-plasminogen. Results presented in this study and that of others highlight that higher thrombin concentrations can impact the fibrin network (Domingues et al., 2016). In addition, the concentrations thrombin used by Falls and Farrell was higher than the required concentration for FXIII activation (0.0088 U/mL) (Brummel et al., 2002). Potentially the concentration of thrombin and FXIII may provide additional fibrinolysis resistance which may not be observed during internal fibrinolysis. A study using plasma purified fibrinogen with low, normal, and high γ'-chain levels observed no difference in internal fibrinolysis between normal and high γ'-chain levels in the absence of FXIII, which agrees observations in this study (Macrae et al., 2021). However, with the addition of FXIII, the Macrae et al. study showed an increase in time to 50 % lysis observed between normal and high γ'-chain

levels. Interestingly, the average rate of lysis observed for normal (-0.0008 δOD/seconds), and high γ'-chain (-0.0007 δOD/seconds) levels was like average rate of fibrinolysis observed for γ'/γ' (-0.0006 δOD/seconds) within this study. Furthermore, the study observed a shorting of time to 50 % with the inclusion of FXIII, whereas this study observed similar time to 50 % with and without FXIII. This discrepancy may be related to differences in experimental conditions as higher concentration of fibrinogen (plasma purified compared to recombinant), thrombin, plasminogen, and t-PA were used but a similar concentration of FXIII. A study into the relationship between plasminogen and γ'-chain found that plasminogen had reduced binding to the γ'-chain but this was related to FpB cleavage as γ'-chain fibrinogen had slower FpB cleavage (Doolittle and Pandi, 2006;Kim et al., 2014b). Although Fp release was not investigated in this study, a previous recombinant study found γA/γ' to be the same as normal whereas γ'/γ' was more readily released (Gersh et al., 2009b). Plasma purified γA/γ' has been observed to have slower FpB release (Cooper et al., 2003; Allan et al., 2012).

While the above studies and the current study have used internal fibrinolysis for investigations, external fibrinolysis omits differences in delayed plasminogen binding or delays in FpB cleavage. Previous studies into external fibrinolysis have observed a similar and extended fibrinolysis time for fibrinogen with the γ'-chain, with studies using LSCM to monitor fibrinolysis. Fibrinolysis resistance by external fibrinolysis was increased in recombinant fibrinogen γ'/γ' and authors attributed this resistance to increased FXIII cross-linking (Collet et al., 2004). Another recombinant study observed no difference between WT and γ'/γ' but FXIII was not present, however lysis time was extended for plasma purified γA/γ' compared to γA/γA (Guedes et al., 2018a; Guedes et al., 2018b). These two studies used the same concentration of plasminogen and t-PA. However, plasma purified fibrinogen is likely to have contained FXIII, resulting in extended lysis time mirroring the earlier observation by Collet et al. It is important to appreciate the differences in observations for internal and external fibrinolysis as increased γ'-chain levels are observed in CVD and this could influence success of patient treatment with thrombolysis (Lovely et al., 2002; Appiah et al., 2015).

The presence of γ'-chain residues resulted in alterations in viscoelastic properties compared to WT. There was a stepwise reduction observed with increased γ'-chain residues, which was evident from γ'12. The frequencies examined are related to points of deformation, with 0.1Hz and below deformation events occurring at branch points and along fibres. At 1 Hz, are deformation events at fibre level (twisting or stretching) and 10 Hz is at the molecular level (Allan, 2012). G' (clot stiffness) showed the greatest change at 10 Hz and then at 1 Hz,

indicating the γ'-chain and γ'-chain residues impact the fibrin network at the molecular and fibre level. Reduced clot stiffness agrees with previous observation with plasma purified γA/γ' (Allan et al., 2012; Guedes et al., 2018a). However, a recombinant study observed no difference in clot stiffness between WT and γ'/γ' (Collet et al., 2004). The differences observed may be due to techniques used, as the plasma purified fibrinogen and the present study used magnetic rheology whereas the recombinant study used torsion pendulum device (Collet et al., 2004; Allan et al., 2012; Guedes et al., 2018a). The G" (clot viscosity) was significantly reduced for γ'-chain variants containing 12 and above at 1 Hz, whereas the γ'-chain residues did not differ compared to WT at 0.1 and 10 Hz. A previous studies have observed a higher G" in plasma purified γA/γ' compared to WT but the frequency studied was not stated (Allan et al., 2012).

Tan delta was similar between the γ'-chain variants and WT at 0.1 Hz and 10 Hz, however, reduced tan delta was observed at 1 Hz for γ'/γ' and γ'16 compared to WT indicating the clots were less viscous and less deformable. A previous study observed no difference in tan delta between recombinant WT and γ'/γ', but the frequency of the tan delta was not stated, however it could potentially agree with the observations at 0.1 or 10 Hz (Guedes et al., 2018b). An early study of plasma purified showed higher tan delta for γA/γ' compared to WT but the frequency examined was not stated (Allan et al., 2012). Fibrinogen with γ'-chain containing residues had greater effect on clot stiffness compared to clot viscosity. Clot stiffness or viscosity was similar between γ'0 and WT at all the frequencies, indicating that the presence of the γ'-chain residues causes the observed changes in viscoelastic properties. Viscoelastic properties were influenced the greatest, at the fibre level. The presence of 12 residues of the γ'-chain impacted mechanical clot properties which was further emphasised with the inclusion of more γ'-chain residues.

Investigations into clots formed with recombinant γ'-chain variants showed that with increasing residues of the γ'-chain, the γ'-chain can influence the rate of clotting, fibre structure and viscoelastic properties. Additionally, the more residues of the γ'-chain present the greater impact there was on clot behaviour.

6.3.1 Key Findings

- The presence of γ'-chain residues influences the rate of clotting in the presence and absence of FXIII.
- Clot structure is altered by the increased residues of the γ'-chain.
- Clot viscoelastic properties are altered by increased residues of the γ'-chain.
- Reduced G' and G" was observed following the addition of the first 12 residues of the γ' sequence and was particularly prominent at the fibre level.

Chapter 7 Characterisation of γ'-chain Variants in Plasma and Whole Blood

7.1 Introduction

The previous chapter showed that more residues of the γ'-chain resulted in reduced rate of clotting, increased curvature of fibrin fibres and influenced clot mechanics. However, the γ'-chain residues did not appear to influence fibrinolysis or maximum OD as observed in other plasma purified and recombinant studies (Gersh et al., 2009b; Allan et al., 2012; Kim et al., 2014b).

There have been few studies into effects of the γ'-chain in plasma based clots; one study found that with increasing γ'-chain maximal OD was reduced and lysis time prolonged but the clotting rates were not affected (Pieters et al., 2013). In agreement with this, plasma samples with higher percentage of the γ'-chain showed reduced maximal OD and prolonged lysis time in another study (Macrae et al., 2021). In addition, the latter study also observed reduced porosity and increased fibre density with increasing percentage of the γ'-chain. Whether the structural observations are a result of interactions with plasma proteins which were not removed by purification in the plasma purified investigations or additional PTM to the fibrinogen in the circulating plasma is unclear, as there were also some differing observations between two previous recombinant studies (Collet et al., 2004;Gersh et al., 2009b).

Flow cytometry based investigations into fibrinogen:platelet interactions in 5.4.2 observed no increase in either fibrinogen positive platelets or median fluorescent intensity with platelet activation compared to basal for γ'0 and γ'/γ'. This agrees with previous observations into γ'-chain and platelet aggregation, where fibrinogen homozygous for the γ'-chain did not support platelet aggregation (Farrell et al., 1992; Rooney et al., 1996). Other studies have shown that presence of the γ'-chain does not prevent clot contraction but that the interaction with $_{\alpha IIB\beta 3}$ between fibrinogen and fibrin differs (Rooney et al., 1996; Litvinov et al., 2016). Furthermore, multiple binding sites within the $_{\alpha IIB}$ have been shown to bind fibrin and inhibition of $_{\alpha IIB\beta 3}$ by abciximab can effect clot contraction (Podolnikova et al., 2014; Kim et al., 2017). Whether the absence of part of the γ'-chain affects interaction of $\alpha_{IIB}\beta_3$ and fibrin during clot contraction is not known.

There have not been extensive studies into γ'-chain in whole blood either *ex vivo* or *in vivo*, including murine studies of arterial and venous thrombosis. The main challenge with these studies is that mice do not express the γ'-chain and therefore the relevance to humans would be unclear. However, polymerisation of purified human fibrinogen (γA/γA or γA/γ')

by either human or murine thrombin shows no difference in maximum OD but a shorter lag phase was observed using murine thrombin (Walton et al., 2014). Plasma studies with murine or human plasma supplemented with γA/γA or γA/γ' showed reduced maximum OD for γA/γ' mirroring previous observations into human γA/γ' purified studies (Cooper et al., 2003; Allan et al., 2012; Walton et al., 2014). These results do indicate that *in vivo* studies using murine models likely reflect observations in humans for γ'-fibrinogen. Additionally, murine studies into the effects of γ'-chain in thrombosis models have shown that it can modify thrombotic risk by modulating thrombin binding as well as reducing the thrombotic potential of the factor V Leiden mutation (Mosesson et al., 2009; Walton et al., 2014). These observations confirm previous studies that have shown γ'-chain binding to thrombin (Pineda et al., 2007). Furthermore, there was no difference observed in thrombus volume in a venous thrombosis model comparing WT mice with heterozygous mice for the human γ'-chain (Mosesson et al., 2009). However, fibrinogen infusion of either γA/γA or γA/γ' into mice before arterial thrombus formation showed faster time to carotid artery occlusion in γA/γA compared to γA/γ' (Walton et al., 2014). In agreement with the time to occlusion turbidimetric assay showed increased Vmax for γA/γA compared to γA/γ'.

In contrast to the murine models, a study investigating thrombosis formation under arterial and venous shear rates, showed faster fibrin deposition and larger thrombi with increasing percentage of human γ' for both shear rates (Macrae et al., 2021). The three studies were experimentally different, the flow model used pre-formed human platelet aggregates, and human plasma with various percentage ratios of γ' fibrinogen was next flowed over at venous and arterial flow rate (Macrae et al., 2021). In the arterial model the vessels were harvested after 30 minutes and sections were prepared for histology where thrombus volume was calculated (Mosesson et al., 2009). In mice infused with γA/γA and γA/γ', the $FeCl_3$ injury model was used and the time to occlusion was shortened in γA/γA compared to γA/γ' (Walton et al., 2014). Furthermore, the flow model used pre-formed human platelet aggregates, which mitigates the step of aggregation of platelets, which is impacted by the presence of the γ'-chain, which may be why the time to occlusion was shorter for γA/γA compared to γA/γ' (Walton et al., 2014; Macrae et al., 2021).

This chapter further investigates fibrinogen γ'-chain variants to understand if the differences observed in previous studies (Cooper et al., 2003; Allan et al., 2012) were due to potential interactions with other proteins within the plasma. The studies in this chapter were performed using turbidimetric assays and LSCM with fibrinogen deficient plasma and plasma from patients with afibrinogenemia, and clotting was initiated with thrombin or tissue factor. Whole blood investigations into the influence of γ'-chain residues on clot contraction,

clot formation and whole blood clot structure were also performed. These investigations are performed using whole blood from *FGA*$^{-/-}$ mice followed by supplementation with either fibrinogen γ'-chain variants or WT. Clot formation studies were performed by ROTEM analysis, and the clots formed will be investigated by scanning electron microscopy. Clot contraction analysis is used to investigate RBC and platelet incorporation into the clot.

7.1.1 Hypothesis

The γ'-chain residues can influence clot structure, function and contraction in plasma and whole blood.

7.1.2 Aims

To uncover γ'-chain residues that are responsible for the observations in plasma studies and their effects in whole blood.

Secondary Aims:

- To observe any structural differences using microscopy and turbidimetric assays.
- Study how the γ'-chain residues influence whole blood clot formation and contraction by ROTEM analysis and *ex-vivo* whole blood contraction assay.

7.2 Results

7.2.1 Influence of Plasma on γ'-chain Variants

7.2.1.1 Reduced Maximum Optical Densities for γ'-chain Variants in Plasma

The previous chapter showed no difference in maximum OD for the γ'-chain variants compared to WT. Previous investigations with plasma purified γA/γ' had shown reduced maximum OD (Allan et al., 2012). To uncover if the reduced maximum OD was a result of an interaction between γ'-chain and plasma proteins, fibrinogen deficient plasma supplemented with recombinant γ'-chain variants were incubation at 37 °C for a 1 hour, followed by turbidimetric assays.

Figure 50A polymerisation curve showed reduced Maximum OD for the γ'-chain variants compared to WT. There was an increase in lag phase for the γ'-chain variants (γ'/γ' 298.0±114.8 seconds p=0.4548, γ'12 396.0±140.6 seconds p=0.0707, γ'0 234.0±140.0 seconds p=0.08906) but this was only significant for γ'16 (450.0±78.7 seconds p=0.0220) compared to WT (179.5±28.8 seconds p=0.0220) (Figure 50B).

All γ'-chain variants (γ'0 0.259±0.065 OD p=0.0022, γ'12 0.258±0.044 OD p=0.0039, γ'16 0.185±0.014 OD p<0.0001 and γ'/γ' 0.294±0.005 OD p=0.0027) had reduced maximum OD compared to WT (0.388±0.028 OD) (Figure 50C).

There was no difference in average rate of clotting for the γ'-chain variants compared to WT (Figure 50D). A reduced Vmax was observed for γ'16 (0.000449±0.000042 δOD/seconds p=0.0265) compared to WT (0.001070±0.001288 δOD/seconds). No difference was observed for the other γ'-chain variants compared to WT.

No difference was observed in time to 50 % clotting or time to maximum OD for any of the γ'-chain truncations or γ'/γ' compared to WT (Figure 50F and G).

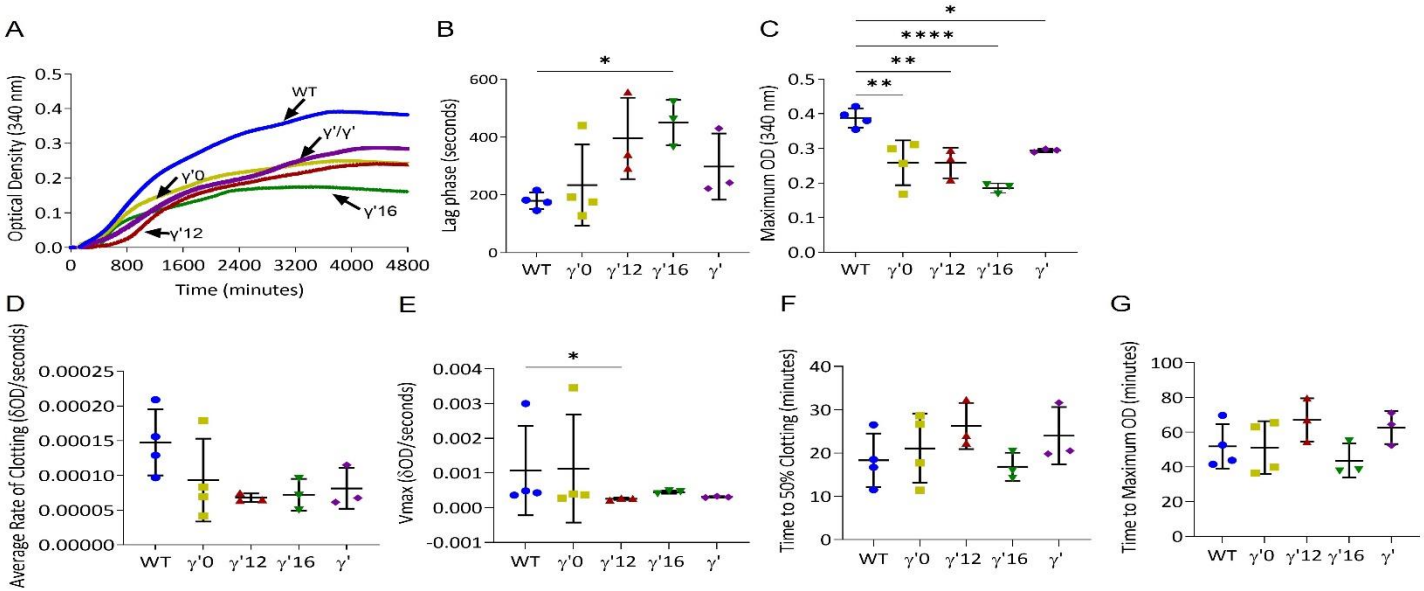

Figure 50 Reduced Maximum OD for γ'-chain Variants using Thrombin Initiated Clotting

Polymerisation curves for WT and γ'-chain variants (A). Lag Phase for WT and γ'-chain variants (B). Maximum optical density (OD) for WT and γ'-chain variants (C). Average rate of clotting for WT and γ'-chain variants (D). Vmax for WT and γ'-chain variants (E). Reduced Vmax observed for γ'12 compared to WT. Time to 50 % clotting (F) and time to maximum OD (G) for WT and γ'-chain variants. Clotting was initiated with 0.1 U/mL thrombin and 10 mM $CaCl_2$. Results shown as mean ± standard deviation, *n*=4 WT and γ'0, *n*=3 γ'1, γ'16 and γ'/γ' *p=0.05 **p=0.01 by one-way ANOVA with Dunnett's multiple comparison test (maximum OD and Vmax) or Kruskal-Wallis test with Dunn's multiple comparison test (lag phase) relative to the WT. Error bars not shown on A.

7.2.1.2 Reduced Maximum OD Observed for γ'12 and γ'16 by Tissue factor Initiated Clotting

Following the observation of reduced maximum OD for fibrinogen deficient plasma supplemented with γ' variants by thrombin-initiated clotting. Clotting was initiated by the addition of 1 pM of tissue factor to observe if a similar reduction in OD occurred when clotting was initiated earlier in the coagulation cascade.

Figure 51A shows turbidimetric curves for WT and γ' variants. Reduced maximum OD was observed for all the γ' variants compared to WT. No difference was observed in lag phase for any of the γ' variants compared to WT (Figure 51A). Like thrombin-initiated clotting, a significantly reduced maximum OD was observed for γ'12 (0.223±0.042 OD p=0.0154) and γ'16 (0.196±0.014 OD p=0.0088) compared to WT (0.359±0.050 OD) (Figure 51C). A reduced maximum OD was observed for γ'/γ' (0.270±0.0.38 OD p=0.6676) and γ'0 (0.239±0.074 OD p=0.112) but this was not significant compared to WT.

No difference was observed between the γ'-chain variants to the WT for average rate of clotting, Vmax, time to 50 % clotting or time to maximum OD (Figure 51D-G).

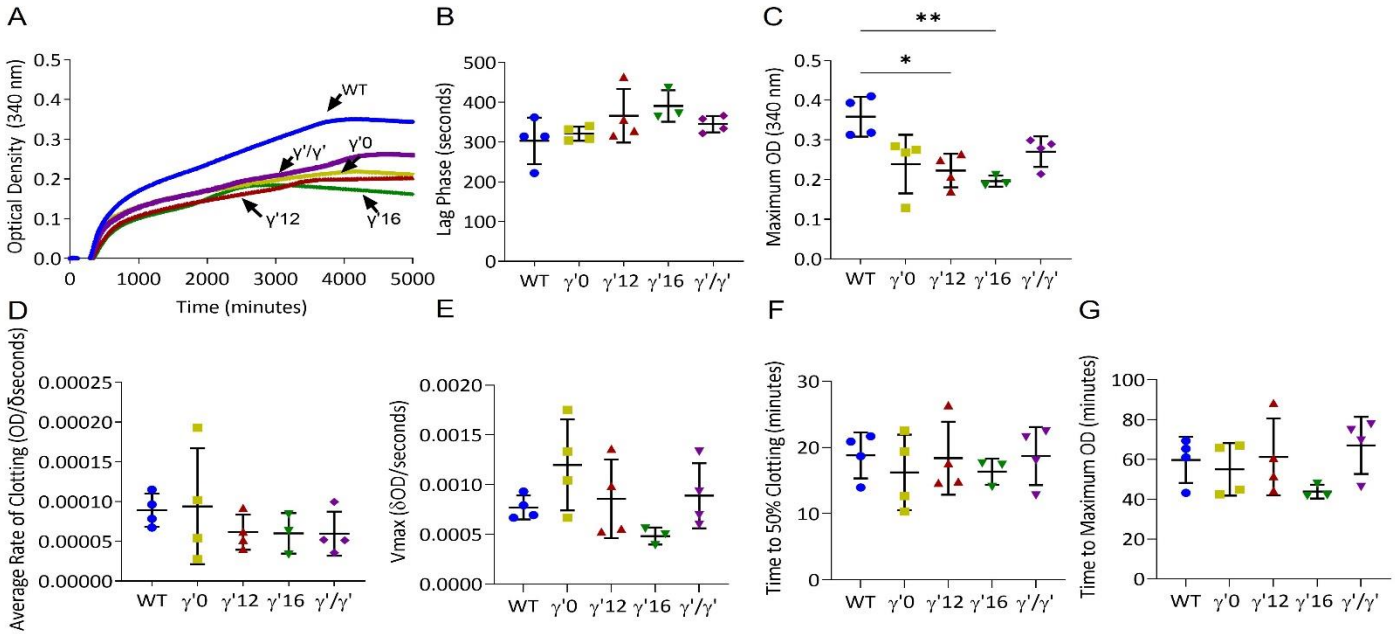

Figure 51 Fibrinogen Deficient Plasma Supplemented with γ'12 and γ'16 Showed Reduced Maximum OD for Tissue Factor Initiated Clotting

Polymerisation Curves for WT and γ'-chain variants (A). Lag Phase for WT and γ'-chain variants (B). Maximum OD for WT and γ'-chain variants (C). Average rate of clotting (D), Vmax (E), time to 50 % clotting (F) and time to maximum OD (G) for WT and γ'-chain variants. Clotting was initiated with 1 pM tissue factor and 10 mM $CaCl_2$. Results shown as mean ± standard deviation, *n*=4 WT, γ'0 γ'12, γ'16 and γ'/γ' *n*=3 γ'16, **p*=0.05 ***p*=0.01 by Kruskal-Wallis test with Dunn's multiple comparison test relative to the WT. Error bars not shown on A.

7.2.1.3 Reduced Maximum Optical Density for γ'-chain Variants in Afibrinogenemia Plasma

Following the observations using the commercial sourced plasma depleted fibrinogen, turbidimetric assay was undertaken using plasma from three patients with afibrinogenemia and clotting was initiated by thrombin. The plasma samples were kindly given by Dr Alexandro Cassini from the University of Geneva.

Figure 52A shows the turbidimetric curves for the γ'-chain variants compared to WT. All the γ' variants showed a reduced OD compared to WT. The plasma from the patients without added fibrinogen did not show an increase in OD indicating that the clotting observed was due to the addition of the recombinant fibrinogen. The maximum OD was significantly reduced for all γ'-chain variants (γ'/γ' 0.220±0.017 OD p=0.0002, γ'16 0.126±0.025 OD p<0.0001, γ'12 0.285±0.050 OD p=0.043 and γ'0 0.267±0.052 OD p=0.0015) compared to WT (0.413±0.017OD). No difference was observed between the γ'-chain variants compared with WT for lag phase, average rate of clotting, Vmax, time to 50 % clotting or time to maximum OD (Figure 52B, D-G).

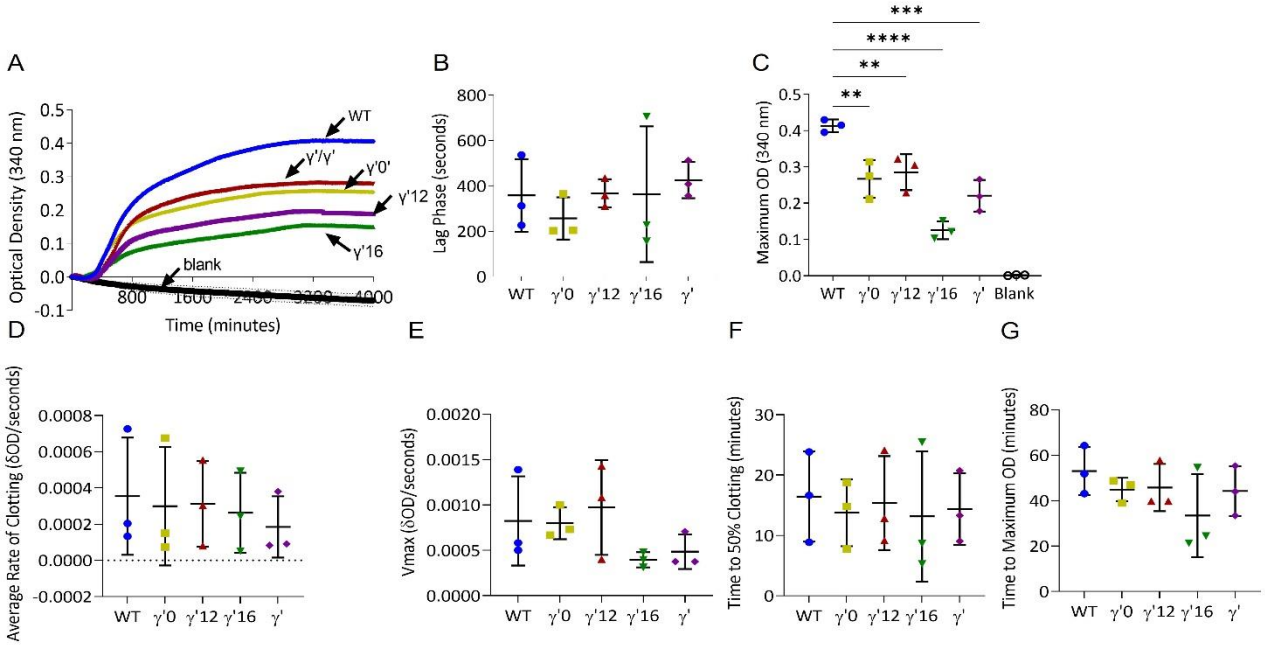

Figure 52 Reduced Maximum Optical Density for γ'-chain Variants in Afibrinogenemia Plasma

Polymerisation curves for WT and γ'-chain variants (A). Lag Phase for WT and γ'-chain variants (B). Maximum OD for WT and γ'-chain variants (C). Average rate of clotting (D), Vmax (E), time to 50 % clotting (F) and time to maximum OD (G) for WT and γ'-chain variants. Clotting was initiated with 0.1 U/mL thrombin and 10 mM $CaCl_2$. Blank is afibrinogenemia plasma where clotting was initiated but no fibrinogen was included. Results shown as mean ± standard deviation, n=3, **p=0.01, ***p=0.001, ****p<0.0001 by one-way ANOVA with Dunnett's multiple comparison test relative to the WT. Error bars not shown on A.

7.2.1.4 Reduction in Maximum Optical Densities in γ'-chain Variants with Incubation in Plasma

To uncover if the effects observed in the initial experiments with fibrinogen deficient plasma supplemented with γ'-chain variants was time dependant, the fibrinogens were incubated with fibrinogen deficient plasma for either 5 minutes or no incubation before clotting was initiated by thrombin.

Maximum OD was significant reduced for γ'0 (0.213±0.069 OD p=0.0108) and γ'12 (0.209±0.066 OD p=0.0027) compared to WT (0.359±0.042 OD) with no incubation in plasma. No difference was observed between WT and γ'/γ' (0.260±0.045 OD p=0.1026) with no incubation in plasma. Following a 5-minute incubation there was a significantly reduced maximum OD for all the γ'-chain variants (γ'0 0.263±0.064 OD p=0.0008, γ'12 0.271±0.036 OD p=0.0002 and γ'/ γ' 0.266±0.037 OD p=0.0009) compared to WT (0.458±0.098 OD) (Figure 53A).

No differences were observed in lag phase at either no incubation or after 5 minutes for γ'/γ' and γ'0 compared to WT (Figure 53B), whereas a significant increase in lag phase was observed for γ'12 (584±150.6 seconds p=0.0270) compared to WT (0.346.8±66.5 seconds) at 0 incubation. There was no significant difference after a 5-minute incubation γ'12 (459±94.8 seconds p=0.2341) compared to WT (0294±91.7 seconds).

There was no difference in average rate of clotting with no incubation of γ'-chain variants in the depleted plasma (Figure 53C). A reduced rate of clotting was observed for γ'/γ' (0.00007±0.00002 δOD/seconds p=0.0395) compared to WT (0.00025±0.00012 δOD/seconds) after 5-minute incubation in plasma. No difference was observed for the other γ'-chain variants compared to WT. Neither condition showed any difference in Vmax for any of the γ'-chain variants compared to WT (Figure 53D).

No difference was observed in time to 50 % clotting or time to maximum OD for any of the γ'-chain truncations or γ'/γ' compared to WT which agrees with the previous experiments in plasma (Figure 53E and F, Figure 50F and G, Figure 51F and G).

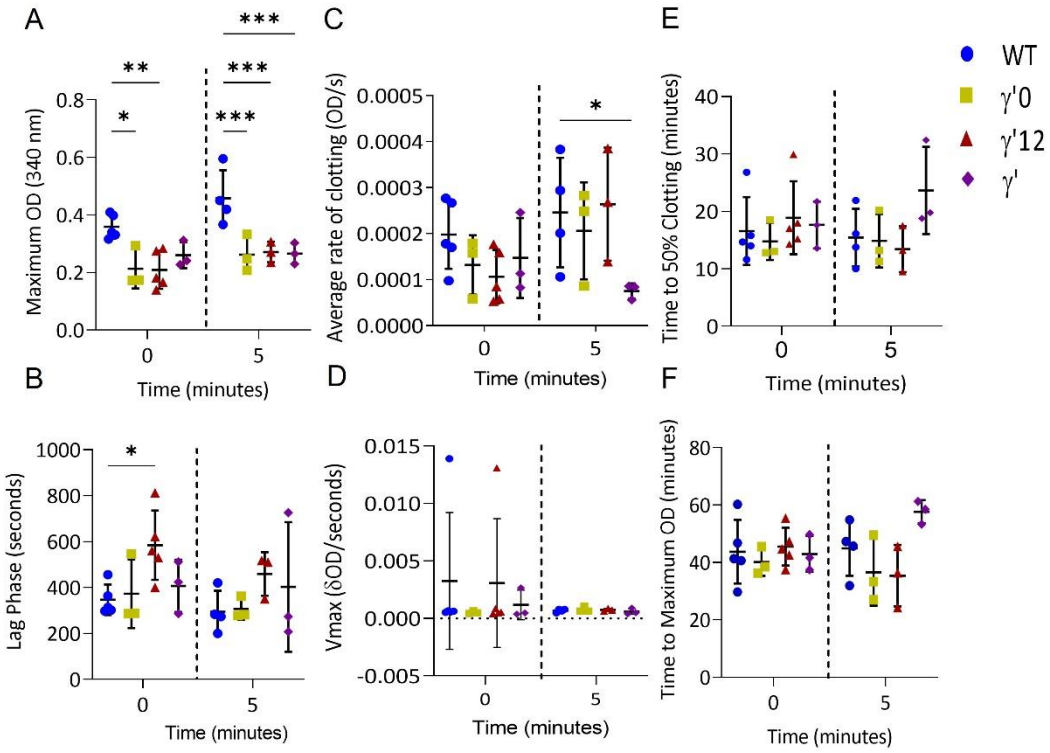

Figure 53 Further Reduction in Maximum OD with Increased Duration in Plasma Observed for γ'-chain Variants

Maximum OD (optical density) for WT and γ'-chain variants (A). Lag Phase for WT and γ'-chain variants (B). Average rate of clotting WT and γ'-chain variants (C). Vmax (D), time to 50 % clotting (E) and time to maximum OD (F) for WT and γ'-chain variants. The various fibrinogen proteins were either incubated after 5 minutes incubation in fibrinogen deficient plasma or had no incubation before clotting was initiated with 0.1 U/mL thrombin and 10 mM $CaCl_2$. Results shown as mean ± standard deviation, *n*=3, **p*=0.05, ***p*=0.01, ****p*=0.001 by two-way ANOVA with Dunnett's multiple comparison test relative to the WT.

Altered Structure Observed in Plasma Supplemented with γ'-chain Residues Following the observation in the turbidimetric assays with the γ'-chain showing reduced maximum OD when the fibrinogen variants were combined with either commercially sourced fibrinogen depleted plasma or plasma from patients, to further explore these observations, laser-scanning confocal microscopy was performed. Clots were prepared in TBS or fibrinogen-depleted plasma and clotting was initiated via thrombin.

No difference was observed in fibrin fibre count for the γ'-chain variants compared to WT in fibrinogen depleted plasma or compared to the corresponding variant in TBS (Figure 54A and B). Alike the observation in chapter 6 in LSCM, clots formed with increasing length of residues of the γ'-chain the fibres became more curved.

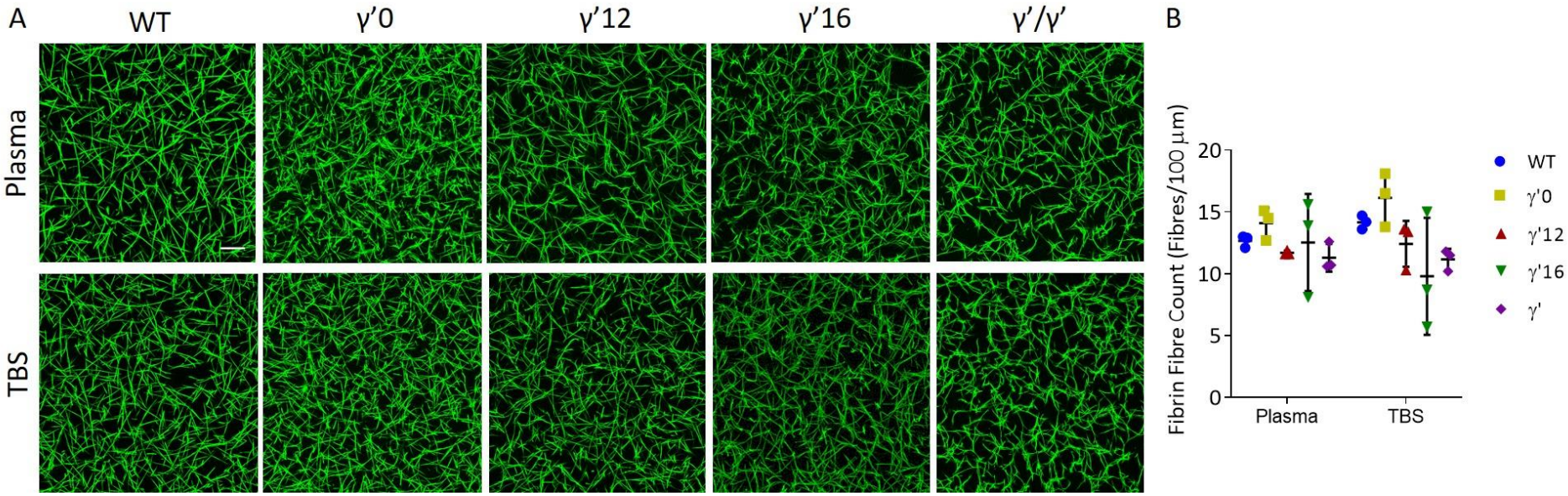

Figure 54 Altered Structure Observed for Clots Containing γ'-chain Residues

Representative z stack image clots composed of WT or γ'-chain fibrinogen variants reconstituted into fibrinogen deficient plasma or TBS (A). Clots were visualised with 5 % Alexa-488® labelled corresponding fibrinogen. Fibrin fibre count of clots composed of WT or γ'-chain variants formed in plasma deficient fibrinogen or TBS (B). Images taken on a LSM880 inverted laser scanning confocal microscope, using the x40 objective, z-stack is over 20.30 µm and composed of 29 slices; scale bar is 20 µm, *n*=3.

7.2.2 Whole Blood

7.2.2.1 γ'-chain Variants Did not Impair Clot Contraction

To determine if any loss of a portion of residues of the γ'-chain impacted the formation of clots in whole blood and their ability to contract, a clot contraction assay was developed using whole blood from *FGA*$^{-/-}$ combined with either γ'-chain variants or WT fibrinogen. Clotting was initiated by the addition of tissue factor and $CaCl_2$. A sample of the whole blood and fibrinogen mixture was collected before clot initiation (pre-activated sample) and the unclotted supernatant (post-activated supernatant) at the final time point for determination of RBC and platelet incorporation within the contracted clot. To determine if any background clotting was occurring. Two control tubes containing *FGA*$^{-/-}$ were used, without the addition of fibrinogen. One of the tubes was to confirm if any clotting was due to the siliconized coating of the tube and the other to confirm if the contraction was due to the addition of fibrinogen, as in this tube the activation mix was included.

Figure 55A shows clot formation and contraction of clots over 2 hours. All γ'-chain variants were able to form clots in whole blood and the formed clots did contract. There was no difference in contracted clot weight comparing WT (28.7±5.8 mg) and γ'-chain variants (γ'0 22.7±1.5 mg, γ'12 22.7±7.1 mg, γ'16 38.3±13.6 mg and γ'/γ' 32.3±4.7 mg). No difference was observed in whole blood clot contraction comparing WT and γ'-chain variants (Figure 55C). RBC incorporation into the contracted clot was similar comparing WT (77.9±7.8 %) and γ'-chain variants (γ'0 74.8±14.0 %, γ'12 66.6±13.7 %, γ'16 85.8±9.4 % and γ'/γ' 84.7±8.5 %). The two control tubes lacking fibrinogen showed limited RBC incorporation as expected.

Platelet incorporation in the contracted clot was measured by flow cytometry. The platelet count was used to compare the platelet numbers before sample activation and the collected supernatant at 2 hours. Flow cytometry was performed by Dr Matthew Hindle, platelets were stained with anti-CD41 (binds α_{IIB}, part of the integrin $_{\alpha IIB\beta 3}$ complex), which was used to gate the platelets.

Figure 56A shows representative forward and side scatter plots of pre-activated sample and post-activated supernatant. The scatter plots for all fibrinogen variants showed a considerable reduction in the number of platelets from the post-activation supernatant of the contracted clot compared to the pre-activated sample.

The scatter profile of the supernatant of the two controls showed increased platelets in the post-activation supernatant. The activated control showed a shift in the scatter profile, indicating the activation of platelets and the change in morphology of post-activation

supernatant. This shift in the scatter was not observed in the supernatant of the non-activated control.

The platelet counts for the supernatant confirmed that most of the platelets were contained within the contracted clot (Figure 56).

The activated control also showed a reduction in platelet count in the post-activation supernatant 224.0±38.0 platelets/µL compared to pre-activated sample (532.4±131.6 platelets/µL). The reduction in platelet count for activated control is due to a loss of platelets through normal activation, and therefore the formation of platelet aggregates. Furthermore, platelet aggregates were not counted as the flow cytometer was gated for single platelets and as noted above the profile of activated platelets causes an increase in SSC/FITC profile. There was a similar platelet count for the non-activated control between the pre-activated sample (517.3±146.3 platelets/µL) and post-activation supernatant (557.5±114.7 platelets/µL), endorsing the concept that the loss of platelets observed in the activated control is due to the formation of platelet aggregates and therefore not counted by the flow cytometer.

Clot contraction was not impacted by varying lengths of the γ'-chain, and the platelet and RBC incorporation was not influenced either.

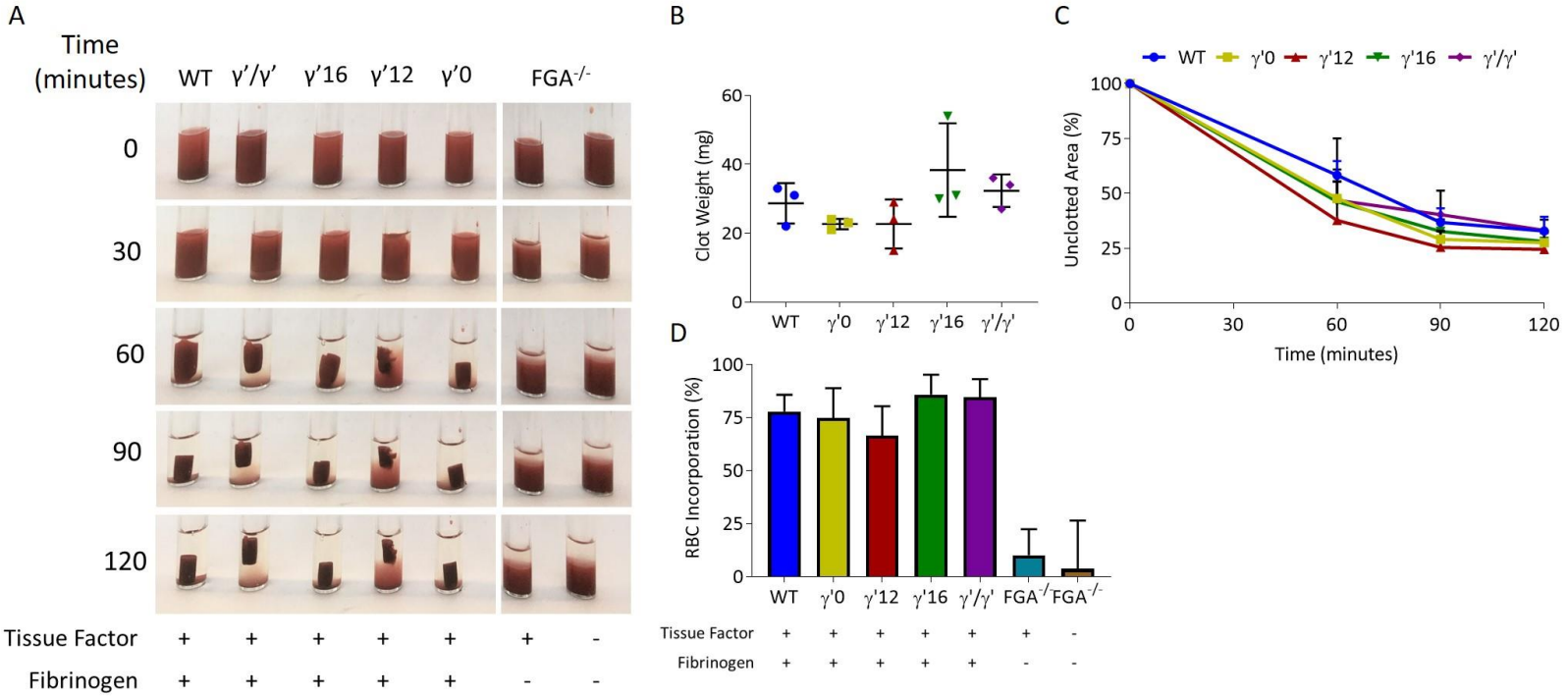

Figure 55 γ'-chain Variants Did Not Impair Whole Blood Clot Contraction

Representative images of tissue factor initiated whole blood clot formation and contraction over time in *FGA*$^{-/-}$ blood supplemented with WT and γ'-chain variants (A). Clot weight of the contracted clot (B). Percentage of unclotted area over time for WT and γ'-chain variants (C). RBC incorporation in contracted clot (D). *n*=3

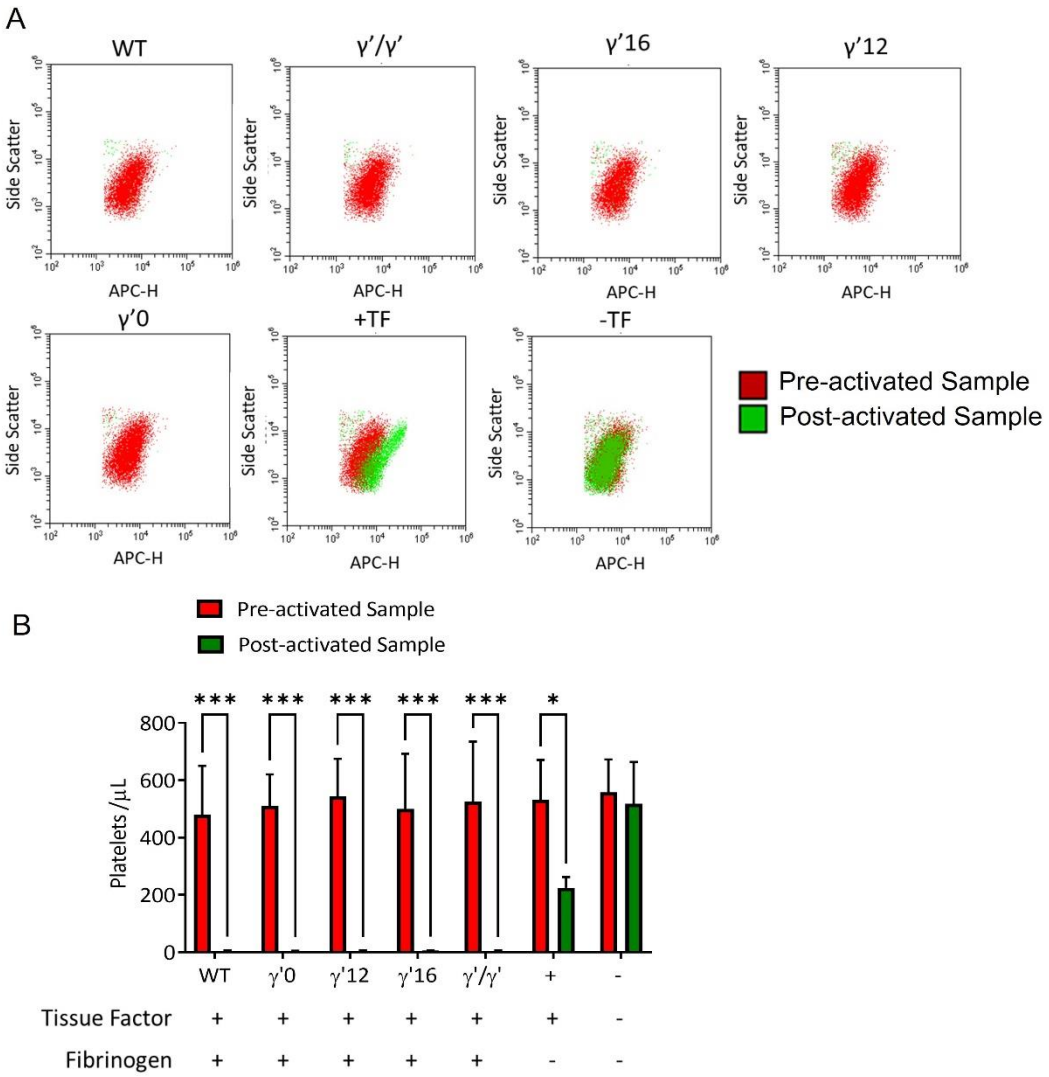

Figure 56 Majority of Platelets were Contained in Contracted Clots

Representative forward and side scatter plots for WT, γ'-chain variants and controls (A). APC-H is fluorescence measured from antibody CD41-APC700, H denotes the peak of fluorescence pulse, following excitation at 488 nm. Platelets were gated by CD41-APC700 (clone MWReg30). Platelet count in non-activated and activated samples from WT, γ'-chain variants and controls (B). Results shown as mean ±standard deviation, n=3, *p=0.05 and *** p=0.001 by two-way ANOVA with Šídák's multiple comparisons test (B).

7.2.2.2 Reduced Maximum Clot Firmness Observed for γ'-chain Containing Variants

ROTEM analysis was used to investigate whole blood clot formation of the γ'-chain variants. The initial investigations were performed using EXTEM, where clotting is started through the extrinsic pathway using TF. The assay is influenced by fibrinogen, platelets and the extrinsic coagulation factors.

Figure 57A shows similar clot firmness curves for the γ'-chain variants and WT. The clotting time was extended for γ'16 (113.3±27.1 seconds) and γ'/γ' (153.0±12.8 seconds) compared to WT (71.0±10.4 seconds) *p*=0.0239 and *p*=0.0003 respectively. No difference was observed between for γ'0 (106.3±12.4 seconds) and γ'12 (75.0±6.6 seconds) compared to WT (Figure 57B). No difference was observed in maximum clot firmness between the truncations (γ'0 (42.0±3.4 mm), γ'12 (47.0±6.6 mm) and γ'16 (40.0±6.0 mm)) and γ'/γ' (39.0±1.7 mm) to WT (42.7±1.2 mm) (Figure 57C).

Surprisingly, the results in EXTEM showed no difference in maximum clot firmness between the γ'-chain variants. As the EXTEM result is influenced by platelets and extrinsic coagulation factors in addition to the fibrinogen itself. To explore this further FIBTEM analysis was performed, the assay includes cytochalasin D therefore platelet function is inhibited allowing the study of fibrinogen on clot formation without the contribution of the platelets.

Figure 57D shows similar clot firmness curves from FIBTEM analysis, in contrast to EXTEM, all γ'-chain variants had reduced clot firmness compared to WT and there was further decrease in clot firmness with the inclusion of additional residues of the γ'-chain. No difference was observed in clotting time between truncations (γ'0 (39.3±8.1 seconds), γ'12 (40.8±4.9 seconds) and γ'16 (39.8±6.2 seconds) and γ'/γ' (63.0±10.8 seconds) to WT (40.0±9.5 seconds) (Figure 57E). The maximum clot firmness was reduced for all the fibrinogen variants compared to EXTEM analysis highlighting the contribution of platelets to whole blood clot mechanics. In contrast to the EXTEM maximum clot firmness, there was further reduction in maximum clot firmness for γ'-chain variants reaching significance for γ'16 (9.0±1.8 mm) and γ'/ γ' (4.7±2.3 mm) compared to WT (14.0±1.7 mm) *p*=0.0439 and *p*=0.0009 respectively (Figure 57F).

Reflecting maximum clot firmness, a reduced shear elastic modulus strength was observed with increasing inclusion of residues in the γ'-chain. There was significant reduction shear elastic modulus for γ'16 (504.0±96.8 G) and γ'/ γ' (253.3±117.1 G) compared to WT (832.0±133.5mm) *p*=0.0416 and *p*=0.0014 respectively (Figure 57G).

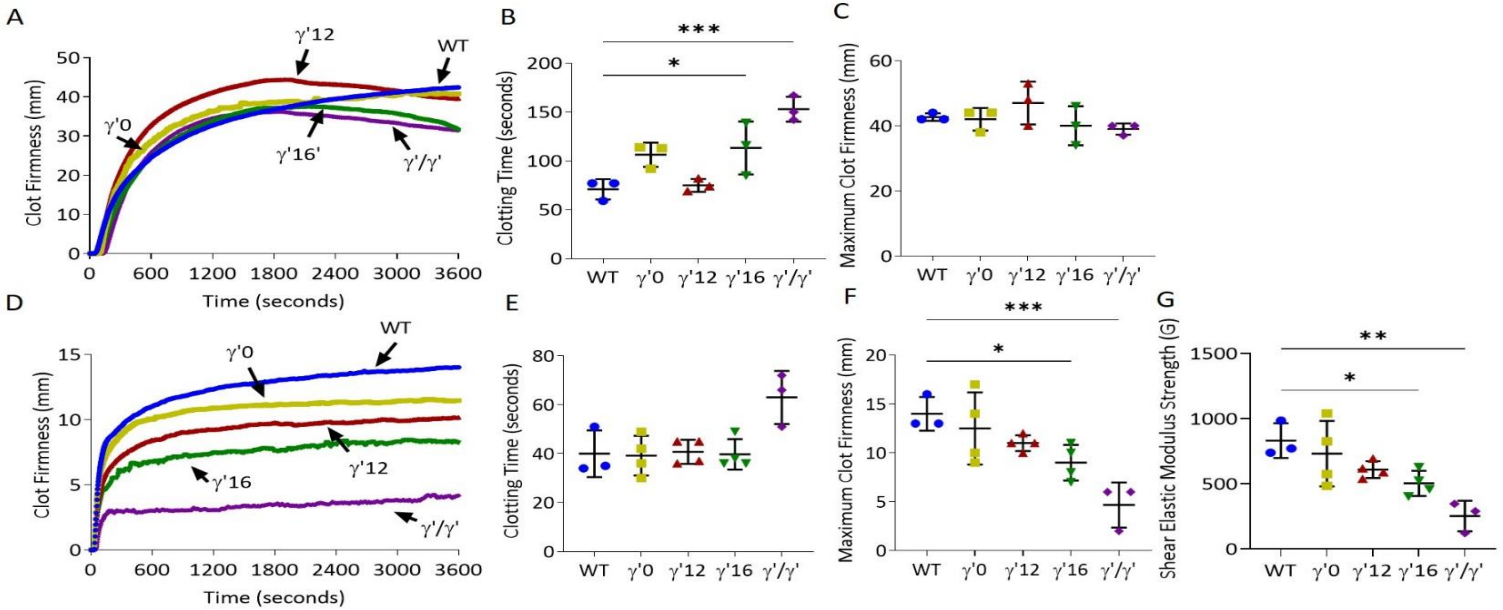

Figure 57 Reduced Maximum Clot Firmness Observed for γ'-chain Containing Variants

Clot firmness curves for EXTEM whole blood from *FGA*$^{-/-}$ mice supplemented with either WT or γ'-chain variants (A). EXTEM clotting time for WT and γ'-chain variants (B). EXTEM maximum clot firmness for WT and γ'-chain variants (C). Clot firmness curves for FIBTEM for WT or γ'-chain variants (D). FIBTEM clotting time for WT and γ'-chain variants (E). FIBTEM maximum clot firmness for WT and γ'-chain variants (F). FIBTEM shear elastic modulus strength (G) for WT and γ'-chain variants. Results shown as mean ±standard deviation, *n*=3 EXTEM and FIBTEM WT and γ'/γ', *n*=4 FIBTEM γ'0, γ'12 and γ'16, **p*=0.05, ***p*=0.01, and ****p*=0.001 by one-way ANOVA with Dunnett's multiple comparison relative to the WT. Error bars not shown on A and D.

7.2.2.2.1 Heterogeneous Clot Architecture Observed in Whole Blood Clots

Figure 58 and Figure 59 show representative images for the clots collected and prepared for scanning electron microscopy following EXTEM and FIBTEM experiments respectively. Whole blood clots images following EXTEM and FIBTEM showed various RBC morphology for WT and γ'-chain variants. The compressed shapes of RBC (polyhedrocytes and polyhedrocyte-intermediates) were seen for WT and γ'-chain variants in EXTEM and FIBTEM suggesting the clots had undergone clot contraction during ROTEM analysis (Weisel and Litvinov, 2019). Compared to EXTEM, in FIBTEM no polyhedrocytes were observed in the clots. Furthermore, fibrin fibres were seen compressing RBC in the whole blood clots for γ'/γ' (Figure 59). In addition, limited platelets were observed in whole blood clots for WT and all γ'-chain variants in either EXTEM or FIBTEM experiments, potentially due to the platelets being localised to the centre of the clot.

There were various fibrin structures observed within the whole blood clots from EXTEM and FIBTEM, bundles and individual fibres, mesh networks of thin fibres, as well as fibrin film and intermediate film. These structures have previously been described in thrombi collected from patients following mechanical thrombectomies (Chernysh et al., 2020a; Khismatullin et al., 2020). Altogether, whole blood clots formed following EXTEM and FIBTEM were heterogeneous in WT and γ'-chain variants, which mirrors observations from scanning electron microscopy studies of thrombi collected in patients.

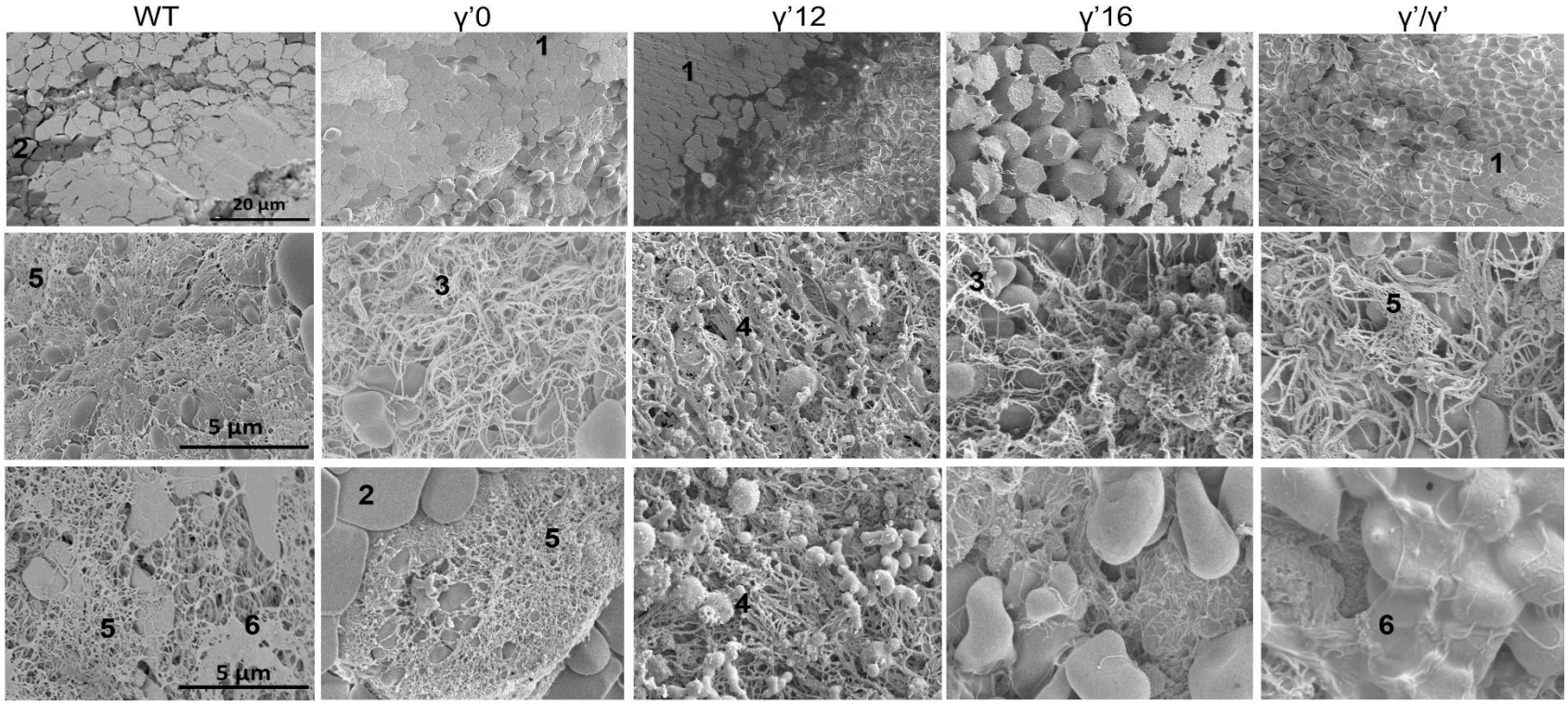

Figure 58 Various Morphologies Observed in Whole Blood Clots

Representative scanning electron microscopy images at x2,000 (top) and x10,000 (middle and bottom) of whole blood clots made with WT and γ'-chain variants. Clots were collected and fixed after ROTEM EXTEM analysis. All clots were heterogeneous in fibrin composition and RBC structure. Areas labelled as "1" are polyhedrocytes and "2" polyhedrocyte-intermediates, "3" are individual fibres, bundles are "4" and mesh networks of thin fibres are shown as "5" and fibrin film as "6". Images taken on a Hitachi SU8230 Ultra-High-Resolution Scanning Electron Microscope. Three clots were imaged for all fibrinogen variants.

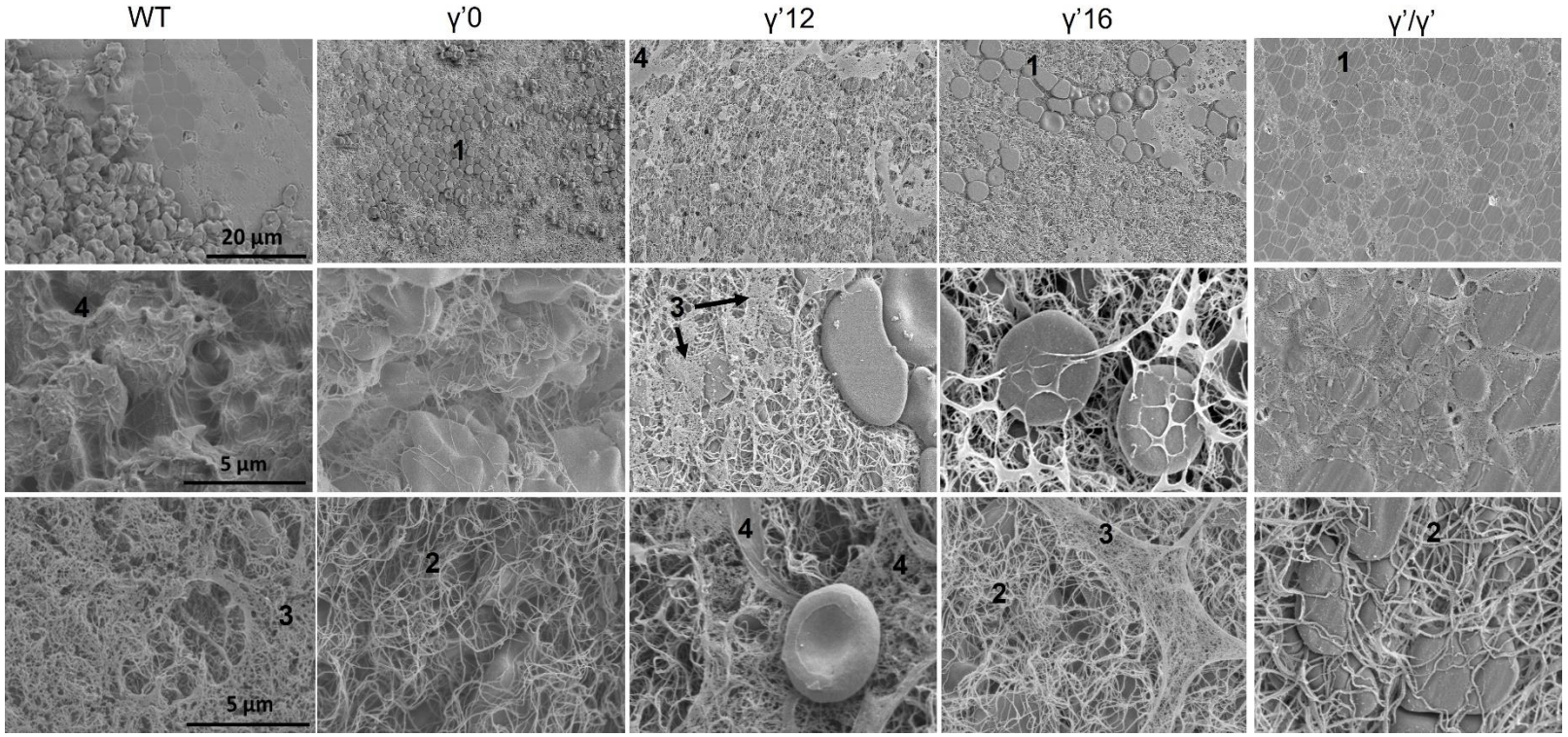

Figure 59 Inhibition of Platelets Prevented Formation of Polyhedrocytes

Representative scanning electron microscopy images at x2,000 (top) and x10,000 (middle and bottom) of whole blood clots made with WT and γ'-chain variants. Clots were collected and fixed after ROTEM FIBTEM analysis. All clots were heterogeneous, in fibrin composition and RBC structure. Areas labelled as "1" are polyhedrocytes intermediates, "2" are individual fibres, and mesh networks of thin fibres are shown as "3" and fibrin sheet as "4". Images taken on a Hitachi SU8230 Ultra-High-Resolution Scanning Electron Microscope. Three clots were imaged for WT and γ'/γ' and four clots for γ'0, γ'12 and γ'16.

7.2.2.3 γ'/γ' Showed Early Sensitivity to Fibrinolysis

The γ'-chain variants were investigated for their susceptibility to fibrinolysis in whole blood clots via ROTEM EXTEM with the addition of t-PA at the point of initiation. There were similar clot firmness profiles for γ'0 and γ'12 to WT, whereas γ'/γ' had an earlier reduction in clot firmness (Figure 60A). There was no difference in clotting time between the variants (γ'0 (59.5±20.9 seconds), γ'12 (72.3±26.1 seconds) and γ'/γ' (63.0±35.9 seconds)) to WT (54.5±17.8 seconds) (Figure 60B). Alike the standard EXTEM assay, no difference was observed in maximum clot firmness comparing the variants (γ'0 (45.3±7.9 mm), γ'12 (46.7±7.3 mm) and γ'/γ' (42.0±6.7 mm)) to WT (40.0±5.9 mm) (Figure 60C). Mirroring maximum clot firmness, no difference was observed between shear elastic modulus strength amongst the truncations (γ'0 (3627.0±1745.0 mm), γ'12 (4472.0±1392.0 G), and γ'/γ' (3665.0±934.7 G)) compared to WT (3049.0±336.4 G) (Figure 60D). As observed in the clot firmness curve there was a difference between γ'/γ' (936.8±140.3 seconds) and WT (1804.0±325.8 seconds p=0.0004) in lysis onset time (Figure 60E). No difference was observed between γ'0 (1675.0±145.6 seconds p=0.7370) and γ'12 (1577.0±164.6 seconds p=0.4058)) compared to WT. No difference was seen in lysis time for γ'/γ' (1931.0±642.0 seconds), γ'0 (2757.0±892.2 seconds) and γ'12 (3146.0±151.8 seconds) compared to WT (2356.0±423.2 seconds).

The measurement of both lysis measurements is linked to the maximum clot firmness and both measurements begin from clotting time. Lysis on set time is the decrease of maximum clot firmness amplitude by 15 % whereas lysis time is a decrease to 10 % of the maximum clot firmness. The results indicate that although there is a faster initial loss of maximum clot firmness observed in γ'/γ', however the decrease to 10 % of the maximum clot firmness was like WT.

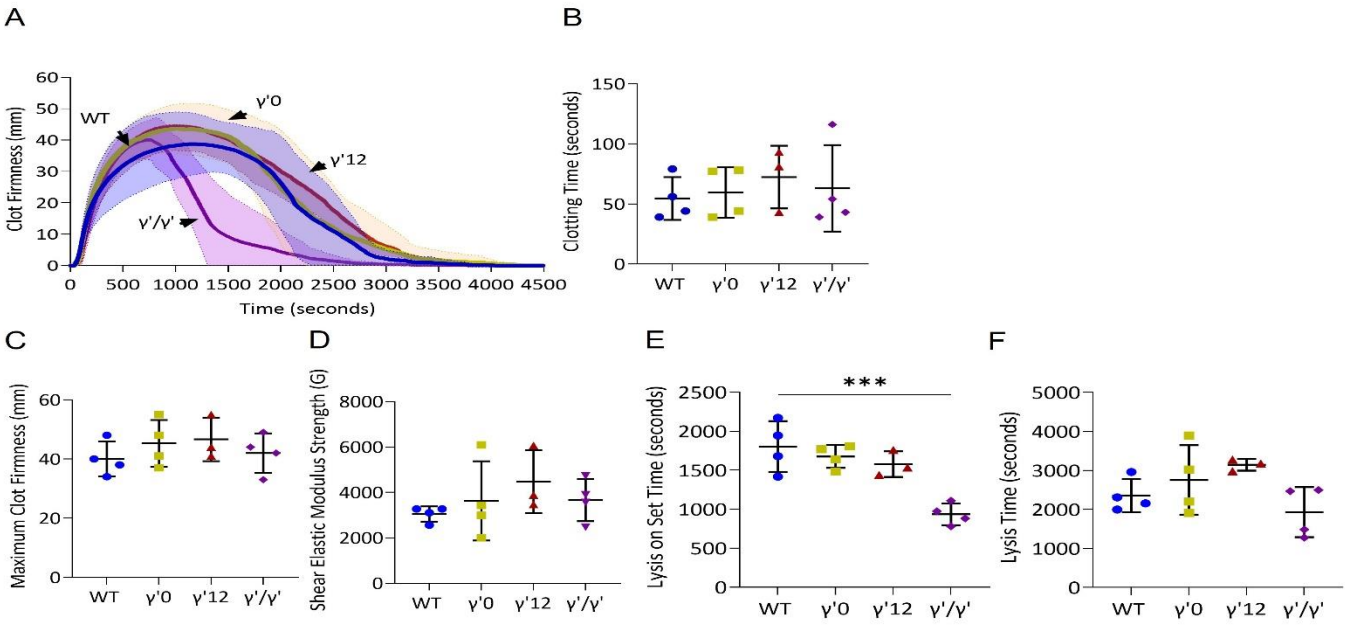

Figure 60 γ'/γ' Exhibited Earlier Sensitivity to Fibrinolysis

Clot firmness curves for EXTEM supplemented with 5 nM t-PA whole blood from *FGA*$^{-/-}$ mice supplemented with either WT, γ'0, γ'12 or γ'/γ' (A). Clotting time for WT, γ'0, γ'12 and γ'/γ' (B). Maximum clot firmness (C) and shear elastic modulus strength (D) for WT, γ'0, γ'12 or γ'/γ'. Lysis on set time for WT, γ'0, γ'12 or γ'/γ' (E). Lysis time for WT, γ'0, γ'12 or γ'/γ'. (F). Results shown as mean ±standard deviation, *n*=3 γ'12 and *n*=4 WT, γ'0 and γ'/γ', ***p=0.001 by one-way ANOVA with Dunnett's multiple comparison test relative to the WT.

7.3 Discussion

The focus of this chapter was to understand the role of the truncated γ'-chain variants in plasma and whole blood *ex vivo* assays and to elucidate how the γ'-chain can influence clot function. The incubation of γ'-chain variants in plasma from fibrinogen depleted plasma and from patients with afibrinogenemia showed reduced maximum OD compared to WT. The truncations to the γ'-chain did not prevent or alter whole blood clot contraction and could incorporate RBC and platelets alike the WT. Whole blood formation assay showed increased clotting time with the inclusion of more γ'-chain residues, although no difference in maximum clot firmness was observed in ROTEM EXTEM. However, when the effect of platelets was omitted, reduced clot firmness was observed for γ'16 and γ'/γ' indicating a potential compensatory effect from platelets.

Following the introduction of γ'-chain variants to fibrinogen deficient plasma, a reduction in maximum OD was observed, mirroring observation of studies with plasma and purified γA/γ' (Allan et al., 2012; Walton et al., 2014; Macrae et al., 2021). This reduction in maximum OD was observed in plasma from patients with afibrinogenemia as well as commercially fibrinogen depleted plasma. The reduction in OD was also observed with no and 5-minute incubation of the recombinant fibrinogen in fibrinogen deficient plasma and observed when either thrombin or tissue factor (γ'12 and γ'16) was used to initiate clotting. There was no difference in observed in fibre count when fibrin was formed in fibrinogen plasma. The maximum OD in the turbidimetric assay is directly related to the average cross-sectional area of fibre (Carr and Hermans, 1978). Investigations using scanning electron microscopy may uncover if there is a range of fibre thickness observed in the γ'-chain variants compared to WT and therefore confirming the results observed in the turbidimetric studies. However, this is more challenging in whole blood clots compared to purified clots as individual fibres can be less distinguishable between the blood cells and the clot structure is not uniform.

In plasma studies, the average rate of clotting was not changed for the γ'-chain variants compared to WT which differs from the purified studies in Chapter 6, however this mirrors the observation of the patient plasma and purified fibrinogen (Macrae et al., 2021).

The altered fibrin structure was still visible in the LSCM for γ'16 and γ'/γ' when repleted in fibrinogen deficient plasma. Interestingly, LSCM studies with purified fibrinogen with either 3, 10 or 40 % γ'-chain, exhibited the same fibre structure, however plasma from patients at the same percentage of γ'-chain did not show this phenotype (Macrae et al., 2021). This observation is unlikely an effect of purification as several methods has been used in the

literature and altered fibrin structure has been observed (Allan et al., 2012; Guedeset al., 2018b; Macrae et al., 2021).

The γ'-chain or γ'-chain truncations did not impede clot contraction or impact the incorporation of RBC or platelets. This agrees with previous studies that the γ'-chain or absence of QAGDV on γA-chain does not prevent clot contraction (Rooney et al., 1996; Holmbäck et al., 1996). In addition, it has been shown that the interaction with $\alpha_{IIB}\beta_3$ alters between fibrinogen and fibrin (Litvinov et al., 2016). This agrees with the investigations in Chapter 5 using flow cytometry showing limited binding of fibrinogen in the absence of the AGDV to activated platelets while post-activated supernatant from clot contraction assays demonstrated platelets within the contracted clot. The truncations within the γ'-chain did not hinder clot contraction indicating that the binding site in the γ'-chains are not crucial for clot contraction and that residues of the C-terminal γA-chain may have a larger role. It has been reported that there are multiple binding sites within the α_{IIB} that can interact with fibrin and the inhibition of $_{\alpha IIB\beta3}$ by abciximab can affect clot contraction. (Podolnikova et al., 2014; Kim et al., 2017).

Analysis of the γ'-chain variants by whole blood ROTEM (FIBTEM) analysis showed reduced maximum clot firmness and shear elastic modulus strength with increased number of residues of the γ'-chain. Previous investigations into purified γA/γA and γA/γ' by ROTEM analysis, where thrombin was used to trigger clot and the purified fibrinogen proteins were mixed into fibrinogen deficient plasma (Domingues et al., 2016), showed reduced maximum clot firmness at 0.1 U/mL thrombin for γA/γ' compared to γA/γA. As there were no platelets included, it agrees with the result of the FIBTEM assay, where platelet function is inhibited. However, investigations into thromboelastometry using TEG where purified fibrinogen γA/γA and γA/γ' were used, and clotting was initiated with a range of thrombin concentrations (1, 2 or 20 U/mL), γA/γ' had a higher maximum amplitude at 1 and 2 U/mL of thrombin (Siebenlist et al., 2005). In the ROTEM experiments performed on the γ'-chain variants, clotting was initiated by tissue factor and it has shown that clot formation occurs at thrombin concentrations below 0.2 U/mL with 0.135 U/mL and 0.177 U/mL required for FpA and FpB cleavage respectively (Brummel et al., 2002). Interestingly, EXTEM analysis showed no difference in maximum clot firmness between the WT and the γ'-chain variants. It has previously been reported that platelets can "sense their environment" (Lam et al., 2011; Qiu et al., 2014) and thus potentially compensate for weaker fibrinogen.

Investigations into whole blood fibrinolysis showed a faster lysis on set time for γ'/γ' compared to WT, however no difference was observed in lysis time. Investigations with human dermal microvascular endothelial cells (HMEC-1) showed that high concentrations

of γA/γ' (30 %) influences the secretion of uPA and PAI-1, with higher secretion of these proteins in the supernatant of HMEC-1 (Cantero et al., 2019). With platelet activation, α-granules can release plasminogen, α_2-antiplasmin, TAFI and PAI-1 (Flaumenhaft, 2013; Whyte et al., 2017). Whether a similar observation can occur in platelets with fibrinogen or fibrin containing the γ'-chain, where they are able influence the secretion of α-granules by modulating thrombin activity.

Previous investigations using TEG with purified fibrinogen γA/γA and γA/γ' showed that γA/γ' clots were more resistant to lysis, however, interestingly the percentage lysis at 30 minutes remained similar at all the range of thrombin concentrations (1, 2 and 20 U/mL) for either γA/γA and γA/γ' (Siebenlist et al., 2005). Another study using TEG with whole blood samples from patients found no association between percentage lysis at 30 minutes and fibrinogen γ' level (Farrell et al., 2020). Following the initial quicker lysis onset observed in γ'/γ', no difference was observed lysis time between WT and the γ'-chain variants. The measurements for the ROTEM are all based on mechanically properties of the clot, the γ'/γ' showed an initial loss in amplitude compared to maximum clot firmness faster than WT. Where the duration of the γ'/γ' to reach 10 % of maximum clot firmness was not different than the WT. If the γ'-chain can influence the structure following initial susceptibility to fibrinolysis resulting in structurally rearrangements and influencing mechanically properties causing fibrinolytic resistance requires further investigation. Additionally, there may be interplay between γ'-chain between RBC and/or platelets providing fibrinolytic susceptibility and resistance.

Clots formed and imaged following ROTEM analysis exhibited qualities observed in thrombi collected in patients from arterial and venous thrombosis (Silvain et al., 2011; Di Meglio et al., 2019; Zabczyk et al., 2019; Chernysh et al., 2020a). There were various fibrin morphologies (bundles and individual fibres, mesh networks of thin fibres and fibrin sheet and intermediate sheet) observed in clots collected following EXTEM and FIBTEM analysis. Clots formed by the γ'-chain variants and WT were heterogeneous, which agrees with previous studies of thrombi (Chernysh et al., 2020a). The presence of polyhedrocytes in the clots has been reported to be a sign of clot contraction (Tutwiler et al., 2018; Khismatullin et al., 2020). This shows that the during ROTEM analysis, the process of clot contract can occur, which is most prominent in the first hour. Although there were polyhedrocyte-intermediates observed following EXTEM and FIBTEM analysis, polyhedrocytes were only observed in EXTEM clots, given inhibition of platelet function with FIBTEM assays.

Whole blood and plasma studies have shown that fibrinogen γ'-chain variants can influence maximum OD in plasma and causes curvature of fibre network with increased number

residues found in the γ'-chain. Fibrinogen γ'-chain or partial absence of the γ'-chain did not inhibit whole blood clot contraction or prevent incorporation of RBC or platelets within the contracted clot. Whole blood formation studies observed reduced maximum clot firmness with inclusion of residues of the γ'-chain when the influence of platelets was absent. Fibrinogen γ'/γ' exhibited faster lysis on set but had no difference in complete lysis.

7.3.1 Key findings

- Partial absence of the γ'-chain did not inhibit whole blood clot contraction
- Whole blood clot formation showed reduced maximum clot firmness with increased number of residues of the γ'-chain presence.
- Platelets may compensate for weaker fibrin network.
- Whole blood clot architecture observed following ROTEM analysis is complex with polyhedrocytes, fibrin fibre and fibrin film.

Chapter 8 Limitations and Future Work

8.1 Study Limitations; Protein Expression Challenges

A major challenge faced for the investigations into the αC-region of fibrinogen was the low yield of expression of fibrinogens with αC-region truncations. There are some improvements that could be made to increase the likelihood of selecting high expressing clones. Flow cytometry could be used to uncover the location of where the cells are within the cell cycle, as having most of the cells within S-phase results in higher transfectability. Alternative methods of transfection (FuGENE® or Lipofectamine®) and transfecting different ratios of the fibrinogen chains also might optimise expression levels. The current pMLP plasmid does not carry a selection maker, subsequently the selection process is not directed to cells that have acquired the pMLP plasmid, which could lead to growth of non-transfected cells. Having the selection marker on the plasmid alongside the fibrinogen sequence would permit direct selection. During production, CHO cells could be grown at reduced temperature therefore maintaining the cells within the G1 phase of the cycle and as a result the cells would be more likely to produce more fibrinogen. However, the recent murine *FGA*$^{270/270}$ model also showed reduced circulating fibrinogen indicating that it would be unlikely to achieve a similar level of expression of Aα-chain truncations as observed for WT (Hur et al., 2021).

As a result of the low expression yield, it was not possible to investigate the produced fibrinogen variants using *in vivo* models in *FGA*$^{-/-}$ mice. To overcome this, several *ex-vivo* whole blood assays using blood from *FGA*$^{-/-}$ mice supplemented with the recombinant fibrinogen variants (clot contraction and ROTEM) were performed. Further investigations with flow models could be used to study the variants under various shear rates. Additionally, if a murine model of either α390 or α220 was established it would have reduced circulating fibrinogen therefore making it difficult to establish the *in vivo* effects of truncated fibrinogen vs reduced yield, like the observation in *FGA*$^{270/270}$ mice where the authors needed to knock-down the concentration of WT fibrinogen in mice using siRNA technology to compare (Hur et al., 2021). Also, it is unlikely that a murine model of α220 would secrete detectable fibrinogen as the patient cases which truncations either side of α220 have afibrinogenemia (Aα219 and Egyptian Aα221). The first reported case of an αC-region mutant not resulting in afibrinogenemia is fibrinogen Otago which is the same as the murine model *FGA*$^{270/270}$ (Ridgway et al., 1997; Vlietman et al., 2002; Abdel Wahab et al., 2010).

The production of homodimers was essential for α-chain investigations as previous studies in patients with dysfibrinogenemia of the αC-region or fragment X have made interpreting the results more challenging due to their heterodimer character.

In the case of investigations of the γ'-chain, there is limited γ'/γ' observed in circulation compared to γA/γ'. Previously, recombinant γA/γ' was generated using a transfection ratio of 1:2 γ' to γA and had an additional purification step to separate γA/γA and γ'/γ' from γA/γ' (Gersh et al., 2009b). It is therefore possible to produce the γ'-chain truncations this way to produce heterodimers. The γ'-chain variants could be produced to make variant heterodimers and then a range of percentages of the γ'-chain to γA-chain could be used explore the γ'-chain variants over ratios found in circulation. In contrast to the α-chain truncations the γ'-chain variants were expressed at higher levels as expected, as it is a physiological variant. Additionally, within the circulation the range of γ'-chain can be between 3-40 % (Macrae et al., 2021).

8.2 αC-region Future Studies

The removal of the entire αC-region resulted in clots that underwent rapid fibrinolysis compared to WT and α390 (which only lacks the αC-domain). Further investigations are required to uncover if this increased fibrinolysis is driven either by structural changes, enabling easier movement of the plasmin and t-PA through the fibre network, or due to the cryptic binding sites for t-PA and plasminogen already exposed in α220. Investigations into plasmin and t-PA binding to fibrinogen/fibrin have previously used monoclonal antibodies, synthetic peptides and surface plasmon resonance (Schielen et al., 1989; Dunn et al., 2006; Mutch et al., 2010b). To investigate plasmin, plasminogen, and t-PA binding in the αC-region truncations, ELISA or surface plasmon resonance could be employed. Furthermore, a plasmin generation assay could be performed on the truncations to see if plasmin is generated faster in the truncations compared to WT, therefore impacting the sensitivity to fibrinolysis (Dunn et al., 2006; Mutch et al., 2010b). Previously, trypsin digests have been used to assess the sensitivity of fragment X to fibrinolysis (Schaefer et al., 2006). Trypsin cleaves proteins indiscriminately rather than recognising specific consensus peptide sequences meaning that the speed of clot lysis is dependent on overall clot structure rather than plasminogen binding and subsequent activation rate. This method could be used to investigation the structural susceptibility of the αC-region truncations to fibrinolysis.

The experiment investigating the effects of α_2-antiplasmin on fibrinolysis showed an extension in time to 50 % fibrinolysis for α390 compared to WT with FXIII and α_2-antiplasmin. This could potentially be explained by denser clot structure formed by α390 fibrinogen in purified experiments and that the assay was done under static conditions. To explore these

observations further and to determine if the static conditions or clot structure is inhibiting the movement of fibrinolytic enzymes and therefore providing fibrinolytic resistance in the fibrinolysis assay. Permeation could be utilised to investigate fibrinolysis during flow of fibrinolytic enzymes through the clot, thus leading to an increase in clot porosity that can be calculated. In addition, the flow-through could be collected and assessed for an increase in D-dimer concentration. Furthermore, there are established flow models which could be used to study fibrinolysis such as the Maastricht flow chamber or other microfluidic devices (Neeves et al., 2010; De Witt et al., 2014; Li and Diamond, 2014; Whyte et al., 2015; Provenzale et al., 2019)

The ROTEM experiments highlighted that there is some fibrinolysis occurring in α390 which was not observed in the WT, indicating that α390 is more sensitive to fibrinolysis than WT in whole blood. Additionally, fibrinolysis susceptibility in whole blood for α390 was not as drastic as was observed for α220. The ROTEM experiment did not included any further initiators of fibrinolysis and it would be interesting to examine the fibrinolytic susceptibility further for α390 using whole blood either by ROTEM or the Chandler Loop by the addition of t-PA or comparing glu- and lys-plasminogen.

Platelet:fibrinogen interactions were not showed to be altered in this thesis with the loss of the αC-domain even though there is loss of the RGD sites, although there was less binding per platelet observed when then entire αC-region was absent (Farrell et al., 1992). It has been suggested that the integrin $_{\alpha IIB\beta 3}$ has a higher affinity conformation and displays differential binding between fibrinogen and fibrin (Litvinov et al., 2016). It would be worthwhile to investigate platelet:fibrin and platelet:fibrinogen relationships with the αC-region truncations, to discover if there is structural alterations in binding on the conversion to fibrin with loss of the αC-domain RGD site as well as the reported GPVI binding site within the αC-region (Xu et al., 2021).

Previously, AFM was used to study mechanics of single platelets and contractile forces applied to fibrinogen, reporting that platelets can apply stronger forces to stiffer surfaces (Lam et al., 2011). As fibrinogen has two $\alpha_{IIB}\beta_3$ binding sites on in each D-region, which are used for platelet:fibrinogen:platelet interactions during platelet aggregation (Hayward and Moffat, 2013), it would be interesting to investigate the effects of this interaction in α220 to uncover if it is able to facilitate the interaction. If so, to what degree? Or is it reduced due to destabilisation of the coiled-coil or D-region from the lost the αC-region? These investigations could be performed with α220 with the γ-chain carrying the γ’ or γ’0 sequence, with and without inhibitors to $_{\alpha IIB\beta 3}$ such as abciximab or eptifibatide.

Laser-scanning confocal microscopy experiments showed that WT fibrinogen and αC-region truncated fibrinogen can form clots. The formation of fibrin this way could occur by inclusion of partially degraded fibrin during excessive bleeding from trauma, patients who are heterozygous for a αC-region dysfibrinogenaemia or patients following t-PA thrombolysis treatment that experience bleeding. The treatment of ischaemic stroke with t-PA (Alteplase®) has a variable patient outcome and there is an increased risk of intracerebral haemorrhage (Chatterjee, 1995; Campbell et al., 2018). In a study of serum levels of fibrinogen degradation products following t-PA treatment for acute myocardial infarction of 242 patients (Arnold et al., 1989), bleeding was observed in 62 patients and of these patients bleeding was observed more often in patients with higher levels of fibrinogen degradation products. Following t-PA treatment, fragment X was observed within 30 minutes of treatment, which stayed in the circulation for at least 24 hours. This t-PA treatment saw that 30 % of fibrinogen was converted to fragment X (Owen et al., 1987). Furthermore, another study observed a reduction in fibrinogen levels following t-PA treatment which was nearly 50 % with 60 mg of t-PA infusion after 90 minutes and 30 % with 40 mg t-PA infusion (Arnold et al., 1989). A study where α_2-antiplasmin was supplemented with t-PA induced fibrinolysis was found to inhibit t-PA induced bleeding with reduced fragment X formation, therefore bleeding risk is potentially due to the incorporation of fragment X into clots as it is clotable (Weitz et al., 1993). In addition, a study with healthy individuals measuring rates of plasmin generation in plasma, concluded that the rate of plasmin generation varied over an 8-fold range, and that this range was further impacted by age, sex, and use of the contraceptive pill (Medcalf and Keragala, 2021). As the incorporation of fragment X into clots showed increased rate in plasmin formation as well as greater sensitivity to proteolysis (Schaefer et al., 2006), the two α-chain truncated fibrinogens described in this thesis can be used to explore sensitivity of hybrid fibrinogen and how clot structure can influence function *in vitro* and in whole blood.

8.3 Fibrinogen γ' Future Studies

Although plasma studies with γ'-chain variants showed a similar fibre count in LSCM, maximum OD was reduced compared to WT. However, it may be beneficial to observe if there is a reduced fibre diameter for the γ'-chain variants when clotting is performed in plasma. As fibre count was not different by LSCM analysis but reduced maximum OD was observed in turbidimetric assay therefore providing conflicting results.

The altered fibre structure could be further studied to explore if it is independent of thrombin by using reptilase as only FpA is cleaved, and then the subsequent clot structure could be studied by microscopy.

Interestingly, ROTEM showed earlier onset of fibrinolysis for γ'/γ' but no difference in lysis time from onset to complete lysis. It is currently not clear whether there is fibre rearrangement or interactions with platelets or RBCs or another blood cell providing fibrinolytic resistance. The EXTEM assay showed no difference in maximum clot firmness for the γ'-chain variants compared to WT but there was a stepwise decrease in maximum clot firmness for the γ'-chain variants compared to WT in FIBTEM, highlighting that the platelets to some extent can compensate for weaker fibrin. A study into plasminogen and the γ'-chain found that there was delayed plasminogen binding and activation but similar kinetics observed for γA/γA and γA/γ' clots with plasmin (Kim et al., 2014b). These experiments were only performed in a purified system and whether there are similar effects of plasminogen/plasmin in plasma or whole blood is not known.

As the ROTEM experiments were performed using whole blood from *FGA*$^{-/-}$ mice, it would be beneficial if fibrinolysis observations could be explored further using whole blood from either a patient with afibrinogenaemia or supplementing fibrinogen deficient plasma with γ'-chain variants with platelets and RBC. This is particularly relevant as mice do not have fibrinogen γ'-chain splice variation, although there is currently no evidence for differences in interaction between human or murine proteins with this variant. Furthermore, a study comparing activation of the murine fibrinolytic system compared to human found that murine t-PA can initiate lysis of human plasma clot, and vice versa murine plasma clots can be lysed by human t-PA. Overall, the murine fibrinolytic system is more resistant to activation than the human system (Lijnen et al., 1994). Indicating that the hybrid human and mice used within this study is unlikely to have influenced the results.

Fibrinogen can undergo numerous PTM and these can influence structure and function. The types of PTM fibrinogen can undergo are oxidation, glycosylation, glycation and acetylation along with other modifications (De Vries et al., 2019). In addition, there are increased fibrinogen levels observed with age due to a slower rate of disposal, therefore these PTM on fibrinogen are going to be present within the circulation for longer periods of time (Aizhong et al., 1998; Kotzé et al., 2014). A study showed that the ratio of fibrinogen γ' in a study of healthy individuals did not increase with age (Kotzé et al., 2014). A small study of plasma samples from healthy individuals below 60 and above 60 showed that there was increased glycosylation with age (but not advanced-glycation end products), and older individuals had reduced clotting time and a more densely packed clot structure (Gligorijević et al., 2018). Recombinant fibrinogen produced in the presence and absence of aspirin showed that there was altered clot structure and function with increasing concentrations of aspirin and a similar observation was observed in healthy volunteers following 1 week of

daily aspirin (Ajjan et al., 2009). In CVD there are likely to be increased fibrinogen levels with PTM in the circulation, whether this is due to extended duration of fibrinogen with PTM within the circulation or the influence of medication or a combination of the two is also unknown. Finally, the influence of various PTM and γ'-chain is unknown and can be identified using mass spectrometry-based techniques.

Chapter 9 General Discussion

The focus of this thesis was to explore the residues of the γ-chain splice variant γ' and the αC-region subregions (αC-domain and αC-connector) and how these regions influence clot structure and function. The investigations into these regions occurred through the production and analysis of recombinant fibrinogens. In total, five truncations were made to the γ'-chain, each one shorter than the last (γ'16, γ'12, γ'8, γ'4 and γ'0), as well as a full-length homodimer (γ'/γ'). For γ'0 in addition to lacking all γ'-chain residues, the final four residues of γA were also absent. Although γ'8 and γ'4 were cloned in CHO cells, they were not produced on a large scale as initial turbidimetric studies did not show a stepwise increase in maximum OD towards the WT with decreasing residues of γ'-chain.

9.1 αC-region

The two α-chain truncations were used to investigate the subregions of the αC-region, α390 which lacks the C-terminal αC-domain and α220 which is without the αC-connector along with the αC-domain. Both truncations to the αC-region resulted in altered clot architecture with the loss of the αC-domain producing a clot that was denser and composed of structure fibres. The removal of αC-domain and αC-connector resulted in clot structure that was porous with short, stunted fibres. In purified assays fibrinogen missing the αC-region was mechanically weak and highly susceptible to fibrinolysis. However, fibrinogen without the αC-domain did not show mechanical weakness or vulnerability to fibrinolysis. Although in whole blood investigations α390 did exhibit sensitivity to fibrinolysis and had reduced clot firmness suggesting that the denser clot structure observed within the purified experiments was providing protection. The initial studies in whole blood via clot contract for α220 failed to form a visible clot and therefore no clot contract was observed. Monitoring whole blood clot formation showed a clot forming and breaking down within the course of the assay. When inhibitors of fibrinolysis were added it revealed that the premature fibrinolysis was occurring. Additionally, the lack of the αC-domain and αC-connector resulted a critically weak clot. Both the αC-domain and αC-connector are required for fibrin stability.

There have previously been several recombinant fibrinogen proteins produced of the αC-region, only two of these αC-region truncations produced mirror patient cases (fibrinogen Egyptian (Aα221) and Zaghouan (Aα252)) and both patients had afibrinogenemia (Abdel Wahab et al., 2010; Amri et al., 2016). However, afibrinogenemic cases can be studied using mammalian expression systems, yet these truncations do secrete less protein compared to WT expression systems. Using the CHO-cell expression model, the two αC-subregion could be studied, as α220 is one residue shorter than fibrinogen Egyptian, which would likely result

in afibrinogenemia if found in a patient. Whereas α390 is potentially more likely to be expressed in a patient case, however there are number of patient cases around the end of the αC-connector and the start of the αC-domain that show hypofibrinogenemia (Fibrinogen Italy Aα373) or dysfibrinogenaemia (Fibrinogen Austin (Aα 381) and Caracas II (Aα 434)) (Maekawa et al., 1991; Castaman et al., 2015; Brennan et al., 2015). Fibrinogen Italy was a homozygous mutant, and this resulted in a premature termination of the α-chain, whereas Fibrinogen Austin and Caracas II are both point mutations and were heterozygous in the patient cases. Furthermore, many of the patients' cases with truncations situated within the tandem repeat region of the αC-connector (Aα261-391) present with hypofibrinogenemia and experience bleeding highlighting the critical role the αC-connector has on clot stability.

The study into the αC-region highlights the importance that this fibrinogen region has on clot formation and clot stability, however the two αC-subregions appear to have distinct roles. The loss of either the entire αC-region or the αC-domain did not critically impact clotability; this is an important observation as patients with dysfibrinogenemia or following bleeding, trauma, or treatment by fibrinolytic agents could result in multiple fibrinogens or fibrin monomers of various sizes within the circulation. Furthermore, mixed fibrinogen proteins could form clots and therefore the structural, mechanical, and fibrinolytic properties would be influenced by hybrid fibrin, which potentially could result in clot instability and further bleeding or secondary thrombus formation in circulation leading to adverse effects in these patients.

Previous studies have shown that the αC-region was involved in lateral aggregation. The studies have ranged from recombinant fibrinogen, fragment X and patient studies. Together, the studies have shown impaired lateral aggregation by turbidimetric assays and microscopy showing the fibrin to be composed of thinner fibres. The production of the αC-subregions has allowed the further exploration into polymerisation and how the two subregions support fibre growth. Through the combination of AFM, turbidimetric assays and microscopy, it was demonstrated that the loss of the αC-connector produced fibrinogen that was stunted in length and showed limited protofibril growth. In contrast, α390 which retained the αC-connector showed similar protofibril length to WT. In addition to lateral aggregation, it appears that the αC-region is essential for longitudinal fibre growth which was previously not known.

Interestingly, functional studies into α390 showed that it exhibited many similarities to WT, but it was structurally distinct. Potentially the dense clot structure formed by α390 gives rise to the fibrinolytic resistance and increased mechanical stiffness that was observed. Fibrinolytic observations by LSCM showed multiple lysis fronts for α220, which is likely due

the porous architecture observed for the fibrin clots, highlighting that macro-structure can influence external fibrinolysis. The *ex-vivo* whole blood assay highlighted that α390 had fibrinolytic sensitivity and furthermore was mechanically weak although it was not as critically weak or showed the same degree premature fibrinolysis as observed by α220. As it has been demonstrated that plasmin lyses individual fibres at multiple points, the rates of digestion were variable because of longitudinal sliding and loss of protofibril sections (Lynch et al., 2022). Furthermore, there is likely to be increased lysis rates when fibres are composed of fibrin which was more susceptible to fibrinolysis or is mechanically weak and therefore less able to compensate for longitudinal sliding, resulting in fibre breakdown occurring sooner. This could further explain the rapid fibrinolysis observed for α220.

The process of clot contraction results in resistance to fibrinolysis, and no difference was observed in clot weight between WT and α390. However, ROTEM analysis did observe fibrinolysis and reduced clot firmness for α390 compared to WT. As these assays covered a similar experimental time frame it would potentially be of interest to see if there was a higher concentration of D-dimer or fibrin degradation products for α390 in the clot contraction supernatant compared to WT. Additionally, although neither experiment is under a shear rate, the ROTEM does have some mechanical movement, which may explain why there was no differences observed between α390 and WT in static clot contraction but there was in ROTEM. Additionally, RBCs can provide lytic resistance by supressing t-PA activation of plasminogen (Wohner et al., 2011). Potentially there is a tipping point where the lytic resistance provided RBC and platelet contraction is not able to compensate for fibrin instability. Together these results demonstrate the importance of studying proteins in different systems to pinpoint how structure affects function.

9.2 γ'-chain

Investigations into the residues of the γ'-chain showed that there was a stepwise reduction in the rate of clotting and mechanical weakness with the inclusion of more residues of the γ'-chain. The γ'-chain residues influenced viscoelastic properties the greatest, at the fibre level. The presence of 12 residues of the γ'-chain affected mechanical clot properties which was further highlighted with the inclusion of more γ'-chain residues. These studies indicate that G" was dominating and therefore it would be less likely there would be the formation of emboli. In addition, the fibre network is likely to be able to rearrange which may be what was observed in the ROTEM lysis experiments as there was initial sensitivity observed for γ'/γ' to fibrinolysis however no difference was observed in lysis time. Additional studies are required to further validate this hypothesis and could be initially explored by investigating if there is a link between γ'-levels in patients and risk of embolism. The residues of the γ'-chain

did not influence fibrinolysis in purified experiments. The presence of the γ'-chain altered clot structure. In fibrinogen whole blood *ex-vivo* assay showed that the truncations to the γ'-chain do not impede clot contraction or causes reduction in the incorporation of platelets or RBC. ROTEM analysis observed a stepwise reduction in mechanical strength inclusion of more residues of the γ'-chain.

Many of the negatively charged residues found within the γ'-chain are between γ'12 and γ'/γ', potentially the fibre curvature observed in LSCM is due to presence of these negatively charged residues within the γ' as it was not observed in WT or γ'0. Interestingly, the fibre curvature was observed in recombinant (γ'/γ') and plasma purified γA/γ' studies which have used fibrinogen from different commercial suppliers and batches. Additionally, the commercially supplied fibrinogen will contain fibrinogen from a pool of donors, of which the details are unknown (ages, ethnicities, health, and number of donors) and it is known that there are multiple factors and modifications that fibrinogen can undergo that can affect structure and function. Interestingly, the LSCM images of 3 patients with low, normal, and high γ'-levels from the Leeds Aneurysm Development Study did not show the altered fibre structure. Perhaps other plasma patients showed altered structure or there are other factors that can influence clot structure in plasma furthermore the LSCM images could have been from plasma from patients or controls.

An interesting observation is that turbidimetric assays do not always align with observations in structural studies which again shows why it is important to use multiple methods for investigations. For example, Aα251 polymerisation curves showed a lower maximum OD, however the differences in OD were limited at lower fibrinogen levels. The difference in maximum OD of Aα251 compared to WT was considerably less (0.03 OD) than observed between WT and α390 (0.19 OD), and both these truncations show a similar clot structure via microscopy. A further contrasting observation between maximum OD and microscopy was the recombinant γA/γ' which has a lower maximum OD but thicker fibres were observed by scanning electron microscopy (Gersh et al., 2009b). The maximum OD from turbidimetric assays is related to fibre diameter but the fibres need to be uniformly distributed, therefore clot porosity and fibre bundles impact the result.

Fibrinogen γ'0, which lacks the final four γA residues and contains no γ' residues, showed reduced maximum OD in both thrombin initiated purified and plasma assays, in addition to a reduced fibre diameter which was observed in scanning electron microscopy. Of note, the γ-chain C-terminal residues 395-411 were not resolved by crystallography. A murine model (γA5/γA5), where the final 5 residues of the γA chain are absent, exhibited similar features to γ'0 with defective platelet aggregation and normal clot retraction (Holmbäck et al., 1996).

Interestingly, the mice had uncontrollable blood loss following surgical challenge, even though platelet counts, and fibrinogen levels were normal. Previously, it has been observed that γ'-chain fibrinogen produces shorter oligomers and the negative charge of the γ'-chain may disrupt the D:D interface (Allan et al., 2012). However, the γA5/γA5 mice had a normal thrombin time and therefore it is unlikely that there is an issue with fibrin formation that is driving the phenotype. Potentially this could be due to issues in primary haemostasis between the platelets and fibrinogen which has a subsequent effect in secondary haemostasis that is not apparent in *ex-vivo* or *in vitro* assays. Furthermore, two subpopulations of platelets have been described proaggregatory (directs platelet aggregation and clot retraction) and procoagulant (drives coagulation factors and thrombin generation) (Hindle et al., 2021). Inhibitory effect of γ'-chain on thrombin and relationship it has with $\alpha_{IIb}\beta_3$, possibly the γ'-chain could play a further role with platelet thrombus development.

The clots collected and imaged following ROTEM analysis showed similarities to clots collected from patient thrombi. It may be of interest to investigate the γ' levels of these patients to observe if there is a particular fibrin structure observed associated with γ' levels. Additionally, as this and other studies show that γ' influences clot mechanical properties, it would be worth knowing how easy it would be to remove the thrombi from the site of formation by thrombectomy and if this is associated with γ' levels. A study of fibrinogen containing various percentages of γ'-chain under arterial and venous flow showed faster and increased fibrin deposition and a larger clot volume with higher concentration of the γ'-chain (Macrae et al., 2021). The duration of the assay was just over 8 minutes, and it would be interesting to observe the clots over a longer time frame to see if there were differences with the rate of clot contraction following formation with higher concentration of the γ'-chain. Additionally, it would be interesting to study if over time there was a reduction of the clot due to the formation of emboli with higher concentration of the γ'-chain.

The cross-linking of fibrinogen chains by FXIIIa provides substantial stability to the clot. Although in this study the addition of FXIII did not show a difference in extension of time to 50 % lysis, this could potentially be due to the $FXIIIA_2B_2$ that was used and perhaps also due to no pre-incubation of the fibrinogen with FXIII. Previously it has been shown that there is a lag in cross-linking by $FXIIIA_2B_2$ compared to FXIIIa (Siebenlist et al., 2001). There was a notable difference in increased stiffness with the magnetic tweezer assay for the α-chain truncations, which is likely due to the time frame of clotting before the start of the assay. Within the circulation, fibrinogen and FXIII bind together in a complex although based on the molar concentration of each present in plasma, only 1 % of fibrinogen can have $FXIIIA_2B_2$

bound at most. Even though there is a small percentage, it does provide the cross-linking required to stabilise the clot and provide fibrinolytic resistance by cross-linking α2-antiplasmin to fibrin. Additionally, FXIIIa is exposed on stimulated platelets which is an additionally source of FXIIIa, importantly is localised within the thrombi (Mitchell et al., 2014).

9.3 Clinical Implications

Fibrinogen is a dynamic protein within coagulation with many roles in primary and secondary haemostasis. Furthermore, fibrinogen and fibrin have distinct qualities which is remarkable considering it only differs by the loss of 2 sets of 16 residues and 14 residues in the FpA and FpB respectively from a large multi-chain protein (Cilia La Corte et al., 2011). Fibrin stability is important as mechanical weakness and/or increased susceptibility to fibrinolysis which may result in thrombus instability leading to bleeding events such as a prolonged mild bleeding event or extensive bleeding following trauma. Furthermore, thrombus instability could lead to the release of emboli leading to thromboembolic events. Interestingly, haemorrhagic transformation is a common complication with patients with acute ischaemic stroke and is a common side effect following t-PA treatment, however it can also occur independently of t-PA treatment. It may be beneficial to ascertain the species of fibrinogen within circulation and therefore treat patients accordingly. The main challenge with this would be to have a clinically accurate assay which could provide the information rapidly.

In vivo, fibrinolysis will mostly occur via internal fibrinolysis, however treatment of ischaemic stroke via t-PA exploits molecular mechanisms involved in external fibrinolysis. Furthermore, clot contraction, cellular composition, and clot age all impact on the success of treatment whether this is by fibrinolytic or mechanical methods.

Fibrinolysis can also occur during the conversion of fibrinogen to fibrin, therefore, delays in protofibril formation, longitudinal growth and lateral aggregation may amplify the fibrinolytic process. In addition, arterial or venous flow could cause additional destabilisation and delays in the formation of a clot. Low fibrinogen levels are an early marker of postpartum haemorrhage. The recent study in to two fibrinogen concentrates and cryoprecipitate demonstrated that there is variability of fibrin properties in these fibrinogen supplements and the presence of FXIII was important for clot stability (Whyte et al., 2022). Highlighting it is important to appreciate the structure/size of fibrinogen within the concentration or cryoprecipitate as the loss or partial loss of αC-region does not impact clotability.

As fibrin is composed of multiple fibrin molecules it is important to appreciate how individual fibres, fibre network and the entire clot effects the mechanical stability and interactions with

blood cells. The combination of investigations using ROTEM, flow cytometry and clot contraction allowed the delineation of fibrinolysis and mechanical properties. Further studies into the connection between the two and fibrin are required for improvements in treatment of patients with haemorrhagic or thrombotic tendencies

9.4 Conclusions

This thesis reinforces the importance of the fibrinogen αC-region in clot stability and furthermore has uncovered the individual roles of the αC-subregions. The subregions have distinct roles and together contribute to the mechanical and fibrinolytic stability of fibrin.

This thesis has also shown that residues of the γ'-chain can impact clot structure and its mechanical properties, but the relationship between γ'-chain and CVD is governed by many additional factors that add to observations seen in patients.

9.4.1 Key Findings for the Fibrinogen αC-region

- The αC-domain is essential for lateral aggregation, fibre thickness and clot density.
- The αC-connector together with the αC-domain is necessary for longitudinal fibre growth and the continuation of fibrin fibres.
- The lack of the entire αC-region in fibrin causes critical clot weakness.
- Fibrinogen with only the αC-domain can partially recover clot firmness.
- Premature fibrinolysis is observed for fibrin clots made from fibrinogen lacking the entire αC-region.
- The presence of the αC-connector offers some resistance to premature fibrinolysis, but still shows predisposition to fibrinolytic sensitivity.

9.4.2 Key Findings for the Fibrinogen γ'-chain

- Clot structure is altered by increasing residues of the γ'-chain.
- Clot viscoelastic properties are altered by inclusion of 12 or more residues of the γ'-chain, with the effect predominantly at the fibre level.
- Viscosity dominating with inclusion of 12 or more residues of γ'-chain
- Truncations to the γ'-chain did not prohibit whole blood clot contraction.
- Whole blood clot formation showed reduced maximum clot firmness with increased number of residues of the γ'-chain present.

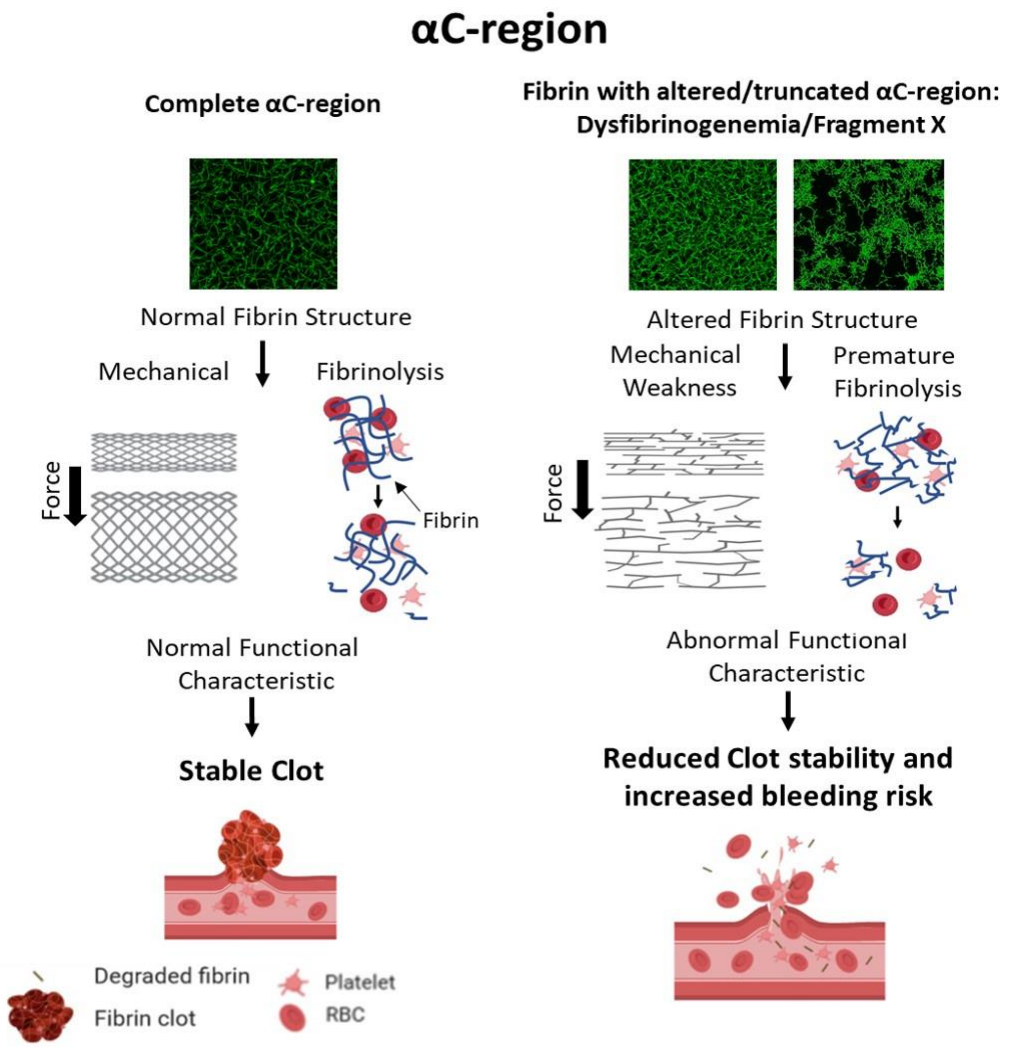

Figure 61 Summary Schematic Highlighting Key Finding for the αC-region Investigations

The αC-region investigations showed that both truncations resulted in altered structure which subsequently altered function and therefore reduced clot stability and increased risk of bleeding.

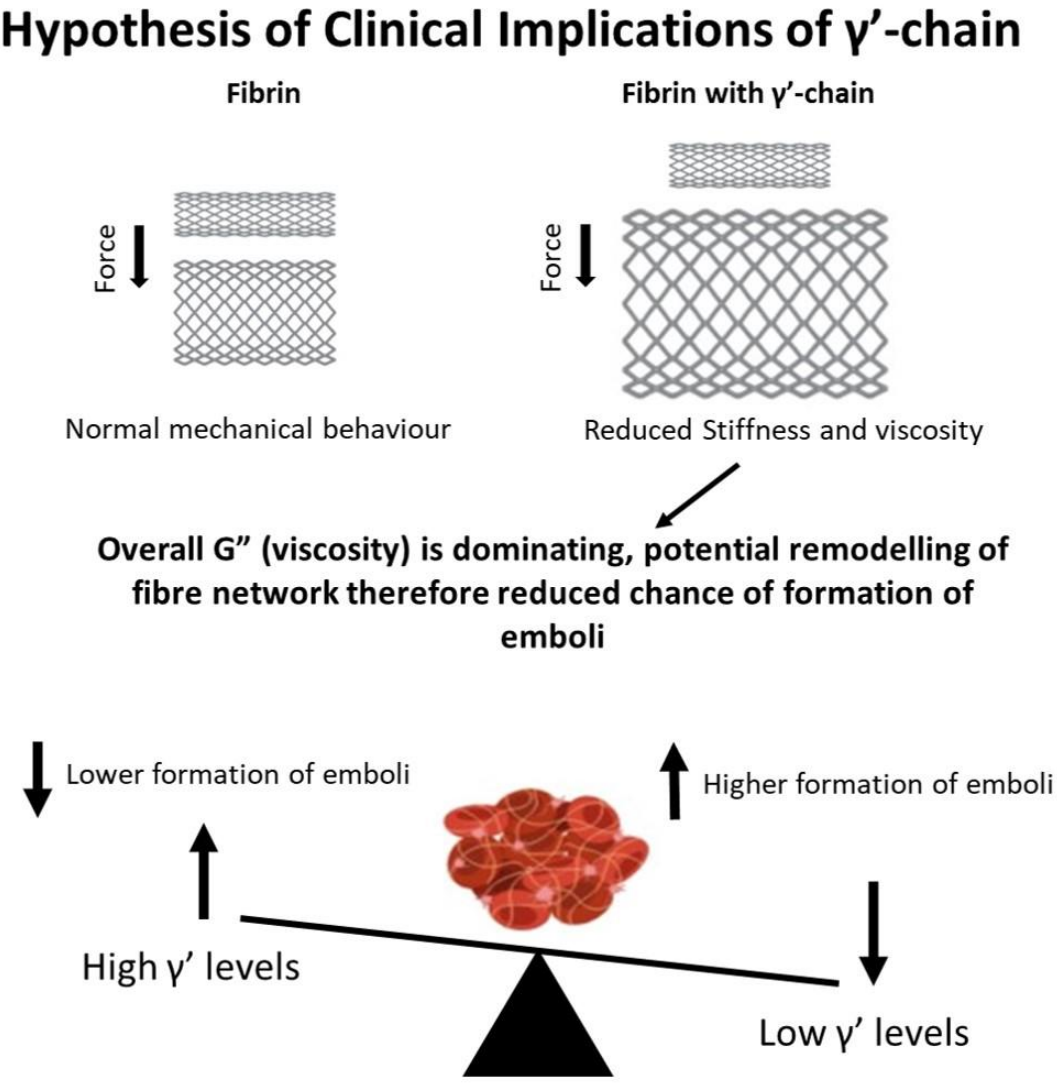

Figure 62 Hypothesis of Clinical Implications of γ' Levels in Patients

Recombinant study of the γ'-chain variants highlighted that the presence of the residues within the γ'-chain resulted in reduced stiffness and viscosity. Furthermore, as the viscosity was dominating there can be remodelling of fibre network and potentially there could be reduced incidence of formation of emboli. Additional studies are required to investigate this hypothesis further. Image created using Biorender and Microsoft PowerPoint.

Chapter 10 References

Abdel Wahab, M., de Moerloose, P., Fish, R.J. and Neerman-Arbez, M. 2010. Identification and functional characterization of a novel nonsense mutation in FGA accounting for congenital afibrinogenemia in six Egyptian patients. *Blood coagulation & fibrinolysis : an international journal in haemostasis and thrombosis*. **21**(2), pp.164–7.

Acevedo, M., Foody, J.A.M., Pearce, G.L. and Sprecher, D.L. 2002. Fibrinogen: associations with cardiovascular events in an outpatient clinic. *American heart journal*. **143**(2), pp.277–282.

Adam, S.S., Key, N.S. and Greenberg, C.S. 2009. D-dimer antigen: Current concepts and future prospects. *Blood*. **113**(13), pp.2878–2887.

Ahn, S.H., Hong, R., Choo, I.S., Heo, J.H., Nam, H.S., Kang, H.G., Kim, H.W. and Kim, J.H. 2016. Histologic features of acute thrombi retrieved from stroke patients during mechanical reperfusion therapy. *International Journal of Stroke*. **11**(9), pp.1036–1044.

Aizhong, F.U., Sreekumaean Nair, K. and Strong, A. 1998. Age effect on fibrinogen and albumin synthesis in humans. *American Journal of Physiology*. **275**(6 PART 1), pp.1023–1030.

Ajjan, R., Lim, B.C.B., Standeven, K.F., Harrand, R., Dolling, S., Phoenix, F., Greaves, R., Abou-Saleh, R.H., Connell, S., Smith, D.A.M., Weisel, J.W., Grant, P.J. and Ariëns, R.A.S. 2008. Common variation in the C-terminal region of the fibrinogen beta-chain: effects on fibrin structure, fibrinolysis and clot rigidity. *Blood*. **111**(2), pp.643–50.

Ajjan, R.A., Standeven, K.F., Khanbhai, M., Phoenix, F., Gersh, K.C., Weisel, J.W., Kearney, M.T., Ariëns, R.A.S. and Grant, P.J. 2009. Effects of aspirin on clot structure and fibrinolysis using a novel in vitro cellular system. *Arteriosclerosis, Thrombosis, and Vascular Biology*. **29**(5), pp.712–717.

Albers, G.W. and Olivot, J.M. 2007. Intravenous alteplase for ischaemic stroke. *Lancet*. **369**(9558), pp.249–250.

Aleman, M.M., Byrnes, J.R., Wang, J.G., Tran, R., Lam, W.A., Paola, J. Di, Mackman, N., Degen, J.L., Flick, M.J. and Wolberg, A.S. 2014. Factor XIII activity mediates red blood cell retention in venous thrombi. *Journal of Clinical Investigation*. **124**(8), pp.3590–3600.

Alkarithi, G., Duval, C., Shi, Y., Macrae, F.L. and Ariëns, R.A.S. 2021. Thrombus Structural Composition in Cardiovascular Disease. *Arteriosclerosis, Thrombosis, and Vascular Biology*. (September), pp.2370–2383.

Allan, P. 2012. Microrheology of Fibrin Clots. . (April), pp.1–253.

Allan, P., Uitte de Willige, S., Abou-Saleh, R.H., Connell, S.D. and Ariëns, R.A.S. 2012. Evidence

that fibrinogen γ′ directly interferes with protofibril growth: Implications for fibrin structure and clot stiffness. *Journal of Thrombosis and Haemostasis*. **10**(6), pp.1072–1080.

Alshehri, O.M., Hughes, C.E., Montague, S., Watson, S.K., Frampton, J., Bender, M. and Watson, S.P. 2015. Fibrin activates GPVI in human and mouse platelets. *Blood*. **126**(13), pp.1601–1608.

Amri, Y., Jouini, H., Becheur, M., Dabboubi, R., Mahjoub, B., Messaoud, T., Sfar, M.T., Casini, A., de Moerloose, P. and Toumi, N.E.H. 2017. Fibrinogen Mahdia: A congenitally abnormal fibrinogen characterized by defective fibrin polymerization. *Haemophilia*. **23**(4), pp.e340–e347.

Amri, Y., Toumi, N.E.H., Hadj Fredj, S. and de Moerloose, P. 2016. Congenital afibrinogenemia: Identification and characterization of two novel homozygous fibrinogen Aα and Bβ chain mutations in two Tunisian families. *Thrombosis Research*. **143**, pp.11–16.

Aoki, N. 1993. Clot Retraction Increases Clot Resistance to Fibrinolysis by Condensing α2-Plasmin Inhibitor Crosslinked to Fibrin. *Thrombosis and Haemostasis*. **70**(02), pp.376–376.

Appiah, D., Schreiner, P.J., MacLehose, R.F. and Folsom, A.R. 2015. Association of Plasma γ′ Fibrinogen With Incident Cardiovascular Disease. *Arteriosclerosis, Thrombosis, and Vascular Biology*. **35**(12), pp.2700–2706.

Arnold, A.E.R., Brower, R.W., Collen, D., van Es, G.A., Lubsen, J., Serruys, P.W., Simoons, M.L. and Verstraete, M. 1989. Increased serum levels of fibrinogen degradation products due to treatment with recombinant tissue-type plasminogen activator for acute myocardial infarction are related to bleeding complications, but not to coronary patency. *Journal of the American College of Cardiology*. **14**(3), pp.581–588.

Asselta, R., Platè, M., Robusto, M., Borhany, M., Guella, I., Soldà, G., Afrasiabi, A., Menegatti, M., Shamsi, T., Peyvandi, F. and Duga, S. 2015a. Clinical and molecular characterisation of 21 patients affected by quantitative fibrinogen deficiency. *Thrombosis and Haemostasis*. **113**(3), pp.567–576.

Asselta, R., Robusto, M., Platé, M., Santoro, C., Peyvandi, F. and Duga, S. 2015b. Molecular characterization of 7 patients affected by dys- or hypo-dysfibrinogenemia: Identification of a novel mutation in the fibrinogen Bbeta chain causing a gain of glycosylation. *Thrombosis Research*. **136**(1), pp.168–174.

Atkins, G.B. and Jain, M.K. 2007. Role of Krüppel-like transcription factors in endothelial biology. *Circulation Research*. **100**(12), pp.1686–1695.

Bagoly, Z., Szegedi, I., Kálmándi, R., Tóth, N.K. and Csiba, L. 2019. Markers of Coagulation and Fibrinolysis Predicting the Outcome of Acute Ischemic Stroke Thrombolysis Treatment: A Review of the Literature. *Frontiers in neurology*. **10**(June), p.513.

Baker, S.R., Zabczyk, M., Macrae, F.L., Duval, C., Undas, A. and Ariëns, R.A.S. 2019. Recurrent venous thromboembolism patients form clots with lower elastic modulus than those formed by patients with non-recurrent disease. *Journal of Thrombosis and Haemostasis*. **17**(4), pp.618–626.

Baumann, R.E. and Henschen, A.H. 1993. Human fibrinogen polymorphic site analysis by restriction endonuclease digestion and allele-specific polymerase chain reaction amplification: Identification of polymorphisms at positions Aα312 and Bβ448. *Blood*. **82**(7), pp.2117–2124.

Beck-Joseph, J. and Lehoux, S. 2021. Molecular Interactions Between Vascular Smooth Muscle Cells and Macrophages in Atherosclerosis. *Frontiers in Cardiovascular Medicine*. **8**(October), pp.1–14.

Bembenek, J.P., Niewada, M., Siudut, J., Plens, K., Członkowska, A. and Undas, A. 2017. Fibrin clot characteristics in acute ischaemic stroke patients treated with thrombolysis: The impact on clinical outcome. *Thrombosis and Haemostasis*. **117**(7), pp.1440–1447.

Bennett, J.S. 2006. Platelet-Fibrinogen Interactions. *Annals of the New York Academy of Sciences*. **936**(1), pp.340–354.

Bentzon, J.F., Otsuka, F., Virmani, R. and Falk, E. 2014. Mechanisms of plaque formation and rupture. *Circulation Research*. **114**(12), pp.1852–1866.

Besser, M., Baglin, C., Luddington, R., Van Hylckama Vlieg, A. and Baglin, T. 2008. High rate of unprovoked recurrent venous thrombosis is associated with high thrombin-generating potential in a prospective cohort study. *Journal of Thrombosis and Haemostasis*. **6**(10), pp.1720–1725.

Bigland, C.H. and Triantaphyllopoulos, D.C. 1961. Chicken prothrombin, thrombin, and fibrinogen. *American Journal of Physiology-Legacy Content*. **200**(5), pp.1013–1017.

Binnie, C.G., Hettasch, J.M., Strickland, E. and Lord, S.T. 1993. Characterization of purified recombinant fibrinogen: partial phosphorylation of fibrinopeptide A. *Biochemistry*. **32**(1), pp.107–13.

Blinc, A., Keber, D., Lahajnar, G., Zupancic, I., Zorec-Karlovsek, M. and Demsar, F. 1992. Magnetic resonance imaging of retracted and nonretracted blood clots during fibrinolysis in vitro. *Haemostasis*. **22**(4), pp.195–201.

Blombäck, B., Carlsson, K., Fatah, K., Hessel, B. and Procyk, R. 1994. Fibrin in human plasma: Gel architectures governed by rate and nature of fibrinogen activation. *Thrombosis*

Research. **76**(5), pp.501–502.

Blombäck, B., Carlsson, K., Hessel, B., Liljeborg, A., Procyk, R. and Åslund, N. 1989. Native fibrin gel networks observed by 3D microscopy, permeation and turbidity. *Biochimica et Biophysica Acta (BBA)/Protein Structure and Molecular*. **997**(1–2), pp.96–110.

Blombäck, B., Hessel, B. and Hogg, D. 1976. Disulfide bridges in nh2 -terminal part of human fibrinogen. *Thrombosis research*. **8**(5), pp.639–58.

Blomback, B., Hessel, B., Hogg, D. and Therkildsen, L. 1978. A two-step fibrinogen-fibrin transition in blood coagulation. *Nature*. **275**(5680), pp.501–505.

Bochenek, M., Zalewski, J., Sadowski, J. and Undas, A. 2013. Type 2 diabetes as a modifier of fibrin clot properties in patients with coronary artery disease. *Journal of Thrombosis and Thrombolysis*. **35**(2), pp.264–270.

Bolyard, M.G. and Lord, S.T. 1989. Expression in Escherichia coli of the human fibrinogen Bβ chain and its cleavage by thrombin. *Blood*. **73**(5), pp.1202–1206.

Bolyard, M.G. and Lord, S.T. 1988. High-level expression of a functional human fibrinogen gamma chain in Escherichia coli. *Gene*. **66**(2), pp.183–192.

Borczuk, A.C., Salvatore, S.P., Seshan, S. V., Patel, S.S., Bussel, J.B., Mostyka, M., Elsoukkary, S., He, B., Del Vecchio, C., Fortarezza, F., Pezzuto, F., Navalesi, P., Crisanti, A., Fowkes, M.E., Bryce, C.H., Calabrese, F. and Beasley, M.B. 2020. COVID-19 pulmonary pathology: a multi-institutional autopsy cohort from Italy and New York City. *Modern Pathology*. **33**(11), pp.2156–2168.

Bouchard, B.A., Silveira, J.R. and Tracy, P.B. 2013. *Interactions Between Platelets and the Coagulation System* [Online] Third Edit. Elsevier Inc. Available from: http://dx.doi.org/10.1016/B978-0-12-387837-3.00021-3.

Bouman, A.C., McPherson, H., Cheung, Y.W., Ten Wolde, M., Ten Cate, H., Ariëns, R.A.S. and Ten Cate-Hoek, A.J. 2016. Clot structure and fibrinolytic potential in patients with post thrombotic syndrome. *Thrombosis Research*. **137**, pp.85–91.

Bowley, S.R., Okumura, N. and Lord, S.T. 2009. Impaired protofibril formation in fibrinogen γN308K is due to altered D:D and 'A:a' interactions. *Biochemistry*. **48**(36), pp.8656–8663.

Brandts, A., Van Hylckama Vlieg, A., Rosing, J., Baglin, T.P. and Rosendaal, F.R. 2007. The risk of venous thrombosis associated with a high endogenous thrombin potential in the absence and presence of activated protein C [3]. *Journal of Thrombosis and Haemostasis*. **5**(2), pp.416–418.

Brennan, S.O., Laurie, A.D., Mo, A. and Grigg, A. 2015. Novel fibrinogen mutations (Aα17Gly→Cys and Aα381Ser→Phe) occurring with a 312Thr→Ala polymorphism:

Allelic phase assigned by direct mass measurement. *Blood Coagulation and Fibrinolysis*. **26**(8), pp.882–886.

Brennan, S.O., Mosesson, M.W., Lowen, R. and Frantz, C. 2006. Dysfibrinogenemia (fibrinogen Wilmington) due to a novel Aα chain truncation causing decreased plasma expression and impaired fibrin polymerisation. *Thrombosis and Haemostasis*. **96**(1), pp.88–89.

Bridge, K.I., Philippou, H. and Ariëns, R.A.S. 2014. Clot properties and cardiovascular disease. *Thrombosis and Haemostasis*. **112**(5), pp.901–908.

Brown, A.E.X., Litvinov, R.I., Discher, D.E., Purohit, P.K. and Weisel, J.W. 2009. Multiscale mechanics of fibrin polymer: gel stretching with protein unfolding and loss of water. *Science (New York, N.Y.)*. **325**(5941), pp.741–4.

Brown, A.J., Gibson, S., Hatton, D. and James, D.C. 2018. Transcriptome-Based Identification of the Optimal Reference CHO Genes for Normalisation of qPCR Data. *Biotechnology journal*. **13**(1).

Brubaker, L.S., Saini, A., Nguyen, T.C., Martinez-Vargas, M., Lam, F.W., Yao, Q., Loor, M.M., Rosengart, T.K. and Cruz, M.A. 2022. Aberrant Fibrin Clot Structure Visualized Ex Vivo in Critically Ill Patients With Severe Acute Respiratory Syndrome Coronavirus 2 Infection. *Critical Care Medicine*. **Publish Ah**, pp.1–12.

Brummel, K.E., Paradis, S.G., Butenas, S. and Mann, K.G. 2002. Thrombin functions during tissue factor-induced blood coagulation. *Blood*. **100**(1), pp.148–152.

Burton, R.A., Tsurupa, G., Hantgan, R.R., Tjandra, N. and Medved, L. 2007. NMR solution structure, stability, and interaction of the recombinant bovine fibrinogen αC-domain fragment. *Biochemistry*. **46**(29), pp.8550–8560.

Burton, R.A., Tsurupa, G., Medved, L. and Tjandra, N. 2006. Identification of an ordered compact structure within the recombinant bovine fibrinogen alphaC-domain fragment by NMR. *Biochemistry*. **45**(7), pp.2257–66.

Byrnes, J.R., Duval, C., Wang, Y., Hansen, C.E., Ahn, B., Mooberry, M.J., Clark, M.A., Johnsen, J.M., Lord, S.T., Lam, W.A., Meijers, J.C.M., Ni, H., Ariëns, R.A.S. and Wolberg, A.S. 2015. Factor XIIIa-dependent retention of red blood cells in clots is mediated by fibrin α-chain crosslinking. *Blood*. **126**(16), pp.1940–1948.

Campbell, B.C.V., Mitchell, P.J., Churilov, L., Yassi, N., Kleinig, T.J., Dowling, R.J., Yan, B., Bush, S.J., Dewey, H.M., Thijs, V., Scroop, R., Simpson, M., Brooks, M., Asadi, H., Wu, T.Y., Shah, D.G., Wijeratne, T., Ang, T., Miteff, F., Levi, C.R., Rodrigues, E., Zhao, H., Salvaris, P., Garcia-Esperon, C., Bailey, P., Rice, H., de Villiers, L., Brown, H., Redmond, K., Leggett, D., Fink, J.N., Collecutt, W., Wong, A.A., Muller, C., Coulthard, A., Mitchell, K.,

Clouston, J., Mahady, K., Field, D., Ma, H., Phan, T.G., Chong, W., Chandra, R. V., Slater, L.-A., Krause, M., Harrington, T.J., Faulder, K.C., Steinfort, B.S., Bladin, C.F., Sharma, G., Desmond, P.M., Parsons, M.W., Donnan, G.A. and Davis, S.M. 2018. Tenecteplase versus Alteplase before Thrombectomy for Ischemic Stroke. *New England Journal of Medicine*. **378**(17), pp.1573–1582.

Cantero, M., Rojas, H., Anglés-Cano, E. and Marchi, R. 2019. Fibrin γ/γ' influences the secretion of fibrinolytic components and clot structure. *BMC Molecular and Cell Biology*. **20**(1), pp.1–9.

Carr, M.E. and Hermans, J. 1978. Size and Density of Fibrin Fibers from Turbidity. *Macromolecules*. **11**(1), pp.46–50.

Carrell, N., Gabriel, D.A., Blatt, P.M., Carr, M.E. and McDonagh, J. 1983. Hereditary dysfibrinogenemia in a patient with thrombotic disease. *Blood*. **62**(2), pp.439–447.

Carter, A.M., Catto, A.J. and Grant, P.J. 1999. Association of the α-fibrinogen Thr312Ala polymorphism with poststroke mortality in subjects with atrial fibrillation. *Circulation*. **99**(18), pp.2423–2426.

Carter, A.M., Catto, A.J., Kohler, H.P., Ariëns, R.A.S.S., Stickland, M.H. and Grant, P.J. 2000. α-Fibrinogen Thr312Ala polymorphism and venous thromboembolism. *Blood*. **96**(3), pp.1177–1179.

Carvalho, F.A., Connell, S., Miltenberger-Miltenyi, G., Pereira, S.V., Tavares, A., Ariëns, R.A.S. and Santos, N.C. 2010. Atomic force microscopy-based molecular recognition of a fibrinogen receptor on human erythrocytes. *ACS Nano*. **4**(8), pp.4609–4620.

Carvalho, F.A., Guedes, A.F., Duval, C., Macrae, F.L., Swithenbank, L., Farrell, D.H., Ariëns, R.A.S. and Santos, N.C. 2018. The 95RGD97 sequence on the Aα Chain of fibrinogen is essential for binding to its erythrocyte receptor. *International Journal of Nanomedicine*. **13**, pp.1985–1992.

Castaman, G., Rimoldi, V., Giacomelli, S.H. and Duga, S. 2015. Congenital hypofibrinogenemia associated with novel homozygous fibrinogen Aα and heterozygous Bβ chain mutations. *Thrombosis Research*. **136**(1), pp.144–147.

Chatterjee, S. 1995. Tissue Plasminogen Activator for Acute Ischemic Stroke. *New England Journal of Medicine*. **333**(24), pp.1581–1588.

Cheresh, D.A., Berliner, S.A., Vicente, V. and Ruggeri, Z.M. 1989. Recognition of distinct adhesive sites on fibrinogen by related integrins on platelets and endothelial cells. *Cell*. **58**(5), pp.945–953.

Chernysh, I.N., Nagaswami, C., Kosolapova, S., Peshkova, A.D., Cuker, A., Cines, D.B., Cambor, C.L., Litvinov, R.I. and Weisel, J.W. 2020a. The distinctive structure and

composition of arterial and venous thrombi and pulmonary emboli. *Scientific Reports*. **10**(1), pp.1–12.

Chernysh, I.N., Nagaswami, C., Purohit, P.K. and Weisel, J.W. 2012. Fibrin clots are equilibrium polymers that can be remodeled without proteolytic digestion. *Scientific Reports*. **2**, pp.1–6.

Chernysh, I.N., Nagaswami, C. and Weisel, J.W. 2011. Visualization and identification of the structures formed during early stages of fibrin polymerization. *Blood*. **117**(17), pp.4609–4614.

Chernysh, I.N., Spiewak, R., Cambor, C.L., Purohit, P.K. and Weisel, J.W. 2020b. Structure, mechanical properties, and modeling of cyclically compressed pulmonary emboli. *Journal of the Mechanical Behavior of Biomedical Materials*. **105**(July 2019), p.103699.

Chueh, J.Y., Wakhloo, A.K., Hendricks, G.H., Silva, C.F., Weaver, J.P. and Gounis, M.J. 2011. Mechanical characterization of thromboemboli in acute ischemic stroke and laboratory embolus analogs. *American Journal of Neuroradiology*. **32**(7), pp.1237–1244.

Chung, D.W. and Davie, E.W. 1984. γ and γ Chains of Human Fibrinogen Are Produced by Alternative mRNA Processing. *Biochemistry*. **23**(18), pp.4232–4236.

Cieslik, J., Mrozinska, S., Broniatowska, E. and Undas, A. 2018. Altered plasma clot properties increase the risk of recurrent deep vein thrombosis: A cohort study. *Blood*. **131**(7), pp.797–807.

Cilia La Corte, A.L., Philippou, H. and Ariëns, R.A.S. 2011. Role of Fibrin Structure in Thrombosis and Vascular Disease *In*: *Advances in Protein Chemistry and Structural Biology* [Online]. Elsevier Inc., pp.75–127. Available from: http://dx.doi.org/10.1016/B978-0-12-381262-9.00003-3.

Collen, A., Maas, A., Kooistra, T., Lupu, F., Grimbergen, J., Haas, F.J.L.M., Biesma, D.H., Koolwijk, P., Koopman, J. and Van Hinsbergh, V.W.M. 2001. Aberrant fibrin formation and cross-linking of fibrinogen Nieuwegein, a variant with a shortened Aα-chain, alters endothelial capillary tube formation. *Blood*. **97**(4), pp.973–980.

Collet, J.-P., Moen, J.L., Veklich, Y.I., Gorkun, O. V., Lord, S.T., Montalescot, G. and Weisel, J.W. 2005. The alphaC domains of fibrinogen affect the structure of the fibrin clot, its physical properties, and its susceptibility to fibrinolysis. *Blood*. **106**(12), pp.3824–30.

Collet, J.P., Allali, Y., Lesty, C., Tanguy, M.L., Silvain, J., Ankri, A., Blanchet, B., Dumaine, R., Gianetti, J., Payot, L., Weisel, J.W. and Montalescot, G. 2006. Altered fibrin architecture is associated with hypofibrinolysis and premature coronary atherothrombosis. *Arteriosclerosis, Thrombosis, and Vascular Biology*. **26**(11), pp.2567–2573.

Collet, J.P., Nagaswami, C., Farrell, D.H., Montalescot, G. and Weisel, J.W. 2004. Influence of

γ' Fibrinogen Splice Variant on Fibrin Physical Properties and Fibrinolysis Rate. *Arteriosclerosis, Thrombosis, and Vascular Biology*. **24**(2), pp.382–386.

Collet, J.P., Park, D., Lesty, C., Soria, J., Soria, C., Montalescot, G. and Weisel, J.W. 2000. Influence of fibrin network conformation and fibrin diameter on fibrinolysis speed: Dynamic and structural approaches by confocal microscopy. *Arteriosclerosis, Thrombosis, and Vascular Biology*. **20**(5), pp.1354–1361.

Cooper, A. V., Standeven, K.F. and Ariéns, R.A.S. 2003. Fibrinogen gamma-chain splice variant γ' alters fibrin formation and structure. *Blood*. **102**(2), pp.535–540.

Cortet, M., Deneux-Tharaux, C., Dupont, C., Colin, C., Rudigoz, R.C., Bouvier-Colle, M.H. and Huissoud, C. 2012. Association between fibrinogen level and severity of postpartum haemorrhage: Secondary analysis of a prospective trial. *British Journal of Anaesthesia*. **108**(6), pp.984–989.

Cui, S., Chen, S., Li, X., Liu, S. and Wang, F. 2020. Prevalence of venous thromboembolism in patients with severe novel coronavirus pneumonia. *Journal of Thrombosis and Haemostasis*. **18**(6), pp.1421–1424.

Davie, E.W. and Ratnoff, O.D. 1964. WATERFALL SEQUENCE FOR INTRINSIC BLOOD CLOTTING. *Science (New York, N.Y.)*. **145**(3638), pp.1310–2.

Dempfle, C.E., George, P.M., Borggrefe, M., Neumaier, M. and Brennan, S.O. 2009. Demonstration of heterodimeric fibrinogen molecules partially conjugated with albumin in a novel dysfibrinogen: Fibrinogen Mannheim V. *Thrombosis and Haemostasis*. **102**(1), pp.29–34.

Dolhnikoff, M., Duarte-Neto, A.N., Almeida Monteiro, R.A., Silva, L.F.F., Oliveira, E.P., Saldiva, P.H.N., Mauad, T. and Negri, E.M. 2020. Pathological evidence of pulmonary thrombotic phenomena in severe COVID-19. *Journal of Thrombosis and Haemostasis*. **18**(6), pp.1517–1519.

Domingues, M.M., Macrae, F.L., Duval, C., McPherson, H.R., Bridge, K.I., Ajjan, R.A., Ridger, V.C., Connell, S.D., Philippou, H. and Ariëns, R.A.S. 2016. Thrombin and fibrinogen γ' impact clot structure by marked effects on intrafibrillar structure and protofibril packing. *Blood*. **127**(4), pp.487–495.

Doolittle, R.F., Goldbaum, D.M. and Doolittle, L.R. 1978. Designation of sequences involved in the 'coiled-coil' interdomainal connections in fibrinogen: Construction of an atomic scale model. *Journal of Molecular Biology*. **120**(2), pp.311–325.

Doolittle, R.F. and Kollman, J.M. 2006. Natively unfolded regions of the vertebrate fibrinogen molecule. *Proteins*. **63**(2), pp.391–7.

Doolittle, R.F. and Pandi, L. 2006. Erratum: Binding of synthetic B knobs to fibrinogen

changes the character of fibrin and inhibits its ability to activate tissue plasminogen activator and its destruction by plasmin (Biochemistry (February 28, 2006) 45, 8 (2657-2667)). *Biochemistry*. **45**(13), p.4338.

Doolittle, R.F., Spraggon, G. and Everse, S.J. 1998. Three-dimensional structural studies on fragments of fibrinogen and fibrin. *Current Opinion in Structural Biology*. **8**(6), pp.792–798.

Doolittle, R.F., Watt, K.W.K., Cottrell, B.A., Strong, D.D. and Riley, M. 1979. The amino acid sequence of the α-chain of human fibrinogen. *Nature*. **280**(5722), pp.464–468.

Ducloy-Bouthors, A.S., Duhamel, A., Kipnis, E., Tournoys, A., Prado-Dupont, A., Elkalioubie, A., Jeanpierre, E., Debize, G., Peynaud-Debayle, E., Deprost, D., Huissoud, C., Rauch, A. and Susen, S. 2016. Postpartum haemorrhage related early increase in D-dimers is inhibited by tranexamic acid: Haemostasis parameters of a randomized controlled open labelled trial. *British Journal of Anaesthesia*. **116**(5), pp.641–648.

Dunn, E.J., Ariëns, R.A.S. and Grant, P.J. 2005. The influence of type 2 diabetes on fibrin structure and function. *Diabetologia*. **48**(6), pp.1198–1206.

Dunn, E.J., Philippou, H., Ariëns, R.A.S. and Grant, P.J. 2006. Molecular mechanisms involved in the resistance of fibrin to clot lysis by plasmin in subjects with type 2 diabetes mellitus. *Diabetologia*. **49**(5), pp.1071–1080.

Duval, C., Allan, P., Connell, S.D.A., Ridger, V.C., Philippou, H. and Ariëns, R.A.S. 2014. Roles of fibrin α- and γ-chain specific cross-linking by FXIIIa in fibrin structure and function. *Thrombosis and Haemostasis*. **111**(5), pp.842–850.

Duval, C., Profumo, A., Aprile, A., Salis, A., Millo, E., Damonte, G., Gauer, J.S., Ariëns, R.A.S. and Rocco, M. 2020. Fibrinogen αC-regions are not directly involved in fibrin polymerization as evidenced by a “Double-Detroit” recombinant fibrinogen mutant and knobs-mimic peptides. *Journal of Thrombosis and Haemostasis*. **18**(4), pp.802–814.

Erickson, H.P. and Fowler, W.E. 1983. Electron Microscopy of Fibrinogen, Its Plasmic Fragments and Small Polymers. *Annals of the New York Academy of Sciences*. **408**(1), pp.146–163.

Esmon, C.T. 2009. Basic mechanisms and pathogenesis of venous thrombosis. *Blood Reviews*. **23**(5), pp.225–229.

Everse, S.J., Spraggon, G., Veerapandian, L. and Doolittle, R.F. 1999. Conformational changes in fragments D and double-D from human fibrin(ogen) upon binding the peptide ligand Gly-His-Arg-Pro-Amide. *Biochemistry*. **38**(10), pp.2941–2946.

Everse, S.J., Spraggon, G., Veerapandian, L., Riley, M. and Doolittle, R.F. 1998. Crystal

structure of fragment double-D from human fibrin with two different bound ligands. *Biochemistry*. **37**(24), pp.8637–8642.

Evtugina, N.G., Peshkova, A.D., Pichugin, A.A., Weisel, J.W. and Litvinov, R.I. 2020. Impaired contraction of blood clots precedes and predicts postoperative venous thromboembolism. *Scientific Reports*. **10**(1), pp.1–11.

Falls, L.A. and Farrell, D.H. 1997. Resistance of γA/γ' fibrin clots to fibrinolysis. *Journal of Biological Chemistry*. **272**(22), pp.14251–14256.

Falvo, M.R., Millard, D., O'Brien, E.T., Superfine, R. and Lord, S.T. 2008. Length of tandem repeats in fibrin's alphaC region correlates with fiber extensibility. *Journal of thrombosis and haemostasis : JTH*. **6**(11), pp.1991–3.

Farag, M., Spinthakis, N., Gue, Y.X., Srinivasan, M., Sullivan, K., Wellsted, D. and Gorog, D.A. 2019. Impaired endogenous fibrinolysis in ST-segment elevation myocardial infarction patients undergoing primary percutaneous coronary intervention is a predictor of recurrent cardiovascular events: The RISK PPCI study. *European Heart Journal*. **40**(3), pp.295–305.

Farrell, D.H. and Al-Mondhiry, H.A. 1997. Human fibroblast adhesion to fibrinogen. *Biochemistry*. **36**(5), pp.1123–1128.

Farrell, D.H., Mulvihill, E.R., Huang, S.M., Chung, D.W. and Davie, E.W. 1991. Recombinant human fibrinogen and sulfation of the gamma' chain. *Biochemistry*. **30**(39), pp.9414–20.

Farrell, D.H., Rick, E.A., Dewey, E.N., Schreiber, M.A. and Rowell, S.E. 2020. γ' fibrinogen levels are associated with blood clot strength in traumatic brain injury patients. *American journal of surgery*. **220**(2), pp.459–463.

Farrell, D.H., Thiagarajan, P., Chung, D.W. and Davie, E.W. 1992. Role of fibrinogen α and γ chain sites in platelet aggregation. *Proceedings of the National Academy of Sciences of the United States of America*. **89**(22), pp.10729–10732.

Feichtinger, J., Hernández, I., Fischer, C., Hanscho, M., Auer, N., Hackl, M., Jadhav, V., Baumann, M., Krempl, P.M., Schmidl, C., Farlik, M., Schuster, M., Merkel, A., Sommer, A., Heath, S., Rico, D., Bock, C., Thallinger, G.G. and Borth, N. 2016. Comprehensive genome and epigenome characterization of CHO cells in response to evolutionary pressures and over time. *Biotechnology and Bioengineering*. **113**(10), pp.2241–2253.

Felgner, P.L. 1990. Particulate systems and polymers for in vitro and in vivo delivery of polynucleotides. *Advanced Drug Delivery Reviews*. **5**(3), pp.163–187.

Fernández-Cadenas, I., Penalba, A., Boada, C., Msc, C.C., Bueno, S.R., Quiroga, A., Monasterio, J., Delgado, P., Anglés-Cano, E. and Montaner, J. 2016. Exome sequencing

and clot lysis experiments demonstrate the R458C mutation of the alpha chain of fibrinogen to be associated with impaired fibrinolysis in a family with thrombophilia. *Journal of Atherosclerosis and Thrombosis*. **23**(4), pp.431–440.

Fibrinogen Studies Collaboration, Danesh, J., Lewington, Sarah, Thompson, S.G., Lowe, G.D.O., Collins, R., Kostis, J.B., Wilson, A.C., Folsom, A.R., Wu, K., Benderly, M., Goldbourt, U., Willeit, J., Kiechl, S., Yarnell, J.W.G., Sweetnam, P.M., Elwood, P.C., Cushman, M., Psaty, B.M., Tracy, R.P., Tybjaerg-Hansen, A., Haverkate, F., de Maat, M.P.M., Fowkes, F.G.R., Lee, A.J., Smith, F.B., Salomaa, V., Harald, K., Rasi, R., Vahtera, E., Jousilahti, P., Pekkanen, J., D'Agostino, R., Kannel, W.B., Wilson, P.W.F., Tofler, G., Arocha-Piñango, C.L., Rodriguez-Larralde, A., Nagy, E., Mijares, M., Espinosa, R., Rodriquez-Roa, E., Ryder, E., Diez-Ewald, M.P., Campos, G., Fernandez, V., Torres, E., Marchioli, R., Valagussa, F., Rosengren, A., Wilhelmsen, L., Lappas, G., Eriksson, H., Cremer, P., Nagel, D., Curb, J.D., Rodriguez, B., Yano, K., Salonen, J.T., Nyyssönen, K., Tuomainen, T.-P., Hedblad, B., Lind, P., Loewel, H., Koenig, W., Meade, T.W., Cooper, J.A., De Stavola, B., Knottenbelt, C., Miller, G.J., Cooper, J.A., Bauer, K.A., Rosenberg, R.D., Sato, S., Kitamura, A., Naito, Y., Palosuo, T., Ducimetiere, P., Amouyel, P., Arveiler, D., Evans, A.E., Ferrieres, J., Juhan-Vague, I., Bingham, A., Schulte, H., Assmann, G., Cantin, B., Lamarche, B., Després, J.-P., Dagenais, G.R., Tunstall-Pedoe, H., Woodward, M., Ben-Shlomo, Y., Davey Smith, G., Palmieri, V., Yeh, J.L., Rudnicka, A., Ridker, P., Rodeghiero, F., Tosetto, A., Shepherd, J., Ford, I., Robertson, M., Brunner, E., Shipley, M., Feskens, E.J.M., Kromhout, D., Dickinson, A., Ireland, B., Juzwishin, K., Kaptoge, S., Lewington, S, Memon, A., Sarwar, N., Walker, M., Wheeler, J., White, I. and Wood, A. 2005. Plasma fibrinogen level and the risk of major cardiovascular diseases and nonvascular mortality: an individual participant meta-analysis. *JAMA*. **294**(14), pp.1799–809.

Fineschi, V., Turillazzi, E., Neri, M., Pomara, C. and Riezzo, I. 2009. Histological age determination of venous thrombosis: A neglected forensic task in fatal pulmonary thrombo-embolism. *Forensic Science International*. **186**(1–3), pp.22–28.

Fish, R.J. and Neerman-Arbez, M. 2012. Fibrinogen gene regulation. *Thrombosis and Haemostasis*. **108**(3), pp.419–426.

Flaumenhaft, R. 2013. *Platelet Secretion* [Online] Third Edit. Elsevier Inc. Available from: http://dx.doi.org/10.1016/B978-0-12-387837-3.00018-3.

Fleury, V. and Anglés-Cano, E. 1991. Characterization of the Binding of Plasminogen to Fibrin Surfaces: The Role of Carboxy-Terminal Lysines. *Biochemistry*. **30**(30), pp.7630–7638.

Flood, V.H., Al-Mondhiry, H.A., Rein, C.M., Alexander, K.S., Lovely, R.S., Shackleton, K.M.,

David, L.L. and Farrell, D.H. 2008. Fibrinogen Hershey IV: A novel dysfibrinogen with a γV411I mutation in the integrin αIIbβ3 binding site. *Thrombosis and Haemostasis*. **99**(6), pp.1008–1012.

Fornace, A.J., Cummings, D.E., Comeau, C.M., Kant, J.A. and Crabtree, G.R. 1984. Structure of the human γ-fibrinogen gene. Alternate mRNA splicing near the 3' end of the gene produces γA and γB forms of γ-fibrinogen. *Journal of Biological Chemistry*. **259**(20), pp.12826–12830.

Francis, C.W., Marder, V.J. and Martin, S.E. 1980. Demonstration of a large molecular weight variant of the gamma chain of normal human plasma fibrinogen. *Journal of Biological Chemistry*. **255**(12), pp.5599–5604.

Fraser, S.R., Booth, N.A. and Mutch, N.J. 2011. The antifibrinolytic function of factor XIII is exclusively expressed through α2-antiplasmin cross-linking. *Blood*. **118**(26), p.6993.

Fredenburgh, J.C., Stafford, A.R., Leslie, B.A. and Weitz, J.I. 2008. Bivalent binding to γA/γ'-fibrin engages both exosites of thrombin and protects it from inhibition by the antithrombin-heparin complex. *Journal of Biological Chemistry*. **283**(5), pp.2470–2477.

Fuller, G.M., Otto, J.M., Woloski, B.M., McGary, C.T. and Adams, M.A. 1985. The effects of hepatocyte stimulating factor on fibrinogen biosynthesis in hepatocyte monolayers. *Journal of Cell Biology*. **101**(4), pp.1481–1486.

Fuller, G.M. and Zhang, Z. 2001. Transcriptional control mechanism of fibrinogen gene expression. *Annals of the New York Academy of Sciences*. **936**, pp.469–479.

Furlan, M., Steinmann, C., Jungo, M., Bogli, C., Baudo, F., Redaelli, R., Fedeli, F. and Lammle, B. 1994. A frameshift mutation in exon V of the Aα-chain gene leading to truncated Aα-chains in the homozygous dysfibrinogen Milano III. *Journal of Biological Chemistry*. **269**(52), pp.33129–33134.

Gailani, D. and Renne, T. 2007. The intrinsic pathway of coagulation: a target for treating thromboembolic disease? *Journal of Thrombosis and Haemostasis*. **5**(6), pp.1106–1112.

GEHT, H.F.D. n.d. GEHT - Human Fibrinogen Database. [Accessed 15 June 2021]. Available from: https://site.geht.org/base-de-donnees-fibrinogene/.

Gersh, K., Nagaswami, C. and Weisel, J. 2009a. Fibrin network structure and clot mechanical properties are altered by incorporation of erythrocytes. *Thrombosis and Haemostasis*. **102**(12), pp.1169–1175.

Gersh, K.C. and Lord, S.T. 2006. An Investigation of Factor XIII Binding to Recombinant γ'/γ' and γ/γ' Fibrinogen. *Blood*. **108**(11), pp.1705–1705.

Gersh, K.C., Nagaswami, C., Weisel, J.W. and Lord, S.T. 2009b. The presence of gamma' chain

impairs fibrin polymerization. *Thrombosis research*. **124**(3), pp.356–63.

Giannis, D., Ziogas, I.A. and Gianni, P. 2020. Coagulation disorders in coronavirus infected patients: COVID-19, SARS-CoV-1, MERS-CoV and lessons from the past. *Journal of Clinical Virology*. **127**(March), p.104362.

Gligorijević, N., Zámorová Križáková, M., Penezić, A., Katrlík, J. and Nedić, O. 2018. Structural and functional changes of fibrinogen due to aging. *International Journal of Biological Macromolecules*. **108**, pp.1028–1034.

Gorkun, O. V., Henschen-Edman, A.H., Ping, L.F. and Lord, S.T. 1998. Analysis of Aα251 fibrinogen: The αC domain has a role in polymerization, albeit more subtle than anticipated from the analogous proteolytic fragment X. *Biochemistry*. **37**(44), pp.15434–15441.

Gorkun, O. V., Veklich, Y.I., Weisel, J.W., Medved, L. V. and Henschen, A.H. 1994. Role of the αC Domains of Fibrin in Clot Formation. *Biochemistry*. **33**(22), pp.6986–6997.

Greenberg, C.S. and Shuman, M.A. 1982. The zymogen forms of blood coagulation factor XIII bind specifically to fibrinogen. *Journal of Biological Chemistry*. **257**(11), pp.6096–6101.

Grosjean, F., Batard, P., Jordan, M. and Wurm, F.M. 2002. S-phase synchronized CHO cells show elevated transfection efficiency and expression using CaPi. *Cytotechnology*. **38**(1–3), pp.57–62.

Guedes, A.F., Carvalho, F.A., Domingues, M.M., Macrae, F.L., McPherson, H.R., Sabban, A., Martins, I.C., Duval, C., Santos, N.C. and Ariëns, R.A. 2018b. Impact of γ'γ' fibrinogen interaction with red blood cells on fibrin clots. *Nanomedicine (London, England)*. **13**(19), pp.2491–2505.

Guedes, A.F., Carvalho, F.A., Domingues, M.M., Macrae, F.L., McPherson, H.R., Santos, N.C. and Ariëns, R.A.S. 2018a. Sensing adhesion forces between erythrocytes and γ' fibrinogen, modulating fibrin clot architecture and function. *Nanomedicine: Nanotechnology, Biology, and Medicine*. **14**(3), pp.909–918.

Gulledge, A.A., McShea, C., Schwartz, T., Koch, G. and Lord, S.T. 2003. Effects of hyperfibrinogenemia on vasculature of C57BL/6 mice with and without atherogenic diet. *Arteriosclerosis, Thrombosis, and Vascular Biology*. **23**(1), pp.130–135.

Gulledge, A.A., Rezaee, F., Verheijen, J.H. and Lord, S.T. 2001. A novel transgenic mouse model of hyperfibrinogenemia. *Thrombosis and Haemostasis*. **86**(2), pp.511–516.

Gunning, G.M., McArdle, K., Mirza, M., Duffy, S., Gilvarry, M. and Brouwer, P.A. 2018. Clot friction variation with fibrin content; implications for resistance to thrombectomy. *Journal of NeuroInterventional Surgery*. **10**(1), pp.34–38.

Hafiane, A. 2019. Vulnerable plaque, characteristics, detection, and potential therapies.

Journal of Cardiovascular Development and Disease. **6**(3), pp.1–24.

Haidaris, P., Francis, C., Sporn, L., Arvan, D., Collichio, F. and Marder, V. 1989. Megakaryocyte and hepatocyte origins of human fibrinogen biosynthesis exhibit hepatocyte-specific expression of gamma chain-variant polypeptides. *Blood*. **74**(2), pp.743–750.

Haidaris, P.J. and Courtney, M.A. 1990. Tissue-specific and ubiquitous expression of fibrinogen gamma-chain mRNA. *Blood coagulation & fibrinolysis : an international journal in haemostasis and thrombosis*. **1**(4–5), pp.433–7.

Hanss, M., Ffrench, P., Vinciguerra, C., Bertrands, M.A. and De Mazancourt, P. 2005. Four cases of hypofibrinogenemia associated with four novel mutations [2]. *Journal of Thrombosis and Haemostasis*. **3**(10), pp.2347–2349.

Hanss, M., Vergnes, C., Rugeri, L., Ffrench, P. and De Mazancourt, P. 2008. A new electrophoretic variant of fibrinogen associated with venous thromboembolism, fibrinogen Bordeaux Aα Arg439 → Cys. *Journal of Thrombosis and Haemostasis*. **6**(8), pp.1422–1424.

Hanss, M.M.L., Ffrench, P.O., Mornex, J.F., Chabuet, M., Biot, F., De Mazancourt, P. and Dechavanne, M. 2003. Two novel fibrinogen variants found in patients with pulmonary embolism and their families. *Journal of Thrombosis and Haemostasis*. **1**(6), pp.1251–1257.

Hantgan, R., Fowler, W., Erickson, H. and Hermans, J. 1980. Fibrin Assembly: A Comparison of Electron Microscopic and Light Scattering Results. *Thrombosis and Haemostasis*. **44**(03), pp.119–124.

Harrand, R. 2007. *The Viscoelastic Properties of Fibrin Clots Studied Using Magnetic Tweezers*. University of Leeds.

Hartwig, R. and Danishefsky, K.J. 1991. Studies on the assembly and secretion of fibrinogen. *The Journal of biological chemistry*. **266**(10), pp.6578–85.

Hayward, C.P.M. and Moffat, K.A. 2013. *Platelet Aggregation* [Online] Third Edit. Elsevier Inc. Available from: http://dx.doi.org/10.1016/B978-0-12-387837-3.00028-6.

von Heijne, G. 1991. Proline kinks in transmembrane α-helices. *Journal of Molecular Biology*. **218**(3), pp.499–503.

Helms, C.C., Ariëns, R.A.S., Uitte De Willige, S., Standeven, K.F. and Guthold, M. 2012. α-α Cross-links increase fibrin fiber elasticity and stiffness. *Biophysical Journal*. **102**(1), pp.168–175.

Helms, J., Tacquard, C., Severac, F., Leonard-Lorant, I., Ohana, M., Delabranche, X., Merdji, H., Clere-Jehl, R., Schenck, M., Fagot Gandet, F., Fafi-Kremer, S., Castelain, V., Schneider, F., Grunebaum, L., Anglés-Cano, E., Sattler, L., Mertes, P.M. and Meziani, F.

2020. High risk of thrombosis in patients with severe SARS-CoV-2 infection: a multicenter prospective cohort study. *Intensive Care Medicine*. **46**(6), pp.1089–1098.

Henriques de Gouveia, R., Van der Wal, A.C., Van der Loos, C.M. and Becker, A.E. 2002. Sudden unexpected death in young adults: Discrepancies between initiation of acute plaque complications and the onset of acute coronary death. *European Heart Journal*. **23**(18), pp.1433–1440.

Hethershaw, E.L., Cilia La Corte, A.L., Duval, C., Ali, M., Grant, P.J., Ariëns, R.A.S. and Philippou, H. 2014. The effect of blood coagulation factor XIII on fibrin clot structure and fibrinolysis. *Journal of Thrombosis and Haemostasis*. **12**(2), pp.197–205.

Hindle, M.S., Spurgeon, B.E.J., Cheah, L.T., Webb, B.A. and Naseem, K.M. 2021. Multidimensional flow cytometry reveals novel platelet subpopulations in response to prostacyclin. *Journal of Thrombosis and Haemostasis*. **19**(7), pp.1800–1812.

Hirashima, M., Imamura, T., Yano, K., Kawamura, R., Meta, A., Tokieda, Y. and Nakashima, T. 2016. High-level expression and preparation of recombinant human fibrinogen as biopharmaceuticals. *Journal of Biochemistry*. **159**(2), pp.261–270.

Hoffman, M. 2003. A cell-based coagulation factor Vlla and the role of. *Blood Reviews*. **17**, pp.S1–S5.

Hoffman, M. and Monroe, D.M. 2001. A cell-based model of hemostasis. *Thrombosis and Haemostasis*. **85**(6), pp.958–965.

Holm, B., Brosstad, F., Kierulf, P. and Godal, H.C. 1985. Polymerization properties of two normally circulating fibrinogens, HMW and LMW. Evidence that the COOH-terminal end of the a-chain is of importance for fibrin polymerization. *Thrombosis research*. **39**(5), pp.595–606.

Holm, B., Nilsen, D.W.T. and Godal, H.C. 1986. Evidence that low molecular fibrinogen (LMW) is formed in man by degradation of high molecular weight fibrinogen (HMW). *Thrombosis Research*. **41**(6), pp.879–884.

Holmbäck, K., Danton, M.J.S., Suh, T.T., Daugherty, C.C. and Degen, J.L. 1996. Impaired platelet aggregation and sustained bleeding in mice lacking the fibrinogen motif bound by integrin α(IIb)β3. *EMBO Journal*. **15**(21), pp.5760–5771.

Homer, V.M., Mullin, J.L., Brennan, S.O., Barr, A. and George, P.M. 2003. Novel Aα chain truncation (fibrinogen Perth) resulting in low expression and impaired fibrinogen polymerization. *Journal of Thrombosis and Haemostasis*. **1**(6), pp.1245–1250.

Houser, J.R., Hudson, N.E., Ping, L., O'Brien, E.T., Superfine, R., Lord, S.T. and Falvo, M.R. 2010. Evidence that αC region is origin of low modulus, high extensibility, and strain stiffening in fibrin fibers. *Biophysical Journal*. **99**(9), pp.3038–3047.

Hoylaerts, M., Rijken, D.C., Lijnen, H.R. and Collen, D. 1982. Kinetics of the activation of plasminogen by human tissue plasminogen activator. Role of fibrin. *Journal of Biological Chemistry*. **257**(6), pp.2912–2919.

Huang, S., Mulvihill, E.R., Farrell, D.H., Chung, D.W. and Davie, E.W. 1993. Biosynthesis of human fibrinogen. Subunit interactions and potential intermediates in the assembly. *The Journal of biological chemistry*. **268**(12), pp.8919–26.

Hudson, N.E. 2017. Biophysical Mechanisms Mediating Fibrin Fiber Lysis. *BioMed Research International*. **2017**.

Hunt, B.J. 2009. The prevention of hospital-acquired venous thromboembolism in the United Kingdom. *British Journal of Haematology*. **144**(5), pp.642–652.

Hur, W.S., Paul, D.S., Bouck, E.G., Negron, O., Mwiza, J.M.N., Poole, L.G., Cline-Fedewa, H.M., Clark, E.G., Juang, L.J., Leung, J., Kastrup, C.J., Ugarova, T.P., Wolberg, A.S., Luyendyk, J.P., Bergmeier, W. and Flick, M.J. 2021. Hypofibrinogenemia with preserved hemostasis and protection from thrombosis in mice with a Fga truncation mutation . *Blood*.

Van Hylckama Vlieg, A., Christiansen, S.C., Luddington, R., Cannegieter, S.C., Rosendaal, F.R. and Baglin, T.P. 2007. Elevated endogenous thrombin potential is associated with an increased risk of a first deep venous thrombosis but not with the risk of recurrence. *British Journal of Haematology*. **138**(6), pp.769–774.

Ikeda, M., Arai, S., Mukai, S., Takezawa, Y., Terasawa, F. and Okumura, N. 2015. Novel heterozygous dysfibrinogenemia, Sumida (AαC472S), showed markedly impaired lateral aggregation of protofibrils and mildly lower functional fibrinogen levels. *Thrombosis Research*. **135**(4), pp.710–717.

Jayapal, K.P., Wlaschin, K.F., Hu, W.S. and Yap, M.G.S. 2007. Recombinant protein therapeutics from CHO Cells - 20 years and counting. *Chemical Engineering Progress*. **103**(10), pp.40–47.

Jolugbo, P. and Ariëns, R.A.S. 2021. Thrombus Composition and Efficacy of Thrombolysis and Thrombectomy in Acute Ischemic Stroke. *Stroke*. **52**(3), pp.1131–1142.

Kant, J.A., Fornace, A.J., Saxe, D., Simon, M.I., McBride, O.W. and Crabtree, G.R. 1985. Evolution and organization of the fibrinogen locus on chromosome 4: Gene duplication accompanied by transposition and inversion. *Proceedings of the National Academy of Sciences of the United States of America*. **82**(8), pp.2344–2348.

Kaptoge, S., White, I.R., Thompson, S.G., Wood, A.M., Lewington, S., Lowe, G.D.O., Danesh, J., Kostis, J.B., Wilson, A.C., Folsom, A.R., Wu, K., Chambless, L., Benderly, M., Goldbourt, U., Willeit, J., Kiechl, S., Yarnell, J.W.G., Sweetnam, P.M., Elwood, P.C.,

Cushman, M., Psaty, B.M., Tracy, R.P., Tybjærg-Hansen, A., Haverkate, F., de Maat, M.P.M., Fowkes, F.G.R., Lee, A.J., Smith, F.B., Salomaa, V., Harald, K., Rasi, V., Vahtera, E., Jousilahti, P., Pekkanen, J., D'Agostino, R., Kannel, W.B., Wilson, P.W.F., Tofler, G., Levy, D., Marchioli, R., Valagussa, F., Rosengren, A., Wilhelmsen, L., Lappas, G., Eriksson, H., Cremer, P., Nagel, D., Curb, J.D., Rodriguez, B., Yano, K., Salonen, J.T., Nyyssönen, K., Tuomainen, T.P., Hedblad, B., Engström, G., Berglund, G., Loewel, H., Koenig, W., Hense, H.W., Meade, T.W., Cooper, J.A., Stavola, B.D., Knottenbelt, C., Miller, G.J., Bauer, K.A., Rosenberg, R.D., Sato, S., Kitamura, A., Naito, Y., Iso, H., Palosuo, T., Ducimetiere, P., Amouyel, P., Arveiler, D., Evans, A.E., Ferrieres, J., Juhan-Vague, I., Bingham, A., Schulte, H., Assmann, G., Cantin, B., Lamarche, B., Després, J.P., Dagenais, G.R., Tunstall-Pedoe, H., Woodward, M., Ben-Shlomo, Y., Davey Smith, G., Palmieri, V., Yeh, J.L., Rudnicka, A., Brennan, P., Ridker, P., Rodeghiero, F., Tosetto, A., Shepherd, J., Ford, I., Robertson, M., Brunner, E., Shipley, M., Feskens, E.J.M., Kromhout, D., Collins, R., Angelantonio, E.D., Sarwar, N., Walker, M. and Watson, S. 2007. Associations of plasma fibrinogen levels with established cardiovascular disease risk factors, inflammatory markers, and other characteristics: Individual participant meta-analysis of 154,211 adults in 31 prospective studies. *American Journal of Epidemiology*. **166**(8), pp.867–879.

Kaufmann, H., Mazur, X., Fussenegger, M. and Bailey, J.E. 1999. Influence of low temperature on productivity, proteome and protein phosphorylation of CHO cells. *Biotechnology and Bioengineering*. **63**(5), pp.573–582.

Keavney, B., Danesh, J., Parish, S., Palmer, A., Clark, S., Youngman, L., Delépine, M., Lathrop, M., Peto, R. and Collins, R. 2006. Fibrinogen and coronary heart disease: Test of causality by 'Mendelian randomization'. *International Journal of Epidemiology*. **35**(4), pp.935–943.

Khismatullin, R.R., Nagaswami, C., Shakirova, A.Z., Vrtková, A., Procházka, V., Gumulec, J., Mačák, J., Litvinov, R.I. and Weisel, J.W. 2020. Quantitative Morphology of Cerebral Thrombi Related to Intravital Contraction and Clinical Features of Ischemic Stroke. *Stroke*. (December), pp.3640–3650.

Kim, O. V., Litvinov, R.I., Alber, M.S. and Weisel, J.W. 2017. Quantitative structural mechanobiology of platelet-driven blood clot contraction. *Nature Communications*. **8**(1), pp.1–10.

Kim, O. V., Litvinov, R.I., Weisel, J.W. and Alber, M.S. 2014a. Structural basis for the nonlinear mechanics of fibrin networks under compression. *Biomaterials*. **35**(25), pp.6739–6749.

Kim, P.Y., Vu, T.T., Leslie, B.A., Stafford, A.R., Fredenburgh, J.C. and Weitz, J.I. 2014b.

Reduced plasminogen binding and delayed activation render γ'-fibrin more resistant to lysis than γA-fibrin. *The Journal of biological chemistry*. **289**(40), pp.27494–503.

Kimura, S. and Aoki, N. 1986. Cross-linking site in fibrinogen for α2-plasmin inhibitor. *Journal of Biological Chemistry*. **261**(33), pp.15591–15595.

Klok, F.A., Kruip, M.J.H.A., van der Meer, N.J.M., Arbous, M.S., Gommers, D.A.M.P.J., Kant, K.M., Kaptein, F.H.J., van Paassen, J., Stals, M.A.M., Huisman, M. V and Endeman, H. 2020. Incidence of thrombotic complications in critically ill ICU patients with COVID-19. *Thrombosis research*. **191**(January), pp.145–147.

Klovaite, J., Nordestgaard, B.G., Tybjrg-Hansen, A. and Benn, M. 2013. Elevated fibrinogen levels are associated with risk of pulmonary embolism, but not with deep venous thrombosis. *American Journal of Respiratory and Critical Care Medicine*. **187**(3), pp.286–293.

Klykov, O., Van Der Zwaan, C., Heck, A.J.R., Meijer, A.B. and Scheltema, R.A. 2020. Missing regions within the molecular architecture of human fibrin clots structurally resolved by XL-MS and integrative structural modeling. *Proceedings of the National Academy of Sciences of the United States of America*. **117**(4), pp.1976–1987.

Kollman, J.M., Pandi, L., Sawaya, M.R., Riley, M. and Doolittle, R.F. 2009. Crystal structure of human fibrinogen. *Biochemistry*. **48**(18), pp.3877–3886.

Koopman, J., Haverkate, F., Grimbergen, J., Egbring, R. and Lord, S.T.S.T. 1992. Fibrinogen Marburg: a homozygous case of dysfibrinogenemia, lacking amino acids A alpha 461-610 (Lys 461 AAA-->stop TAA). *Blood*. **80**(8), pp.1972–1979.

Koopman, J., Haverkate, F., Grimbergen, J., Lord, S.T., Mosesson, M.W., DiOrio, J.P., Siebenlist, K.S., Legrand, C., Soria, J., Soria, C. and Caen, J.P. 1993. Molecular basis for fibrinogen Dusart (Aα 554 Arg → Cys) and its association with abnormal fibrin polymerization and thrombophilia. *Journal of Clinical Investigation*. **91**(4), pp.1637–1643.

Kotlín, R., Suttnar, J., Čápová, I., Hrachovinová, I., Urbánková, M. and Dyr, J.E. 2012. Fibrinogen Šumperk II: Dysfibrinogenemia in an individual with two coding mutations. *American Journal of Hematology*. **87**(5), pp.555–557.

Kotzé, R.C.M., Ariëns, R.A.S., De Lange, Z. and Pieters, M. 2014. CVD risk factors are related to plasma fibrin clot properties independent of total and or γ' fibrinogen concentration. *Thrombosis Research*. **134**(5), pp.963–969.

Kramer, M.C.A., Van Der Wal, A.C., Koch, K.T., Ploegmakers, J.P.H.M., Van Der Schaaf, R.J., Henriques, J.P.S., Baan, J., Rittersma, S.Z.H., Vis, M.M., Piek, J.J., Tijssen, J.G.P. and De Winter, R.J. 2008. Presence of older thrombus is an independent predictor of long-term

mortality in patients with ST-elevation myocardial infarction treated with thrombus aspiration during primary percutaneous coronary intervention. *Circulation*. **118**(18), pp.1810–1816.

Lam, W.A., Chaudhuri, O., Crow, A., Webster, K.D., Li, T. De, Kita, A., Huang, J. and Fletcher, D.A. 2011. Mechanics and contraction dynamics of single platelets and implications for clot stiffening. *Nature Materials*. **10**(1), pp.61–66.

Lancellotti, S., Rutella, S., De Filippis, V., Pozzi, N., Rocca, B. and De Cristofaro, R. 2008. Fibrinogen-elongated γ chain inhibits thrombin-induced platelet response, hindering the interaction with different receptors. *Journal of Biological Chemistry*. **283**(44), pp.30193–30204.

Laurens, N., Koolwijk, P. and de Maat, M.P. 2006. Fibrin structure and wound healing. *Journal of thrombosis and haemostasis : JTH*. **4**(5), pp.932–939.

Lee, Y.U., Lee, A.Y., Humphrey, J.D. and Rausch, M.K. 2015. Histological and biomechanical changes in a mouse model of venous thrombus remodeling. *Biorheology*. **52**(3), pp.235–245.

Lefebvre, P., Velasco, P.T., Dear, A., Lounes, K.C., Lord, S.T., Brennan, S.O., Green, D. and Lorand, L. 2004. Severe hypodysfibrinogenemia in compound heterozygotes of the fibrinogen AalphaIVS4 + 1G>T mutation and an AalphaGln328 truncation (fibrinogen Keokuk). *Blood*. **103**(7), pp.2571–6.

Levrat, E., Aboukhamis, I., De Moerloose, P., Farho, J., Chamaa, S., Reber, G., Fort, A. and Neerman-Arbez, M. 2011. A novel frameshift mutation in FGA (c.1846 del A) leading to congenital afibrinogenemia in a consanguineous Syrian family. *Blood Coagulation and Fibrinolysis*. **22**(2), pp.148–150.

Levy, J.H., Welsby, I. and Goodnough, L.T. 2014. Fibrinogen as a therapeutic target for bleeding: a review of critical levels and replacement therapy. *Transfusion*. **54**(5), pp.1389–405; quiz 1388.

Li, J.F., Lin, Y., Yang, Y.H., Gan, H.L., Liang, Y., Liu, J., Yang, S.Q., Zhang, W.J., Cui, N., Zhao, L., Zhai, Z.G., Wang, J. and Wang, C. 2013. Fibrinogen Aα Thr312Ala Polymorphism Specifically Contributes to Chronic Thromboembolic Pulmonary Hypertension by Increasing Fibrin Resistance. *PLoS ONE*. **8**(7), pp.1–7.

Li, R. and Diamond, S.L. 2014. Detection of platelet sensitivity to inhibitors of COX-1, P2Y1, and P2Y12 using a whole blood microfluidic flow assay. *Thrombosis Research*. **133**(2), pp.203–210.

Libby, P., Buring, J.E., Badimon, L., Hansson, G.K., Deanfield, J., Bittencourt, M.S., Tokgözoğlu, L. and Lewis, E.F. 2019. Atherosclerosis. *Nature Reviews Disease Primers*.

5(1), pp.1–18.

Lijnen, H.R. 2001. Elements of the fibrinolytic system. *Annals of the New York Academy of Sciences*. **936**, pp.226–236.

Lijnen, H.R., Van Hoef, B., Beelen, V. and Collen, D. 1994. Characterization of the Murine Plasma Fibrinolytic System. *European Journal of Biochemistry*. **224**(3), pp.863–871.

Lin, C., Chen, Y., Chen, B., Zheng, K., Luo, X. and Lin, F. 2020. D-Dimer Combined with Fibrinogen Predicts the Risk of Venous Thrombosis in Fracture Patients. *Emergency Medicine International*. **2020**, pp.1–7.

Litvinov, R.I., Evtugina, N.G., Peshkova, A.D., Safiullina, S.I., Andrianova, I.A., Khabirova, A.I., Nagaswami, C., Khismatullin, R.R., Sannikova, S.S. and Weisel, J.W. 2021. Altered platelet and coagulation function in moderate-to-severe COVID-19. *Scientific Reports*. **11**(1), pp.1–14.

Litvinov, R.I., Faizullin, D.A., Zuev, Y.F. and Weisel, J.W. 2012. The α-helix to β-sheet transition in stretched and compressed hydrated fibrin clots. *Biophysical Journal*. **103**(5), pp.1020–1027.

Litvinov, R.I., Farrell, D.H., Weisel, J.W. and Bennett, J.S. 2016. The platelet integrin αIIbβ3 differentially interacts with fibrin versus fibrinogen. *Journal of Biological Chemistry*. **291**(15), pp.7858–7867.

Litvinov, R.I., Khismatullin, R.R., Shakirova, A.Z., Litvinov, T.R., Nagaswami, C., Peshkova, A.D. and Weisel, J.W. 2018. Morphological Signs of Intravital Contraction (Retraction) of Pulmonary Thrombotic Emboli. *BioNanoScience*. **8**(1), pp.428–433.

Litvinov, R.I., Yakovlev, S., Tsurupa, G., Gorkun, O. V, Medved, L. and Weisel, J.W. 2007. Direct evidence for specific interactions of the fibrinogen alphaC-domains with the central E region and with each other. *Biochemistry*. **46**(31), pp.9133–42.

Liu, W., Carlisle, C.R., Sparks, E.A. and Guthold, M. 2010. The mechanical properties of single fibrin fibers. *Journal of thrombosis and haemostasis : JTH*. **8**(5), pp.1030–6.

Liu, W., Jawerth, L.M., Sparks, E.A., Falvo, M.R., Hantgan, R.R., Superfine, R., Lord, S.T. and Guthold, M. 2006. Fibrin fibers have extraordinary extensibility and elasticity. *Science (New York, N.Y.)*. **313**(5787), p.634.

Lodigiani, C., Iapichino, G., Carenzo, L., Cecconi, M., Ferrazzi, P., Sebastian, T., Kucher, N., Studt, J.D., Sacco, C., Alexia, B., Sandri, M.T. and Barco, S. 2020. Venous and arterial thromboembolic complications in COVID-19 patients admitted to an academic hospital in Milan, Italy. *Thrombosis Research*. **191**(January), pp.9–14.

Longstaff, C. and Kolev, K. 2015. Basic mechanisms and regulation of fibrinolysis. *Journal of Thrombosis and Haemostasis*. **13**(S1), pp.S98–S105.

López-Terrada, D., Cheung, S.W., Finegold, M.J. and Knowles, B.B. 2009. Hep G2 is a hepatoblastoma-derived cell line. *Human Pathology*. **40**(10), pp.1512–1515.

Lord, S.T. 1985. Expression of a Cloned Human Fibrinogen cDNA in Escherichia coli: Synthesis of an a Alpha Polypeptide. *Dna*. **4**(1), pp.33–38.

Lord, S.T., Binnie, C.G., Hettasch, J.M. and Strickland, E. 1993. Purification and characterization of recombinant human fibrinogen. *Blood coagulation & fibrinolysis : an international journal in haemostasis and thrombosis*. **4**(1), pp.55–9.

Lovely, R.S., Boshkov, L.K., Marzec, U.M., Hanson, S.R. and Farrell, D.H. 2007. Fibrinogen γ' chain carboxy terminal peptide selectively inhibits the intrinsic coagulation pathway. *British Journal of Haematology*. **139**(3), pp.494–503.

Lovely, R.S., Falls, L.A., Al-Mondhiry, H.A., Chambers, C.E., Sexton, G.J., Ni, H. and Farrell, D.H. 2002. Association of γA/γ' fibrinogen levels and coronary artery disease. *Thrombosis and Haemostasis*. **88**(1), pp.26–31.

Lovely, R.S., Moaddel, M. and Farrell, D.H. 2003. Fibrinogen γ' chain binds thrombin exosite II. *Journal of Thrombosis and Haemostasis*. **1**(1), pp.124–131.

Lu, G., Broze, G.J. and Krishnaswamy, S. 2004. Formation of factors IXa and Xa by the extrinsic pathway: Differential regulation by tissue factor pathway inhibitor and antithrombin III. *Journal of Biological Chemistry*. **279**(17), pp.17241–17249.

Lynch, S.R., Laverty, S.M., Bannish, B.E. and Hudson, N.E. 2022. Microscale structural changes of individual fibrin fibers during fibrinolysis. *Acta biomaterialia*. (xxxx).

Macek, B., Forchhammer, K., Hardouin, J., Weber-Ban, E., Grangeasse, C. and Mijakovic, I. 2019. Protein post-translational modifications in bacteria. *Nature reviews. Microbiology*. **17**(11), pp.651–664.

MacFarlane, R.G. 1964. An Enzyme Cascade in the Blood Clotting Mechanism, and its Function as a Biochemical Amplifier. *Nature*. **202**(4931), pp.498–499.

Machlus, K.R., Cardenas, J.C., Church, F.C. and Wolberg, A.S. 2011. Causal relationship between hyperfibrinogenemia, thrombosis, and resistance to thrombolysis in mice. *Blood*. **117**(18), pp.4953–4963.

Macrae, F.L., Domingues, M.M., Casini, A. and Ariëns, R.A.S. 2016. The (Patho)physiology of Fibrinogen γ'. *Seminars in thrombosis and hemostasis*. **42**(4), pp.344–55.

Macrae, F.L., Duval, C., Papareddy, P., Baker, S.R., Yuldasheva, N., Kearney, K.J., McPherson, H.R., Asquith, N., Konings, J., Casini, A., Degen, J.L., Connell, S.D., Philippou, H., Wolberg, A.S., Herwald, H. and Ariëns, R.A.S. 2018. A fibrin biofilm covers blood clots and protects from microbial invasion. *Journal of Clinical Investigation*. **128**(8), pp.3356–3368.

Macrae, F.L., Swieringa, F., Heemskerk, J.W.M. and Ariëns, R.A.S. 2021. High fibrinogen γ' levels in patient plasma increase clot formation at arterial and venous shear. *Blood advances*. **5**(17), pp.3468–3477.

Maekawa, H., Yamazumi, K., Muramatsu -i., S., Kaneko, M., Hirata, H., Takahashi, N., De Bosch, N.B., Carvajal, Z., Ojeda, A., Arocha-Pinango, C.L. and Matsuda, M. 1991. An Aα Ser-434 to N-glycosylated Asn substitution in a dysfibrinogen, fibrinogen caracas II, characterized by impaired fibrin gel formation. *Journal of Biological Chemistry*. **266**(18), pp.11575–11581.

Mammadova-Bach, E., Ollivier, V., Loyau, S., Schaff, M., Dumont, B., Favier, R., Freyburger, G., Latger-Cannard, V., Nieswandt, B., Gachet, C., Mangin, P.H. and Jandrot-Perrus, M. 2015. Platelet glycoprotein VI binds to polymerized fibrin and promotes thrombin generation. *Blood*. **126**(5), pp.683–691.

Maners, J., Gill, D., Pankratz, N., Laffan, M.A., Wolberg, A.S., de Maat, M.P.M., Ligthart, S., Tang, W., Ward-Caviness, C.K., Fornage, M., Debette, S., Dichgans, M., McKnight, B., Boerwinkle, E., Smith, N.L., Morrison, A.C., Dehghan, A. and de Vries, P.S. 2020. A mendelian randomization of γ' and total fibrinogen levels in relation to venous thromboembolism and ischemic stroke. *Blood*. **136**(26), pp.3062–3069.

Mannila, M.N., Lovely, R.S., Kazmierczak, S.C., Eriksson, P., Samnegård, A., Farrell, D.H., Hamsten, A. and Silveira, A. 2007. Elevated plasma fibrinogen γ' concentration is associated with myocardial infarction: Effects of variation in fibrinogen genes and environmental factors. *Journal of Thrombosis and Haemostasis*. **5**(4), pp.766–773.

Marchi, R., Carvajal, Z., Meyer, M., Soria, J., Ruiz-Saez, A., Arocha-Piñango, C.L. and Weisel, J.W. 2006. Fibrinogen Guarenas, an abnormal fibrinogen with an Aα-chain truncation due to a nonsense mutation at Aα 467 Glu (GAA) → stop (TAA). *Thrombosis Research*. **118**(5), pp.637–650.

Marchi, R., Lundberg, U., Grimbergen, J., Koopman, J., Torres, A., De Bosch, N.B., Haverkate, F. and Arocha Piñango, C.L. 2000. Fibrinogen Caracas V, an abnormal fibrinogen with an Aα 532 Ser→Cys substitution associated with thrombosis. *Thrombosis and Haemostasis*. **84**(2), pp.263–270.

Marchi, R., Meyer, M., De Bosch, N., Soria, J., Arocha-Piñango, C.L. and Weisel, J.W. 2004. Biophysical characterization of fibrinogen Caracas I with an Aα-chain truncation at Aα-466 Ser: Identification of the mutation and biophysical characterization of properties of clots from plasma and purified fibrinogen. *Blood Coagulation and Fibrinolysis*. **15**(4), pp.285–293.

Marchi, R.C., Carvajal, Z., Boyer-Neumann, C., Anglés-Cano, E. and Weisel, J.W. 2006.

Functional characterization of fibrinogen Bicêtre II: A γ 308 Asn→Lys mutation located near the fibrin D:D interaction sites. *Blood Coagulation and Fibrinolysis*. **17**(3), pp.193–201.

Marder, V.J. and Francis, C.W. 1983. Plasmin degradation of cross-linked fibrin. *Annals of the New York Academy of Sciences*. **408**, pp.397–406.

Margaglione, M., Vecchione, G., Santacroce, R., D'Angelo, F., Casetta, B., Papa, M.L., Grandone, E. and Di Minno, G. 2001. A frameshift mutation in the human fibrinogen Aα-chain gene (Aα[499]Ala frameshift stop) leading to dysfibrinogen San Giovanni Rotondo. *Thrombosis and Haemostasis*. **86**(6), pp.1483–1488.

Martinez, M.R., Cuker, A., Mills, A.M., Crichlow, A., Lightfoot, R.T., Chernysh, I.N., Nagaswami, C., Weisel, J.W. and Ischiropoulos, H. 2014. Enhanced lysis and accelerated establishment of viscoelastic properties of fibrin clots are associated with pulmonary embolism. *American Journal of Physiology - Lung Cellular and Molecular Physiology*. **306**(5), pp.397–404.

Mazur, P., Sobczyński, R., Ząbczyk, M., Babiarczyk, P., Sadowski, J. and Undas, A. 2013. Architecture of fibrin network inside thrombotic material obtained from the right atrium and pulmonary arteries: Flow and location matter. *Journal of Thrombosis and Thrombolysis*. **35**(1), pp.127–129.

McMichael, M. 2012. New Models of Hemostasis. *Topics in Companion Animal Medicine*. **27**(2), pp.40–45.

McNeil, J.S. and Kleiman, A.M. 2017. Fulminant Hyperfibrinolysis Diagnosed by Rotational Thromboelastometry. *Anesthesiology*. **127**(5), pp.892–892.

Medcalf, R.L. and Keragala, C.B. 2021. The Fibrinolytic System: Mysteries and Opportunities. *HemaSphere*.

Medved, L. and Nieuwenhuizen, W. 2003. Molecular mechanisms of initiation of fibrinolysis by fibrin. *Thrombosis and Haemostasis*. **89**(3), pp.409–419.

Medved, L. V., Gorkun, O. V. and Privalov, P.L. 1983. Structural organization of C-terminal parts of fibrinogen Aα-chains. *FEBS Letters*. **160**(1–2), pp.291–295.

Medved, L. and Weisel, J.W. 2021. The story of the fibrin(ogen) αC-domains: evolution of our view on their structure and interactions. *Thrombosis and Haemostasis*.

Medved, L., Weisel, J.W. and Fibrinogen and Factor XIII Subcommittee of Scientific Standardization Committee of International Society on Thrombosis and Haemostasis 2009. Recommendations for nomenclature on fibrinogen and fibrin. *Journal of thrombosis and haemostasis : JTH*. **7**(2), pp.355–9.

Di Meglio, L., Desilles, J.P., Ollivier, V., Nomenjanahary, M.S., Di Meglio, S., Deschildre, C.,

Loyau, S., Olivot, J.M., Blanc, R., Piotin, M., Bouton, M.C., Michel, J.B., Jandrot-Perrus, M., Ho-Tin-Noé, B. and Mazighi, M. 2019. Acute ischemic stroke thrombi have an outer shell that impairs fibrinolysis. *Neurology*. **93**(18), pp.E1686–E1698.

Mfoumou, E., Tripette, J., Blostein, M. and Cloutier, G. 2014. Time-dependent hardening of blood clots quantitatively measured in vivo with shear-wave ultrasound imaging in a rabbit model of venous thrombosis. *Thrombosis Research*. **133**(2), pp.265–271.

Middeldorp, S., Coppens, M., Haaps, T.F., Foppen, M., Vlaar, A.P., Müller, M.C.A., Bouman, C.C.S., Beenen, L.F.M., Kootte, R.S., Heijmans, J., Smits, L.P., Bonta, P.I. and Es, N. 2020. Incidence of venous thromboembolism in hospitalized patients with COVID-19. *Journal of Thrombosis and Haemostasis*. **18**(8), pp.1995–2002.

Migliacci, R., Becattini, C., Pesavento, R., Davi, G., Vedovati, M.C., Guglielmini, G., Falcinelli, E., Ciabattoni, G., Valle, F.D., Prandoni, P., Agnelli, G. and Gresele, P. 2007. Endothelial dysfunction in patients with spontaneous venous thromboembolism. *Haematologica*. **92**(6), pp.812–818.

Milosevic, I., Korac, M., Zerjav, S., Urosevic, A., Lavadinovic, L., Milosevic, B. and Jevtovic, D. 2013. Non-specific inflammatory parameters in patients with pandemic H1N1 influenza. *Biomedicine and Pharmacotherapy*. **67**(3), pp.218–220.

Minet, C., Lugosi, M., Savoye, P.Y., Menez, C., Ruckly, S., Bonadona, A., Schwebel, C., Hamidfar-Roy, R., Dumanoir, P., Ara-Somohano, C., Ferretti, G.R. and Timsit, J.F. 2012. Pulmonary embolism in mechanically ventilated patients requiring computed tomography: Prevalence, risk factors, and outcome. *Critical Care Medicine*. **40**(12), pp.3202–3208.

Mitchell, J.L., Lionikiene, A.S., Fraser, S.R., Whyte, C.S., Booth, N.A. and Mutch, N.J. 2014. Functional factor XIII-A is exposed on the stimulated platelet surface. *Blood*. **124**(26), pp.3982–3990.

Moaddel, M., Farrell, D.H., Daugherty, M.A. and Fried, M.G. 2000. Interactions of human fibrinogens with factor XIII: Roles of calcium and the γ' peptide. *Biochemistry*. **39**(22), pp.6698–6705.

Monaldini, L., Asselta, R., Duga, S., Peyvandi, F., Karimi, M., Malcovati, M. and Tenchini, M.L. 2007. Mutational screening of six afibrinogenemic patients: Identification and characterization of four novel molecular defects. *Thromb Haemost*. **97**(04), pp.546–551.

Morrissey, J.H. 2012. Polyphosphate: a link between platelets, coagulation and inflammation. *International journal of hematology*. **95**(4), pp.346–52.

Mosesson, M.W. 2005. Fibrinogen and fibrin structure and functions. *Journal of thrombosis*

and haemostasis : JTH. **3**(8), pp.1894–904.

Mosesson, M.W., Cooley, B.C., Hernandez, I., Diorio, J.P. and Weiler, H. 2009. Thrombosis risk modification in transgenic mice containing the human fibrinogen thrombin-binding γ′ chain sequence. *Journal of Thrombosis and Haemostasis*. **7**(1), pp.102–110.

Mosesson, M.W. and Finlayson, J.S. 1963. Biochemical and chromatographic studies of certain activities associated with human fibrinogen preparations. *The Journal of clinical investigation*. **42**(6), pp.747–55.

Mosesson, M.W., Finlayson, J.S. and Umfleet, R.A. 1972. Human Fibrinogen Heterogeneities. *Journal of Biological Chemistry*. **247**(16), pp.5223–5227.

Mosesson, M.W., Hernandez, I., Raife, T.J., Medved, L., Yakovlev, S., Simpson-Haidaris, P.J., Uitte De Willige, S. and Bertina, R.M. 2007. Plasma fibrinogen γ′ chain content in the thrombotic microangiopathy syndrome. *Journal of Thrombosis and Haemostasis*. **5**(1), pp.62–69.

Mosesson, M.W., Siebenlist, K.R. and Meh, D.A. 2001. The structure and biological features of fibrinogen and fibrin. *Annals of the New York Academy of Sciences*. **936**, pp.11–30.

Mouapi, K.N., Bell, J.D., Smith, K.A., Ariëns, R.A.S., Philippou, H. and Maurer, M.C. 2016. Ranking reactive glutamines in the fibrinogen αC region that are targeted by blood coagulant factor XIII. *Blood*. **127**(18), pp.2241–2248.

Mukai, S., Nagata, K., Ikeda, M., Arai, S., Sugano, M., Honda, T. and Okumura, N. 2016. Genetic analyses of novel compound heterozygous hypodysfibrinogenemia, Tsukuba I: FGG c.1129 + 62_65 del AATA and FGG c.1299 + 4 del A. *Thrombosis Research*. **148**, pp.111–117.

Mutch, Nicola J., Engel, R., De Willige, S.U., Philippou, H. and Ariëns, R.A.S. 2010b. Polyphosphate modifies the fibrin network and down-regulates fibrinolysis by attenuating binding of tPA and plasminogen to fibrin. *Blood*. **115**(19), pp.3980–3988.

Mutch, N. J., Koikkalainen, J.S., Fraser, S.R., Duthie, K.M., Griffin, M., Mitchell, J., Watson, H.G. and Booth, N.A. 2010a. Model thrombi formed under flow reveal the role of factor XIII-mediated cross-linking in resistance to fibrinolysis. *Journal of Thrombosis and Haemostasis*. **8**(9), pp.2017–2024.

Mutch, N.J., Robbie, L.A. and Booth, N.A. 2001. Human thrombi contain an abundance of active thrombin. *Thrombosis and Haemostasis*. **86**(4), pp.1028–1034.

Ndrepepa, G., Braun, S., King, L., Fusaro, M., Keta, D., Cassese, S., Tada, T., Schömig, A. and Kastrati, A. 2013. Relation of fibrinogen level with cardiovascular events in patients with coronary artery disease. *American Journal of Cardiology*. **111**(6), pp.804–810.

Nechipurenko, D.Y., Receveur, N., Yakimenko, A.O., Shepelyuk, T.O., Yakusheva, A.A.,

Kerimov, R.R., Obydennyy, S.I., Eckly, A., Léon, C., Gachet, C., Grishchuk, E.L., Ataullakhanov, F.I., Mangin, P.H. and Panteleev, M.A. 2019. Clot Contraction Drives the Translocation of Procoagulant Platelets to Thrombus Surface. *Arteriosclerosis, Thrombosis, and Vascular Biology*. **39**(1), pp.37–47.

Neerman-Arbez, M. and de Moerloose, P. 2007. Mutations in the fibrinogen gene cluster accounting for congenital afibrinogenemia: an update and report of 10 novel mutations. *Human mutation*. **28**(6), pp.540–53.

Neerman-Arbez, M., De Moerloose, P., Bridel, C., Honsberger, A., Schönbörner, A., Rossier, C., Peerlinck, K., Claeyssens, S., Di Michele, D., D'Oiron, R., Dreyfus, M., Laubriat-Bianchin, M., Dieval, J., Antonarakis, S.E. and Morris, M.A. 2000. Mutations in the fibrinogen Aα gene account for the majority of cases of congenital afibrinogenemia. *Blood*. **96**(1), pp.149–152.

Neerman-Arbez, M., De Moerloose, P., Honsberger, A., Parlier, G., Arnuti, B., Biron, C., Borg, J.Y., Eber, S., Meili, E., Peter-Salonen, K., Ripoll, L., Vervel, C., D'Oiron, R., Staeger, P., Antonarakis, S.E. and Morris, M.A. 2001. Molecular analysis of the fibrinogen gene cluster in 16 patients with congenital afibrinogenemia: Novel truncating mutations in the FGA and FGG genes. *Human Genetics*. **108**(3), pp.237–240.

Neeves, K.B., Illing, D.A.R. and Diamond, S.L. 2010. Thrombin flux and wall shear rate regulate fibrin fiber deposition state during polymerization under flow. *Biophysical Journal*. **98**(7), pp.1344–1352.

Nieuwenhuizen, W. and Gravesen, M. 1981. Anticoagulant and calcium-binding properties of high molecular weight derivatives of human fibrinogen, produced by plasmin (fragments X). *BBA - Protein Structure*. **668**(1), pp.81–88.

Nowak-Gött, U., Weiler, H., Hernandez, I., Thedieck, S., Seehafer, T., Schulte, T. and Stoll, M. 2009. Fibrinogen α and γ genes and factor VLeiden in children with thromboembolism: Results from 2 family-based association studies. *Blood*. **114**(9), pp.1947–1953.

Omarova, F., Uitte De Willige, S., Ariëns, R.A.S., Rosing, J., Bertina, R.M. and Castoldi, E. 2013. Inhibition of thrombin-mediated factor V activation contributes to the anticoagulant activity of fibrinogen γ'. *Journal of Thrombosis and Haemostasis*. **11**(9), pp.1669–1678.

Omarova, F., Uitte de Willige, S., Simioni, P., Ariëns, R.A.S., Bertina, R.M., Rosing, J. and Castoldi, E. 2014. Fibrinogen γ' increases the sensitivity to activated protein C in normal and factor V Leiden plasma. *Blood*. **124**(9), pp.1531–8.

Owen, J., Friedman, K.D., Grossman, B.A., Wilkins, C., Berke, A.D. and Powers, E.R. 1987. Quantitation of fragment X formation during thrombolytic therapy with streptokinase and tissue plasminogen activator. *Journal of Clinical Investigation*. **79**(6), pp.1642–

1647.

Page, E.M. and Ariëns, R.A.S. 2021. Mechanisms of thrombosis and cardiovascular complications in COVID-19. *Thrombosis Research*. **200**(January), pp.1–8.

Park, R., Doh, H.J., An, S.S.A., Choi, J.R., Chung, K.H. and Song, K.S. 2006. Anovel fibrinogen variant (fibrinogen Seoul II; AαGln328Pro) characterized by impaired fibrin α-chain cross-linking. *Blood*. **108**(6), pp.1919–1924.

Park, R., Ping, L., Song, J., Seo, J.-Y.Y., Choi, T.-Y.Y., Choi, J.-R.R., Gorkun, O. V. and Lord, S.T. 2013. An engineered fibrinogen variant AαQ328,366P does not polymerise normally, but retains the ability to form α cross-links. *Thrombosis and haemostasis*. **109**(2), pp.199–206.

Pechlivani, N., Kearney, K.J. and Ajjan, R.A. 2021. Fibrinogen and antifibrinolytic proteins: Interactions and future therapeutics. *International Journal of Molecular Sciences*. **22**(22).

Peerschke, E., Francis, C. and Marder, V. 1986. Fibrinogen binding to human blood platelets: effect of gamma chain carboxyterminal structure and length. *Blood*. **67**(2), pp.385–390.

Perisanidis, C., Psyrri, A., Cohen, E.E., Engelmann, J., Heinze, G., Perisanidis, B., Stift, A., Filipits, M., Kornek, G. and Nkenke, E. 2015. Prognostic role of pretreatment plasma fibrinogen in patients with solid tumors: A systematic review and meta-analysis. *Cancer Treatment Reviews*. **41**(10), pp.960–970.

Perrella, G., Nagy, M., Watson, S.P. and Heemskerk, J.W.M. 2021. Platelet gpvi (glycoprotein vi) and thrombotic complications in the venous system. *Arteriosclerosis, Thrombosis, and Vascular Biology*. (November), pp.2681–2692.

Peshkova, A., Malyasyov, D., Bredikhin, R., Le Minh, G., Andrianova, I., Tutwiler, V., Nagaswami, C., Weisel, J. and Litvinov, R. 2018. Reduced Contraction of Blood Clots in Venous Thromboembolism Is a Potential Thrombogenic and Embologenic Mechanism. *TH Open*. **02**(01), pp.e104–e115.

Pieters, M., Kotze, R.C., Jerling, J.C., Kruger, A. and Ariëns, R.A.S. 2013. Evidence that fibrinogen γ' regulates plasma clot structure and lysis and relationship to cardiovascular risk factors in black Africans. *Blood*. **121**(16), pp.3254–3260.

Pineda, A.O., Chen, Z.W., Marino, F., Mathews, F.S., Mosesson, M.W. and Di Cera, E. 2007. Crystal structure of thrombin in complex with fibrinogen γ' peptide. *Biophysical Chemistry*. **125**(2–3), pp.556–559.

Ping, L., Huang, L., Cardinali, B., Profumo, A., Gorkun, O. V and Lord, S.T. 2011. Substitution of the human αC region with the analogous chicken domain generates a fibrinogen with severely impaired lateral aggregation: fibrin monomers assemble into protofibrils

but protofibrils do not assemble into fibers. *Biochemistry*. **50**(42), pp.9066–75.

Pisano, J.J., Finlayson, J.S. and Peyton, M.P. 1968. [Cross-link in fibrin polymerized by factor 13: epsilon-(gamma-glutamyl)lysine]. *Science (New York, N.Y.)*. **160**(3830), pp.892–3.

Podolnikova, N.P., Yakovlev, S., Yakubenko, V.P., Wang, X., Gorkun, O. V. and Ugarova, T.P. 2014. The interaction of integrin αiIb β3 with fibrin occurs through multiple binding sites in the α IIb β-propeller domain. *Journal of Biological Chemistry*. **289**(4), pp.2371–2383.

Podoplelova, N.A., Sveshnikova, A.N., Kotova, Y.N., Eckly, A., Receveur, N., Nechipurenko, D.Y., Obydennyi, S.I., Kireev, I.I., Gachet, C., Ataullakhanov, F.I., Mangin, P.H. and Panteleev, M.A. 2016. Coagulation factors bound to procoagulant platelets concentrate in cap structures to promote clotting. *Blood*. **128**(13), pp.1745–1755.

Pong, R.P., Leveque, J.C.A., Edwards, A., Yanamadala, V., Wright, A.K., Herodes, M. and Sethi, R.K. 2018. Effect of tranexamic acid on blood loss, D-dimer, and fibrinogen kinetics in adult spinal deformity surgery. *Journal of Bone and Joint Surgery - American Volume*. **100**(9), pp.758–764.

Pospisil, C.H., Stafford, A.R., Fredenburgh, J.C. and Weitz, J.I. 2003. Evidence that both exosites on thrombin participate in its high affinity interaction with fibrin. *Journal of Biological Chemistry*. **278**(24), pp.21584–21591.

Previtali, E., Bucciarelli, P., Passamonti, S.M. and Martinelli, I. 2011. Risk factors for venous and arterial thrombosis. *Blood transfusion = Trasfusione del sangue*. **9**(2), pp.120–38.

Protopopova, A.D., Barinov, N.A., Zavyalova, E.G., Kopylov, A.M., Sergienko, V.I. and Klinov, D. V. 2015. Visualization of fibrinogen αC regions and their arrangement during fibrin network formation by high-resolution AFM. *Journal of Thrombosis and Haemostasis*. **13**(4), pp.570–579.

Protopopova, A.D., Litvinov, R.I., Galanakis, D.K., Nagaswami, C., Barinov, N.A., Mukhitov, A.R., Klinov, D. V. and Weisel, J.W. 2017. Morphometric characterization of fibrinogen's αC regions and their role in fibrin self-assembly and molecular organization. *Nanoscale*. **9**(36), pp.13707–13716.

Provenzale, I., Brouns, S.L.N., van der Meijden, P.E.J., Swieringa, F. and Heemskerk, J.W.M. 2019. Whole blood based multiparameter assessment of thrombus formation in standard microfluidic devices to proxy in vivo haemostasis and thrombosis. *Micromachines*. **10**(11).

Purohit, P.K., Litvinov, R.I., Brown, A.E.X., Discher, D.E. and Weisel, J.W. 2011. Protein unfolding accounts for the unusual mechanical behavior of fibrin networks. *Acta Biomaterialia*. **7**(6), pp.2374–2383.

Qiu, Y., Brown, A.C., Myers, D.R., Sakurai, Y., Mannino, R.G., Tran, R., Ahn, B., Hardy, E.T., Kee, M.F., Kumar, S., Bao, G., Barker, T.H. and Lam, W.A. 2014. Platelet mechanosensing of substrate stiffness during clot formation mediates adhesion, spreading, and activation. *Proceedings of the National Academy of Sciences of the United States of America*. **111**(40), pp.14430–5.

Ramanathan, R., Gram, J., Feddersen, S., Nybo, M., Larsen, A. and Sidelmann, J.J. 2013. Dusart Syndrome in a Scandinavian family characterized by arterial and venous thrombosis at young age. *Scandinavian Journal of Clinical and Laboratory Investigation*. **73**(7), pp.585–590.

Ramos-Pachón, A., López-Cancio, E., Bustamante, A., Pérez De La Ossa, N., Millán, M., Hernández-Pérez, M., Garcia-Berrocoso, T., Cardona, P., Rubiera, M., Serena, J., Ustrell, X., Garcés, M., Terceño, M., Dávalos, A. and Montaner, J. 2021. D-Dimer as Predictor of Large Vessel Occlusion in Acute Ischemic Stroke. *Stroke*. (March), pp.852–858.

Rasmussen-Torvik, L.J., Cushman, M., Tsai, M.Y., Zhang, Y., Heckbert, S.R., Rosamond, W.D. and Folsom, A.R. 2007. The association of α-fibrinogen Thr312Ala polymorphism and venous thromboembolism in the LITE study. *Thrombosis Research*. **121**(1), pp.1–7.

Redman, C.M. and Xia, H. 2000. A review of the expression, assembly, secretion and intracellular degradation of fibrinogen. *Fibrinolysis and Proteolysis*. **14**(2–3), pp.198–205.

Reed, G.L., Houng, A.K., Singh, S. and Wang, D. 2017. α2-Antiplasmin: New Insights and Opportunities for Ischemic Stroke. *Seminars in Thrombosis and Hemostasis*. **43**(2), pp.191–199.

Reinhart, D., Damjanovic, L., Kaisermayer, C., Sommeregger, W., Gili, A., Gasselhuber, B., Castan, A., Mayrhofer, P., Grünwald-Gruber, C. and Kunert, R. 2019. Bioprocessing of Recombinant CHO-K1, CHO-DG44, and CHO-S: CHO Expression Hosts Favor Either mAb Production or Biomass Synthesis. *Biotechnology Journal*. **14**(3), p.1700686.

Remijn, J.A., IJsseldijk, M.J.W. and de Groot, P.G. 2003. Role of the fibrinogen gamma-chain sequence gamma316-322 in platelet-mediated clot retraction. *Journal of Thrombosis and Haemostasis*. **1**(10), pp.2245–2246.

Remijn, J.A., Ijsseldijk, M.J.W., Van Hemel, B.M., Galanakis, D.K., Hogan, K.A., Lounes, K.C., Lord, S.T., Sixma, J.J. and De Groot, P.G. 2002. Reduced platelet adhesion in flowing blood to fibrinogen by alterations in segment γ316-322, part of the fibrin-specific region. *British Journal of Haematology*. **117**(3), pp.650–657.

Ridgway, H.J., Brennan, S.O., Faed, J.M. and George, P.M. 1997. Fibrinogen Otago: a major alpha chain truncation associated with severe hypofibrinogenaemia and recurrent

miscarriage. *British Journal of Haematology*. **98**(3), pp.632–9.

Ridgway, H.J., Brennan, S.O., Gibbons, S. and George, P.M. 1996. Fibrinogen Lincoln: a new truncated alpha chain variant with delayed clotting. *British journal of haematology*. **93**(1), pp.177–84.

Ritchie, H. and Roser, M. 2019. Cause of Death. *Our World in Data*.

Rittersma, S.Z.H., Van Der Wal, A.C., Koch, K.T., Piek, J.J., Henriques, J.P.S., Mulder, K.J., Ploegmakers, J.P.H.M., Meesterman, M. and De Winter, R.J. 2005. Plaque instability frequently occurs days or weeks before occlusive coronary thrombosis: A pathological thrombectomy study in primary percutaneous coronary intervention. *Circulation*. **111**(9), pp.1160–1165.

Roberts, H., Hoffman, M. and Monroe, D. 2006. A Cell-Based Model of Thrombin Generation. *Seminars in Thrombosis and Hemostasis*. **32**(S 1), pp.032–038.

Roberts, I., Shakur, H., Coats, T., Hunt, B., Balogun, E., Barnetson, L., Cook, L., Kawahara, T., Perel, P., Prieto-Merino, D., Ramos, M., Cairns, J. and Guerriero, C. 2013. The CRASH-2 trial: A randomised controlled trial and economic evaluation of the effects of tranexamic acid on death, vascular occlusive events and transfusion requirement in bleeding trauma patients. *Health Technology Assessment*. **17**(10), pp.1–80.

Rooney, M.M., Farrell, D.H., van Hemel, B.M., de Groot, P.G. and Lord, S.T. 1998. The contribution of the three hypothesized integrin-binding sites in fibrinogen to platelet-mediated clot retraction. *Blood*. **92**(7), pp.2374–2381.

Rooney, M.M., Parise, L. V. and Lord, S.T. 1996. Dissecting clot retraction and platelet aggregation: Clot retraction does not require an intact fibrinogen γ chain C terminus. *Journal of Biological Chemistry*. **271**(15), pp.8553–8555.

Roy, S., Overton, O. and Redman, C. 1994. Overexpression of any fibrinogen chain by Hep G2 cells specifically elevates the expression of the other two chains. *The Journal of biological chemistry*. **269**(1), pp.691–5.

Roy, S.N., Procyk, R., Kudryk, B.J. and Redman, C.M. 1991. Assembly and secretion of recombinant human fibrinogen. *Journal of Biological Chemistry*. **266**(8), pp.4758–4763.

Sabater-Lleal, M., Huang, J., Chasman, D., Naitza, S., Dehghan, A., Johnson, A.D., Teumer, A., Reiner, A.P., Folkersen, L., Basu, S., Rudnicka, A.R., Trompet, S., Mälarstig, A., Baumert, J., Bis, J.C., Guo, X., Hottenga, J.J., Shin, S.Y., Lopez, L.M., Lahti, J., Tanaka, T., Yanek, L.R., Oudot-Mellakh, T., Wilson, J.F., Navarro, P., Huffman, J.E., Zemunik, T., Redline, S., Mehra, R., Pulanic, D., Rudan, I., Wright, A.F., Kolcic, I., Polasek, O., Wild, S.H., Campbell, H., Curb, J.D., Wallace, R., Liu, S., Eaton, C.B., Becker, D.M., Becker, L.C., Bandinelli, S., Räikkönen, K., Widen, E., Palotie, A., Fornage, M., Green, D., Gross, M.,

Davies, G., Harris, S.E., Liewald, D.C., Starr, J.M., Williams, F.M.K., Grant, P.J., Spector, T.D., Strawbridge, R.J., Silveira, A., Sennblad, B., Rivadeneira, F., Uitterlinden, A.G., Franco, O.H., Hofman, A., Van Dongen, J., Willemsen, G., Boomsma, D.I., Yao, J., Swords Jenny, N., Haritunians, T., McKnight, B., Lumley, T., Taylor, K.D., Rotter, J.I., Psaty, B.M., Peters, A., Gieger, C., Illig, T., Grotevendt, A., Homuth, G., Völzke, H., Kocher, T., Goel, A., Franzosi, M.G., Seedorf, U., Clarke, R., Steri, M., Tarasov, K. V., Sanna, S., Schlessinger, D., Stott, D.J., Sattar, N., Buckley, B.M., Rumley, A., Lowe, G.D., McArdle, W.L., Chen, M.H., Tofler, G.H., Song, J., Boerwinkle, E., Folsom, A.R., Rose, L.M., Franco-Cereceda, A., Teichert, M., Ikram, M.A., Mosley, T.H., Bevan, S., Dichgans, M., Rothwell, P.M., Sudlow, C.L.M., Hopewell, J.C., Chambers, J.C., Saleheen, D., Kooner, J.S., Danesh, J., Nelson, C.P., Erdmann, J., Reilly, M.P., Kathiresan, S., Schunkert, H., Morange, P.E., Ferrucci, L., Eriksson, J.G., Jacobs, D., Deary, I.J., Soranzo, N., Witteman, J.C.M., De Geus, E.J.C., Tracy, R.P., Hayward, C., Koenig, W., Cucca, F., Jukema, J.W., Eriksson, P., Seshadri, S., Markus, H.S., Watkins, H., Samani, N.J., Wallaschofski, H., Smith, N.L., Tregouet, D., Ridker, P.M., Tang, W., Strachan, D.P., Hamsten, A. and O'Donnell, C.J. 2013. Multiethnic meta-analysis of genome-wide association studies in >100 000 subjects identifies 23 fibrinogen-associated loci but no strong evidence of a causal association between circulating fibrinogen and cardiovascular disease. *Circulation*. **128**(12), pp.1310–1324.

Sadowski, M., Zabczyk, M. and Undas, A. 2014. Coronary thrombus composition: Links with inflammation, platelet and endothelial markers. *Atherosclerosis*. **237**(2), pp.555–561.

Sakata, Y. and Aoki, N. 1982. Significance of cross-linking of α2-plasmin inhibitor to fibrin in inhibition of fibrinolysis and in hemostasis. *Journal of Clinical Investigation*. **69**(3), pp.536–542.

Sakka, M., Connors, J.M., Hékimian, G., Martin-Toutain, I., Crichi, B., Colmegna, I., Bonnefont-Rousselot, D., Farge, D. and Frere, C. 2020. Association between D-Dimer levels and mortality in patients with coronavirus disease 2019 (COVID-19): a systematic review and pooled analysis. *JMV-Journal de Medecine Vasculaire*. **45**(5), pp.268–274.

Santacroce, R., Cappucci, F., Pisanelli, D., Perricone, F., Papa, M.L., Santoro, R., Grandone, E. and Margaglione, M. 2006. Inherited abnormalities of fibrinogen: 10-Year clinical experience of an Italian group. *Blood Coagulation and Fibrinolysis*. **17**(4), pp.235–240.

Sato, H. and Swadesh, J.K. 1993. Structural difference between polymerized and non-polymerized fragment X, obtained by plasmin digest of fibrinogen. *International Journal of Biological Macromolecules*. **15**(6), pp.323–327.

Sato, H. and Weisel, J.W. 1990. Polymerization of fibrinogen-derived fragment X and

subsequent rearrangement of fibers. *Thrombosis research*. **58**(3), pp.205–12.

Satterfield, B.A., Bhatt, D.L. and Gersh, B.J. 2021. Cardiac involvement in the long-term implications of COVID-19. *Nature Reviews Cardiology*.

Schaefer, A.V.L., Leslie, B.A., Rischke, J.A., Stafford, A.R., Fredenburgh, J.C. and Weitz, J.I. 2006. Incorporation of fragment X into fibrin clots renders them more susceptible to lysis by plasmin. *Biochemistry*. **45**(13), pp.4257–4265.

Schielen, W., Adams, H., van Leuven, K., Voskuilen, M., Tesser, G. and Nieuwenhuizen, W. 1991. The sequence gamma-(312-324) is a fibrin-specific epitope. *Blood*. **77**(10), pp.2169–2173.

Schielen, W.J.G., Voskuilen, M., Tesser, G.I. and Nieuwenhuizen, W. 1989. The sequence Aα-(148-160) in fibrin, but not in fibrinogen, is accessible to monoclonal antibodies. *Proceedings of the National Academy of Sciences of the United States of America*. **86**(22), pp.8951–8954.

Schmaier, A.H. 2008. The elusive physiologic role of Factor XII. *Journal of Clinical Investigation*. **118**(9), pp.3006–3009.

Schmitt, L.R., Henderson, R., Barrett, A., Darula, Z., Issaian, A., D'Alessandro, A., Clendenen, N. and Hansen, K.C. 2019. Mass spectrometry– based molecular mapping of native FXIIIa cross-links in insoluble fibrin clots. *Journal of Biological Chemistry*. **294**(22), pp.8773–8778.

Sevitt, S. 1974. The structure and growth of valve-pocket thrombi in femoral veins. *Journal of Clinical Pathology*. **27**(7), pp.517–528.

Shakur, H., Roberts, I., Fawole, B., Chaudhri, R., El-Sheikh, M., Akintan, A., Qureshi, Z., Kidanto, H., Vwalika, B., Abdulkadir, A., Etuk, S., Noor, S., Asonganyi, E., Alfirevic, Z., Beaumont, D., Ronsmans, C., Arulkumaran, S., Grant, A., Afsana, K., Gülmezoglu, M., Hunt, B., Olayemi, O., Chalmers, I., Lumbiganon, P., Piaggio, G., Brady, T., Elbourne, D., Balogun, E., Pepple, T., Prowse, D., Quashi, N., Barneston, L., Barrow, C., Cook, L., Frimley, L., Gilbert, D., Gilliam, C., Jackson, R., Kawahara, T., Miah, H., Kostrov, S., Ramos, M., Edwards, P., Godec, T., Huque, S., Okunade, O., Adetayo, O., Kayani, A., Javaid, K., Biryabarema, C., Tchounzou, R., Regmi, M., Dallaku, K., Sahani, M., Akhter, S., Meda, N., Dah, A.K., Odekunle, O., Monehin, O., Ojo, A., Akinbinu, G., Offiah, I., Akpan, U., Udofia, U., Okon, U., Omoronyia, E., James, O., Bello, N., Adeyemi, Blessed, Aimakhu, C., Akinsanya, O., Adeleye, B., Adeyemi, O., Oluwatosin, K., Aboyeji, A., Adeniran, A., Adewale, A., Olaomo, N., Omo-Aghoja, L., Okpako, E., Oyeye, L., Alu, F., Ogudu, J., Ladan, E., Habib, I., Okusanya, B., Onafowokan, O., Isah, D., Aye, A., Okogbo, F., Aigere, E., Ogbiti, M., Onile, T., Salau, O., Amode, Y., Shoretire, K., Owodunni, A.,

Ologunde, K., Ayinde, A., Alao, M., Awonuga, O., Awolaja, B., Adegbola, O., Habeebu-Adeyemi, F., Okunowo, A., Idris, H., Okike, O., Madueke, N., Mutihir, J., Joseph, N., Adebudo, B., Fasanu, A., Akintunde, O., Abidoye, O., Opreh, O., Udonwa, S., Dibia, G., Bazuaye, S., Ifemeje, A., Umoiyoho, A., Inyang-Etoh, E., Yusuf, S., Olayinka, K., Adeyemi, Babalola, Ajenifuja, O., Ibrahim, U., Adamu, Y.B., Akinola, O., Adekola-Oni, G., Kua, P., Iheagwam, R., Idrisa, A., Geidam, A., Jogo, A., Agulebe, J., Ikechebelu, J., Udegbunam, O., Awoleke, J., Adelekan, O., Sulayman, H., Ameh, N., Onaolapo, N., Adelodun, A., Golit, W., Audu, D., Adeniji, A., Oyelade, F., Dattijo, L., Henry, P., Loto, O., Umeora, O., Onwe, A., Nzeribe, E., Okorochukwu, B., Adeniyi, A., Gbejegbe, E., Ikpen, A., Nwosu, I., Sambo, A., Ladipo, O., Abubakar, S., Okike, O.N., Nduka, E.C., Ezenkwele, E.P., Onwusulu, D., Irinyenikan, T.A., Singh, S., Bariweni, A., Galadanci, H., Achara, P., Osayande, O., Gana, M., Jabeen, K., Mobeen, A., Mufti, S., Zafar, M., Ahmad, B., Munawar, M., Gul, J., Usman, N., Shaheen, F., Tariq, M., Sadiq, N., Batool, R., Ali, H.S., Jaffer, M., Baloch, A., Mukhtiar, N., Ashraf, T., Asmat, R., Khudaidad, S., Taj, G., Qazi, R., Dars, S., Sardar, F., Ashfaq, S., Majeed, S., Jabeen, S., Karim, R., Burki, F., Bukhari, S.R., Gul, F., Jabeen, M., Sherin, A., Ain, Q., Rao, S., Shaheen, U., Manzoor, Samina, Masood, S., Rizvi, S., Ali, Anita, Sajid, A., Iftikhar, A., Batool, S., Dar, L., Sohail, S., Rasul, S., Humayun, S., Sultana, R., Manzoor, Sofia, Mazhar, S., Batool, A., Nazir, A., Tasnim, N., Masood, H., Khero, R., Surhio, N., Aleem, S., Israr, N., Javed, S., Bashir, L., Iqbal, Samina, Aleem, F., Sohail, R., Iqbal, Saima, Dojki, S., Bano, A., Saba, N., Hafeez, M., Akram, N., Shaheen, R., Hashmi, H., Arshad, S., Hussain, R., Khan, S., Shaheen, N., Khalil, S., Sachdev, P., Arain, G., Zarreen, A., Saeed, S., Hanif, S., Tariq, N., Jamil, M., Chaudhry, S., Rajani, H., Wasim, T., Aslam, S., Mustafa, N., Quddusi, H., Karim, S., Sultana, S., Harim, M., Chohan, M., Salman, N., Waqar, F., Sadia, S., Kahloon, L., Manzoor, Shehla, Amin, S., Akram, U., Ikram, A., Kausar, S., Batool, T., Naila, B., Kyani, T., Bulime, R., Akello, R., Lwasa, B.N., Ayikoru, J., Namulwasira, C., Komagum, P., Rebecca, I., Annet, N., Nuulu, N., Nionzima, E., Bwotya, R., Nankya, M., Babirye, S., Ngonzi, J., Sanchez, C., Innocent, N., Anitah, K., Jackson, A., Ndagire, E., Nanyongo, C., Drametu, D., Meregurwa, G., Banya, F., Atim, R., Byaruhanga, E., Felix, L., Iman, H., Oyiengo, V., Waigi, P., Wangui, R., Nassir, F., Soita, M., Msengeti, R., Zubier, Z., Mabeya, H., Wanjala, A., Mwangi, H., Liyayi, B., Muthoka, E., Osoti, A., Otara, A., Ongwae, V., Wanjohi, V., Musila, B., Wekesa, K., Bosire, A.N., Ntem, A., Njoache, A., Ashu, A., Simo, A., Keka, D., Bruno, K., Ndouoya, A., Saadio, M., Tchana, M., Gwan, O., Assomo, P., Mutsu, V., Eric, N., Foumane, P., Nsem, P., Fouedjio, J., Fouelifack, Y., Tebeu, P.M., Nko'ayissi, G., Mbong, E.N., Nabag, W., Desougi, R., Mustafa, H., Eltaib, H., Umbeli, T., Elfadl, K.,

Ibrahim, M., Mohammed, A., Ali, Awadia, Abdelrahiem, S., Musa, M., Awadalla, K., Ahmed, S., Bushra, M., Babiker, O., Abdullahi, H., Ahmed, M., Safa, E., Almardi, H., Rayis, D., Abdelgabar, S.A., Houghton, G., Sharpe, A., Thornton, J., Grace, N., Smith, C., Hinshaw, K., Edmundson, D., Ayuk, P., Bates, A., Bugg, G., Wilkins, J., Tower, C., Allibone, A., Oteng-Ntim, E., Kazumari, A., Danford, A., Ngarina, M., Abeid, M., Mayumba, K., Zacharia, M., Mtove, G., Madame, L., Massinde, A., Mwambe, B., Onesmo, R., Ganyaka, S.K., Gupta, S., Bhatt, R., Agrawal, A., Pradhan, P., Dhakal, N., Yadav, P., Karki, G., Shrestha, B.R., Lubeya, M.K., Mumba, J., Silwimba, W., Hansingo, I., Bopili, N., Makukula, Z., Kawimbe, A., Mtambo, W., Ng'ambi, M., Cenameri, S., Tasha, I., Kruja, A., Brahimaj, B., Tola, A., Kaza, L., Tshombe, D., Buligho, E., Paluku-Hamuli, R., Kacha, C., Faida, K., Musau, B., Kalyana, H., Simisi, P., Mulyumba, S., Jason, N.K., Lubamba, J.R., Missumba, W., Islam, F., Begum, N., Chowdhury, F., Begum, R., Basher, F., Nargis, N., Kholdun, A., Jesmin, S., Paul, S., Segni, H., Ayana, G., Haleke, W., Hussien, H., Geremew, F., Bambara, M., Somé, A., Ly, A., Pabakba, R., Fletcher, H., Samuels, L., Opare-Addo, H., Larsen-Reindorf, R., Nyarko-Jectey, K., Mola, G., Wai, M., El Rahman, M., Basta, W., Khamis, H., Escobar, M.F., Vallecilla, L. and Faye, G.E. 2017. Effect of early tranexamic acid administration on mortality, hysterectomy, and other morbidities in women with post-partum haemorrhage (WOMAN): an international, randomised, double-blind, placebo-controlled trial. *The Lancet*. **389**(10084), pp.2105–2116.

Sheen, C., Brennan, S., Jabado, N. and George, P. 2006. Fibrinogen Montreal: A novel missense mutation (Aα D496N) associated with hypofibrinogenaemia. *Thrombosis and Haemostasis*. **96**(08), pp.231–232.

Shen, L.L., McDonagh, R.P., McDonagh, J. and Hermans, J. 1977. Early events in the plasmin digestion of fibrinogen and fibrin: Effects of plasmin on fibrin polymerization. *Journal of Biological Chemistry*. **252**(17), pp.6184–6189.

Shen, Y.M., Trang, V., Sarode, R. and Brennan, S. 2014. Fibrinogen Dusart presenting as recurrent thromboses in the hepatic portal system. *Blood Coagulation and Fibrinolysis*. **25**(4), pp.392–394.

Shojaie, M., Pourahmad, M., Eshraghian, A., Izadi, H.R. and Naghshvar, F. 2009. Fibrinogen as a risk factor for premature myocardial infarction in Iranian patients: A case control study. *Vascular Health and Risk Management*. **5**, pp.673–676.

Siebenlist, K.R., Meh, D.A. and Mosesson, M.W. 1996. Plasma factor XIII binds specifically to fibrinogen molecules containing γ' chains. *Biochemistry*. **35**(32), pp.10448–10453.

Siebenlist, K.R., Meh, D.A. and Mosesson, M.W. 2001. Protransglutaminase (factor XIII)

mediated crosslinking of fibrinogen and fibrin. *Thrombosis and Haemostasis*. **86**(5), pp.1221–1228.

Siebenlist, K.R., Mosesson, M.W., Hernandez, I., Bush, L.A., Di Cera, E., Shainoff, J.R., Di Orio, J.P. and Stojanovic, L. 2005. Studies on the basis for the properties of fibrin produced from fibrinogen-containing γ′ chains. *Blood*. **106**(8), pp.2730–2736.

Siegerink, B., Rosendaal, F.R. and Algra, A. 2009. Genetic variation in fibrinogen; its relationship to fibrinogen levels and the risk of myocardial infarction and ischemic stroke. *Journal of Thrombosis and Haemostasis*. **7**(3), pp.385–390.

Silvain, J., Collet, J.P., Guedeney, P., Varenne, O., Nagaswami, C., Maupain, C., Empana, J.P., Boulanger, C., Tafflet, M., Manzo-Silberman, S., Kerneis, M., Brugier, D., Vignolles, N., Weisel, J.W., Jouven, X., Montalescot, G. and Spaulding, C. 2017. Thrombus composition in sudden cardiac death from acute myocardial infarction. *Resuscitation*. **113**, pp.108–114.

Silvain, J., Collet, J.P., Nagaswami, C., Beygui, F., Edmondson, K.E., Bellemain-Appaix, A., Cayla, G., Pena, A., Brugier, D., Barthelemy, O., Montalescot, G. and Weisel, J.W. 2011. Composition of coronary thrombus in acute myocardial infarction. *Journal of the American College of Cardiology*. **57**(12), pp.1359–1367.

Silver, M.J., Kawakami, R., Jolly, M.A., Huff, C.M., Phillips, J.A., Sakamoto, A., Kawai, K., Kutys, B., Guo, L., Cornelissen, A., Mori, M., Sato, Y., Romero, M., Virmani, R. and Finn, A. V. 2021. Histopathologic analysis of extracted thrombi from deep venous thrombosis and pulmonary embolism: Mechanisms and timing. *Catheterization and Cardiovascular Interventions*. **97**(7), pp.1422–1429.

Simpson-Haidaris, P.J. and Rybarczyk, B. 2001. Tumors and fibrinogen: The role of fibrinogen as an extracellular matrix protein. *Annals of the New York Academy of Sciences*. **936**, pp.406–425.

Simsek, I., De Mazancourt, P., Horellou, M.H., Erdem, H., Pay, S., Dinc, A. and Samama, M.M. 2008. Afibrinogenemia resulting from homozygous nonsense mutation in A alpha chain gene associated with multiple thrombotic episodes. *Blood Coagulation and Fibrinolysis*. **19**(3), pp.247–253.

Siniarski, A., Baker, S.R., Duval, C., Malinowski, K.P., Gajos, G., Nessler, J. and Ariëns, R.A.S. 2021. Quantitative analysis of clot density, fibrin fiber radius, and protofibril packing in acute phase myocardial infarction. *Thrombosis Research*. **205**(May), pp.110–119.

Smalberg, J.H., Koehler, E., Murad, S.D., Plessier, A., Seijo, S., Trebicka, J., Primignani, M., Rijken, D.C., de Maat, M.P.M., Garcia-Pagan, J.C., Valla, D.C., Janssen, H.L.A. and Leebeek, F.W.G. 2013. Fibrinogen γ′ and variation in fibrinogen gamma genes in the

etiology of portal vein thrombosis. *Thrombosis and Haemostasis*. **109**(3), pp.558–560.

Smith, K.A., Adamson, P.J., Pease, R.J., Brown, J.M., Balmforth, A.J., Cordell, P.A., Ariëns, R.A.S., Philippou, H. and Grant, P.J. 2011. Interactions between factor XIII and the αC region of fibrinogen. *Blood*. **117**(12), pp.3460–3468.

Smith, S.A. 2009. The cell-based model of coagulation: State-Of-The-Art Review. *Journal of Veterinary Emergency and Critical Care*. **19**(1), pp.3–10.

Sobel, J.H. and Gawinowicz, M.A. 1996. Identification of the α chain lysine donor sites involved in factor XIII(a) fibrin cross-linking. *Journal of Biological Chemistry*. **271**(32), pp.19288–19297.

Soepandi, P.Z., Burhan, E., Mangunnegoro, H., Nawas, A., Aditama, T.Y., Partakusuma, L., Isbaniah, F., Ikhsan, M., Swidarmoko, B., Sutiyoso, A., Malik, S., Benamore, R., Baird, J.K. and Taylor, W.R.J. 2010. Clinical course of avian influenza A(H5N1) in patients at the Persahabatan Hospital, Jakarta, Indonesia, 2005-2008. *Chest*. **138**(3), pp.665–673.

Soria, J., Mirshahi, S.S.Q.S.S.Q.S.S.Q., Mirshahi, S.S.Q.S.S.Q.S.S.Q., Varin, R., Pritchard, L.L., Soria, C. and Mirshahi, M. 2019. Fibrinogen αC domain: Its importance in physiopathology. *Research and Practice in Thrombosis and Haemostasis*. **3**(2), pp.173–183.

Soria, J., Soria, C. and Caen, J.P. 1983. A new type of congenital dysfibrinogenaemia with defective fibrin lysis—Dusard syndrome: possible relation to thrombosis. *British Journal of Haematology*. **53**(4), pp.575–586.

Sovova, Z., Pecankova, K., Majek, P. and Suttnar, J. 2021. Extension of the Human Fibrinogen Database with Detailed Clinical Information—The αC-Connector Segment. *International Journal of Molecular Sciences*. **23**(1), p.132.

Spraggon, G., Everse, S.J. and Doolittle, R.F. 1997. Crystal structures of fragment D from human fibrinogen and its crosslinked counterpart from fibrin. *Nature*. **389**(6650), pp.455–62.

Staessens, S., François, O., Brinjikji, W., Doyle, K.M., Vanacker, P., Andersson, T. and De Meyer, S.F. 2021. Studying Stroke Thrombus Composition After Thrombectomy: What Can We Learn? *Stroke*. (November), pp.1–10.

Standeven, K.F., Carter, A.M., Grant, P.J., Weisel, J.W., Chernysh, I., Masova, L., Lord, S.T. and Ariëns, R.A.S. 2007. Functional analysis of fibrin γ-chain cross-linking by activated factor XIII: Determination of a cross-linking pattern that maximizes clot stiffness. *Blood*. **110**(3), pp.902–907.

Standeven, K.F., Grant, P.J., Carter, A.M., Scheiner, T., Weisel, J.W. and Ariëns, R.A.S. 2003. Functional analysis of the fibrinogen Aα Thr312Ala polymorphism: Effects on fibrin

structure and function. *Circulation*. **107**(18), pp.2326–2330.

Stein-Merlob, A.F., Kessinger, C.W., Sibel Erdem, S., Zelada, H., Hilderbrand, S.A., Lin, C.P., Tearney, G.J., Jaff, M.R., Reed, G.L., Henke, P.K., McCarthy, J.R. and Jaffer, F.A. 2015. Blood accessibility to fibrin in venous thrombosis is thrombus age-dependent and predicts fibrinolytic efficacy: An in vivo fibrin molecular imaging study. *Theranostics*. **5**(12), pp.1317–1327.

Suh, T.T., Holmbäck, K., Jensen, N.J., Daugherty, C.C., Small, K., Simon, D.I., Potter, S. and Degen, J.L. 1995. Resolution of spontaneous bleeding events but failure of pregnancy in fibrinogen-deficient mice. *Genes & development*. **9**(16), pp.2020–33.

Sumaya, W., Wallentin, L., James, S.K., Siegbahn, A., Gabrysch, K., Bertilsson, M., Himmelmann, A., Ajjan, R.A. and Storey, R.F. 2018. Fibrin clot properties independently predict adverse clinical outcome following acute coronary syndrome: A PLATO substudy. *European Heart Journal*. **39**(13), pp.1078–1085.

Sumitha, E., Jayandharan, G.R., Arora, N., Abraham, A., David, S., Devi, G.S., Shenbagapriya, P., Nair, S.C., George, B., Mathews, V., Chandy, M., Viswabandya, A. and Srivastava, A. 2013. Molecular basis of quantitative fibrinogen disorders in 27 patients from India. *Haemophilia*. **19**(4), pp.611–618.

Suntharalingam, J., Goldsmith, K., Van Marion, V., Long, L., Treacy, C.M., Dudbridge, F., Toshner, M.R., Pepke-Zaba, J., Eikenboom, J.C.J. and Morrell, N.W. 2008. Fibrinogen Aα Thr312Ala polymorphism is associated with chronic thromboembolic pulmonary hypertension. *European Respiratory Journal*. **31**(4), pp.736–741.

Tajdar, M., Orlando, C., Casini, A., Herpol, M., De Bisschop, B., Govaert, P., Neerman-Arbez, M. and Jochmans, K. 2018. Heterozygous FGA p.Asp473Ter (fibrinogen Nieuwegein) presenting as antepartum cerebral thrombosis. *Thrombosis Research*. **163**(August), pp.185–189.

Takebe, M., Soe, G., Kohno, I., Sugo, T. and Matsuda, M. 1995. Calcium ion-dependent monoclonal antibody against human fibrinogen: preparation, characterization, and application to fibrinogen purification. *Thrombosis and haemostasis*. **73**(4), pp.662–7.

Tamura, T., Arai, S., Nagaya, H., Mizuguchi, J. and Wada, I. 2013. Stepwise assembly of fibrinogen is assisted by the endoplasmic reticulum lectin-chaperone system in HepG2 cells. *PloS one*. **8**(9), p.e74580.

Tang, N., Li, D., Wang, X. and Sun, Z. 2020. Abnormal coagulation parameters are associated with poor prognosis in patients with novel coronavirus pneumonia. *Journal of Thrombosis and Haemostasis*. **18**(4), pp.844–847.

Tarumi, T., Martincic, D., Thomas, A., Janco, R., Hudson, M., Baxter, P. and Gailani, D. 2000.

Familial thrombophilia associated with fibrinogen Paris V: Dusart syndrome. *Blood*. **96**(3), pp.1191–1193.

Tihanyi, B. and Nyitray, L. 2021. Recent advances in CHO cell line development for recombinant protein production. *Drug Discovery Today: Technologies*. **xxx**(xx), pp.1–10.

Tojo, N., Miyagi, I., Miura, M. and Ohi, H. 2008. Recombinant human fibrinogen expressed in the yeast Pichia pastoris was assembled and biologically active. *Protein expression and purification*. **59**(2), pp.289–96.

Tomaiuolo, M., Brass, L.F. and Stalker, T.J. 2017. Regulation of Platelet Activation and Coagulation and Its Role in Vascular Injury and Arterial Thrombosis. *Interventional Cardiology Clinics*. **6**(1), pp.1–12.

Topol, E.J., George, B.S., Kereiakes, D.J., Stump, D.C., Candela, R.J., Abbottsmith, C.W., Aronson, L., Pickel, A., Boswick, J.M., Lee, K.L., Ellis, S.G. and Califf, R.M. 1989. A randomized controlled trial of intravenous tissue plasminogen activator and early intravenous heparin in acute myocardial infarction. *Circulation*. **79**(2), pp.281–286.

Troisi, R., Balasco, N., Autiero, I., Vitagliano, L. and Sica, F. 2021. Exosite binding in thrombin: A global structural/dynamic overview of complexes with aptamers and other ligands. *International Journal of Molecular Sciences*. **22**(19).

Tsurupa, G., Hantgan, R.R., Burton, R.A., Pechik, I., Tjandra, N. and Medved, L. 2009. Structure, stability, and interaction of the fibrin(ogen) alphaC-domains. *Biochemistry*. **48**(51), pp.12191–201.

Tsurupa, G. and Medved, L. 2001. Identification and characterization of novel tPA- and plasminogen-binding sites within fibrin(ogen) alpha C-domains. *Biochemistry*. **40**(3), pp.801–8.

Tsurupa, G., Pechik, I., Litvinov, R.I., Hantgan, R.R., Tjandra, N., Weisel, J.W. and Medved, L. 2012. On the mechanism of αC polymer formation in fibrin. *Biochemistry*. **51**(12), pp.2526–38.

Tsurupa, G., Yakovlev, S., McKee, P. and Medved, L. 2010. Noncovalent interaction of α2-antiplasmin with fibrin(ogen): Localization of α2-antiplasmin-binding sites. *Biochemistry*. **49**(35), pp.7643–7651.

Tutwiler, V., Litvinov, R.I., Lozhkin, A.P., Peshkova, A.D., Lebedeva, T., Ataullakhanov, F.I., Spiller, K.L., Cines, D.B. and Weisel, J.W. 2016. Kinetics and mechanics of clot contraction are governed by the molecular and cellular composition of the blood. *Blood*. **127**(1), pp.149–159.

Tutwiler, V., Mukhitov, A.R., Peshkova, A.D., Le Minh, G., Khismatullin, R.R., Vicksman, J.,

Nagaswami, C., Litvinov, R.I. and Weisel, J.W. 2018. Shape changes of erythrocytes during blood clot contraction and the structure of polyhedrocytes. *Scientific Reports*. **8**(1), pp.1–14.

Tutwiler, V., Peshkova, A.D., Le Minh, G., Zaitsev, S., Litvinov, R.I., Cines, D.B. and Weisel, J.W. 2019. Blood clot contraction differentially modulates internal and external fibrinolysis. *Journal of Thrombosis and Haemostasis*. **17**(2), pp.361–370.

Tutwiler, V., Wang, H., Litvinov, R.I., Weisel, J.W. and Shenoy, V.B. 2017. Interplay of Platelet Contractility and Elasticity of Fibrin/Erythrocytes in Blood Clot Retraction. *Biophysical Journal*. **112**(4), pp.714–723.

Uitte De Willige, S., Rietveld, I.M., De Visser, M.C.H., Vos, H.L. and Bertina, R.M. 2007. Polymorphism 10034C>T is located in a region regulating polyadenylation of FGG transcripts and influences the fibrinogen γ'/γA mRNA ratio. *Journal of Thrombosis and Haemostasis*. **5**(6), pp.1243–1249.

Uitte de Willige, S., de Visser, M.C.H., Houwing-Duistermaat, J.J., Rosendaal, F.R., Vos, H.L. and Bertina, R.M. 2005. Genetic variation in the fibrinogen gamma gene increases the risk for deep venous thrombosis by reducing plasma fibrinogen gamma' levels. *Blood*. **106**(13), pp.4176–83.

Undas, A. and Ariëns, R.A.S. 2011. Fibrin clot structure and function: A role in the pathophysiology of arterial and venous thromboembolic diseases. *Arteriosclerosis, Thrombosis, and Vascular Biology*. **31**(12), pp.88–99.

Undas, A., Slowik, A., Wolkow, P., Szczudlik, A. and Tracz, W. 2010a. Fibrin clot properties in acute ischemic stroke: relation to neurological deficit. *Thrombosis Research*. **125**(4), pp.357–361.

Undas, A., Stępień, E., Rudziński, P. and Sadowski, J. 2010b. Architecture of a pulmonary thrombus removed during embolectomy in a patient with acute pulmonary embolism. *The Journal of Thoracic and Cardiovascular Surgery*. **140**(3), pp.e40–e41.

Undas, A., Zawilska, K., Ciesla-Dul, M., Lehmann-Kopydłowska, A., Skubiszak, A., Ciepłuch, K. and Tracz, W. 2009. Altered fibrin clot structure/function in patients with idiopathic venous thromboembolism and in their relatives. *Blood*. **114**(19), pp.4272–4278.

Veklich, Y., Francis, C.W., White, J. and Weisel, J.W. 1998. Structural studies of fibrinolysis by electron microscopy. *Blood*. **92**(12), pp.4721–4729.

Veklich, Y.I., Gorkun, O. V., Medved, L. V., Nieuwenhuizen, W. and Weisel, J.W. 1993. Carboxyl-terminal portions of the alpha chains of fibrinogen and fibrin. Localization by electron microscopy and the effects of isolated alpha C fragments on polymerization. *The Journal of biological chemistry*. **268**(18), pp.13577–13585.

Vilar, R., Fish, R.J., Casini, A. and Neerman-Arbez, M. 2020. Fibrin(ogen) in human disease: Both friend and foe. *Haematologica*. **105**(2), pp.284–296.

Vlietman, J.J., Verhage, J., Vos, H.L., van Wijk, R., Remijn, J.A., van Solinge, W.W. and Brus, F. 2002. Congenital afibrinogenaemia in a newborn infant due to a novel mutation in the fibrinogen aalpha gene. *British journal of haematology*. **119**(1), pp.282–3.

Vos, B.E., Martinez-Torres, C., Burla, F., Weisel, J.W. and Koenderink, G.H. 2020. Revealing the molecular origins of fibrin's elastomeric properties by in situ X-ray scattering. *Acta Biomaterialia*. **104**, pp.39–52.

De Vries, J.J., Snoek, C.J.M., Rijken, D.C. and De Maat, M.P.M. 2019. Effects of post-translational modifications of fibrinogen on clot formation, clot structure, and fibrinolysis: A systematic review. *Arteriosclerosis, Thrombosis, and Vascular Biology*. (March), pp.554–569.

Wada, Y. and Lord, S.T. 1994. A correlation between thrombotic disease and a specific fibrinogen abnormality (Aα 554 Arg → Cys) in two unrelated kindred, Dusart and Chapel Hill III. *Blood*. **84**(11), pp.3709–3714.

Walton, B.L., Getz, T.M., Bergmeier, W., Lin, F.C., Uitte de Willige, S. and Wolberg, A.S. 2014. The fibrinogen γA/γ′ isoform does not promote acute arterial thrombosis in mice. *Journal of Thrombosis and Haemostasis*. **12**(5), pp.680–689.

Wang, J., Ning, R. and Wang, Y. 2016. Plasma D-dimer Level, the Promising Prognostic Biomarker for the Acute Cerebral Infarction Patients. *Journal of Stroke and Cerebrovascular Diseases*. **25**(8), pp.2011–2015.

Ward-Caviness, C.K., De Vries, P.S., Wiggins, K.L., Huffman, J.E., Yanek, L.R., Bielak, L.F., Giulianini, F., Guo, X., Kleber, M.E., Kacprowski, T., Groß, S., Petersman, A., Smith, G.D., Hartwig, F.P., Bowden, J., Hemani, G., Müller-Nuraysid, M., Strauch, K., Koenig, W., Waldenberger, M., Meitinger, T., Pankratz, N., Boerwinkle, E., Tang, W., Fu, Y.P., Johnson, A.D., Song, C., De Maat, M.P.M., Uitterlinden, A.G., Franco, O.H., Brody, J.A., McKnight, B., Chen, Y.D.I., Psaty, B.M., Mathias, R.A., Becker, D.M., Peyser, P.A., Smith, J.A., Bielinski, S.J., Ridker, P.M., Taylor, K.D., Yao, J., Tracy, R., Delgado, G., Trompet, S., Sattar, N., Jukema, J.W., Becker, L.C., Kardia, S.L.R., Rotter, J.I., März, W., Dörr, M., Chasman, D.I., Dehghan, A., O'Donnell, C.J., Smith, N.L., Peters, A. and Morrison, A.C. 2019. Mendelian randomization evaluation of causal effects of fibrinogen on incident coronary heart disease. *PLoS ONE*. **14**(5), pp.1–18.

Weisel, J.W. 2004. The mechanical properties of fibrin for basic scientists and clinicians. *Biophysical Chemistry*. **112**(2-3 SPEC. ISS.), pp.267–276.

Weisel, J.W. and Litvinov, R.I. 2017. Fibrin Formation, Structure and Properties. *Sub-cellular*

biochemistry. **82**, pp.405–456.

Weisel, J.W. and Litvinov, R.I. 2019. Red blood cells: the forgotten player in hemostasis and thrombosis. *Journal of Thrombosis and Haemostasis*. **17**(2), pp.271–282.

Weisel, J.W. and Medved, L. 2001. The structure and function of the alpha C domains of fibrinogen. *Annals of the New York Academy of Sciences*. **936**, pp.312–27.

Weisel, J.W., Nagaswami, C., Korsholm, B., Petersen, L.C. and Suenson, E. 1994. Interactions of plasminogen with polymerizing fibrin and its derivatives, monitored with a photoaffinity cross-linker and electron microscopy. *Journal of molecular biology*. **235**(3), pp.1117–35.

Weisel, J.W. and Papsun, D.M. 1987. Involvement of the COOH-terminal portion of the alpha-chain of fibrin in the branching of fibers to form a clot. *Thrombosis research*. **47**(2), pp.155–63.

Weissbach, L. and Grieninger, G. 1990. Bipartite mRNA for chicken α-fibrinogen potentially encodes an amino acid sequence homologous to β- and γ-fibrinogens. *Proceedings of the National Academy of Sciences of the United States of America*. **87**(13), pp.5198–5202.

Weitz, J.I., Leslie, B., Hirsh, J. and Klement, P. 1993. α2-Antiplasmin supplementation inhibits tissue plasminogen activator- induced fibrinogenolysis and bleeding with little effect on thrombolysis. *Journal of Clinical Investigation*. **91**(4), pp.1343–1350.

Westbury, S.K., Duval, C., Philippou, H., Brown, R., Lee, K.R., Murden, S.L., Phillips, E., Reilly-Stitt, C., Whalley, D., Ariëns, R.A. and Mumford, A.D. 2013. Partial deletion of the αC-domain in the Fibrinogen Perth variant is associated with thrombosis, increased clot strength and delayed fibrinolysis. *Thrombosis and Haemostasis*. **110**(12), pp.1135–1144.

WHO n.d. Disability, Global Health Estimates: Life expectancy and leading causes of death and. [Accessed 4 January 2022]. Available from: https://www.who.int/data/gho/data/themes/mortality-and-global-health-estimates.

Whyte, C.S., Mitchell, J.L. and Mutch, N.J. 2017. Platelet-Mediated Modulation of Fibrinolysis. *Seminars in Thrombosis and Hemostasis*. **43**(2), pp.115–128.

Whyte, C.S., Rastogi, A., Ferguson, E., Donnarumma, M. and Mutch, N.J. 2022. The Efficacy of Fibrinogen Concentrates in Relation to Cryoprecipitate in Restoring Clot Integrity and Stability against Lysis. *International Journal of Molecular Sciences*. **23**(6).

Whyte, C.S., Swieringa, F., Mastenbroek, T.G., Lionikiene, A.S., Lancé, M.D., Van Der Meijden, P.E.J., Heemskerk, J.W.M. and Mutch, N.J. 2015. Plasminogen associates with phosphatidylserine-exposing platelets and contributes to thrombus lysis under flow.

Blood. **125**(16), pp.2568–2578.

Wilkins, E., Wilson, L., Wickramasinghe, K. and Bhatnagar, P. 2017. European Cardiovascular Disease Statistics 2017. *European Heart Network*., pp.94–100.

De Witt, S.M., Swieringa, F., Cavill, R., Lamers, M.M.E., Van Kruchten, R., Mastenbroek, T., Baaten, C., Coort, S., Pugh, N., Schulz, A., Scharrer, I., Jurk, K., Zieger, B., Clemetson, K.J., Farndale, R.W., Heemskerk, J.W.M. and Cosemans, J.M.E.M. 2014. Identification of platelet function defects by multi-parameter assessment of thrombus formation. *Nature Communications*. **5**(May).

Wohner, N., Sótonyi, P., MacHovich, R., Szabó, L., Tenekedjiev, K., Silva, M.M.C.G., Longstaff, C. and Kolev, K. 2011. Lytic resistance of fibrin containing red blood cells. *Arteriosclerosis, Thrombosis, and Vascular Biology*. **31**(10), pp.2306–2313.

Wolberg, A.S. 2007. Thrombin generation and fibrin clot structure. *Blood Reviews*. **21**(3), pp.131–142.

Wolberg, A.S., Monroe, D.M., Roberts, H.R. and Hoffman, M. 2003. Elevated prothrombin results in clots with an altered fiber structure: A possible mechanism of the increased thrombotic risk. *Blood*. **101**(8), pp.3008–3013.

Wolberg, A.S., Rosendaal, F.R., Weitz, J.I., Jaffer, I.H., Agnelli, G., Baglin, T. and Mackman, N. 2015. Venous thrombosis. *Nature reviews. Disease primers*. **1**, p.15006.

Wool, G.D. and Miller, J.L. 2021. The Impact of COVID-19 Disease on Platelets and Coagulation. *Pathobiology*. **88**(1), pp.15–27.

Wygrecka, M., Birnhuber, A., Seeliger, B., Michalick, L., Pak, O., Schultz, A., Schramm, F., Zacharias, M., Gorkiewicz, G., David, S., Welte, T., Schmidt, J.J., Weissmann, N., Schermuly, R.T., Barreto, G., Schaefer, L., Markart, P., Brack, M.C., Hippenstiel, S., Kurth, F., Sander, L.E., Witzenrath, M., Kuebler, W.M., Kwapiszewska, G. and Preissner, K.T. 2022. Altered fibrin clot structure and dysregulated fibrinolysis contribute to thrombosis risk in severe COVID-19. *Blood advances*. **6**(3), pp.1074–1087.

Xu, R.G., Gauer, J.S., Baker, S.R., Slater, A., Martin, E.M., McPherson, H.R., Duval, C., Manfield, I.W., Bonna, A.M., Watson, S.P. and Ariëns, R.A.S. 2021. GPVI (Glycoprotein VI) interaction with fibrinogen is mediated by avidity and the fibrinogen αc-Region. *Arteriosclerosis, Thrombosis, and Vascular Biology*. (March), pp.1092–1104.

Xu, X.R., Carrim, N., Neves, M.A.D., McKeown, T., Stratton, T.W., Coelho, R.M.P., Lei, X., Chen, P., Xu, J., Dai, X., Li, B.X. and Ni, H. 2016. Platelets and platelet adhesion molecules: Novel mechanisms of thrombosis and anti-thrombotic therapies. *Thrombosis Journal*. **14**(Suppl 1).

Yakovlev, S., Makogonenko, E., Kurochkina, N., Nieuwenhuizen, W., Ingham, K. and Medved,

L. 2000. Conversion of fibrinogen to fibrin: Mechanism of exposure of tPA- and plasminogen-binding sites. *Biochemistry*. **39**(51), pp.15730–15741.

Yang, H., Lang, S., Zhai, Z., Li, L., Kahr, W.H.A.A., Chen, P., Brkić, J., Spring, C.M., Flick, M.J., Degen, J.L., Freedman, J. and Ni, H. 2009. Fibrinogen is required for maintenance of platelet intracellular and cell-surface P-selectin expression. *Blood*. **114**(2), pp.425–36.

Yee, V.C., Pratt, K.P., Côté, H.C.F., Le Trong, I., Chung, D.W., Davie, E.W., Stenkamp, R.E. and Teller, D.C. 1997. Crystal structure of a 30 kDA C-terminal fragment from the γ chain of human fibrinogen. *Structure*. **5**(1), pp.125–138.

Yoon, S.K., Song, J.Y. and Lee, G.M. 2003. Effect of low culture temperature on specific productivity, transcription level, and heterogeneity of erythropoietin in Chinese hamster ovary cells. *Biotechnology and Bioengineering*. **82**(3), pp.289–298.

Yu, S., Sher, B., Kudryk, B. and Redman, C.M. 1983. Intracellular assembly of human fibrinogen. *The Journal of biological chemistry*. **258**(22), pp.13407–10.

Zabczyk, M., Natorska, J., Zalewski, J. and Undas, A. 2019. Fibrin biofilm can be detected on intracoronary thrombi aspirated from patients with acute myocardial infarction. *Cardiovascular Research*. **115**(6), pp.1026–1028.

Zhang, J., Liu, L., Tao, J., Song, Y., Fan, Y., Gou, M. and Xu, J. 2019. Prognostic role of early D-dimer level in patients with acute ischemic stroke. *PLoS ONE*. **14**(2), pp.1–10.

Zhang, Y., Zhu, C.G., Guo, Y.L., Xu, R.X., Li, S., Dong, Q. and Li, J.J. 2014. Higher fibrinogen level is independently linked with the presence and severity of new-onset coronary atherosclerosis among han Chinese population. *PLoS ONE*. **9**(11), pp.1–14.

Zhmurov, A., Brown, A.E.X., Litvinov, R.I., Dima, R.I., Weisel, J.W. and Barsegov, V. 2011. Mechanism of fibrin(ogen) forced unfolding. *Structure*. **19**(11), pp.1615–1624.

Zhmurov, A., Protopopova, A.D., Litvinov, R.I., Zhukov, P., Weisel, J.W. and Barsegov, V. 2018. Atomic Structural Models of Fibrin Oligomers. *Structure (London, England : 1993)*. **26**(6), pp.857-868.e4.

Chapter 11 Appendix

11.1 Sequencing Primer Sequence

Table 12 Sequencing primers

Primer	Sequencing Primer Sequence
γ-F2	5'-GTACTGCAGACTATGCCATGTTC-3'
Aα-F1	5'-TTCTCATTCGTTGACCACTAATATA-3'
Aα-F2	5'-GAAACCCTGGGAGCTCTG-3'
pMLP-F1	5'-CTCTCGAGTGAATTGTCG-3'
pMLP-F3	5'-CCTTTCTCTCCACAGGTGTC-3'
pMLP-R1	5'-TTGTTGTTAACTTGTTTATTGCAGC-3'

11.2 Mutagenesis Primer Sequence

Table 13 Sequence of the mutagenesis primers

Bases highlighted green were used to establish the stop codon within the cDNA

Primer	Mutagenesis Primer Sequence
FbgAa390-F	5'-CGAGGCCTAACAACCCAGACTAGGGCACATTTG-3'
FbgAa390-R	5'-CAAATGTGCCCTAGTCTGGGTTGTTAGGCCTCG-3'
FbgAa220-F	5'-CCGGAAATTTTAAGAGCTAGCTTCAGAAGGTACCC-3'
FbgAa220-R	5'-GGGTACCTTCTGAAGCTAGCTCTTAAAATTTCCGG-3'
Fbgγ'16-F	5'-ACAGAATATGACTCACTTTACCCTTAGGATGATTTGTAGAGAG-3'
Fbgγ'16-R	5'-CTCTCTACAAATCATCCTAAGGGTAAAGTGAGTCATATTCTGT-3'
Fbgγ'12-F	5'-CCCTGCGGAAACAGAATATGACTGACTTTACCCTGA-3'
Fbgγ'12-R	5'-TCAGGGTAAAGTCAGTCATATTCTGTTTCCGCAGGG-3'
Fbgγ'8-F	5'-GACCAGAGCACCCTGCGGAATGAGAATATGACTCAC-3'
Fbgγ'8-R	5'-GTGAGTCATATTCTCATTCCGCAGGGTGCTCTGGTC-3'
Fbgγ'4-F	5'-CAAACAGGTCAGACCAGAGTAGCCTGCGGAAACAGAATATG-3'
Fbgγ'4-R	5'-CATATTCTGTTTCCGCAGGCTACTCTGGTCTGACCTGTTTG-3'
Fbgγ'0-F	5'-GGGGGGAGCCAAACAGTAGAGACCAGAGCACCCTG-3'
Fbgγ'0-R	5'-CAGGGTGCTCTGGTCTCTACTGTTTGGCTCCCCCC-3'

11.3 Real Time PCR Primers

Table 14 Primer and Sequence of Primers used for real-time PCR

Housekeeper primers Gnb1 and FbpK1a and fibrinogen primers

Primer	Sequence
FGA-F	5’-CCGGAAGTGAAGCCGATCATGA-3’
FGA-R	5’-CCTGAAGGATGTGTTTGGAGGAC-3’
FGB-F	5’-CAACGGCATGTTCTTCAGCACG-3’
FGB-R	5’-GTATCTGCCGTTTGGATTGGCTG-3’
FGG-F	5’-GAAGGCAACTGTGCTGAACAGG-3’
FGG-R	5’-GAAGGCAACTGTGCTGAACAGG-3’
Gnb1-F	5’-CCATATGTTTCTTTCCCAATGGC-3’
Gnb1-R	5’-AAGTCGTCGTACCCAGCAAG-3’
FbpK1a-F	5’-CTCTCGGGACAGAAACAAGC-3’
FbpK1a-R	5’-GACCTACACTCATCTGGGCTAC-3’

11.4 Plasmid Map

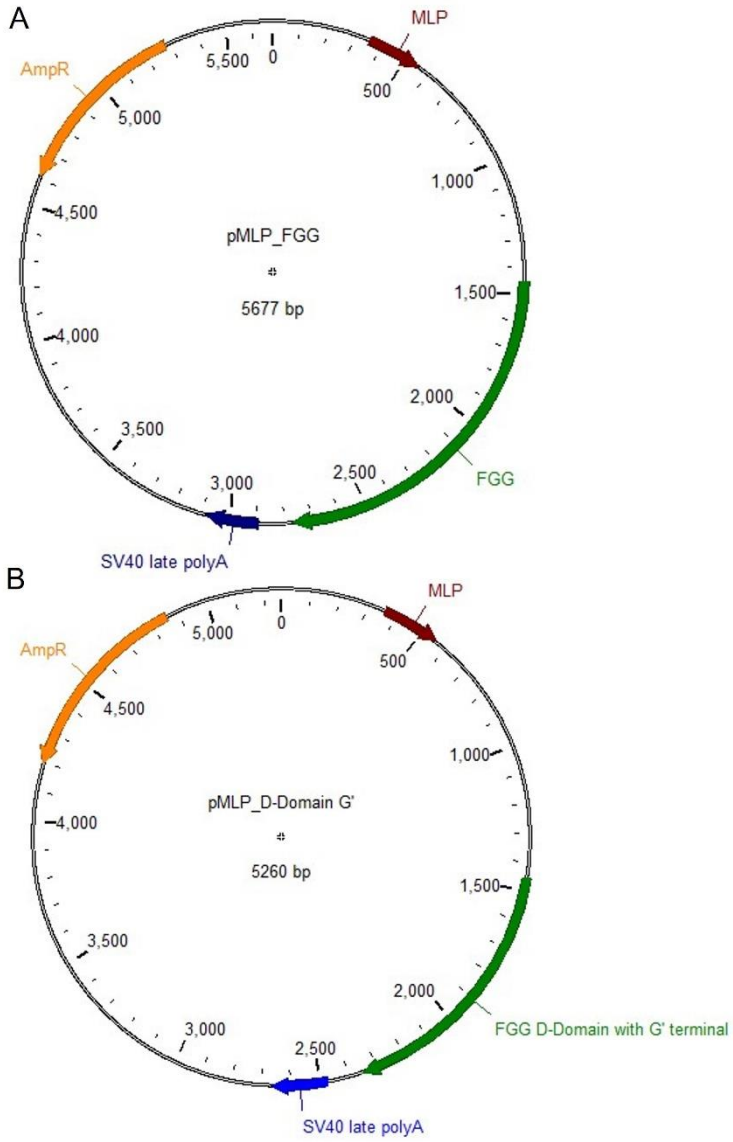

Figure 63 Plasmid Maps of pMLP FGG and PMLP D-domain γ'

Plasmid maps of pMLP FGG (A) and pMLP D-domain γ' (B). The major late promoter (MLP) shown in red, cDNA shown in green, SV40 late polyadenylation signal in blue and the ampicillin resistance marker (AmpR) in orange.

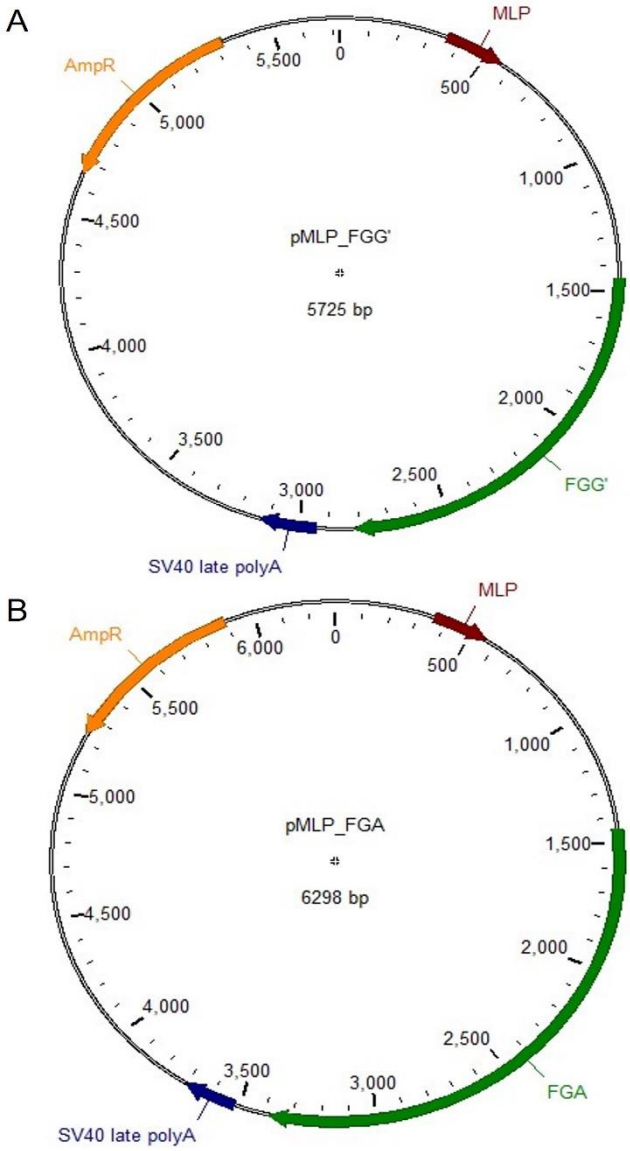

Figure 64 Plasmid maps of pMLP FGA and, pMLP FGG'

Plasmid maps of pMLP FGA (A) and pMLP FGG' (B). The major late promoter (MLP) shown in red, cDNA shown in green, SV40 late polyadenylation signal in blue and the ampicillin resistance marker (AmpR) in orange.

11.5 Sequence of pMLP Plasmids

Figure 65 Sequence of pMLP γA

The γA cDNA sequence is located between the start and stop codons (orange). The restriction sites used to establish pMLP γ' BStXI (light grey) and XBal (teal) and the sequencing primers used pMLP F2 (red), pMLP F1 (purple), pMLP γF2 (green) and pMLP R1 (pink).

Figure 66 Sequence of pMLP γ' D-domain

The γ' D-domain cDNA sequence is located between the start and stop codons (orange). The restriction sites used to establish pMLP γ' BStXI (light grey) and XBal (teal) and the sequencing primers used pMLP F2 (red), pMLP F1 (purple), pMLP γF2 (green) and pMLP R1 (pink).

Figure 67 Sequence of plasmid pMLP Aα

The Aα cDNA sequence is located between the start and stop codons (orange). The sequencing primers used pMLP F2 (red), pMLP F1 (purple), pMLP AαF1 (green), pMLP AαF2 (blue) and pMLP R1 (pink).

11.6 Sequence Alignment

Figure 68 Sequence alignment of pMLP γ'12 to reference FGG'

The amino acid sequence alignment showed no difference in sequence compared to reference, until the desired loss of the final 8 residues to establish pMLP γ'12. The γ' amino acid sequence is highlighted in orange, the signal peptide lost in the mature protein is highlighted in red and matched residues are shown by *.

Figure 69 Sequence alignment of γ'8 to reference FGG'

The amino acid sequence alignment showed no difference in sequence compared to reference, until the desired loss of the final 12 residues to establish pMLP γ'8. The γ' amino acid sequence is highlighted in orange, the signal peptide lost in the mature protein is highlighted in red and matched residues are shown by *.

```
FGG'          MSWSLHPRNLILYFYALLFLSSTCVAYVATRDNCCILDERFGSYCPTTCGIADFLSTYQT
pMLP γ'4      MSWSLHPRNLILYFYALLFLSSTCVAYVATRDNCCILDERFGSYCPTTCGIADFLSTYQT
              ************************************************************
FGG'          KVDKDLQSLEDILHQVENKTSEVKQLIKAIQLTYNPDESSKPNMIDAATLKSRKMLEEIM
pMLP γ'4      KVDKDLQSLEDILHQVENKTSEVKQLIKAIQLTYNPDESSKPNMIDAATLKSRKMLEEIM
              ************************************************************
FGG'          KYEASILTHDSSIRYLQEIYNSNNQKIVNLKEKVAQLEAQCQEPCKDTVQIHDITGKDCQ
pMLP γ'4      KYEASILTHDSSIRYLQEIYNSNNQKIVNLKEKVAQLEAQCQEPCKDTVQIHDITGKDCQ
              ************************************************************
FGG'          DIANKGAKQSGLYFIKPLKANQQFLVYCEIDGSGNGWTVFQKRLDGSVDFKKNWIQYKEG
pMLP γ'4      DIANKGAKQSGLYFIKPLKANQQFLVYCEIDGSGNGWTVFQKRLDGSVDFKKNWIQYKEG
              ************************************************************
FGG'          FGHLSPTGTTEFWLGNEKIHLISTQSAIPYALRVELEDWNGRTSTADYAMFKVGPEADKY
pMLP γ'4      FGHLSPTGTTEFWLGNEKIHLISTQSAIPYALRVELEDWNGRTSTADYAMFKVGPEADKY
              ************************************************************
FGG'          RLTYAYFAGGDAGDAFDGFDFGDDPSDKFFTSHNGMQFSTWDNDNDKFEGNCAEQDGSGW
pMLP γ'4      RLTYAYFAGGDAGDAFDGFDFGDDPSDKFFTSHNGMQFSTWDNDNDKFEGNCAEQDGSGW
              ************************************************************
FGG'          WMNKCHAGHLNGVYYQGGTYSKASTPNGYDNGIIWATWKTRWYSMKKTTMKIIPFNRLTI
pMLP γ'4      WMNKCHAGHLNGVYYQGGTYSKASTPNGYDNGIIWATWKTRWYSMKKTTMKIIPFNRLTI
              ************************************************************
FGG'          GEGQQHHLGGAKQVRPEHPAETEYDSLYPEDDL
pMLP γ'4      GEGQQHHLGGAKQVRPE-----------------
              *****************
```

Figure 70 Sequence alignment of γ'4 to reference FGG'

The amino acid sequence alignment showed no difference in sequence compared to reference, until the desired loss of the final 16 residues to establish pMLP γ'4. The γ' amino acid sequence is highlighted in orange, the signal peptide lost in the mature protein is highlighted in red and matched residues are shown by *.

```
FGG'        MSWSLHPRNLILYFYALLFLSSTCVAYVATRDNCCILDERFGSYCPTTCGIADFLSTYQT
pMLP γ'0    MSWSLHPRNLILYFYALLFLSSTCVAYVATRDNCCILDERFGSYCPTTCGIADFLSTYQT
            ************************************************************
FGG'        KVDKDLQSLEDILHQVENKTSEVKQLIKAIQLTYNPDESSKPNMIDAATLKSRKMLEEIM
pMLP γ'0    KVDKDLQSLEDILHQVENKTSEVKQLIKAIQLTYNPDESSKPNMIDAATLKSRKMLEEIM
            ************************************************************
FGG'        KYEASILTHDSSIRYLQEIYNSNNQKIVNLKEKVAQLEAQCQEPCKDTVQIHDITGKDCQ
pMLP γ'0    KYEASILTHDSSIRYLQEIYNSNNQKIVNLKEKVAQLEAQCQEPCKDTVQIHDITGKDCQ
            ************************************************************
FGG'        DIANKGAKQSGLYFIKPLKANQQFLVYCEIDGSGNGWTVFQKRLDGSVDFKKNWIQYKEG
pMLP γ'0    DIANKGAKQSGLYFIKPLKANQQFLVYCEIDGSGNGWTVFQKRLDGSVDFKKNWIQYKEG
            ************************************************************
FGG'        FGHLSPTGTTEFWLGNEKIHLISTQSAIPYALRVELEDWNGRTSTADYAMFKVGPEADKY
pMLP γ'0    FGHLSPTGTTEFWLGNEKIHLISTQSAIPYALRVELEDWNGRTSTADYAMFKVGPEADKY
            ************************************************************
FGG'        RLTYAYFAGGDAGDAFDGFDFGDDPSDKFFTSHNGMQFSTWDNDNDKFEGNCAEQDGSGW
pMLP γ'0    RLTYAYFAGGDAGDAFDGFDFGDDPSDKFFTSHNGMQFSTWDNDNDKFEGNCAEQDGSGW
            ************************************************************
FGG'        WMNKCHAGHLNGVYYQGGTYSKASTPNGYDNGIIWATWKTRWYSMKKTTMKIIPFNRLTI
pMLP γ'0    WMNKCHAGHLNGVYYQGGTYSKASTPNGYDNGIIWATWKTRWYSMKKTTMKIIPFNRLTI
            ************************************************************
FGG'        GEGQQHHLGGAKQVRPEHPAETEYDSLYPEDDL
pMLP γ'0    GEGQQHHLGGAKQ---------------------
            *************
```

Figure 71 Sequence alignment of γ'0 to reference FGG'

The amino acid sequence alignment showed no difference in sequence compared to reference, until the desired loss of the final 20 residues to establish pMLP γ'0. The γ' amino acid sequence is highlighted in orange, the signal peptide lost in the mature protein is highlighted in red and matched residues are shown by *.

Figure 72 Sequence alignment of pMLP α390 and pMLP α220 to reference FGA

The amino acid sequence alignment of pMLP α390 and FGA (A). There was no difference in sequence compared to reference, until the desired point. The amino acid sequence alignment of pMLP α220 and FGA (B). No difference in sequence compared to reference, until the desired point. The signal peptide lost in the mature protein is highlighted in red and the fibrinopeptide A is highlighted in blue. Matched residues are shown by * and - indicates where sequence has ended.